

2016

# Development of Novel Organic Materials with Stimuli-Responsive Applications

Mark James Juetten  
Iowa State University

Follow this and additional works at: <https://lib.dr.iastate.edu/etd>

 Part of the [Organic Chemistry Commons](#)

## Recommended Citation

Juetten, Mark James, "Development of Novel Organic Materials with Stimuli-Responsive Applications" (2016). *Graduate Theses and Dissertations*. 15733.  
<https://lib.dr.iastate.edu/etd/15733>

This Dissertation is brought to you for free and open access by the Iowa State University Capstones, Theses and Dissertations at Iowa State University Digital Repository. It has been accepted for inclusion in Graduate Theses and Dissertations by an authorized administrator of Iowa State University Digital Repository. For more information, please contact [digirep@iastate.edu](mailto:digirep@iastate.edu).

**Development of novel organic materials with stimuli-responsive applications**

by

**Mark James Juetten**

A dissertation submitted to the graduate faculty  
in partial fulfillment of the requirements for the degree of

DOCTOR OF PHILOSOPHY

Major: Organic Chemistry

Program of Study Committee  
Arthur Winter, Major Professor  
William Jenks  
Theresa Windus  
Levi Stanley  
Jason Chen

Iowa State University

Ames, Iowa

2016

## DEDICATION

I dedicate this dissertation to the memory of my father, James F. Juetten. He will always be my hero.

## TABLE OF CONTENTS

DEDICATION.....	ii
ACKNOWLEDGMENTS.....	iv
ABSTRACT.....	vi
CHAPTER 1: INTRODUCTION.....	1
CHAPTER 2: ACESS TO ARYL MELLITIC ACID ESTERS THROUGH A SURPRISING OXIDATIVE ESTERIFICATION REACTION.....	7
CHAPTER 3: MECHANISTIC INSIGHTS INTO AROMATIC ESTERIFICATION REACTION.....	13
CHAPTER 4: A RADICAL SPIN ON VIOLOGEN POLYMERS: ORGANIC SPIN CROSSOVER MATERIALS.....	25
CHAPTER 5: SUPRAMOLECULAR VIOLOGEN BASED LOGIC GATE SYSTEMS.....	34
CHAPTER 6: CONCLUSIONS.....	49
APPENDIX A: SUPPORTING INFORMATION FOR CHAPTER 2.....	51
APPENDIX B: SUPPORTING INFORMATION FOR CHAPTER 3.....	87
APPENDIX C: SUPPORTING INFORMATION FOR CHAPTER 4.....	105
APPENDIX D: SUPPORTING INFORMATION FOR CHAPTER 5.....	119



## ACKNOWLEDGMENTS

I express my sincere gratitude for my major professor, Dr. Arthur Winter. You are among the most skilled teachers that I have ever encountered, and I feel fortunate to have been given the opportunity to learn from you throughout my studies. I have the highest admiration for your philosophical approach to what it means to be a professor of chemistry. Thank you for your patience with me.

I also want to thank my former and current Winter group members. I could not have asked for a better group to be in. I regard you as some of my closest friends. There have been countless times where I have had to lean on you for support, and you have never faltered or let me down. In particular I want to thank my lab mate neighbor for 5 years, Alex Buck. I knew no matter what you would always be there for me, to support me in all things related to chemistry-or not so chemistry related. Our arguments and discussions have been some of the most fulfilling aspects of my career at Iowa State.

My gratitude for the Iowa State chemistry department extends far beyond just the Winter group. I would like to give special acknowledgments to the chemistry department at large and especially Dr. Sadow, Dr. Gordon, Dr. Vela, and their groups for their support in providing me with equipment and expertise that I otherwise lacked. Whenever I encountered a problem, I always felt comfortable going to other groups for guidance (or to borrow Parr bombs, chemicals, gloveboxes, ect.). Thanks also to Dr. Sarah Cady and her endless knowledge of all magnetic instruments. My research would not go without you, and your constant welcoming availability has been of tremendous help.

To my friends who made Ames home, Dave Appy, Zak Weinstien, Paul Cole and many others, you have been great companions to me and I hope you always will be. A special thank you to the weekly poker game and to all involved with making it a place to relieve stress and to sharpen mental acuties on things unrelated to chemistry.

To my family, especially my mother Connie Juetten, thank you for listening, whether it was rambling about my science or me complaining about whatever, I knew I could always call and you would always listen. Your unconditional support will be forever appreciated.

## ABSTRACT

The research herein describes development of fundamental concepts related to new materials that are designed to be stimuli responsive materials. There are two main avenues explored in this dissertation, a synthetic exploration of a novel aromatization reaction and using single electron reduced 4,4'-bipyridine as sensors for several different inputs. The new synthetic reaction described is based off of an oxidation of a cyclohexane in order to obtain a highly functionalized aromatic ring. The particular functionality that was studied in this abstract is related to the hexaester of cyclohexane. The product of such reactions is shown to be a first generation paddlewheel dendrimer. Since the reaction is not known, mechanistic investigations were performed so that the reaction scope may be generalized for further use beyond hexaester cyclohexanes.

The second part of this dissertation shifts away from synthetic methodology into stable organic radical materials. 4,4'-bipyridine shows a paramagnetic radical in its monomer form that forms diamagnetic dimers at higher concentrations. Since the dimerization is a fairly weak interaction, we enhance the degree of diamagnetism by tethering units together. Several of these units can be tethered together in a polymeric fashion. We then show the ability to disturb this diamagnetism with stimuli such as non-covalent binding interactions or the addition of heat. These changes in magnetic properties can be followed by electron paramagnetic resonance (EPR) and UV/vis spectroscopy. In addition to affecting the concentration of paramagnetic radicals by tethering units together, we also explore changing the substituents on our molecules to alter the binding constants obtained. Using the knowledge of tethering several units

together, modulating our binding constants, and affecting the input by heat and non-covalent binding events, we are able to design molecules that display Boolean logic behavior and can act as sensors for a variety of inputs.

## CHAPTER 1: INTRODUCTION

### 1.1 Dissertation organization

The following dissertation is composed of projects that are designed towards the advancement in the scope and breadth of knowledge related towards chemical machinery. The first avenue of discovery is concerned with creating a class of polyester-based first generation dendrimers that have potential applications as chemical amplifiers or to behave as a cog in advanced molecular machines. This will be the focus of chapter 2 of this dissertation, as we optimized a new reaction that opened up access to these unique molecules. My contributions to the manuscript presented herein was the initial discovery of the novel reaction, the purification conditions, the initial optimization tests, and all the mechanistic work done thus far on the reaction.

Chapter 3 of this dissertation further elaborates on the mechanism of the reaction described in chapter 2. It focuses on providing insights into our proposed reaction pathway of a Hell-Volhard-Zelinsky oxidation by looking at computationally determined  $pK_a$ 's of the proposed intermediates. This chapter also discusses the generalization of this aromatization for creating aromatic compounds of other potential substitution patterns.

The focus of chapter 4 shifts to the study of linked 4,4'-bipyridine molecules, and their reduced form. Prior work has focused on a tethered dimer; Chapter 4 discusses tethering several together in a polymeric fashion. The manuscript of the related paper is shown in this thesis. My contribution to this paper was the synthesis of the viologen polymers, the UV/Vis temperature switching, executing the experiment for the Job's plot and writing the manuscript in its entirety.

Chapter 5 continues the work in chapter 3 of experimentation with the 4,4'-bipyridine. The work shown in chapter 4 has not been published in an academic journal as of yet, but it is likely that two manuscripts will result from research so far done and presented in this dissertation. The first publication will focus on the binding constants of different reduced 4,4'-bipyridine molecules. My contribution to the binding constant determination was the synthesis of the "heterosubstituted" compounds, where the two R groups were different, the investigation of the "monosubstituted" compounds, and all the EPR experiments. The other parts of chapter 4, development of molecular machinery related to these 4,4'-bipyridine molecules, I did in its entirety.

Appendices are utilized to give extra details associated with each manuscript when the data was considered less important for the article but would help to the larger story. Appendices A-E are the supporting information associated with the papers composing chapters 2-5 respectively.

## **1.2 Access to mellitic acid esters through surprising aromatic oxidation**

In order to meet with the demands for new and innovative technologies, molecules are increasing in complexity in order to gain a wide variety of functional uses for applications.<sup>1,2</sup> Many challenges accompany these increasing complexities, particularly synthetic challenges. Old synthetic methods often have to be used in innovative new ways to gain success.<sup>3</sup> Increasing chemical complexity, and meeting the challenges of higher difficulty synthesis, has the potential for exciting and rewarding payouts. Chemical machines or molecular machines are a class of molecule, often with many complex "moving" parts that achieve chemical functions.<sup>4-8</sup> Like a mathematical function, a chemical machine has the ability to transform an input into an entirely

different output. In the case of chemical machines, this is usually through a quasi-mechanical movement that are easy to imagine in a macro-world and that often emulate the form of macro machines.<sup>9</sup> The ability of chemical machines to do complex tasks makes the challenge of difficult target molecule synthesis one worth pursuing.

One example of a chemical machine is a chemical amplifier. These chemical amplifiers are structures that translate a single bond-breaking event into release of numerous chemical outputs. In this way, a single bond cleavage input reaction (e.g. a reaction triggered by an analyte, a photon, or an enzyme) can be translated into the release of numerous output chemical cargos.<sup>10-14</sup> Outputs can take the form of reporting molecules (e.g. fluorescent dyes), biomolecules, or drugs. This kind of chemical amplifier has numerous applications in chemical sensing, in drug delivery and a variety of other highly sophisticated tasks, especially when combined with other chemical functionalities as part of increasingly complex chemical machines.

The type of chemical amplifier that we investigated was based on mellitic acid and its hexaester derivatives. This class of molecule is difficult to synthesize and transform, requiring a variety of techniques.<sup>15-20</sup> Because of the synthetic challenges, careful selection of a target was investigated. A self-immolative linker system, based on anhydride formation of a 1,2 carboxylic acid of a six member ring, was chosen to be the target of interest because of a number of reasons: benign byproducts, availability of starting materials, and fast kinetics of release.<sup>21</sup> An unprecedented synthetic technique we used was the oxidative aromatization of substituted cyclohexanes. This technique has very little literature precedence and so we explore it here.

### 1.3 Spin switchable organic probes

Spin switchable organic molecules, organic compounds capable of changing magnetic states between non-magnetic (diamagnetic) and magnetic (paramagnetic), have the potential to be used in molecular electronic devices,<sup>22, 23</sup> organic spintronics,<sup>24-26</sup> and organic polymers with bulk paramagnetism.<sup>27-29</sup> Previous studies have shown that small changes in magnetic properties of these spin switchable compounds can manifest as large changes in chemical properties,<sup>30, 31</sup> including convenient to observe color changes.<sup>32, 33</sup> While the spin switchable nature of organometallic compounds is very well documented,<sup>34, 35</sup> little has been documented in organic molecules. Our lab has previously reported on one such organic molecule, reduced disubstituted 4,4'-bipyridine (viologen cation radicals).<sup>20, 36</sup> The work done thus far regarding these molecules has concentrated on small molecule systems, including simple two viologen linked systems. This dissertation further explores these reduced viologens expanding the scope of focus to include polymeric versions of the small molecule system. Different chain lengths and modifications to the linkers are then investigated for use in higher functionality systems.

### 1.4 Supramolecular viologen based logic gate systems

Expanding on the work described in chapter 3, chapter 4 focuses on finding target viologen substitution patterns for use in molecular logic gates. This is first accomplished by determining the binding constants of many different substitution patterns of the reduced 4,4'-bipyridine. We found that the monosubstituted reduced bipyridine to be uniquely valuable to our purposes since the binding constant is dependent on pH of



aqueous solutions, or water molecules. When combined with previously stimuli-responsive inputs described in chapter 4, we are able to begin to build Boolean logic gates.

1. A. I. Vogel, B. S. Furniss, A. J. Hannaford, P. W. G. Smith and A. R. Tatchell, *Vogel's textbook of practical organic chemistry. 5th ed*, Longman, Harlow, 1989.
2. R. E. Ireland, *Organic synthesis*, Prentice-Hall, Englewood Cliffs, N.J., 1969.
3. B. Pignataro, *New strategies in chemical synthesis and catalysis*, Wiley-VCH ; John Wiley [distributor], Weinheim; Chichester, 2012.
4. A. Prasanna de Silva and N. D. McClenaghan, *J. Am. Chem. Soc.*, 2000, **122**, 3965-3966.
5. D. C. Magri, G. J. Brown, G. D. McClean and A. P. de Silva, *J. Am. Chem. Soc.*, 2006, **128**, 4950-4951.
6. C. W. Rogers and M. O. Wolf, *Coord. Chem. Rev.*, 2002, 341-350.
7. B. L. Feringa, R. A. van Delden, N. Koumura and E. M. Geertsema, *Chem Rev.*, 2000, **100**, 1789-1816.
8. E. Busseron and F. d. r. Coutrot, *J. Org. Chem.*, 2013, **78**, 4099-4106.
9. R. Ballardini, V. Balzani, A. Credi, M. T. Gandolfi and M. Venturi, *Acc Chem Res.*, 2001, **34**, 445-455.
10. D. Astruc, C. Ornelas and J. Ruiz, *Accounts of Chemical Research*, 2008, **41**, 841-856.
11. M. Avital-Shmilovici and D. Shabat, *Soft Matter*, 2010, **6**, 1073-1080.
12. S. J. Guillaudeu, M. E. Fox, Y. M. Haidar, E. E. Dy, F. C. Szoka and J. M. J. Fruchet, *Bioconjugate Chem*, 2008, **19**, 461-469.
13. N. Karton-Lifshin and D. Shabat, *New J. of Chem.*, 2012, **36**, 386-393.
14. D. Shabat, *J. Polym. Sci., Part A: Polym. Chem.*, 2006, **44**, 1569-1578.
15. V. Cadierno, S. E. García-Garrido, J. Gimeno, A. Varela-Álvarez and J. A. Sordo, *J. Am. Chem. Soc.*, 2006, **128**, 1360-1370.
16. A. Geny, N. Agenet, L. Iannazzo, M. Malacria, C. Aubert and V. Gandon, *Angew. Chem. int. ed.*, 2009, **121**, 1842-1845.
17. S. Kotha and P. Khedkar, *Euro. J. Org. Chem.*, 2008, NA-NA.
18. N. Saino, F. Amemiya, E. Tanabe, K. Kase and S. Okamoto, *J. Chem. Inf.*, 2006, **37**.
19. R. Takeuchi and Y. Nakaya, *Org. Lett.*, 2003, **5**, 3659-3662.
20. M. R. Geraskina, A. T. Buck and A. H. Winter, *J. Org. Chem.* 2014, **79**, 7723-7727.
21. K. M. Mahoney, P. P. Goswami and A. H. Winter, *J. Org. Chem.*, 2013, **78**, 702-705.
22. A. Coskun, J. M. Spruell, G. Barin, W. R. Dichtel, A. H. Flood, Y. Y. Botros and J. F. Stoddart, *Chem. Soc. Rev.*, 2012, **41**, 4827.
23. A. N. Shipway, E. Katz and I. Willner, *J. Mach. Mo.*, 237-281.

24. Y. A. Uspenskii, E. T. Kulatov, A. A. Titov, E. V. Tikhonov, F. Michelini and L. Raymond, *J. Magn. Magn. Mater.*, 2012, **324**, 3597-3600.
25. Y. Zhan and M. Fahlman, *J. Polym. Sci. B Polym. Phys.*, 2012, **50**, 1453-1462.
26. I. Bergenti, V. Dediu, M. Prezioso and A. Riminucci, *Philos. Trans. R. Soc. Lon Ser B.*, 2011, **369**, 3054-3068.
27. A. Rajca, *Chem. Rev.*, 1994, **94**, 871-893.
28. A. Rajca, *Chem. Eur. J.* 2002, **8**, 4834-4841.
29. J. V. Yakhmi, *Bull. Mater. Sci.* 2009, **32**, 217-225.
30. A. Rajca, Y. Wang, M. Boska, J. T. Paletta, A. Olankitwanit, M. A. Swanson, D. G. Mitchell, S. S. Eaton, G. R. Eaton and S. Rajca, *J. Am. Chem. Soc.*, 2012, **134**, 15724-15727.
31. B. W. Muir, D. P. Acharya, D. F. Kennedy, X. Mulet, R. A. Evans, S. M. Pereira, K. L. Wark, B. J. Boyd, T.-H. Nguyen, T. M. Hinton, L. J. Waddington, N. Kirby, D. K. Wright, H. X. Wang, G. F. Egan and B. A. Moffat, *Biomater.*, 2012, **33**, 2723-2733.
32. H. J. Kim, W. S. Jeon, Y. H. Ko and K. Kim, *Proc. Natl. Acad. Sci.*, 2002, **99**, 5007-5011.
33. A. T. Buck, J. T. Paletta, S. A. Khindurangala, C. L. Beck and A. H. Winter, *J. Am. Chem. Soc.*, 2013, **135**, 10594-10597.
34. S. Thies, H. Sell, C. Bornholdt, C. Schütt, F. Köhler, F. Tuzcek and R. Herges, *Eur. J. Chem.*, 2012, **18**, 16358-16368.
35. R. G. Hicks, *Nat Chem*, 2011, **3**, 189-191.
36. A. T. Buck, J. T. Paletta, S. A. Khindurangala, C. L. Beck and A. H. Winter, *J. Am. Chem. Soc.*, 2013, **135**, 10594-10597.

## CHAPTER 2. ACCESS TO ARYL MELLITIC ACID ESTERS THROUGH A SURPRISING OXIDATIVE ESTERIFICATION REACTION

A paper published in *The Journal of Organic Chemistry*

Margarita R. Geraskina, Mark J. Juetten, and Arthur H. Winter

### Abstract

A serendipitously discovered oxidative esterification reaction of cyclohexane hexacarboxylic acid with phosphorus pentachloride and phenols provides one-pot access to previously unknown aryl mellitic acid esters. The reaction features a solvent-free digestion and chromatography-free purifications and demonstrates the possibility of cyclohexane-to-benzene conversions under relatively mild, metal-free conditions.

### 2.1 Introduction

Numerous synthetic methods are known to make alkyl esters of mellitic acid,<sup>15-19</sup> but aryl esters of mellitic acid have not been reported to date. We are interested in aryl esters of mellitic acid because of their possible use as scaffolds for fast-releasing domino self-immolative linkers,<sup>21</sup> but they are also structurally interesting paddlewheel motifs that may find use as the cores of hexagonally branched dendrimers. Additionally, some hindered mellitic acid esters are of interest for their anomalous fluorescence behavior.<sup>37</sup> Perhaps unsurprisingly given the absence of all methods to prepare these structures in the literature, all our attempts to prepare aryl mellitic acid esters via its acid chloride or through direct esterification of mellitic acid with standard coupling reagents

(DCC/DMAP, PyBOP, CDI, etc.) were unsuccessful. In contrast, alkyl esters of mellitic acid can be made easily through these methods. The sterically hindered nature of these aryl esters may explain why they are difficult to prepare via direct methods.

## 2.2 Discussion

Fortunately, we serendipitously discovered a surprising oxidative esterification reaction by digesting all-*cis*-1,2,3,4,5,6-cyclohexanhexacarboxylic acid with phosphorus pentachloride and phenols that leads to the ring-oxidized aryl mellitic acid esters in one pot. The aryl esters can be purified through washing procedures, avoiding chromatography. The reaction optimization, which was performed using *p*-

methoxyphenol, included variation of following parameters: equivalents of PCl<sub>5</sub>, temperature, and time for each reaction step (Table 1). It was found that 12 equiv of PCl<sub>5</sub> (2 equiv. per acid moiety) results in the best yield for solvent-free digestion at 130 °C. Addition of pyridine in the final step was used in all cases except for the synthesis of mellitic acid, where addition of water led to

**Table 2.1. Optimization of reaction conditions**

Temp (°C)	PCl <sub>5</sub> (equiv.)	Time (h) <sup>a</sup>	Yield (isolated %)
130	6	1, 4, 2	49
130	9	1, 4, 2	31
130	12	1, 4, 2	63
130	12	1, 1, 1	45
130	12	24, 24, 24	52
130	18	1, 4, 2	0
100	12	1, 4, 2	58
160	12	1, 4, 2	47

<sup>a</sup>The three times are for PCl<sub>5</sub> digestion, addition of phenol, and addition of pyridine respectively

product in the absence of pyridine. The reactions to prepare the aryl mellitic acid esters

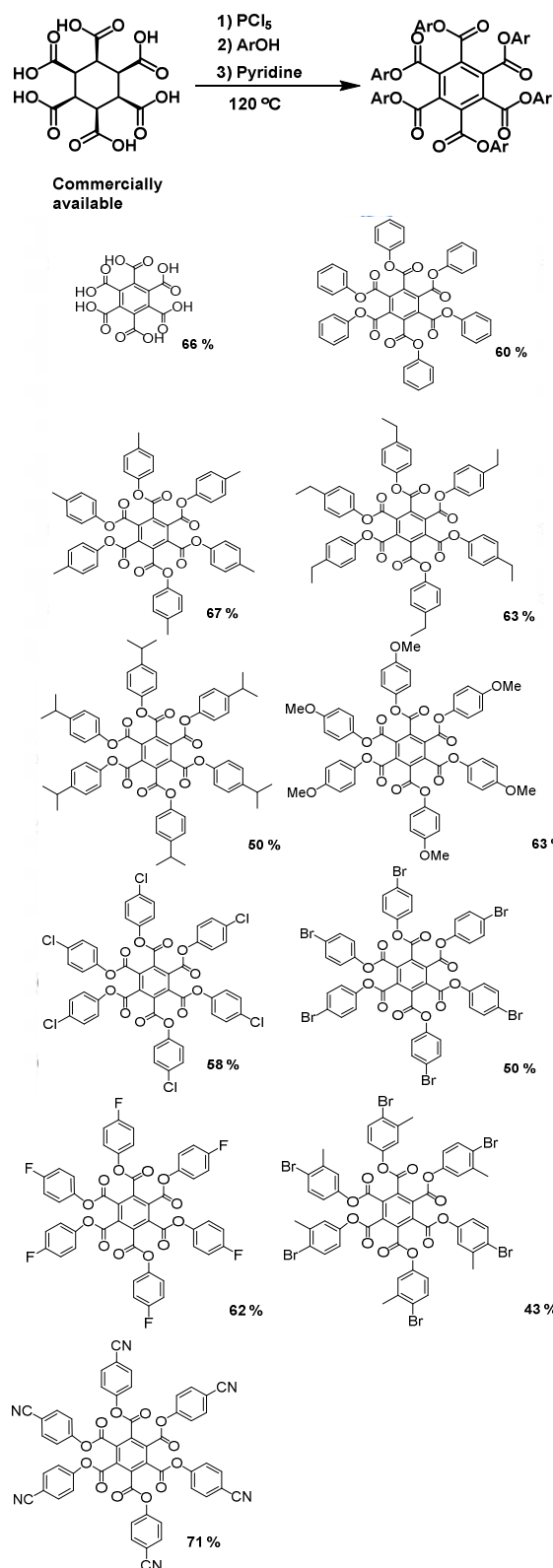


Figure 2.1 scope of aromatic oxidation reaction

are one-pot, solvent-free reactions that can be performed under air and give products that can be purified by washing procedures to free the aryl mellitic acid esters from byproducts (typically  $\text{P}(\text{OAr})_3$ ) and pyridine). As can be seen in Scheme 1, the reaction can tolerate both electron-rich phenols (e.g., p-methoxy phenol, alkyl phenols) as well as some electron-poor phenols (halophenols, cyanophenol) with some exceptions. Using our standard conditions, 4-nitrophenol, 2,2'-bisphenol, 4-52 phenylphenol, 4-acetamidophenol, 4-tert-butylphenol, and 1- and 2-naphthol failed to yield the corresponding mellitic acid ester in significant quantities. Additionally, it was possible to use alkyl alcohols instead of phenols, but we observed some conversion of the alcohols to the alkyl chlorides during the  $\text{PCl}_5$  digestion step and the alkyl esters of

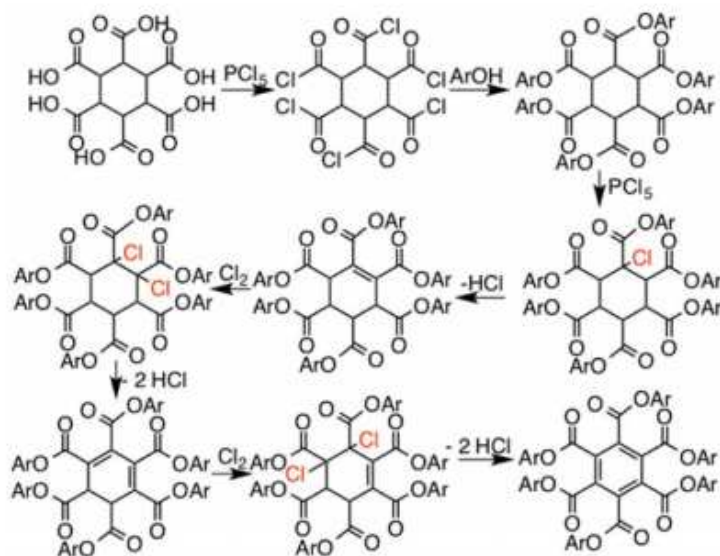


Figure 2.2 Plausible mechanism of oxidative esterification reaction

mellitic acid are difficult to separate from the  $P(OR)_3$  byproduct. Given that there are numerous methods to make alkyl esters of mellitic acid via standard procedures, we did not pursue these oxidative alkyl esterification reactions further. Further, we note that reaction with water instead of a phenol led to mellitic acid as an inseparable mixture with phosphoric acid. Thus, the mellitic acid was converted to its methyl ester to determine the reaction yield in this one case (see the Supporting Information for details).

**Mechanistic Considerations.** A few additional experiments shed some light on the mechanism of this remarkable oxidative esterification reaction. First, the reaction appears to be specific to the 1,2,3,4,5,6-cyclohexanecarboxylic acid scaffold. Subjecting 1,3,5-cyclohexanetricarboxylic acid (all-*cis*) and 1,2-cyclohexanedicarboxylic acid (both *cis* and *trans*) leads to typical esterification with no oxidation of the cyclohexane ring to benzene. Second, given that addition of phenols to the acid chloride of mellitic acid leads to no esterification, it is likely that esterification occurs prior to ring oxidation. In

contrast, esterification of the acid chloride of 1,2,3,4,5,6-cyclohexanehexacarboxylic acid with phenols proceeds to give the cyclohexane hexaester in normal fashion, possibly due to a more flexible cyclohexane ring leading to less steric hindrance between the aryl esters. Finally, subjecting the hexaaryl ester of 1,2,3,4,5,6-cyclohexanehexacarboxylic acid to the reaction conditions leads to oxidation of the cyclohexane to the benzene ring, lending support to the possibility of esterification followed by oxidation.

Additionally, the mechanism is indifferent to the stereochemistry of the starting material. Reacting the all-*trans*-1,2,3,4,5,6-cyclohexanehexacarboxylic acid leads to essentially identical yields as the all-*cis* stereoisomer (although the all-*cis* stereoisomer is available commercially, leading to our preference to using that stereoisomer as the starting material). As to the oxidation mechanism itself, one possibility is that it follows an  $\alpha$  chlorination/elimination mechanism.  $\text{PCl}_5$  is known to be in an equilibrium with  $\text{PCl}_3$  and  $\text{Cl}_2$  at elevated temperatures,<sup>38</sup> so  $\text{Cl}_2$  may play a role in the oxidation process. It may be the case that the contiguous adjacent acid groups in the starting material allow for milder  $\alpha$  chlorination. We tested the importance of  $\text{Cl}_2$  in the oxidation by performing the same reaction with  $\text{PCl}_3$  (which lacks the ability to form  $\text{Cl}_2$ ) and obtained esterified product that was not ring oxidized. This experiment implicates  $\text{Cl}_2$  as the likely oxidant in this reaction. Isolated yields are not affected by running the reaction under air or argon, suggesting molecular oxygen is not playing a role in the oxidation mechanism. We also considered that pyridine might play a role in the oxidation mechanism (e.g., by forming N-chloropyridinium), but given that mellitic acid can be formed by addition of water instead of a phenol without adding pyridine, this possibility seems to be less likely. Additionally, without pyridine we obtain the product esters, albeit in somewhat

diminished yields. The combination of these experiments led us to suggest the mechanism shown in Scheme 2. Although we were unable to obtain X-ray quality crystals of the esters, density functional theory computations (B3LYP/6-31G(d)) on **2** suggest the phenyl rings adopt an interesting paddlewheel-like structure to minimize strain. See Figure 1.

### 2.3 Conclusion

We have developed a simple procedure to access previously unknown aryl mellitic acid esters via a novel oxidative esterification reaction. This approach has obvious synthetic advantages as the reaction is carried out via a solvent-free, one-pot digestion and has a washing workup that avoids chromatography. This reaction is novel because oxidations of cyclohexane rings to benzene typically require high temperatures in excess of 200 °C and a metal catalyst, whereas this reaction is performed in the absence of metal and at comparatively low temperatures. Aryl mellitic acid esters may prove to be useful in domino self-immolative linkers or as the cores of structurally interesting dendrimers.

1. V. Cadierno, S. E. García-Garrido, J. Gimeno, A. Varela-Álvarez and J. A. Sordo, *J. Am. Chem. Soc.*, 2006, **128**, 1360-1370.
2. A. Geny, N. Agenet, L. Iannazzo, M. Malacria, C. Aubert and V. Gandon, *Angew. Chem Int Ed.*, 2009, **121**, 1842-1845.
3. S. Kotha and P. Khedkar, *Euro. J. Org. Chem.*, 2008, NA-NA.
4. N. Saino, F. Amemiya, E. Tanabe, K. Kase and S. Okamoto, *ChemInf.*, 2006, **37**.
5. R. Takeuchi and Y. Nakaya, *Org. Lett.*, 2003, **5**, 3659-3662.
6. K. M. Mahoney, P. P. Goswami and A. H. Winter, *J. Org. Chem.*, 2013, **78**, 702-705.
7. N. Yamasaki, Y. Inoue, T. Yokoyama, A. Tai, A. Ishida and S. Takamuku, *J. Am. Chem. Soc.*, 1991, **113**, 1933-1941.
8. U. Berger, G. Dannhardt and W. Wiegrebe, *Arch. Pharm. Pharm. Med. Chem.*, 1983, **316**, 182-189.



## CHAPTER 3. MECHANISTIC INSIGHTS INTO AROMATIC ESTERIFICATION REACTION

### Introduction

Up until recently, aryl esters of mellitic acid were not known.<sup>39</sup> Previous work in our group, however unlocked access to these potentially valuable snowflake-like molecules via a surprising oxidation reaction. 1,2,3,4,5,6 cyclohexane hexacarboxylic acid could be oxidized to its mellitic acid ester derivatives with phosphorous pentachloride at sufficient temperatures and with a suitable base (see figure 3.1). The studies so far, however, have been limited in their mechanistic insights as well as other types of molecules that could be potentially synthesized through this remarkable one-pot aromatization method.

We previously discussed the possibility of the reaction occurring via a Hell-Volhard-Zelinsky (HVZ) mechanism, since  $\text{PCl}_5$  would provide the chloride necessary to perform the reaction. In order for this to be the case, however, the  $\text{pK}_a$  of the proposed intermediate would have to be investigated since the HVZ reaction typically isn't thought to be feasible with ester compounds. The  $\text{pK}_a$ 's of model compounds were determined via the referential model.

Additionally several new compounds were investigated (figure 3.4) to test the potential scope of this new method for creating aromatic rings.

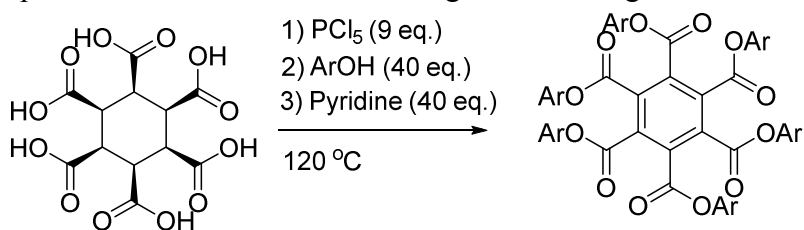


**Figure 3.1** The previously reported oxidative aromatization reaction investigated

### Computational Methods:

All the molecular geometries of the electronic states of all molecules were optimized under the DFT level of theory using the B3LYP functional and the 3-21+G\* basis set.<sup>40</sup> Although the basis set is perhaps unbalanced, the referential method includes a canceling of errors that gives accurate results despite the imbalance. The stationary points were found to have zero imaginary frequencies, and all energies contain a correction for the zero-point energy. All the single-reference computations were computed with Gaussian03/09.<sup>41</sup> The hybrid B3LYP functional used consists of the Becke 3-parameter exchange<sup>42, 43</sup> functional with the correlation functional of Lee, Yang, and Parr<sup>44</sup>. This and related DFT functionals have been shown to give quite reasonable geometries for ground state molecules.<sup>45-47</sup> Polarizable continuum model (PCM) was used to approximate solvent conditions in DMSO.

The pKa calculations followed the proton exchange or relative method. The basic approach of the proton exchange scheme is to consider an acid/base reaction with a reference molecule.<sup>48</sup> This method was chosen because it allows for some canceling in error when the level of theory or basis sets may not otherwise give accurate results. The relative pKa values used were in DMSO and set to pyridine/ pyridinium acid/base pair. Choosing pyridine as the reference base may, however lead to some degree of error because it is a nitrogen based base compared to the carbon acids that we are investigating. Furthermore, since the majority of reactions were done in aprotic solvents, explicit molecule shells were not considered.

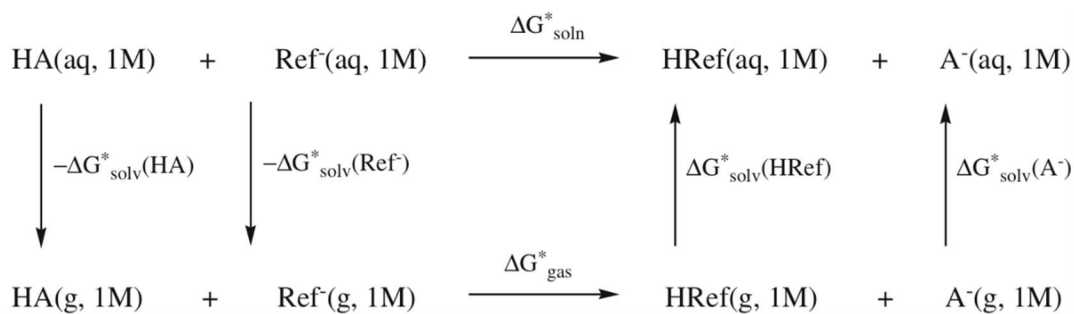


**Figure 3.2** the thermodynamic cycle considered for the relative method of determining  $pK_a$

Given figure 3, the  $pK_a$  could be calculated by the Gibbs free energy equation. To calculate  $pK_a$  the following relations were applied:

$$pK_a = -\log K_a \quad (1)$$

$$\Delta G_s = -RT \ln K_a \quad (2)$$

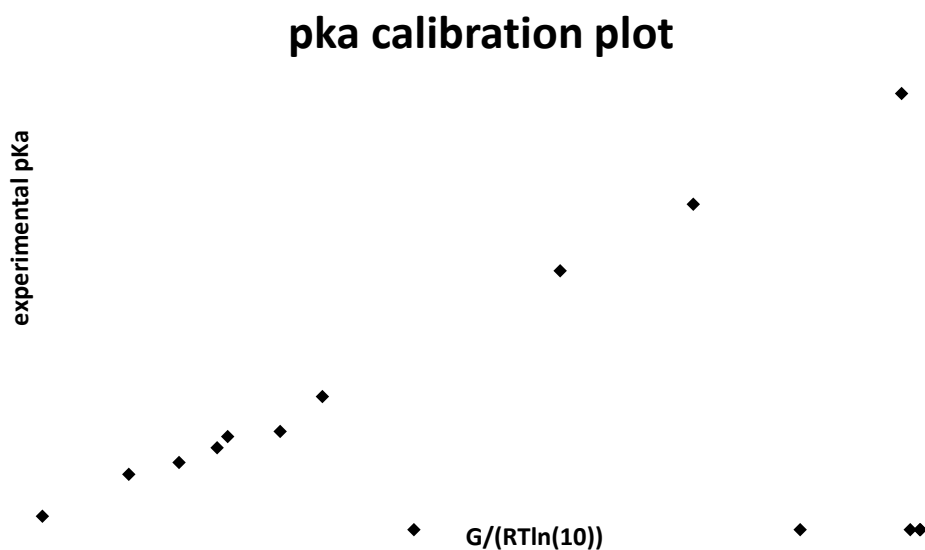
$$pK_a = \frac{\Delta G_s}{RT \ln(10)} \quad (3)$$

Final  $pK_a$  calculations are based on the following modification of equation 3:

$$pK_a = \frac{c_1(G_s(A^-) - G_s(AH))}{RT \ln(10)} + c_2 \quad (4)$$

Where  $c_1$  is the slope of the standardized  $pK_a$  graph (figure 3) and  $c_2$  is the experimental value of the  $pK_a$  of pyridine in DMSO. By plotting several molecules with known  $pK_a$ 's

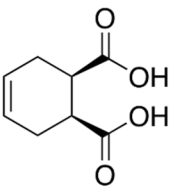
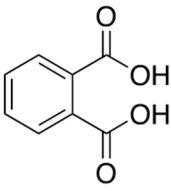
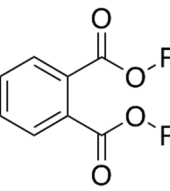
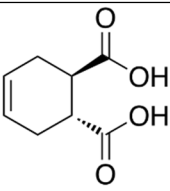
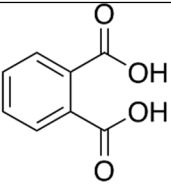
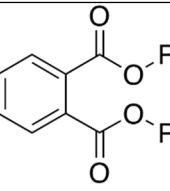
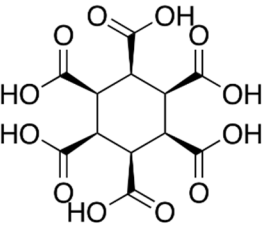
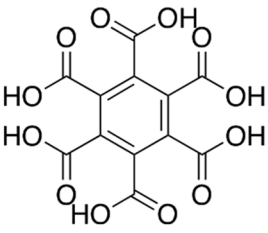
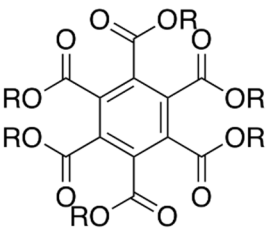
we can get not only the  $c_1$  and  $c_2$  values, but also a relative idea of how accurate our method is. The  $r^2$  value of our data (0.99489) with a wide variety of carbon based acids give a good indication that our method is valid. The plot bellow uses the reference molecules of: 2, 4 pentadione, propane, t-butane, phenol, acetic acid, benzoic acid, cyclohexane, cyclohexanone, propene, 1,4-pentadiene, cyclopentane, hydrochloric acid nitrous acid and p-nitro benzoic acid primarily using the acidities compiled by Bordwell in DMSO.<sup>49</sup>



**Figure 3.3** pKa calibration plot for fitting calculated pKa's using the relative method

## Results and discussion:

The compounds shown below, in figure 2, were all successfully synthesized by the our proposed aromatization method, for the 1,2 carboxylates, structural determination was limited solely to  $^1\text{H-NMR}$ . This set of reactions begins to probe at the overall diversity of the oxidation reaction.

Starting Material	Acid workup	Alcohol Workup
		
		
		

**Figure 3.4** successful oxidative aromatization. The alcohol work-up seems to be fairly diverse, with product with either aliphatic or aromatic esters

The key to our reaction scheme is the source of chlorine. Esterification of the cyclohexane carboxylic acids investigated in this experiment could first be done by producing the acid chloride with thionyl chloride, but with this reagent, no aromatic product was formed. However, when an excess of  $\text{PCl}_5$  is used, some aromatic product is formed. In fact, even when a stoichiometric amount of  $\text{PCl}_5$  is used, some aromatic

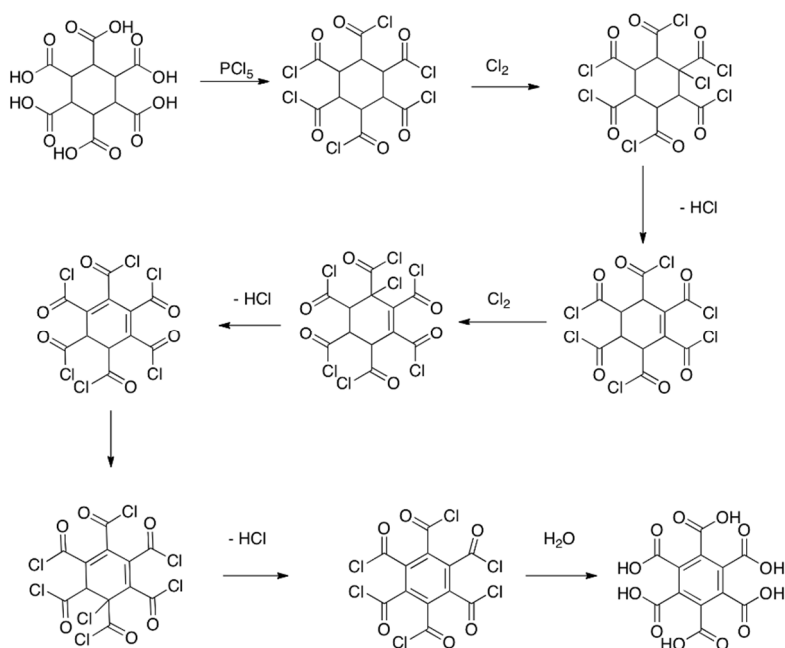


**Figure 3.5** proposed synthetic pathway of formation of mellitic acid. In the case of the hexacyl chloride, the chloride ion is a strong enough base to drive the reaction

product is formed, although yield suffers. It is known that  $\text{PCl}_5$  exists in equilibrium with  $\text{PCl}_3$  and chloride at higher temperatures.<sup>50</sup> This supposition of the source of chlorine being from the  $\text{PCl}_5$  is somewhat consistent with our finding that, in most cases, temperatures in excess of  $120\text{ }^\circ\text{C}$  are required for this reaction to proceed. However,

temperatures in excess of 140 °C seem to cause some unwanted degradations so increasing the temperature beyond this point does not give greater yield.

The dimethyl phthalate that was synthesized with our oxidative aromatization did show some product yielded with temperatures never exceeding 90 °C, but this reaction seems to be the exception and our initial investigations indicate that yields are higher at 120 °C than °C. Even though the cyclohex-4-ene-1,2-dicarboxylic acid did react with  $\text{PCl}_5$  at room temperature, the esterification gave no aromatic results at these conditions. For the hexacarboxylic acid cyclohexane, reaction with  $\text{PCl}_5$  did not take place until 120 °C, so it is difficult to draw conclusions on how lower temperatures affect the reaction, but so far it appears that higher temperatures give more favorable results up to degradation temperatures.

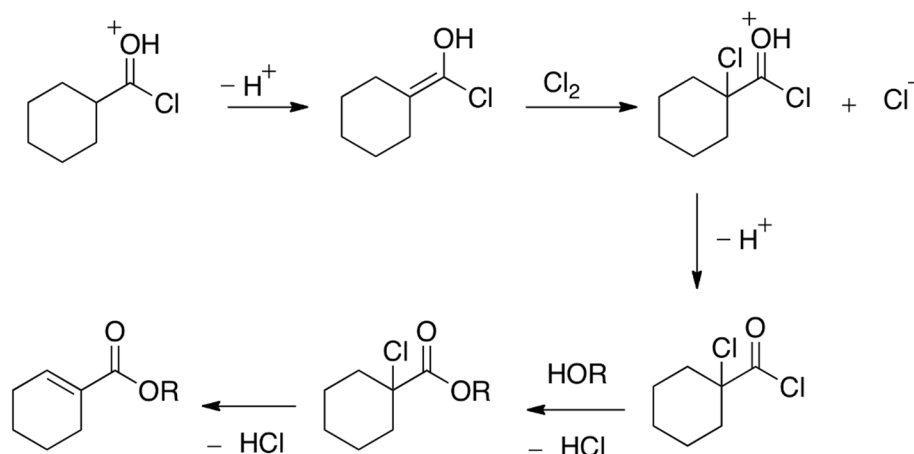


**Figure 3.6** Possible scheme for oxidative aromatization to form hexaesters.

Phosphorus oxychloride chloride ( $\text{POCl}_3$ ) is a side product of the reaction that was intentionally not distilled off before addition of alcohol or water. On addition of water, the phosphoryl chloride reacts and becomes phosphoric acid, which is easily removed. On addition of alcohols, when the ester products are desired, a phosphate ester is produced. This phosphate ester is useful in the work-up since the product is insoluble in the phosphate ester oil, which was yielded on concentration of methylene chloride. This makes filtration a viable and easy purification at the end of the reaction.

Optimizations are currently performed focusing on the 1,2,3,4,5,6 hexacarboxylic acid cyclohexane because this has the most potential utility for use as an amplifier. Aliphatic esters have been shown to be able to be synthesized using the oxidative aromatization as well, however. Reactions concerning carboxylic acids in the 1,3 positions are especially significant since *meta* esters are notoriously difficult to synthesize, investigations into these are currently ongoing.

Mellitic acid can be digested with phosphorus pentachloride at very high temperatures to yield the acyl chloride. On addition of the alcohol or alcohol/catalytic pyridine, however, the ester is not produced. This suggests that the esterification happens before the elimination of the chloride as shown in figure 8.

It is possible that the reaction is not solely undergoing HVZ for chlorination. If the hexaester of the saturated cyclohexane is treated with  $\text{PCl}_5$  and subjected to high temperatures, for an extended period, some aromatic product is formed. It could be that the chlorination can happen radically, since HVZ type halogenation is unlikely with the ester (see  $\text{pK}_a$  study below). These yields are low, however, and require even harsher



conditions (140-180°C and 12 hours). Therefore we believe that this is not the predominate pathway, but rather a competing reaction.

**pKa results and discussion:** The pKa data was collected computationally and is summarized in figure 9. With the computed pKa values being low, it is suggested that the HVZ reaction can happen readily with even fairly mild conjugate bases. Water, is often even suitable for deprotonation. Obviously, the deprotonation barrier of the beta hydrogens are important for rate of elimination and for determining under what conditions the elimination will happen. Less obviously the low pK<sub>a</sub> are important for understanding the initial halogenation. The HVZ halogenation happens to the enolate form of the carboxyl derivatives, and having fairly acidic protons indicate low barriers for the tautomerization. This is why it is generally accepted that the HVZ reaction happens more readily with the acid chloride than with the ester or carboxylic acid.<sup>51</sup> Since our system is particularly acidic, the enol formation must also be investigated and such studies are forthcoming. It is also noteworthy that the more substituted the cyclohexane is, the lower the pK<sub>a</sub>. It is still unclear as to why this is, however it is possible that this is because there is significant axial strain that is being relieved by the deprotonation. This lower pK<sub>a</sub> is in keeping with experimental results of epimerization being rapid in the case of the hexasubstituted cyclohexanes. Unsurprisingly, the more unsaturated the compound is, the lower the pK<sub>a</sub>'s. A consequence of the lower pK<sub>a</sub> is that the reaction towards aromatization

may be accelerating. Therefore, even if the initial halogenation of the HVZ may be disfavored, this reaction may proceed anyway, especially since we expect the aromatic product to be significantly downhill.

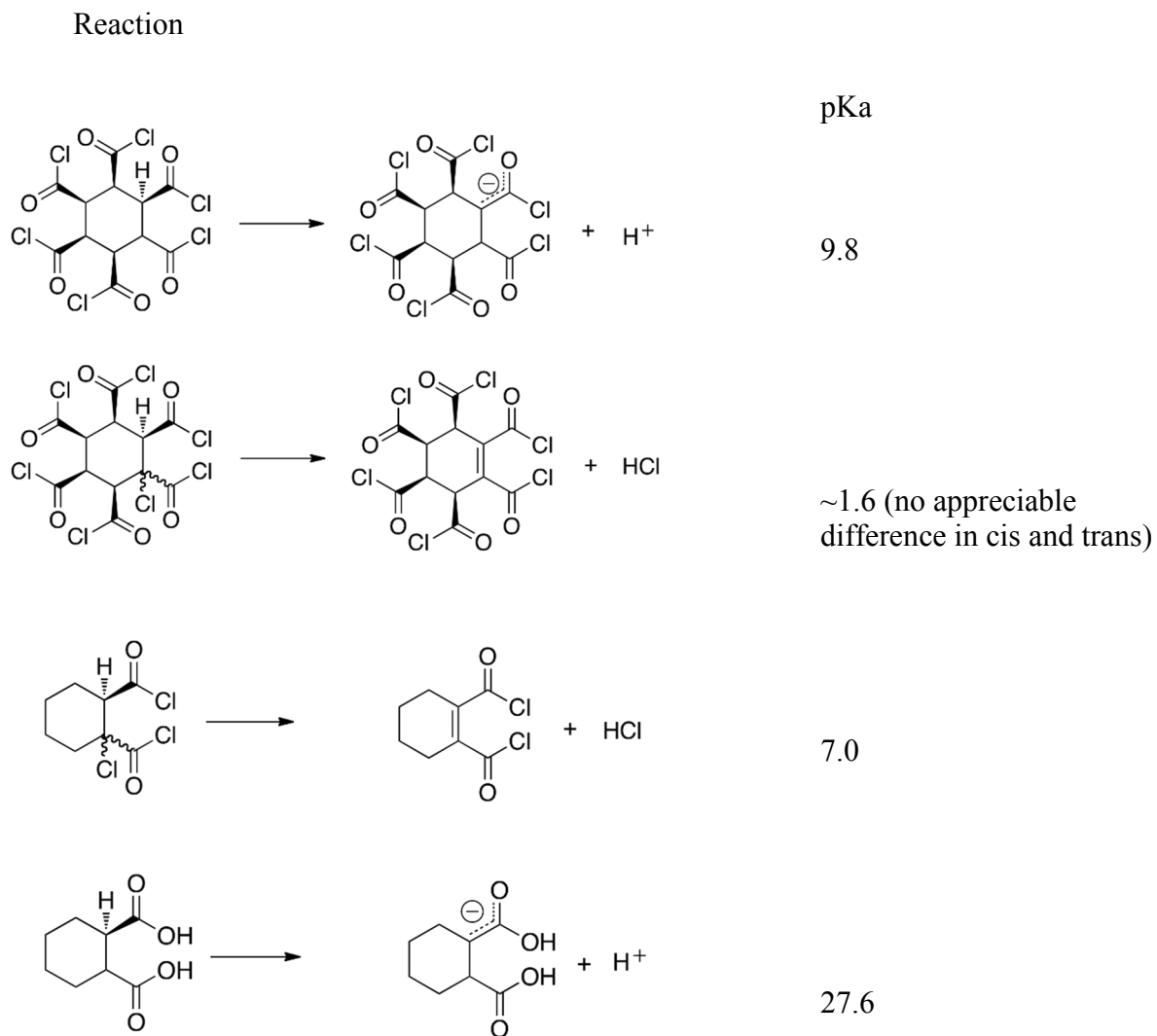


**Figure 3.6:** some of the pK<sub>a</sub> calculated in this study

## Conclusions:

Several ester substituted aromatic compounds were synthesized and characterized by NMR and mass spectroscopy to reasonably show the successful oxidative aromatization. The HVZ mechanism, followed by elimination is consistent with our results and is thus the suggested mechanism, although further computation detail should be considered for a more conclusive reaction scheme and mechanism. Most of these reactions are low yielding, so the synthetic utility is limited to situation where synthesis would otherwise be difficult. The phenolate esters were not able to be prepared from the direct esterification of mellitic acid, showing the HVZ aromatization to be useful for creating highly esterified aromatic derivatives.

1. M. R. Geraskina, M. J. Juetten and A. H. Winter, *The Journal of Organic Chemistry*, 2014, **79**, 5334-5337.
2. K. Andersson, P. A. Malmqvist, B. O. Roos, A. J. Sadlej and K. Wolinski, *J. Phys. Chem.*, 1990, **94**, 5483-5488.
3. M. J. T. Frisch, G. W.; Schlegel, H. B.; Scuseria, G. E.; Robb, M. A.; Cheeseman, J. R.; Scalmani, G.; Barone, V.; Mennucci, B.; Petersson, G. A.; Nakatsuji, H.; Caricato, M.; Li, X.; Hratchian, H. P.; Izmaylov, A. F.; Bloino, J.; Zheng, G.; Sonnenberg, J. L.; Hada, M.; Ehara, M.; Toyota, K.; Fukuda, R.; Hasegawa, J.; Ishida, M.; Nakajima, T.; Honda, Y.; Kitao, O.; Nakai, H.; Vreven, T.; Montgomery, Jr., J. A.; Peralta, J. E.; Ogliaro, F.; Bearpark, M.; Heyd, J. J.; Brothers, E.; Kudin, K. N.; Staroverov, V. N.; Kobayashi, R.; Normand, J.; Raghavachari, K.; Rendell, A.; Burant, J. C.; Iyengar, S. S.; Tomasi, J.; Cossi, M.; Rega, N.; Millam, N. J.; Klene, M.; Knox, J. E.; Cross, J. B.; Bakken, V.; Adamo, C.; Jaramillo, J.; Gomperts, R.; Stratmann, R. E.; Yazyev, O.; Austin, A. J.; Cammi, R.; Pomelli, C.; Ochterski, J. W.; Martin, R. L.; Morokuma, K.; Zakrzewski, V. G.; Voth, G. A.; Salvador, P.; Dannenberg, J. J.; Dapprich, S.; Daniels, A. D.; Farkas, Ö.; Foresman, J. B.; Ortiz, J. V.; Cioslowski, J.; Fox, D. J., *Journal*, 2009.
4. A. D. Becke, *The Journal of Chemical Physics*, 1993, **98**, 5648-5652.
5. A. D. Becke, *Physical Review A*, 1988, **38**, 3098.
6. C. Lee, W. Yang and R. G. Parr, *Physical Review B*, 1988, **37**, 785.
7. C. J. Cramer, F. J. Dulles and D. E. Falvey, *J. Am. Chem. Soc.*, 1994, **116**, 9787-9788.

8. C. J. Cramer, D. G. Truhlar and D. E. Falvey, *J. Am. Chem. Soc.*, 1997, **119**, 12338-12342.
9. C. M. Geise and C. M. Hadad, *J. Org. Chem.*, 2000, **65**, 8348-8356.
10. J. Ho and M. Coote, *Theor Chem Acc*, 2010, **125**, 3-21.
11. F. G. Bordwell, G. E. Drucker and H. E. Fried, *The Journal of Organic Chemistry*, 1981, **46**, 632-635.
12. A. F. A. B. J. B. W. E. M. W. E. W. N. Holleman, *Inorganic chemistry*, Acad. Press [u.a.], San Diego, Calif. [u.a.], 2001.
13. H.-J. Liu and W. Luo, *Synthetic Communications*, 1991, **21**, 2097-2102.

## CHAPTER 4. A RADICAL SPIN ON VIOLOGEN POLYMERS: ORGANIC SPIN CROSSOVER MATERIALS IN WATER

A paper published in *Chemical Communications*

Mark J. Juetten, Alexander T. Buck and Arthur H. Winter

### Abstract

A polymer containing viologen radical cation monomer units is shown to reversibly switch between paramagnetic and diamagnetic states *via* non-covalent host-guest interactions or temperature control in water. Cycling between diamagnetic and paramagnetic forms is accompanied by changes in optical and magnetic properties.

### 3.1 Introduction

Organic materials are prized for their broad range of properties and cheap manufacturing protocols on large scales. Yet while organic polymers have a wealth of physical properties available to them, these material properties typically arise from a static structure. Consequently, there has been long-standing interest in developing new organic materials that adapt their properties in response to environmental cues or other external stimuli.<sup>52</sup>

One way of achieving stimuli-responsive properties in organometallic complexes<sup>34, 53-55</sup> is by invoking a change in the spin state of the metal upon a stimulus. Changes in spin states are often accompanied by large changes in materials properties, including changes in color,<sup>56-58</sup> infrared absorption and emission, luminescence,<sup>59-65</sup> crystallinity,<sup>66, 67</sup> conductivity, and magnetism.<sup>68-72</sup> As a result of such property changes,

spin crossover inorganics that change from low-spin configurations to high-spin configurations upon stimuli such as heating, find use in thermochromic paints<sup>73, 74</sup> and mechanical actuators,<sup>75, 76</sup> and hold promise for use in sensors, displays, and molecular-scale memory storage devices. While such spin-switchable inorganic materials are not uncommon, organic spin-crossover materials are primarily limited to non-polymeric materials,<sup>35, 77-80</sup> Polymers containing paramagnetic building blocks have become

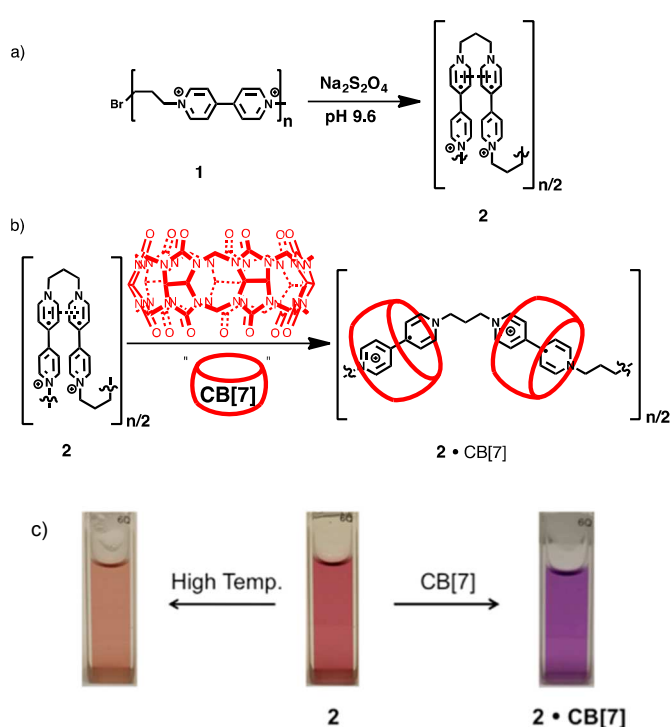


**Figure 4.1** (a) Reduction of 1 to the radical dication 2. (b) Switching between diamagnetic and paramagnetic forms of 2 via binding to a CB[7] host molecule (c) colour changes of 2 in buffered water solution corresponding to a change in temperature or a non-covalent binding event to CB[7].

increasingly sought after for applications such as molecular electronics, spintronics,<sup>81, 82</sup> bulk ferromagnetic polymers,<sup>27, 83</sup> and biological probes for magnetic resonance experiments (e.g. MRI contrast agents<sup>30, 83, 84</sup>). We considered the possibility that organic polymers incorporating spin-switchable building blocks could lead to soft materials with similar changes in properties in response to environmental cues that modulate the molecular spin state of the building blocks.

Prior investigations in our lab have demonstrated that a covalently-linked diradical dyad derived from viologen cation radicals could be reversibly switched between a diamagnetic form and a paramagnetic form via non-covalent stimuli or heating.<sup>20, 33, 85-89</sup> The strategy involved synthesizing two viologen cation radicals tethered with a three carbon linker. This diradical dyad forms a weak pi bond between the two radicals (pimerization), leading to a diamagnetic configuration. Disruption of this weak bond via non-covalent chemistry or heating led to population of a paramagnetic form via disruption of this pi bond.

### 3.2 Discussion

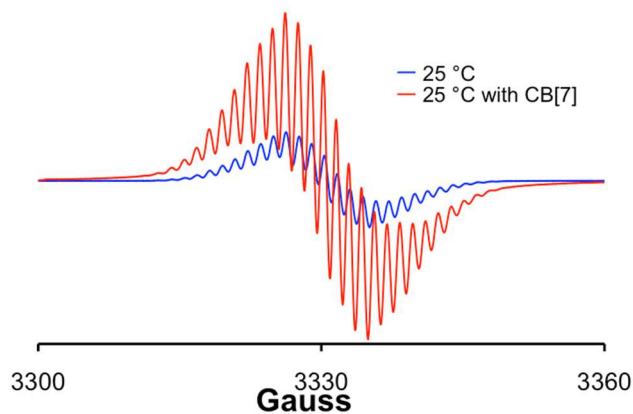


**Figure 4.2** EPR spectrum of 2 (50 mM with respect to the repeat unit) in aqueous buffer solution before binding (blue) and after addition in excess of one equivalent of CB[7] (red).

Here, we report that a polymeric material based on this viologen dication diradical building block can be switched between diamagnetic and paramagnetic forms using non-covalent binding chemistry or by changes in temperature, leading to a bulk organic spin crossover material with stimuli-responsive changes in optical and magnetic properties.

Polymers were prepared via a modified procedure based on a previously reported method.<sup>90</sup> Average molecular weights ( $M_n$ ) were determined by <sup>1</sup>H-NMR endgroup analysis (see Supporting Information) to be around 7,000 daltons, consistent with the

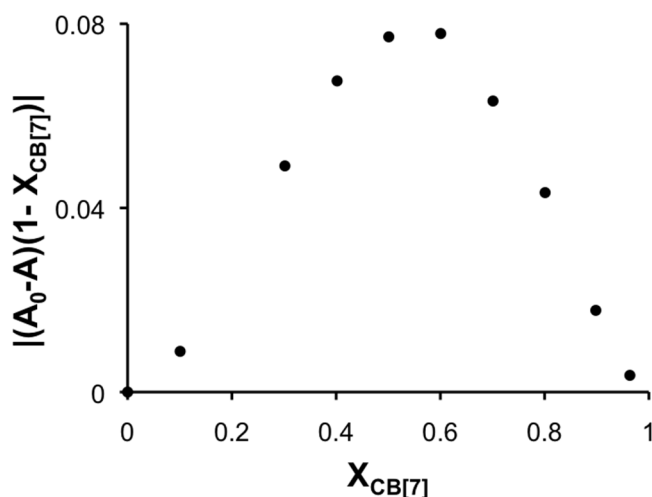
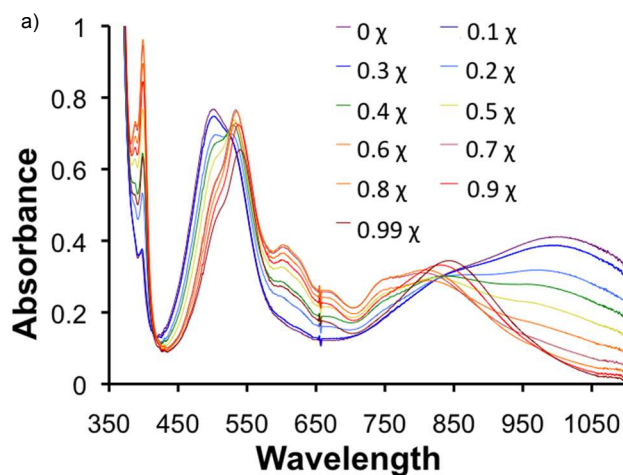


**Figure 4.3** (a) UV-plot of **2** starting at concentration of 100  $\mu\text{M}$  with respect to the repeat unit and adding CB[7] to change molar ratio from 0%-99% viologen:CB[7] (b) UV-Vis Job Plot titration of **2** from the data in (a) monitored at 604 nm.

previously reported ionene complexes. The diamagnetic diradical dimer analogue of the polymer was synthesized by reduction of **1** into **2** using sodium dithionite in buffered water.

The results of the EPR titration studies and UV-Vis switching studies indicate that the poly(propyl viologen cation radical) is a diamagnetic species (with a small thermal population of a paramagnetic form) that can be switched to a paramagnetic form by formation of a complex with CB[7].

Additionally, an increase in temperature from room temperature correlates with an increase in paramagnetism as

seen by EPR measurements. The increase in paramagnetism is fully reversible by decreasing the temperature back to room temperature. Temperature changes can be cycled multiple times with high radical fidelity.



After reduction of 1 to make 2, a weak signal in the EPR spectrum, attributable to the viologen radical cation, is detectable (Fig. 2). We attribute this signal to a thermal population of the dissociated paramagnetic diradical at room temperature and/or spin defects in the material (e.g. monomers radical cations lacking a partner). In order to test whether the paramagnetism could be switched on via non-covalent binding chemistry, in excess of 1 equivalent of CB[7] was added to a 1 mM (by repeat unit concentration) solution of the polymer 2 in buffer solution and the change was monitored by EPR (see

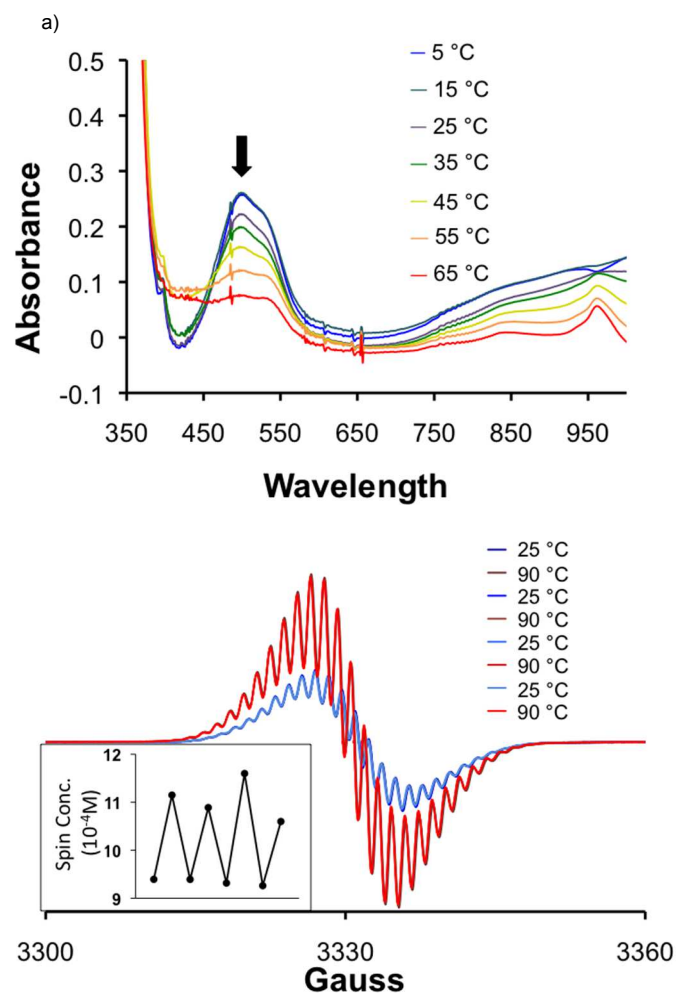


**Figure 4.4** (a) EPR spectra of 1 mM (by viologen repeat units) of 2 in buffer at 25 and 90°C. Inset: four subsequent cycles at 25°C and 90°C are shown (b) UV-Vis plot of 2 at 100  $\mu$ M with respect to the repeat unit with temperature increasing from 5 to 65°C

Fig. 2). We anticipated that CB[7] would thread onto the polymer and bind the cation radical units, leading to a switch-on of EPR signal as the intramolecular dimerization is disrupted (see Fig 1b for a schematic). Indeed, a 3-fold increase of signal (by double integration) was observed after addition of CB[7] (9% spin concentration to 28%), although the lack of complete formation of radical signal by excess CB[7] suggests a low

association constant and/or the presence of spin defects. The addition of more CB[7] was hindered by the limits of its solubility in water.

To determine the binding ratio of CB[7] to the viologens, a Job Plot was obtained (Fig. 3). Since binding to the CB[7] corresponded to a darkening of color, from fuchsia to dark purple (see Fig. 1), UV-Vis was used. A new peak, corresponding to the complex at 604 nm, was monitored as a function of mole fraction of CB[7]. The Job Plot had a maximum at a mole fraction of  $\sim 0.5$ , consistent with a 1:1 CB[7]:viologen repeat unit stoichiometry (see Fig. 3). The binding pocket of CB[7] has been shown to accommodate one viologen unit, and this result was consistent with a single CB[7] binding to each viologen cation radical unit.<sup>33</sup>

While the diamagnetic dimer is favored at room temperature, we anticipated that the diradical form could be favored also by increasing the temperature to demonstrate temperature-dependent spin crossover. To test this idea, variable temperature EPR studies were performed. Accordingly, elevating the temperature from 25°C to 90°C in a buffered water solution leads to a small increase in EPR signal, and this change is highly reversible (Fig. 4). Cycling between high and low temperature reproduced the original spectra with no signs of radical degradation through four iterations. Because no deterioration of signal was detected, these results suggest that 2 is robust to temperature changes, with no apparent radical degradation. This cycling could also be followed by UV-Vis spectroscopy (see appendix C).

The changes in temperature and spin concentration also corresponded to a change in color that could be monitored by UV-Vis spectroscopy between 5 °C and 65 °C.

Temperature was not increased beyond 65°C to avoid the formation of bubbles in the

cuvette, which results in scattering artifacts. Upon heating, we observed a decrease in the absorption band at ~500 nm as well as the broad band between 800-1000 nm. A new band grows in at 958 nm, which we attribute to the paramagnetic diradical. Because of the broad band simultaneously decreasing with the increase of the sharper 958 nm band, a simple straight-line correction was used to monitor the growth of the 958 nm band (see appendix C). The result of the decrease in the visible bands (and a growth of a new band in the near-IR) can be visualized as a change in color from fuchsia to a lighter pink upon heating (see Fig.1).

### 3.3 Conclusions

EPR experiments reveal that the diamagnetic form of a reduced poly(propyl viologen) can be reversibly switched between a diamagnetic form and a paramagnetic form by non-covalent binding or by heating, leading to changes in optical and magnetic properties. Such spin-crossover organic materials may find use in stimuli-responsive bulk materials, where the change in properties of the material arises from a change in the spin configuration of the building blocks.

1. A. Y. Ziganshina, Y. H. Ko, W. S. Jeon and K. Kim, *Chem. Comm.*, 2004, 806-807.
2. E. Evangelio and D. Ruiz-Molina, *C. R. Chim.*, 2008, **11**, 1137-1154.
3. I. Brunlich, A. Suenchez-Ferrer, M. Bauer, R. Schepper, P. Knusel, J. Dshemuchadse, R. Mezzenga and W. Caseri, *Inorg. Chem.*, 2014, **53**, 3546-3557.
4. S. Thies, H. Sell, C. Bornholdt, C. Schütt, F. Köhler, F. Tuzek and R. Herges, *Eur. J. Chem.*, 2012, **18**, 16358-16368.
5. C. Wockerlin, D. Chylarecka, A. Kleibert, K. Mueller, C. Iacovita, F. Nolting, T. A. Jung and N. Ballav, *Nat Commun*, 2010, **1**, 61.

6. D. Benito-Garagorri, L. G. Alves, M. Puchberger, K. Mereiter, L. F. Veiros, M. J. Calhorda, M. D. Carvalho, L. P. Ferreira, M. Godinho and K. Kirchner, *Organometallics*, 2009, **28**, 6902-6914.
7. J. M. G. Laranjeira, H. J. Khoury, W. M. de Azevedo, E. A. de Vasconcelos and E. F. da Silva, Jr., *Mater. Charact.*, 2003, **50**, 127-130.
8. M. Okuhata, Y. Funasako, K. Takahashi and T. Mochida, *Chem. Commun. (Cambridge, U. K.)*, 2013, **49**, 7662-7664.
9. J. T. Culp, D.-L. Chen, J. Liu, D. Chirdon, K. Kauffman, A. Goodman and J. K. Johnson, *Eur. J. Inorg. Chem.*, 2013, **2013**, 511-519.
10. H. Okamura, M. Matsubara, T. Tayagaki, K. Tanaka, Y. Ikemoto, H. Kimura, T. Moriwaki and T. Nanba, *J. Phys. Soc. Jpn.*, 2004, **73**, 1355-1361.
11. C. J. Delbecq and P. H. Yuster, *Phys. Status Solidi B*, 1975, **68**, K21-K23.
12. M. F. Doty, M. Scheibner, I. V. Ponomarev, E. A. Stinaff, A. S. Bracker, V. L. Korenev, T. L. Reinecke and D. Gammon, *Phys. Rev. Lett.*, 2006, **97**, 197201-197204.
13. I. y. A. Gural'skiy, C. M. Quintero, K. Abdul-Kader, M. Lopes, C. Bartual-Murgui, L. Salmon, P. Zhao, G. Molnar, D. Astruc and A. Bousseksoua, *J. Nanophotonics*, 2012, **6**, 063517, 063514 pp.
14. J. Qi, M. Tanaka, J. Sun Ahn and Y. Masumoto, *J. Lumin.*, 2000, **87-89**, 1102-1104.
15. G.-P. Yong, C.-F. Li, Y.-Z. Li and S.-W. Luo, *Chem. Comm.*, 2010, **46**, 3194-3196.
16. D. Boinnard, A. Bousseksou, A. Dworkin, J. M. Savariault, F. Varret and J. P. Tuchagues, *Inorg. Chem.*, 1994, **33**, 271-281.
17. A. D. Naik, K. Robeyns, C. F. Meunier, A. F. Leonard, A. Rotaru, B. Tinant, Y. Filinchuk, B. L. Su and Y. Garcia, *Inorg. Chem.*, 2014, **53**, 1263-1265.
18. S. Bouguessa, K. Herve, S. Golhen, L. Ouahab and J. M. Fabre, *New J. Chem.*, 2003, **27**, 560-564.
19. P. L. Feng, C. J. Stephenson, A. Amjad, G. Ogawa, E. del Barco and D. N. Hendrickson, *Inorg. Chem.*, 2010, **49**, 1304-1306.
20. H. C. Herper, M. Bernien, S. Bhandary, C. F. Hermanns, A. Krueger, J. Miguel, C. Weis, C. Schmitz-Antoniak, B. Krumme, D. Bovenschen, C. Tieg, B. Sanyal, E. Weschke, C. Czekelius, W. Kuch, H. Wende and O. Eriksson, *Phys. Rev. B: Condens. Matter Mater. Phys.*, 2013, **87**, 174425/174421-174425/174415.
21. A. Strozecka, M. Soriano, J. I. Pascual and J. J. Palacios, *Phys. Rev. Lett.*, 2012, **109**, 147202/147201-147202/147205.
22. K.-R. Jeon, B.-C. Min, A. Spiesser, H. Saito, S.-C. Shin, S. Yuasa and R. Jansen, *Nat. Mater.*, 2014, Ahead of Print.
23. A. Seeboth, D. Lotzsch, R. Ruhmann and O. Muehling, *Chem. Rev.*, 2014, **114**, 3037-3068.
24. A. Seeboth, R. Ruhmann and O. Muehling, *Materials*, 2010, **3**, 5143-5168.
25. V. J. Chebny, R. Shukla, S. V. Lindeman and R. Rathore, *Org. Lett.*, 2009, **11**, 1939-1942.
26. A. P. Davis, *Nature*, 1999, **401**, 120-121.

27. A. Alberola, J. Burley, R. J. Collis, R. J. Less and J. M. Rawson, *J. Organomet. Chem.*, 2007, **692**, 2750-2760.
28. W. Fujita, Awaga and Kunio, *Science*, 1999, **286**, 261-262.
29. R. G. Hicks, *Nat Chem*, 2011, **3**, 189-191.
30. J. Hong, E. Bekyarova, W. A. de Heer, R. C. Haddon and S. Khizroev, *ACS Nano*, 2013, **7**, 10011-10022.
31. S. M. Winter, A. Mailman, R. T. Oakley, K. Thirunavukkuarasu, S. Hill, D. E. Graf, S. W. Tozer, J. S. Tse, M. Mito and H. Yamaguchi, *Physical Review B*, 2014, **89**, 214403.
32. C. Herrmann, G. C. Solomon and M. A. Ratner, *J. Am. Chem. Soc.*, 2010, **132**, 3682-3684.
33. B. O. Jahn, H. Ottosson, M. Galperin and J. Fransson, *ACS Nano*, 2013, **7**, 1064-1071.
34. A. Rajca, *Chem. Rev.*, 1994, **94**, 871-893.
35. G. Spagnol, K. Shiraishi, S. Rajca and A. Rajca, *Chem. Comm.*, 2005, 5047-5049.
36. R. M. Davis, A. L. Sowers, W. DeGraff, M. Bernardo, A. Thetford, M. C. Krishna and J. B. Mitchell, *Free Radical Biol. Med.*, 2011, **51**, 780-790.
37. A. Rajca, Y. Wang, M. Boska, J. T. Paletta, A. Olankitwanit, M. A. Swanson, D. G. Mitchell, S. S. Eaton, G. R. Eaton and S. Rajca, *J. Am. Chem. Soc.*, 2012, **134**, 15724-15727.
38. A. T. Buck, J. T. Paletta, S. A. Khindurangala, C. L. Beck and A. H. Winter, *J. Am. Chem. Soc.*, 2013, **135**, 10594-10597.
39. M. R. Geraskina, A. T. Buck and A. H. Winter, *J. Org. Chem.*, 2014, **79**, 7723-7727.
40. A. G. Evans, J. C. Evans and M. W. Baker, *J. Am. Chem. Soc.*, 1977, **99**, 5882-5884.
41. M. Furue and S.-i. Nozakura, *Chem. Lett.*, 1980, **9**, 821-824.
42. W. Geuder, S. Hunig and A. Suchy, *Tetrahedron*, 1986, **42**, 1665-1677.
43. L. Michaelis and E. S. Hill, *J. Gen. Physiol.*, 1933, **16**, 859-873.
44. P. M. S. Monk, N. M. Hodgkinson and S. A. Ramzan, *Dyes Pigment.*, 1999, **43**, 207-217.
45. M. Shimomura, K. Utsugi, J. Horikoshi, K. Okuyama, O. Hatozaki and N. Oyama, *Langmuir*, 1991, **7**, 760-765.

## CHAPTER 5: SUPERMOLECULAR VIOLOGNE BASED LOGIC GATE SYSTEMS

### **Introduction:**

Molecular machinations are of growing interest to the scientific community because of the diverse applications possible of powerful nanomachines.<sup>91-95</sup> Nanomachines of the biological world, such as ATP and myosin, show the ability of these molecules to do incredible work.<sup>96,97</sup> These biological machines are incredibly complex and that complexity makes synthetic design from the bottom up difficult.<sup>96</sup> This makes the need for simple molecular machines, able to take simple inputs and deliver simple outputs, imperative.<sup>96</sup>

One of the possible simple molecular machines revolves around molecular-logic based computing, where molecules are capable of storing different logic levels.<sup>98</sup> While a young field, there has been a vast array of systems already reported in single molecules or supramolecular structures.<sup>98,99</sup> While logic systems of binary nature are common (with only 1 and 0 states available), having different outputs on stimulus of multiple inputs, increases the possibility for molecular computing exponentially.<sup>99</sup> Color shifts that are detectible by UV-Vis chromatography upon different combinations of different inputs offers simple visualization of this Boolean based molecular computing.<sup>98</sup>

Bipyridinium or viologen salts we found as the ideal candidates to be used for this switching behavior due to their ease of reduction.<sup>88, 100-109</sup> Moreover, reduction of viologen salts to form radical cations is a reversible process<sup>110-112</sup> that opens new horizons for even more potential applications and uses such as creating Boolean logic

operations and so on. Previously, it has been reported that the viologen radical cation can undergo self-association due to the  $\pi$ -interaction between two monomeric units<sup>85, 113-115</sup> and exists in equilibrium with its dimer in solution.<sup>116</sup> Despite numerous reports on viologen pi-pi dimerization<sup>105, 117-126</sup> there is little systematic data on the influence of functional substitution on the strength of pi-pi interaction. The output-input that we chose to study revolved around a simple event: dimerization of a molecule. The singly reduced viologen (a 4,4-bipyridine containing two quaternary amines, reduced to a cation radical) molecule was chosen as the molecule of interest because the dimerization of this molecule results in a change in electron configuration. This change in electron configuration is from a paramagnetic triplet that is EPR active to an EPR silent diamagnetic singlet. This switching in electron state is accompanied by changes in several properties, including a color change. In previous studies our group has examined cationic radical viologen that are tethered together by three-carbon  $sp^3$  chains. We have shown these molecules to switch electron states via either a binding event or thermal change. We have also expanded the simple studies of a two viologen system to one of a polymeric nature with many viologen units linked together in a single molecule. However, thus far our studies have not extended beyond the same basic architecture of propyl linked viologens. We believe there is utility in investigating the binding nature of differently substituted viologens with the end goal of modulating the strength of binding in aqueous media, so that different input-outputs may be investigated.

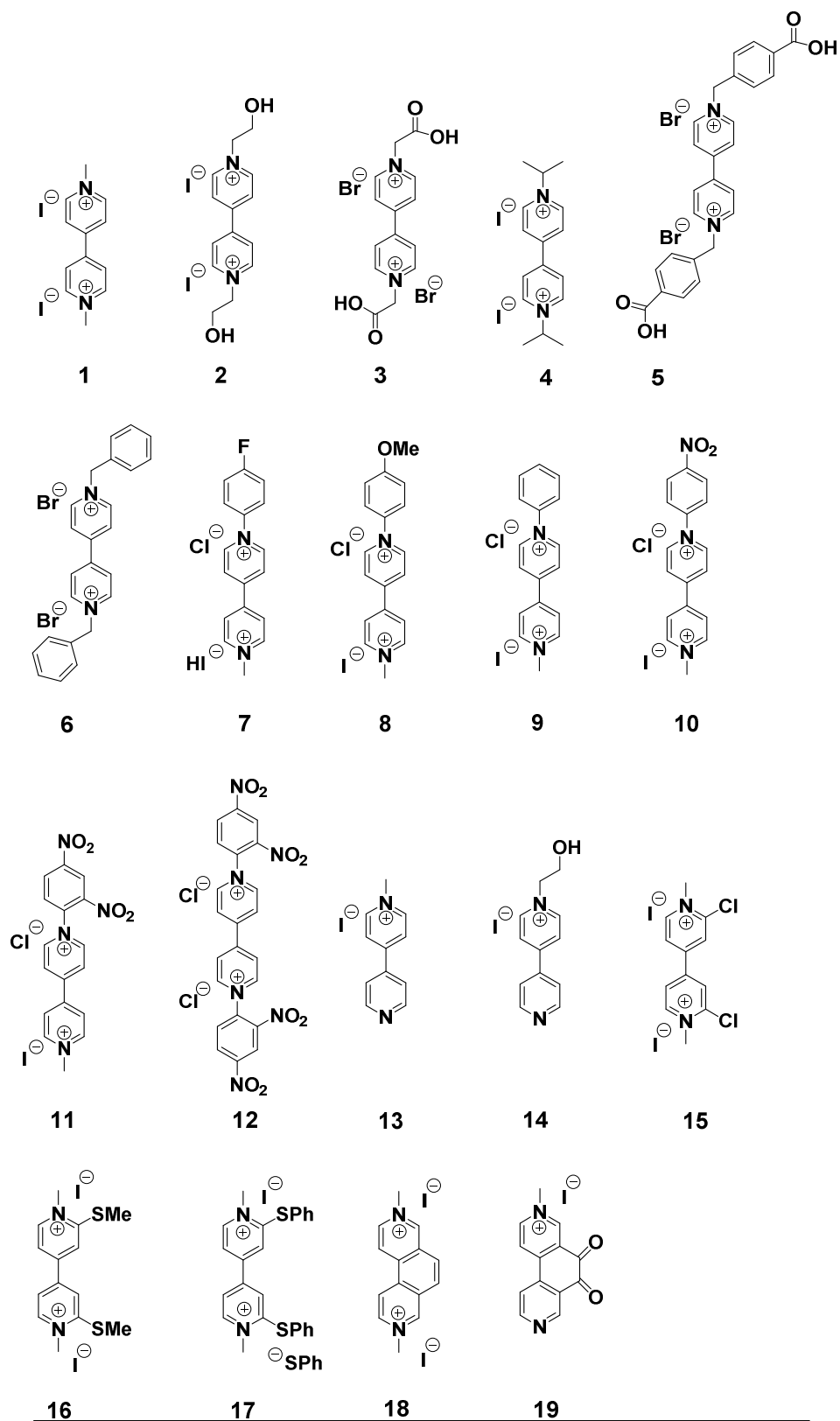


**Figure 5.1** Structures of viologen derivatives (compounds 1-19)



## Results and discussion

We investigated several classes of 4,4 bipyridine radicals: simple alkane substitutions, groups capable of hydrogen bonding, benyl based groups, extended conjugation groups (such as phenyl rings), altering the substitution of the bipyridine rings (referred to herein as “core substituted”), and finally singly substituted 4,4 bipyridine and the protonated version of the singly substituted 4,4 bipyridine. The electron state could be

<b>Table 5.1</b> The apparent association constants by UV-Vis spectroscopy and EPR spectroscopy in aqueous solution at room temperature.				
	<b>UV-Vis</b>		<b>EPR</b>	
<b>Compound</b>	<b>K<sub>a</sub> pH 7, M<sup>-1</sup></b>	<b>K<sub>a</sub> pH 9.6, M<sup>-1</sup></b>	<b>K<sub>a</sub> pH 7, M<sup>-1</sup></b>	<b>K<sub>a</sub> pH 9.6, M<sup>-1</sup></b>
<b>1</b>	1.3 * 10 <sup>3</sup>	4.9 * 10 <sup>2</sup>	1.2 * 10 <sup>3</sup>	4.8 * 10 <sup>2</sup>
<b>2</b>	2.3 * 10 <sup>3</sup>	1.3 * 10 <sup>3</sup>	7.4 * 10 <sup>2</sup>	1.2 * 10 <sup>3</sup>
<b>3</b>	5.0 * 10 <sup>3</sup>	1.1 * 10 <sup>3</sup>	2.3 * 10 <sup>2</sup>	4.2 * 10 <sup>2</sup>
<b>4</b>	2.8 * 10 <sup>3</sup>	1.1 * 10 <sup>3</sup>	1.4 * 10 <sup>3</sup>	7.4 * 10 <sup>2</sup>
<b>5</b>	6.0 * 10 <sup>4</sup>	1.8 * 10 <sup>4</sup>	3.1 * 10 <sup>3</sup>	1.9 * 10 <sup>3</sup>
<b>6*</b>	1.7 * 10 <sup>4</sup>	N/A	N/A	N/A
<b>7*</b>	1.2 * 10 <sup>3</sup>	N/A	N/A	N/A
<b>8*</b>	2.2 * 10 <sup>3</sup>	N/A	N/A	N/A
<b>9*</b>	3.4 * 10 <sup>3</sup>	N/A	N/A	N/A
<b>10*</b>	5.3 * 10 <sup>3</sup>	N/A	N/A	N/A
<b>11*</b>	3.6 * 10 <sup>2</sup>	N/A	N/A	N/A
<b>12*</b>	9.0 * 10 <sup>2</sup>	N/A	N/A	N/A
<b>13</b>	3.9 * 10 <sup>1</sup>	4.2 * 10 <sup>1</sup>	N/A	N/A
<b>14</b>	2.9 * 10 <sup>1</sup>	1.0 * 10 <sup>2</sup>	N/A	N/A
<b>15</b>	9.1 * 10 <sup>3</sup>	1.5 * 10 <sup>4</sup>	1.1 * 10 <sup>4</sup>	N/A
<b>16</b>	1.8 * 10 <sup>4</sup>	5.8 * 10 <sup>3</sup>	2.0 * 10 <sup>3</sup>	N/A
<b>17</b>	3.7 * 10 <sup>3</sup>	N/A	2.3 * 10 <sup>3</sup>	N/A
<b>18</b>	1.5 * 10 <sup>2</sup>	3.2 * 10 <sup>3</sup>	N/A	N/A
<b>19*</b>	N/A	N/A	N/A	N/A

followed by EPR spectroscopy whereas the color changes would be monitored by UV-vis spectroscopy.

Our first analysis of these viologens revolved around observing the differing strengths of binding. To accomplish this task the reduced viologen was observed in varying concentrations by UV-vis and EPR and the change in signal was fitted to a first order binding curve using the ORIGIN software. The results of the binding can be seen summarized in table 5.1.

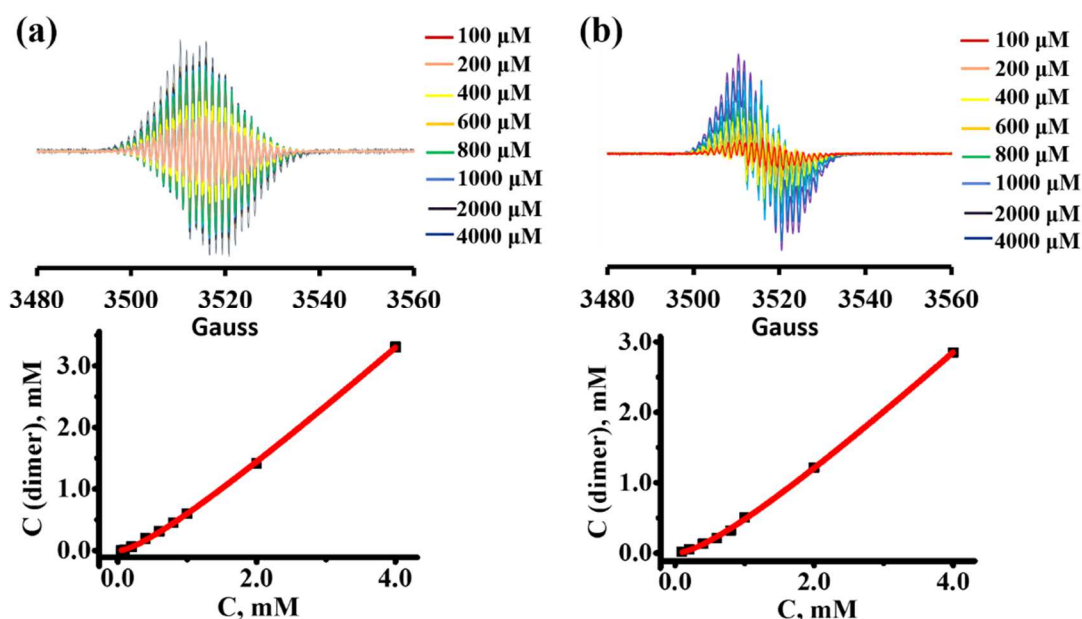


**Figure 5.2** Example of EPR spectra in pH 7 buffer solution for selected compounds (top) and their nonlinear fitting curve the dimer concentration vs total concentration of viologen derivative (bottom): (a) Di-methyl viologen (100 - 4000 μM). (b) Di-ethyl alcohol viologen (100 - 4000 μM).

We found that the alkylated viologens have binding constants on the order of  $K_a=10^3 \text{ mol}^{-1}$  at neutral pH. These binding constants were relatively unchanged (at least to the same order of magnitude) by changing the size of the alkyl group. This change seems to indicate that the steric effects of the substitutions is relatively negligible. Further

modulation, by adding hydrogen bonding able groups, also did not offer much change in apparent binding constants. The highest binding constants were observed to be the viologens with benzyl substituents. This result can be attributed to a hydrophobic effect, and that aggregation results in higher binding constants. While increasing the conjugation did not result in drastically different binding constants, they did become significantly less stable. The stability was too low (i.e. the rate of degradation was too fast) for the binding constants to be obtained via EPR, due to the timing of tuning the instrument would lead to decomposition of our radical. We presume that the conjugation allows for easier reduction to a doubly reduced state, no longer cationic and no longer paramagnetic. The diamagnetic species that is formed over time is insoluble in the aqueous solution that the experiment is performed in, providing evidence of the loss of charge. The core substituted viologens show similar stability issues at higher pH but are stable at pH 7 allowing for binding constants to be obtained via EPR in addition to UV-vis.

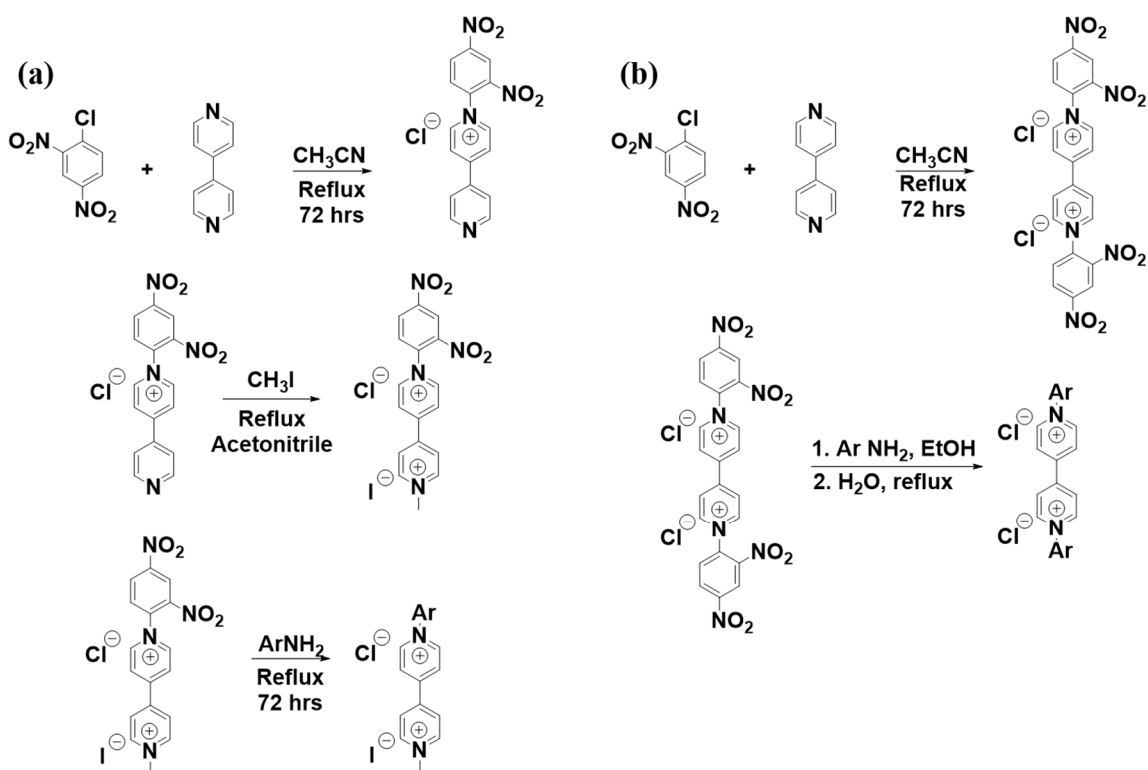


**Figure 5.4** (a) Preparation of hetero-substituted viologen derivatives. (b) Preparation of di-aryl-substituted viologen derivatives.

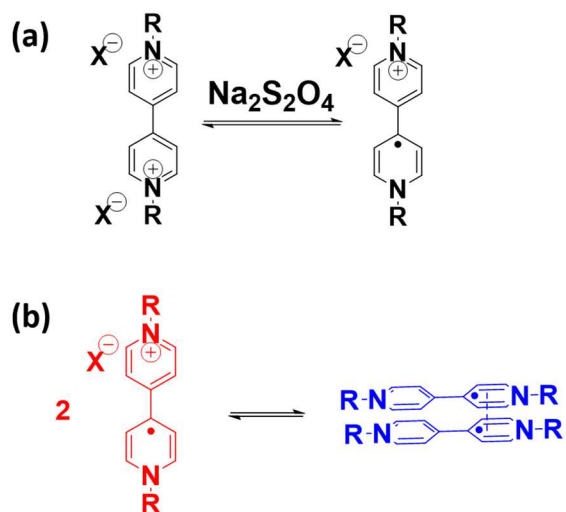


**Figure 5.5** (a) Reduction of dication precursor to radical cation using sodium dithionite. (b) Formation of dimer in aqueous buffer solution.

## UV-Vis

UV-Vis studies were conducted in buffer solutions (pH = 9.6 and pH = 7), as literature precedence include both conditions for viologen radical studies. Our previous studies of viologen radical exploited pH 9.6 conditions.<sup>20, 33, 127</sup> Also, some other publications used pH 7 buffer solutions, in particular studies that discussed hetero-substituted viologen radicals.<sup>117, 118</sup> We have found that hetero-substituted viologen radicals as well as diaryl viologen radicals are more stable in pH=7 buffer while dialkyl viologen derivatives did not show any major differences in stability upon change in pH conditions. Also, it should be mentioned that diaryl substituted viologens have poor solubility upon reduction even at low concentrations in pH 7 buffer solution. Furthermore, these compounds seem to be more sensitive to the amount of sodium dithionite reducing agent. The only diaryl viologen compound that had sufficient solubility for studies was 1,1'-di-2,4-dinitrophenyl-4,4'-bipyridinium dichloride (compound 12, Figure 1). All other diaryl substituted viologens (e.g. 1,1'-di-4-bromophenyl-4,4'-bipyridinium dichloride, 1,1'-di-4-methoxyphenyl-4,4'-bipyridinium dichloride etc) that we synthesized (not included in Figure 1) formed aggregates upon reduction and could not be studied because of the precipitation process at even low concentrations. Due to their poor solubility in aqueous solution upon reduction we did not pursue making more diaryl substituted derivatives.

Overall we are able to modulate the binding constants of different viologens on the order of magnitude between  $10^2 - 10^4 \text{ M}^{-1}$ . Most notably, the mono-substituted 4,4' bipyridines **13**, **14**, and **19** show very low binding constants at pH 9.6, but in more acidic conditions, apparent binding constants, obtained by EPR, are too high to be measured accurately. The UV-vis spectra do not show the same binding peak around 900 nm that is

associated with the dimerization of the viologens, but it is not unreasonable for the peak associated with the dimerization to be shifted to a different wavelength.

### Computational discussion

To further investigate intermolecular interactions of the reduced viologen computational studies were performed using broken-symmetry density functional theory and an universal solvation model (SMD UM06-2X/6-31++G(d,p)) (see SI for details). After optimizing the structure of the triplet and singlet diradical dication we evaluated the energies of the two and found the singlet form to be favored over the triplet (Figure 7).

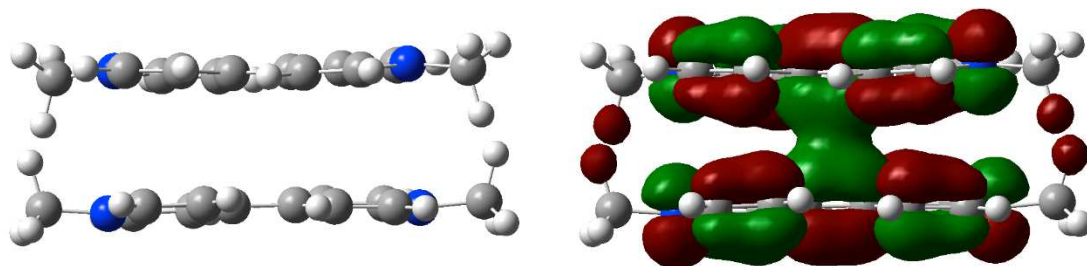


**Figure 5.6** Visualization of the singlet diradical dication HOMO using UM06-2X/631++G(d,p) (isovalue=0.02)

### Logic gates

Linear viologen containing chains have thus far been investigated as simple two system linkers as well as in polymeric chains in previous chapters. As of yet, however, very little work has been done on discrete number of linear viologen units greater than two (bisviologens). Bisviologens have been studied with different length carbon linkers and it has been found that carbon chains with odd number of units are shown to show

intramolecular complexation whereas even number of carbons do not. By alternating carbon chain lengths of  $n=3$  and  $n=4$ , therefore, viologen units can then be “paired together” (see figure 5.7). We modified the literature procedure and synthesized **20**, a straight chain viologens with alternating 3 and 4 carbons linking the viologens.<sup>128</sup> Upon reduction, these viologen units displayed radical signal that was proportional to the number of viologens that were unable to “pair up” (see figure 5.7). In other words, if the viologen was linked to another viologen with 3 carbons linkers, it would be EPR silent, whereas viologen that were linked to neighboring viologens by 4 carbons stayed paramagnetic and thus could be detected by EPR.

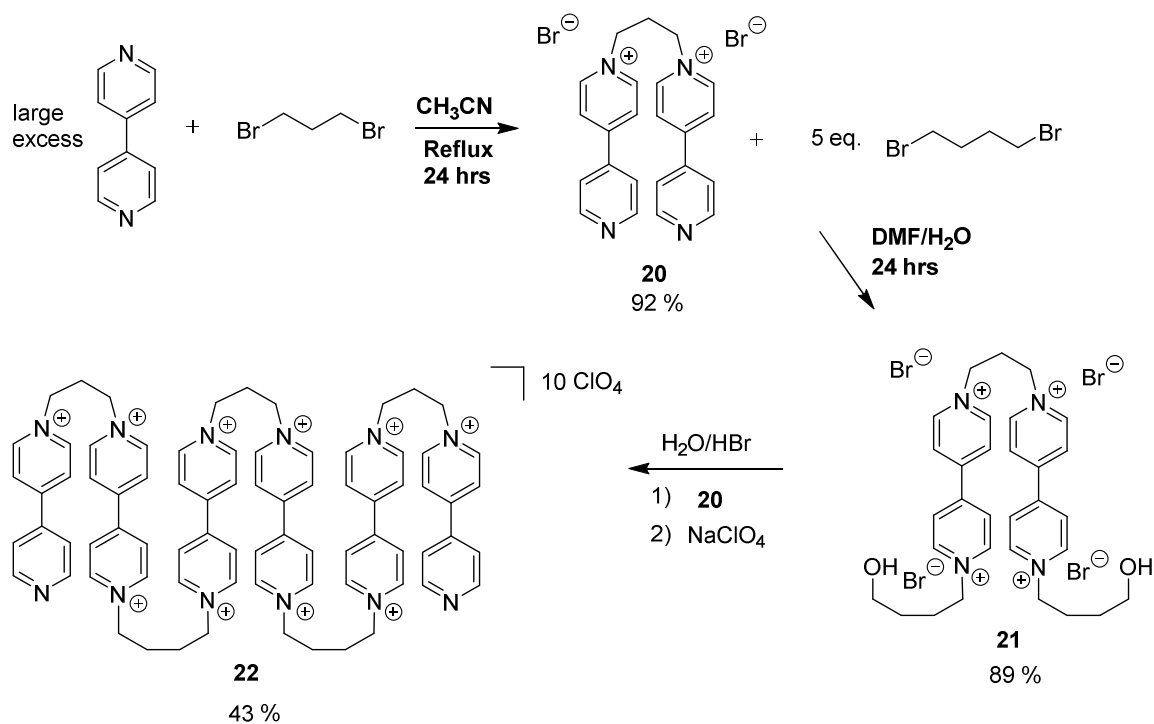


**Figure 5.7** Scheme for synthesis of alternating linker viologen

Having discrete units of viologens allowed for modulation at the end of the chain with the goal of creating tuneable logic gates. Most notably, if the chain is terminated with a singly substituted 4,4'-bipyridine, the properties of the chain would become sensitive to the presence of neutral water or sensitive to changing pH in the case of

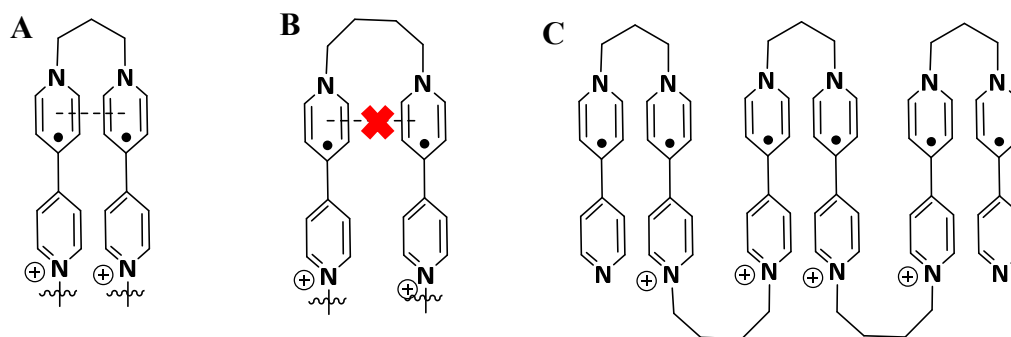


**Figure 5.8** (a) depiction of two reduced viologens linked by 3 carbons that binds tightly and is EPR inactive (b) depiction of two reduced viologens linked by 4 carbons that does not bind tightly and is EPR active (c) the reduced form of **20**, whose EPR behavior and color depends on protonation state and other various inputs.

aqueous solutions. The sensitivity of these 4,4'-bipyridines allows the simple case of a 3-carbon linked 4,4'-bipyridine to be used as a water sensor. In a solution of DMSO, an inverse linear correlation is shown between the radical concentration and the concentration of water, thus acting as an effective “turn off” water sensor. This change in radical concentration is also accompanied by a change in color, going from a blue to red color.

In instances with chains longer than 2 units, leaving the end 4,4'-bipyridine as unsubstituted allows for simple logic gates to be created. In the case of **22**, protonation of the terminal 4,4'-bipyridine switches the molecule from EPR active to EPR silent. A



second input, such as a binding or thermal event, can then be used to create the second “yes no” operation required for simple Boolean logic. These inputs have been previously studied in our group for efficacy in the case of the polymeric viologen chains.

For the case of the protonated singly reduced singly substituted 4,4'-bipyridine the intramolecular binding is too strong to be broken by the intermolecular binding to CB[7]. This binding is clearly demonstrated in the most simple case of the two unit molecule where the radical signal did not increase upon addition of CB[7] unlike in the case of the methyl substituted analogue or in the instance of the polymer. A consequence of

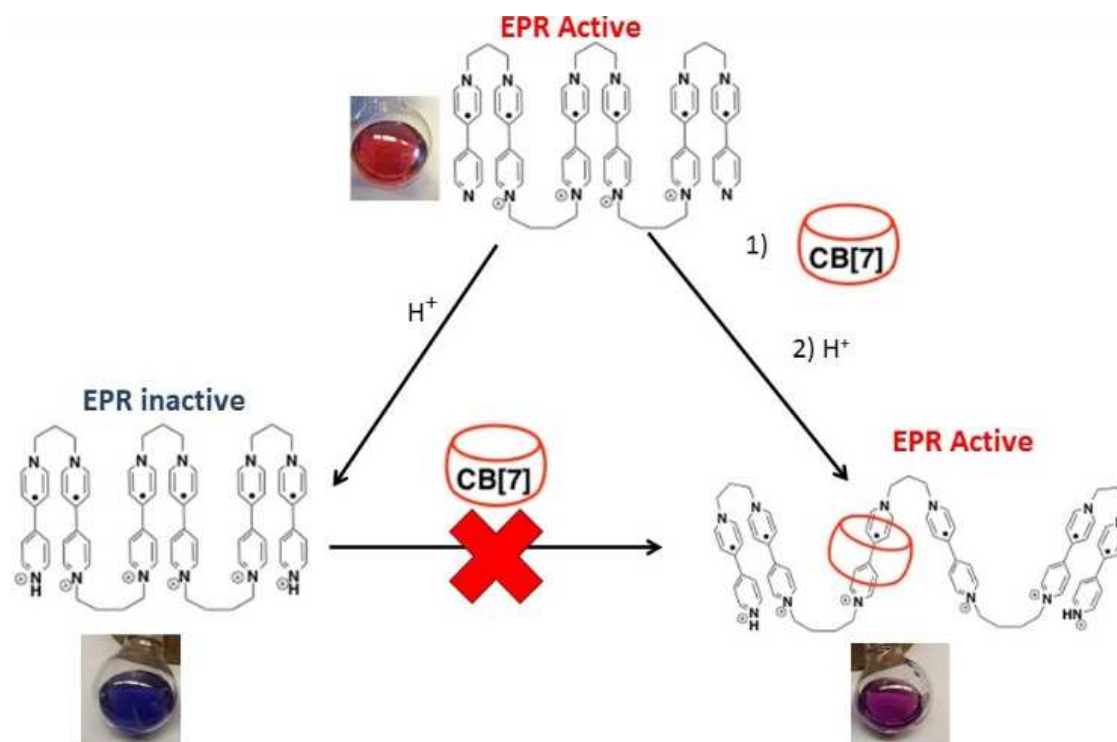


**Figure 5.9** A simple molecular logic gate of the reduced **20**. Different colors can be accessed via addition of different inputs.

decreased radical signal is that the order of addition of the CB[7] is a key component to whether or not **20** shows radical signal; if the CB[7] is added before addition of water, the molecule shows an EPR signal, where if CB[7] is added after water has been introduced,

the molecule remains EPR silent. The implication of the silent nature of the radical is that the CB[7] is not large enough to thread over the “bound together” terminal pairing of bipyridines. The cavity size of CB[7] consistent with previously reported literature, that CB[7] can only include a single viologen molecule. Presumably, then, in the instance of addition of CB[7] before the addition of water, the CB[7] binds to the internal viologens and addition of water “caps” the end creating a rotaxane like supramolecular structure.

In the absence of CB[7], in aqueous solution, **20** can be turned from EPR inactive to EPR active by thermal input. While the diamagnetic dimer is favored at room temperature, we anticipated that the diradical form could be favored also by increasing the temperature to demonstrate temperature-dependent spin crossover. This thermal response is independent of the order of addition of addition of water.

## Conclusions

In conclusion, we investigated the binding affinity of several reduced 4,4'-bipyridine architectures with the purpose of modulating straight chain bipyridine containing monodisperse polymers for use in simple molecular logic gates. We found that the single substituted 4, 4'-bipyridine provided a convenient water sensitive switch. This could be paired with already investigated inputs related to thermal response and supramolecular complexation. The different combinations offer several different types of logic gates. In the case of the supramolecular complexation, the logic gate is order of addition dependent, and in the case of addition of CB[7] prior to addition of water, the resultant structure is a presumed rotaxane. Further investigations are being considered

into different lengths of chains and different combinations of 3 and 4 carbon linkers in order to unlock access to different types of molecular logic gates.

1. V. Balzani, A. Credi, S. Silvi and M. Venturi, *Chem. Soc. Rev.*, 2006, **35**, 1135.
2. V. Balzani, A. Credi and M. Venturi, *Mol. Dev. Mach.*, Wiley-Blackwell, 2008.
3. M. R. Panman, P. Bodis, D. J. Shaw, B. H. Bakker, A. C. Newton, E. R. Kay, A. M. Brouwer, W. J. Buma, D. A. Leigh and S. Woutersen, *Science*, 2010, **328**, 1255-1258.
4. E. R. Kay, D. A. Leigh and F. Zerbetto, *ChemInf.*, 2007, **38**.
5. E. Meyhofer, *Adv. Mater.*, 2004, **16**, 1568-1569.
6. S. Silvi, M. Venturi and A. Credi, *Chem. Comm.*, 2011, **47**, 2483-2489.
7. W. Parak, *ChemPhysChem*, 2005, **6**, 1422-1422.
8. S. J. Bradberry, J. P. Byrne, C. P. McCoy and T. Gunnlaugsson, *Chem. Comm.*, 2015, **51**, 16565-16568.
9. J. Ling, B. Daly, V. A. D. Silversen and A. P. de Silva, *Chem. Comm.*, 2015.
10. R. J. Mortimer and T. S. Varley, *Sol. Energ. Mat. Sol. Cells*, 2013, **109**, 275-279.
11. J. I. Millán, M. Sánchez-Maestre, L. Camacho, J. J. Ruiz and R. Rodríguez-Amaro, *Langmuir*, 1997, **13**, 3860-3865.
12. R. J. Jasinski, *J. Electrochem. Soc.*, 1977, **124**, 637-641.
13. S. G. Mayhew, *Eur. J. Biochem.*, 1978, **85**, 535-547.
14. H. S. Kim, B. Claude and C. Tondre, *The J. Phys. Chem.*, 1990, **94**, 7711-7716.
15. C. L. Bird and A. T. Kuhn, *Chem. Soc Rev.*, 1981, **10**, 49-82.
16. J. G. Gaudiello, P. K. Ghosh and A. J. Bard, *J. Am. Chem. Soc.*, 1985, **107**, 3027-3032.
17. Y. M. Tsou, H. Y. Liu and A. J. Bard, *J. Electrochem. Soc.*, 1988, **135**, 1669-1675.
18. M. Z. Hoffman, *J. Phys Chem.*, 1988, **92**, 3458-3464.
19. D. Meisel, W. A. Mulac and M. S. Matheson, *J. Phys. Chem.*, 1981, **85**, 179-187.
20. L. Michaelis and E. S. Hill, *J. Gen. Phys.*, 1933, **16**, 859-873.
21. K. Maruszewski, A. Hreniak, J. Czyżewski and W. Stręk, *Opt. Mater.*, 2003, **22**, 221-225.
22. L. Pospíšil, J. Fiedler, M. Hromadová, M. Gál, M. Valášek, J. Pecka and J. Michl, *J. Electrochem. Soc.*, 2006, **153**, E179-E183.
23. C. Kahlfuss, E. Métay, M.-C. Duclos, M. Lemaire, M. Oltean, A. Milet, É. Saint-Aman and C. Bucher, *Comptes Rendus Chimie*, 2014, **17**, 505-511.
24. A. G. Evans, J. C. Evans and M. W. Baker, *J. Am. Chem. Soc.*, 1977, **99**, 5882-5884.
25. A. L. Rieger and P. H. Rieger, *J. of Phys. Chem.*, 1984, **88**, 5845-5851.
26. M. Heyrovsky, *Chem Comm.*, 1987, 1856-1857.
27. J. F. Stargardt and F. M. Hawkridge, *Anal. Chim. Acta*, 1983, **146**, 1-8.

28. W. Geuder, S. Hünig and A. Suchy, *Tetrahedron*, 1986, **42**, 1665-1677.
29. L. Zhang, T.-Y. Zhou, J. Tian, H. Wang, D.-W. Zhang, X. Zhao, Y. Liu and Z.-T. Li, *Poly. Chem.*, 2014, **5**, 4715-4721.
30. C. Zhou, J. Tian, J.-L. Wang, D.-W. Zhang, X. Zhao, Y. Liu and Z.-T. Li, *Poly. Chem.*, 2014, **5**, 341-345.
31. E. M. Kosower and J. L. Cotter, *J. Am. Chem. Soc.*, 1964, **86**, 5524-5527.
32. S.G. Mayhew, F. Muller. *Biochem. Soc. Trans.*, 1982, **10**, 176-177.
33. B. Claude-Montigny, A. Merlin and C. Tondre, *J. Phys. Chem.*, 1992, **96**, 4432-4437.
34. O. Johansen, J. W. Loder, A. W. H. Mau, J. Rabani and W. H. F. Sasse, *Langmuir*, 1992, **8**, 2577-2581.
35. K. Y. Tam, R. L. Wang, C. W. Lee and R. G. Compton, *Electroanal.*, 1997, **9**, 219-224.
36. P. A. Quintela, A. Diaz and A. E. Kaifer, *Langmuir*, 1988, **4**, 663-667.
37. P. A. Quintela and A. E. Kaifer, *Langmuir*, 1987, **3**, 769-773.
38. T. Lu, T. M. Cotton, J. K. Hurst and D. H. P. Thompson, *J. Phys. Chem.*, 1988, **92**, 6978-6985.
39. M. R. Geraskina, A. T. Buck and A. H. Winter, *J. Org. Chem.*, 2014, **79**, 7723-7727.
40. A. T. Buck, J. T. Paletta, S. A. Khindurangala, C. L. Beck and A. H. Winter, *J. Am. Chem. Soc.*, 2013, **135**, 10594-10597.
41. M. J. Juetten, A. T. Buck and A. H. Winter, *Chem. Comm.*, 2015, **51**, 5516-5519.
42. L. A. Summers, N. Andriopoulos and A.-L. Channon, *J. Heterocyclic. Chem.*, 1990, **27**, 595-598.

## CHAPTER 6: CONCLUSIONS

### 5.1 Novel aromatic hexaester synthesis.

This dissertation was designed to show the synthesis of a new class of compounds related to the potential application of molecular amplifiers. For more information on the application of these new aromatic compounds for use as molecular amplifiers, see Appendix A. Kinetics and model systems for these molecular amplifiers is further discussed in Appendix A.

For the scope of the main body of this dissertation we focused on demonstrating access to novel mellitic acid esters. In particular we believe that this novel reaction involved a of the Hell-Volhard-Zelinsky reaction. Particularly an application of the HVZ reaction was explored where halogenation was followed by elimination in order to yield a substituted aromatic compound from a saturated or partially unsaturated cyclohexane derivative in a one-pot synthesis. We have shown the ability to generalize this use of the HVZ reaction to oxidize several types of cyclohexane esters of the appropriate substitution pattern. Since the direct synthesis of hexakis substituted benzene esters through the esterification of mellitic acid proved to be a challenging synthesis that is accessible only through electro-cyclization of nonsterically hindered acetylene esters, the oxidative aromatization has great utility in synthesizing previously unknown compounds.

### 5.2 Viologen based EPR probes

In conclusion of the research on the EPR probes, we were able to show a non-covalently bound, reversible organoparamagnetic switch based on a linked-viologen dyad that can be cycled between diamagnetic and paramagnetic forms without radical decomposition.

We were able to use non-covalent chemistry in room-temperature aqueous solution or an

addition of heat in order to initiate this magnetic control. We expanded the scope of previously investigated small molecule viologens to include polymers, with average molecular weights exceeded 10,000 daltons. The polymer could be synthesized via substitution reaction between 1,3-dihalo propane and 4,4'-bipyridine. EPR experiments showed that addition of CB[7] or increase in temperature successfully switched these molecules from diamagnetic forms to a paramagnetic version. This change in electronic properties was accompanied by a change in optical properties, i.e. a color change that could be followed by UV-vis spectroscopy.

We further expanded on the concept of these radical viologens by investigating different substitution patterns of several different types and by UV-Vis and EPR, observed the change in binding affinity. We found that we were able to modulate the binding constants from the order of  $K_a=10^2 \text{ mol}^{-1}$  to  $K_a=10^4 \text{ mol}^{-1}$ . Particular interest was paid to the singly substituted 4,4'-bipyridine since the strength of binding changed drastically depending on the presence of water, or the pH of an aqueous solution. The binding constants shifted from the lowest observed to the highest upon protonation.

The protonation dependence of 4,4'-bipyridine, in addition to providing a convenient sensor to the presence of water, also provides us with a another opportunity for input modulation. By leaving the end of a short chain of 4,4'-bipyridine unsubstituted, we were able to create a molecule sensitive to several different inputs, emulating the Boolean type logic common in computer science. In this way we were able to successfully create a molecular logic gate that has many potential applications for spintronic material devices.

## APPENDIX A. SUPPORTING INFORMATION FOR CHAPTER 2

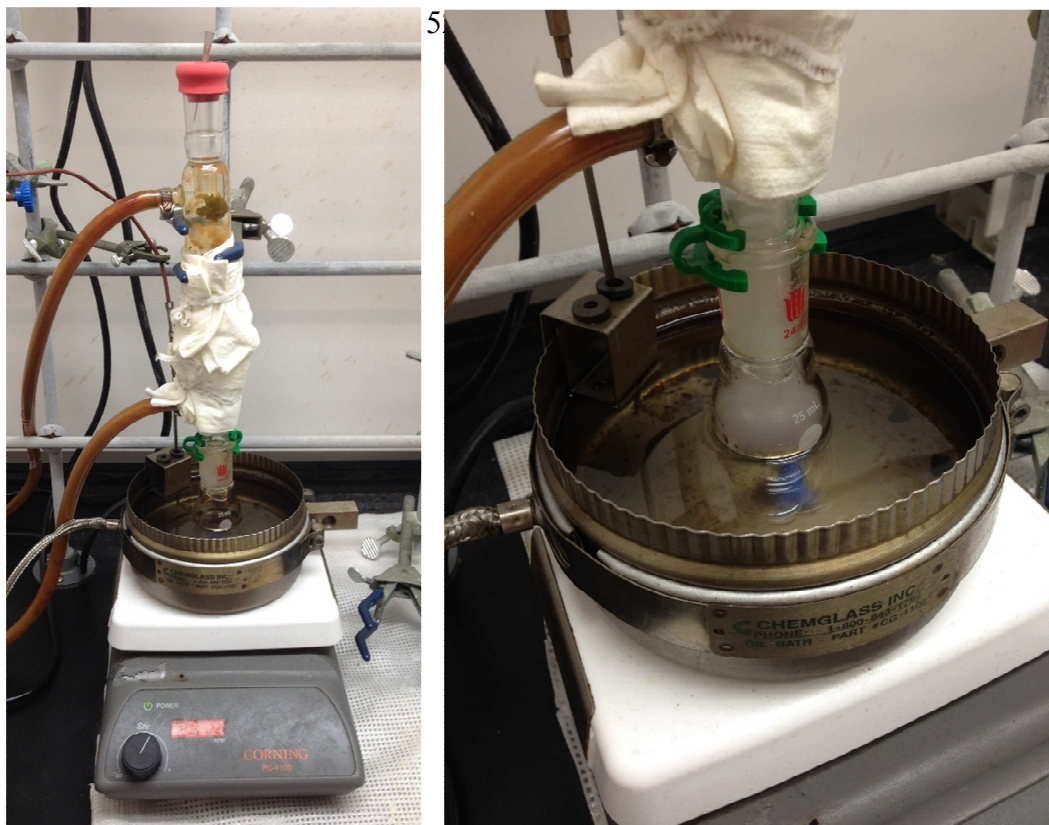
**General information.** Compounds and solvents were used as received from commercial suppliers without prior purification. NMR spectra were obtained using a Bruker AV-III 600 spectrometer (600 and 150 MHz for  $^1\text{H}$  and  $^{13}\text{C}$ , respectively).

**Mellitic acid (1).**  $\text{PCl}_5$  (1.794 g, 8.6 mmol) was added to 1,2,3,4,5,6-cyclohexanehexacarboxylic acid (0.250 g, 0.7 mmol) and digested for 1 h at  $130^\circ\text{C}$ . Then water (10 mL) was added to the reaction mixture and heated at the same temperature for 4 h. Water was removed using rotary evaporator leaving white solid in the flask that contained mellitic acid and phosphoric acid byproduct, which made purification and yield determination difficult. To find the percent yield, the mellitic acid/ byproduct mixture was derivatized by esterification to methyl ester of mellitic acid using a known procedure (Ranganathan, S.; Muraleedharan, K. M.; Chandrashekhara Rao, C. H.; Vairamani, M.; Karle, I. L.; Gilardi, R. D. *Chemical Communications* **2001**, 2544) which has a yield of 81% (published and verified independently). The yield from starting material to the mellitic acid methyl ester was 0.291g (54%). From this, we could determine that the reaction to form mellitic acid 1 affords 0.162 g (66 %).  $^{13}\text{C}$  NMR (150 MHz):  $\delta$ (ppm) 169.3, 133.7.



“Digestion” of 1,2,3,4,5,6-cyclohexanehexacarboxylic acid and  $\text{PCl}_5$





### Addition of pyridine

**Mellitic acid hexaphenyl ester (2).**  $\text{PCl}_5$  (1.794 g, 8.6 mmol) was added to 1,2,3,4,5,6-cyclohexanhexacarboxylic acid (0.250 g, 0.7 mmol) and digested for 1 h at  $130^\circ\text{C}$ . Then, phenol (2.703 g, 28.7 mmol) was added to reaction mixture and heated at the same temperature for 4 h followed by addition of pyridine (3 mL). The reaction mixture was allowed to continue refluxing for 2 h. Pyridine was distilled off and the reaction mixture was filtered and solid product was washed with cold methanol to afford 0.341 g (60%) of the product as a yellow solid. Mp:  $230.5\text{--}231.5^\circ\text{C}$ .  $^1\text{H NMR}$  (600 MHz):  $\delta$ (ppm) 7.35 (t,  $J = 7$  Hz, 2H), 7.28 (t,  $J = 7$  Hz, 1H), 7.14 (d,  $J = 8$  Hz, 2H);  $^{13}\text{C NMR}$  (150 MHz):  $\Delta$  (ppm) 163.2, 150.4, 134.5, 129.8, 127.0, 121.4. **HRMS** (ESI):  $m/z$  calculated for  $\text{C}_{48}\text{H}_{32}\text{O}_{13} [\text{MH}_2\text{O}]^+$ : 816.1843; found: 816.2109.

**Mellitic acid hexa (4-methylphenyl) ester (3).**  $\text{PCl}_5$  (1.794 g, 8.6 mmol) was added to 1,2,3,4,5,6-cyclohexanhexacarboxylic acid (0.250 g, 0.7 mmol) and digested for 1 h at  $130^\circ\text{C}$ . Then 4-methylphenol (*p*-cresol, 3.105 g, 28.7 mmol) was added to reaction mixture and heated at the same temperature for 4 h followed by addition of pyridine (3



mL). The reaction mixture was refluxed for 2 h. Pyridine was distilled off and the reaction mixture was filtered and solid product was washed with cold methanol to afford 0.429 g (67%) of the product as a white solid. Mp: 248.0–249.0 °C. **<sup>1</sup>H NMR** (600 MHz):  $\delta$ (ppm) 7.14 (d,  $J = 8$  Hz, 2H), 7.02 (d,  $J = 9$  Hz, 2H), 2.35 (s, 3H); **<sup>13</sup>C NMR** (150 MHz):  $\delta$  (ppm) 163.5, 148.2, 136.6, 134.5, 130.3, 121.1, 21.1. **HRMS** (ESI):  $m/z$  calculated for C<sub>54</sub>H<sub>42</sub>NaO<sub>12</sub> [MNa]<sup>+</sup>: 905.2574; found: 905.2526.

**Mellitic acid (hexa-4-ethylphenyl) ester (4)**. PCl<sub>5</sub> (1.794 g, 8.6 mmol) was added to 1,2,3,4,5,6-cyclohexanhexacarboxylic acid (0.250 g, 0.7 mmol) and digested for 1 h at 130° C. Then 4-ethylphenol (3.508 g, 28.7 mmol) was added to reaction mixture and heated at the same temperature for 4 h followed by addition of pyridine (3 mL). The reaction mixture was refluxed for 2 h. Pyridine was distilled off and the reaction mixture was filtered and solid product was washed with cold methanol to afford 0.435 g (63%) of the product as a beige solid. Mp: 189.0–190.0 °C. **<sup>1</sup>H NMR** (600 MHz):  $\delta$ (ppm) 7.16 (d,  $J = 8.5$  Hz, 2H), 7.05 (d,  $J = 8.5$  Hz, 2H), 2.65 (q,  $J = 8$  Hz, 2H), 1.24 (t,  $J = 8$  Hz, 3H); **<sup>13</sup>C NMR** (150 MHz):  $\delta$ (ppm) 163.4, 148.4, 142.9, 134.5, 129.1, 121.1, 28.5, 15.7. **HRMS** (ESI):  $m/z$  calculated for C<sub>60</sub>H<sub>54</sub>NaO<sub>12</sub> [MNa]<sup>+</sup>: 989.3513; found: 989.3520.

**Mellitic acid (hexa-4-isopropylphenyl) ester (5)**. PCl<sub>5</sub> (1.794 g, 8.6 mmol) was added to 1,2,3,4,5,6-cyclohexanhexacarboxylic acid (0.250 g, 0.7 mmol) and digested for 1 h at 130°C. Then 4-isopropylphenol (3.911 g, 28.7 mmol) was added to reaction mixture and heated at the same temperature for 4 h followed by addition of pyridine (3 mL). The reaction mixture was refluxed for 2 h. Pyridine was distilled off and the reaction mixture was filtered and solid product was washed with cold methanol to afford 0.169 g (22%) of the product as a yellow solid. Mp: 201.0–203.5 °C. **<sup>1</sup>H NMR** (600 MHz):  $\delta$ (ppm) 7.18 (d,  $J = 8.5$  Hz, 2H), 7.06 (d,  $J = 8.5$  Hz, 2H), 2.91 (m, 1H), 1.25 (s, 6H); **<sup>13</sup>C NMR** (150 MHz):  $\delta$ (ppm) 163.4, 148.4, 147.5, 134.5, 127.6, 121.1, 33.8, 24.1. **HRMS** (ESI):  $m/z$  calculated for C<sub>66</sub>H<sub>66</sub>NaO<sub>12</sub> [MNa]<sup>+</sup>: 1073.4452; found: 1073.4460.

**Mellitic acid (hexa-4-methoxyphenyl) ester (6).**  $\text{PCl}_5$  (1.794 g, 8.6 mmol) was added to 1,2,3,4,5,6-cyclohexanhexacarboxylic acid (0.250 g, 0.7 mmol) and digested for 1 h at  $130^\circ\text{C}$ . Then 4-methoxyphenol (3.565 g, 28.7 mmol) was added to reaction mixture and heated at the same temperature for 4 h followed by addition of pyridine (3 mL). The reaction mixture was refluxed for 2 h. Pyridine was distilled off and the reaction mixture was filtered and solid product was washed with cold methanol to afford 0.442 g (63%) of the product as a white solid. Mp:  $223.0\text{--}223.5^\circ\text{C}$ .  $^1\text{H NMR}$  (600 MHz):  $\delta$ (ppm) 7.05 (d,  $J = 9$  Hz, 2H), 6.85 (d,  $J = 9$  Hz, 2H), 3.80 (s, 3H);  $^{13}\text{C NMR}$  (150 MHz):  $\delta$ (ppm) 163.6, 158.1, 143.9, 134.5, 122.2, 114.8, 55.8. **HRMS** (ESI):  $m/z$  calculated for  $\text{C}_{54}\text{H}_{44}\text{O}_{19}$   $[\text{MH}_2\text{O}]^+$ : 996.2477; found: 996.2730.

**Mellitic acid (hexa-4-chlorophenyl) ester (7).**  $\text{PCl}_5$  (1.794 g, 8.6 mmol) was added to 1,2,3,4,5,6-cyclohexanhexacarboxylic acid (0.250 g, 0.7 mmol) and digested for 1 h at  $130^\circ\text{C}$ . Then 4-chlorophenol (3.692 g, 28.7 mmol) was added to reaction mixture and heated at the same temperature for 4 h followed by addition of pyridine (3 mL). The reaction mixture was refluxed for 2 h. Pyridine was distilled off and the reaction mixture was filtered and solid product was washed with cold acetone to afford 0.423 g (58%) of the product as a white solid. Mp:  $> 260^\circ\text{C}$ .  $^1\text{H NMR}$  (600 MHz):  $\delta$ (ppm) 7.34 (d,  $J = 9$  Hz, 2H), 7.04 (d,  $J = 8.5$  Hz, 2H);  $^{13}\text{C NMR}$  (150 MHz):  $\delta$ (ppm) 162.7, 148.6, 134.4, 132.9, 130.1, 122.5. **HRMS** (ESI):  $m/z$  calculated for  $\text{C}_{48}\text{H}_{24}\text{Cl}_6\text{KO}_{12}$   $[\text{MK}]^+$ : 1042.9006; found: 1043.2923.

**Mellitic acid (hexa-4-bromophenyl) ester (8).**  $\text{PCl}_5$  (1.794 g, 8.6 mmol) was added to 1,2,3,4,5,6-cyclohexanhexacarboxylic acid (0.250 g, 0.7 mmol) and digested for 1 h at  $130^\circ\text{C}$ . Then 4-bromophenol (4.968 g, 28.7 mmol) was added to reaction mixture and heated at the same temperature for 4 h followed by addition of pyridine (3 mL). The reaction mixture was refluxed for 2 h. Pyridine was distilled off and the reaction mixture was filtered and solid product was washed with cold acetone to afford 0.453 g (50%) of the product as a beige solid. Mp:  $> 260^\circ\text{C}$ .  $^1\text{H NMR}$  (600 MHz):  $\delta$ (ppm) 7.49 (d,  $J = 9$  Hz, 2H), 6.97 (d,  $J = 9$  Hz, 2H);  $^{13}\text{C NMR}$  (150 MHz):  $\delta$ (ppm) 162.6, 149.1, 134.4,

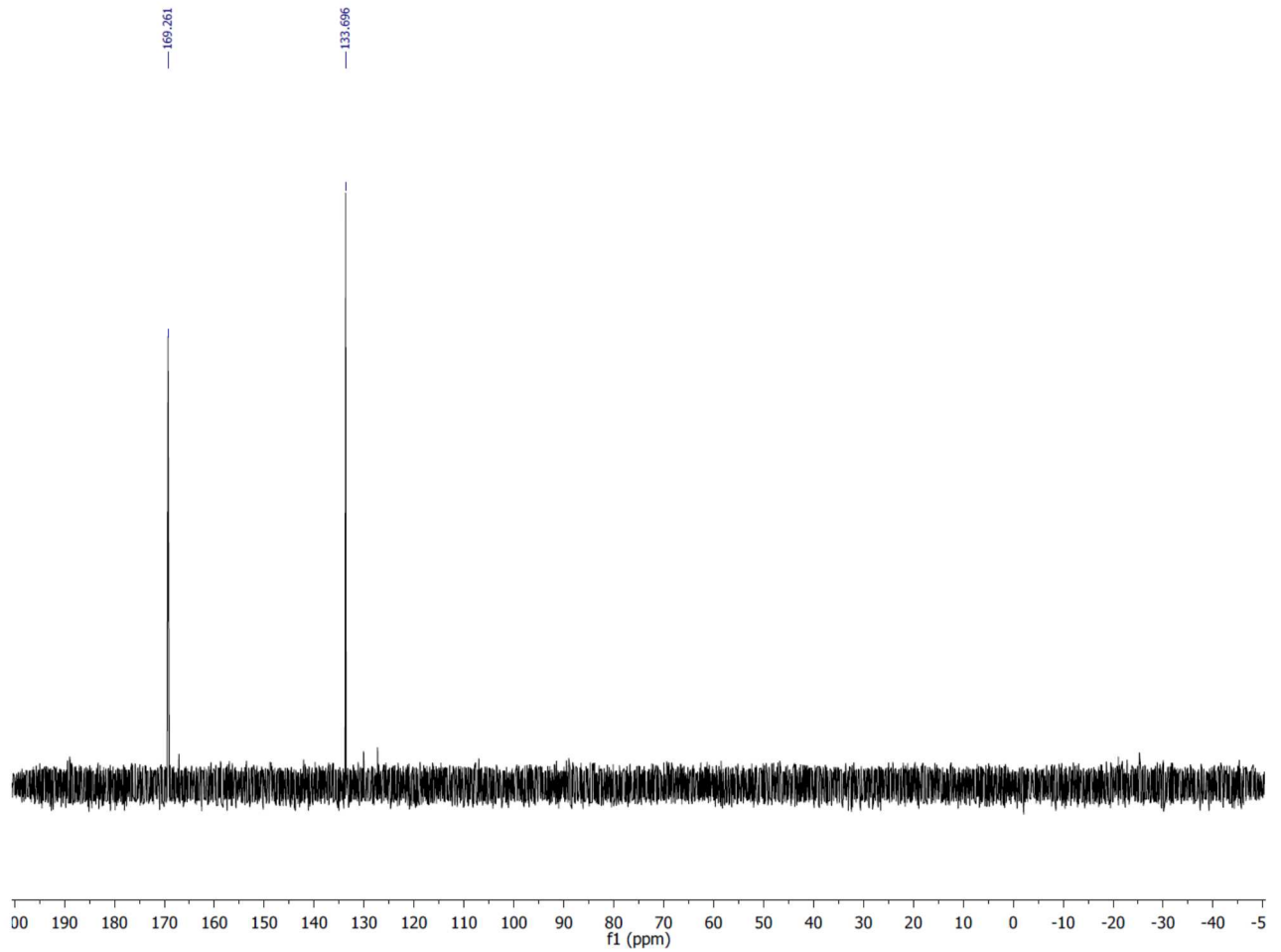
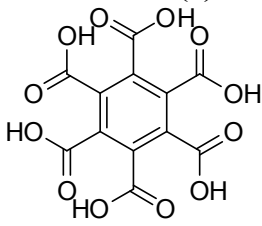
133.1, 122.9, 120.6. **HRMS** (ESI):  $m/z$  calculated for  $C_{48}H_{24}Br_6NaO_{12} [MNa]^+$ : 1294.6204; found: 1294.6212.

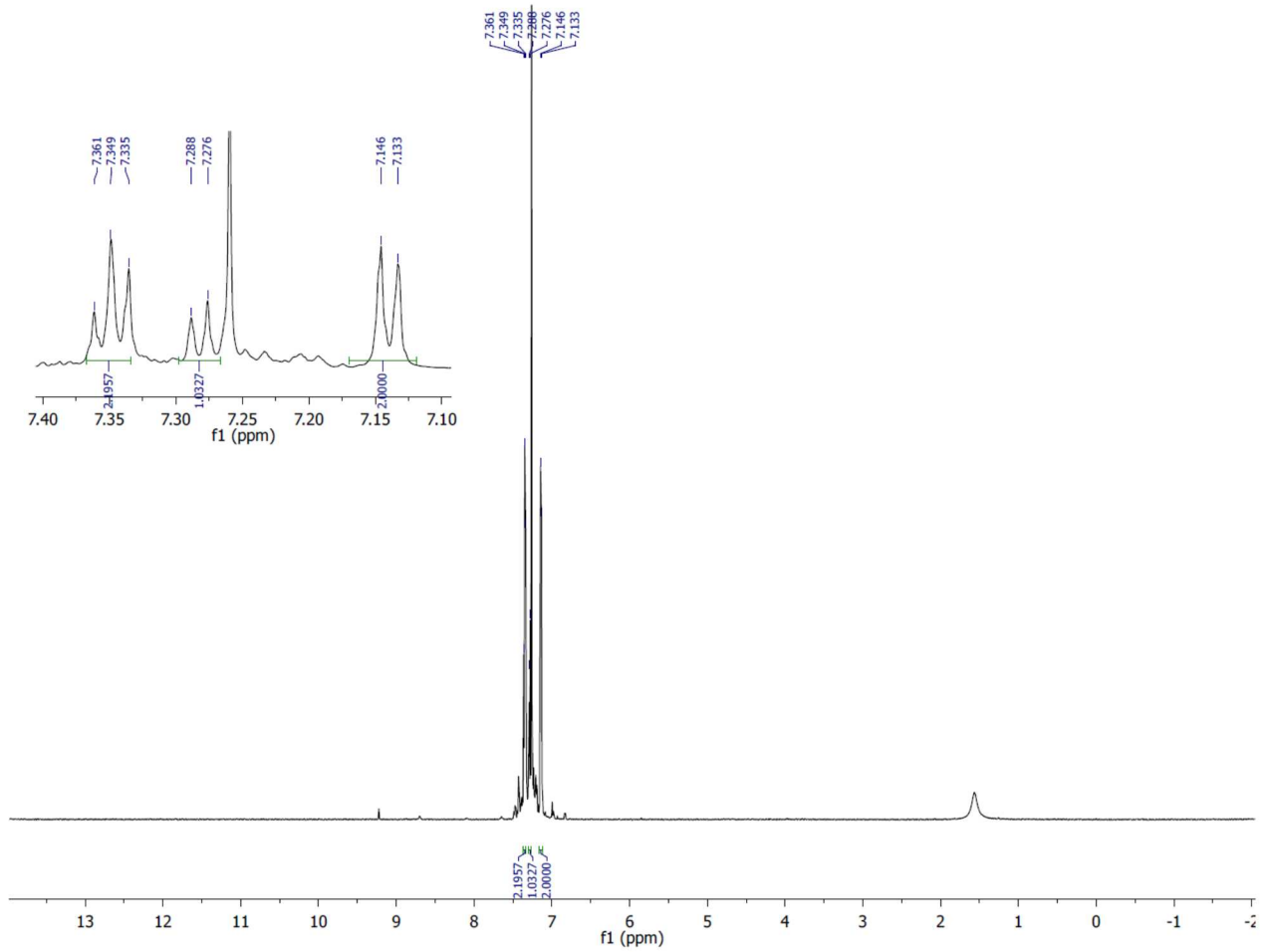
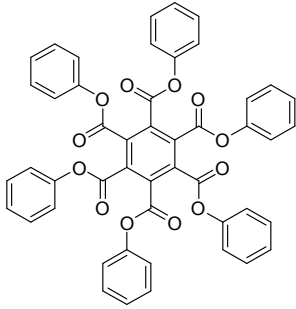
**Mellitic acid (hexa-4-fluorophenyl) ester (9).**  $PCl_5$  (1.794 g, 8.6 mmol) was added to 1,2,3,4,5,6-cyclohexanehexacarboxylic acid (0.250 g, 0.7 mmol) and digested for 1 h at  $130^\circ C$ . Then 4-fluorophenol (3.219 g, 28.7 mmol) was added to reaction mixture and heated at the same temperature for 4 h followed by addition of pyridine (3 mL). The reaction mixture was refluxed for 2 h. Pyridine was distilled off and the reaction mixture was filtered and solid product was washed with cold acetone to afford 0.404 g (62%) of the product as a white solid. Mp:  $210.0\text{--}210.5^\circ C$ .  **$^1H$  NMR** (600 MHz):  $\delta$ (ppm) 7.17 (m, 2H), 7.12 (m, 2H);  **$^{13}C$  NMR** (150 MHz):  $\delta$ (ppm) 163.1, 161.8, 160.2, 146.0, 134.5, 122.7, 116.8. **HRMS** (ESI):  $m/z$  calculated for  $C_{48}H_{24}F_6NaO_{12} [MNa]^+$ : 929.1070; found: 929.1066.

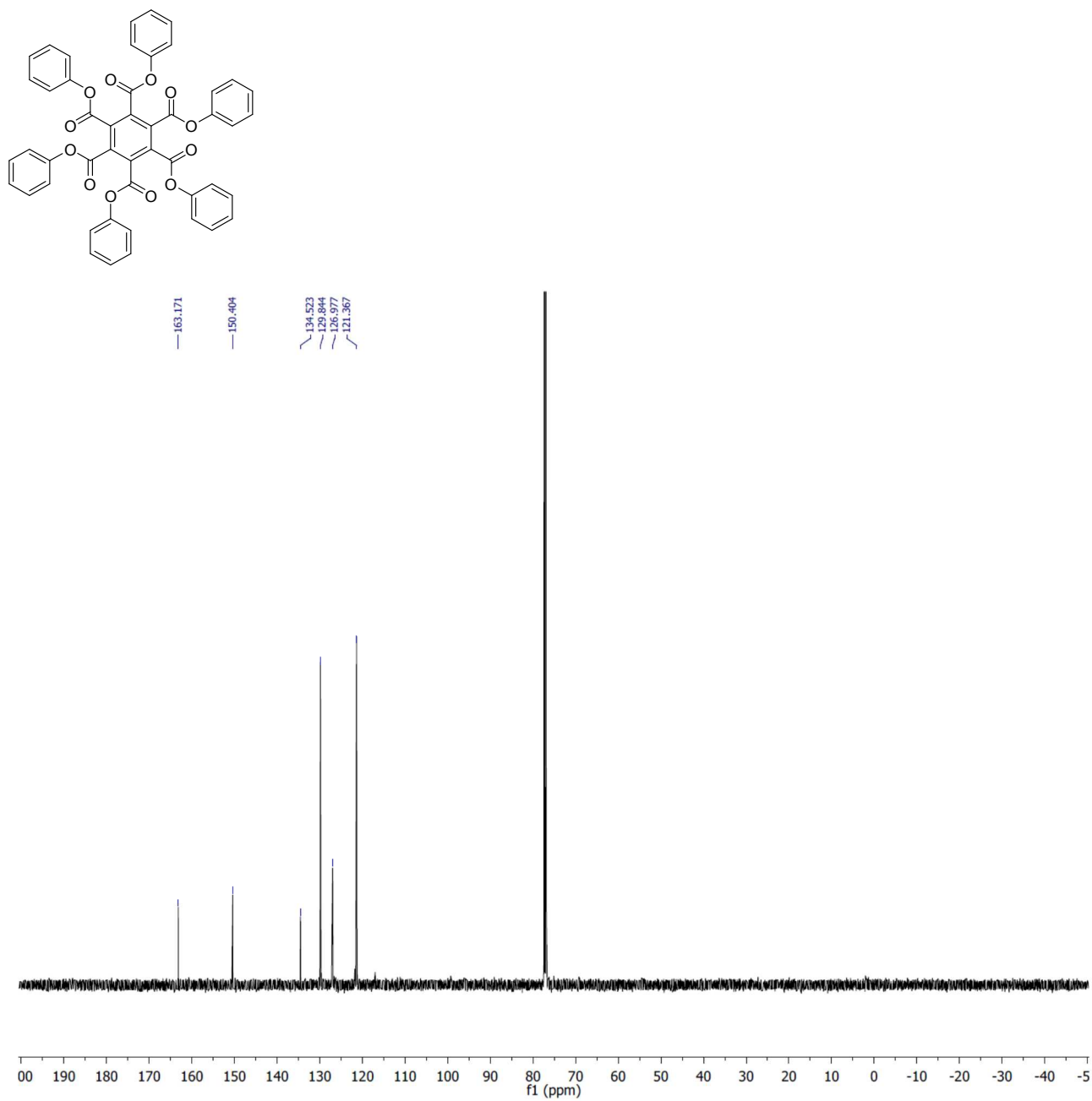
**Mellitic acid (hexa-3-methyl-4-bromophenyl) ester (10).**  $PCl_5$  (1.794 g, 8.6 mmol) was added to 1,2,3,4,5,6-cyclohexanehexacarboxylic acid (0.250 g, 0.7 mmol) and digested for 1 h at  $130^\circ C$ . Then 3-methyl-4-bromophenol (5.371 g, 28.7 mmol) was added to reaction mixture and heated at the same temperature for 4 h followed by addition of pyridine (3 mL). The reaction mixture was refluxed for 2 h. Pyridine was distilled off and the reaction mixture was filtered and solid product was washed with cold acetone to afford 0.416 g (43%) of the product as a beige solid. Mp:  $201.5\text{--}202.5^\circ C$ .  **$^1H$  NMR** (600 MHz):  $\delta$ (ppm) 7.53 (d,  $J = 8.5$  Hz, H), 6.97 (d,  $J = 8.5$  Hz, H), 6.85 (dd, H), 2.31 (s, 3H);  **$^{13}C$  NMR** (150 MHz):  $\delta$ (ppm) 162.7, 149.1, 140.1, 134.4, 133.6, 123.4, 122.9, 120.1, 23.2. **CHN elemental analysis (%)**: Calculated for  $C_{54}H_{36}Br_6O_{12}Na$ : C, 46.98; H, 2.61%. Found C, 46.96; H, 2.44%.

**Mellitic acid (hexa-4-cyanophenyl) ester (11).**  $PCl_5$  (1.794 g, 8.6 mmol) was added to 1,2,3,4,5,6-cyclohexanehexacarboxylic acid (0.250 g, 0.7 mmol) and digested for 1 h at  $130^\circ C$ . Then 4-cyanophenol (3.421 g, 28.7 mmol) was added to reaction mixture and heated at the same temperature for 4 h followed by addition of pyridine (3 mL). The

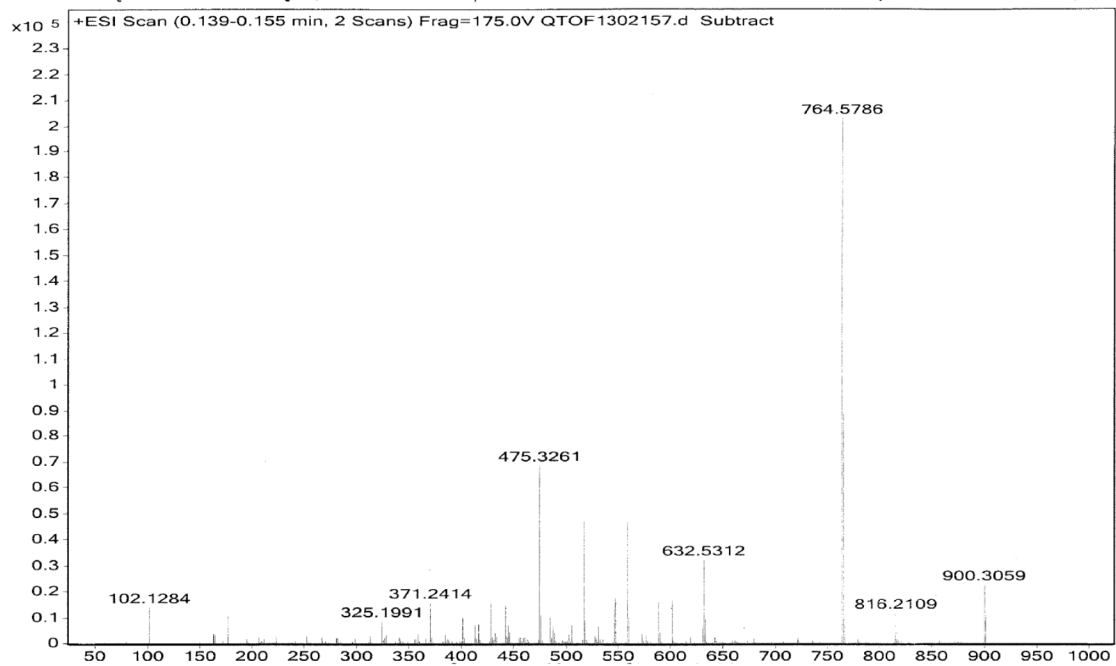
reaction mixture was refluxed for 2 h. Pyridine was distilled off and the reaction mixture was filtered and solid product was washed with cold acetone to afford 0.494 g (71%) of the product as a light brown solid. Mp: > 260 °C. **<sup>1</sup>H NMR** (600 MHz):  $\delta$ (ppm) 7.70 (d,  $J = 8.5$  Hz, 2H), 7.21 (d,  $J = 8.5$  Hz, 2H); **<sup>13</sup>C NMR** (150 MHz):  $\delta$ (ppm) 161.9, 152.8, 134.4, 134.4, 122.1, 117.5, 112.0. **HRMS** (ESI):  $m/z$  calculated for  $C_{54}H_{24}N_6NaO_{12}$  [MNa]<sup>+</sup>: 971.1350; found: 971.1347.

**Mellitic acid (1)****150 MHz, D<sub>2</sub>O**

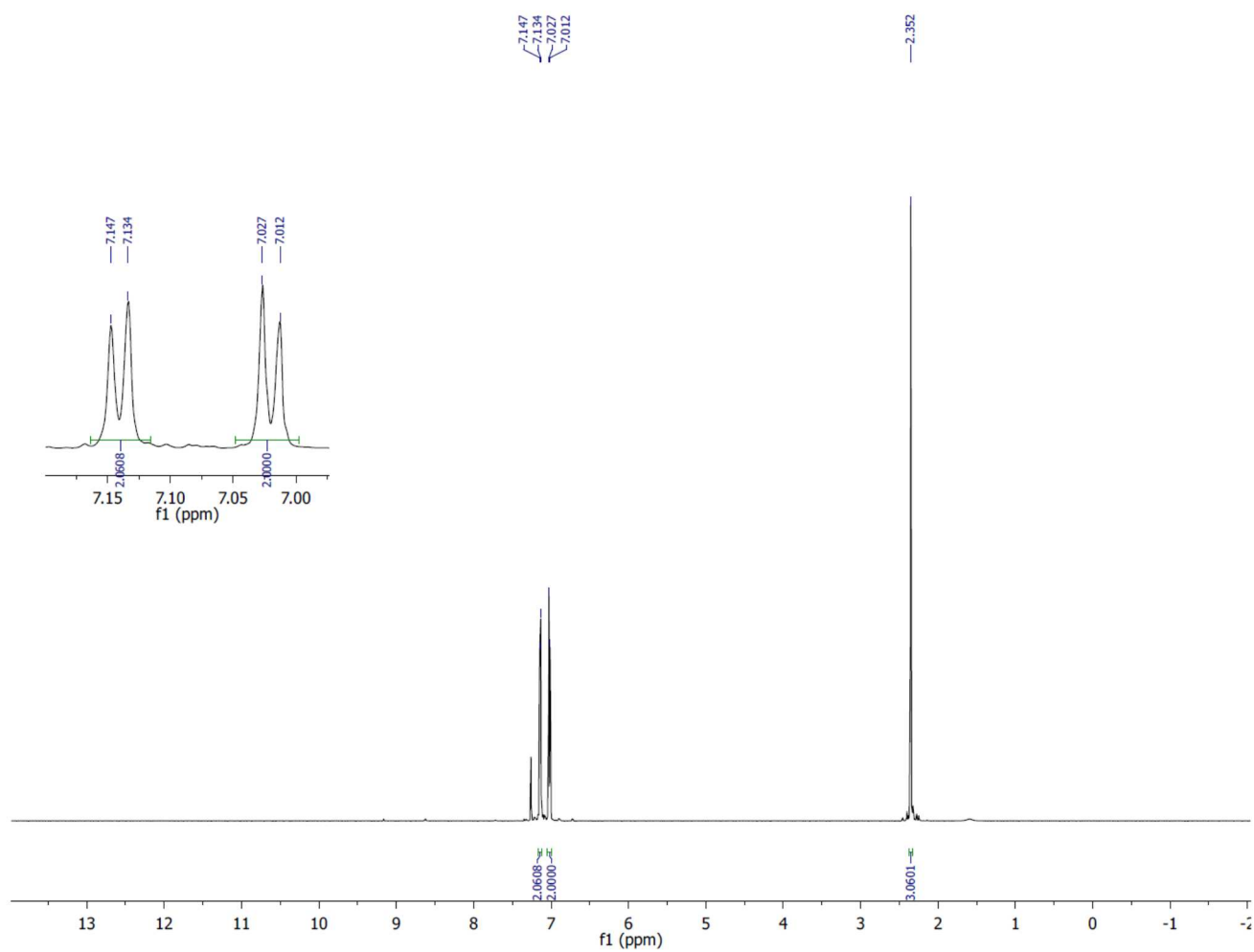
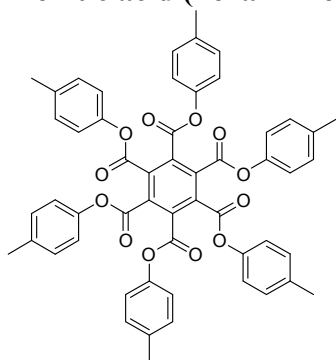
**Mellitic acid (hexaphenyl) ester (2)**

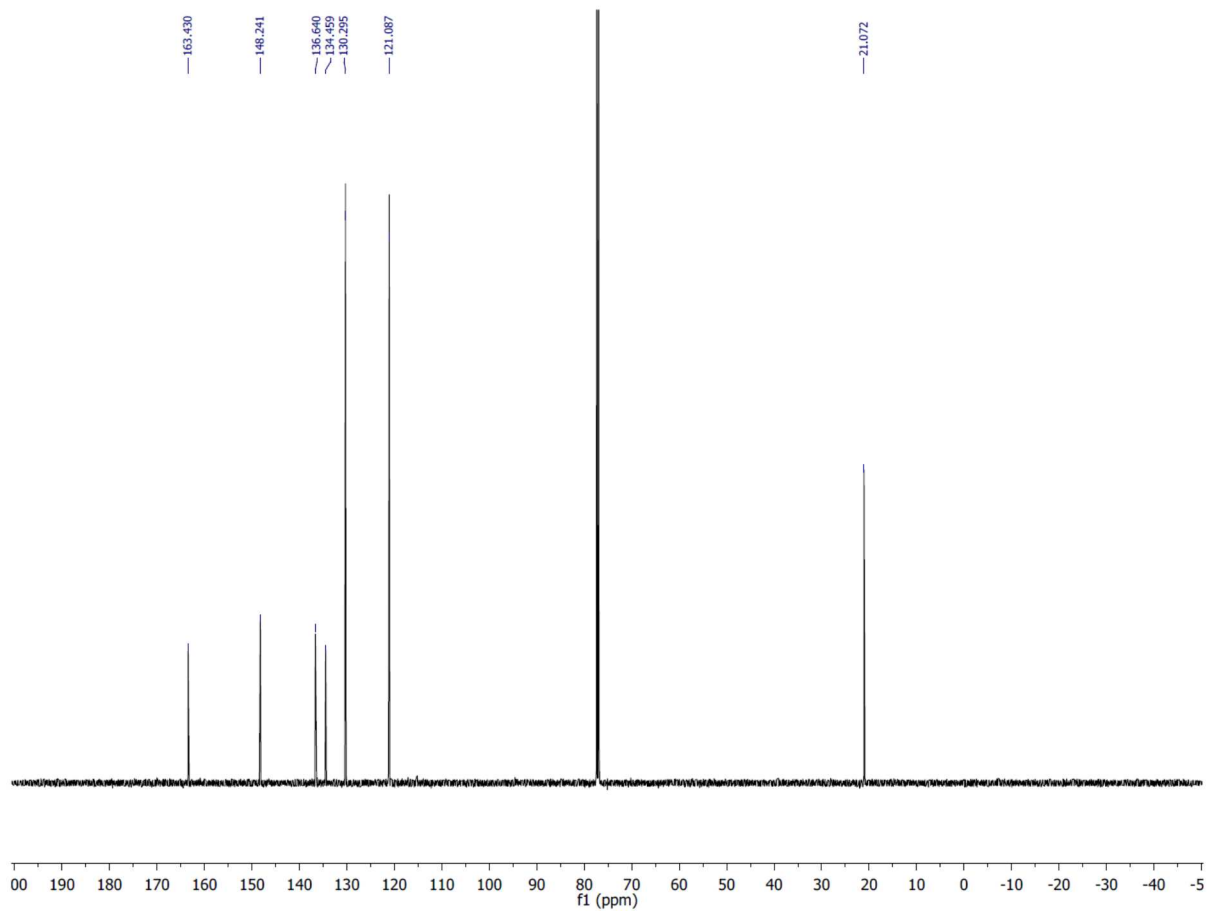
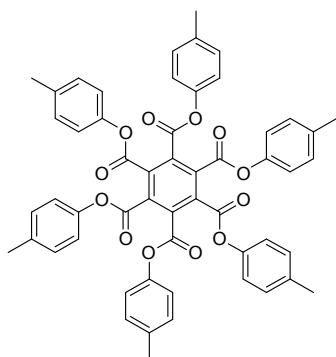


Sample Name	1, Exp36	Position	vial1	Instrument Name	QTOF	User Name	CIF-PC\admin
Inj Vol	2	InjPosition		SampleType	Sample	IRM Calibration Status	Success
Data Filename	QTOF1302157.d	ACQ Method	AESI-100-1000-pos.m	Comment		Acquired Time	7/31/2013 11:07:10



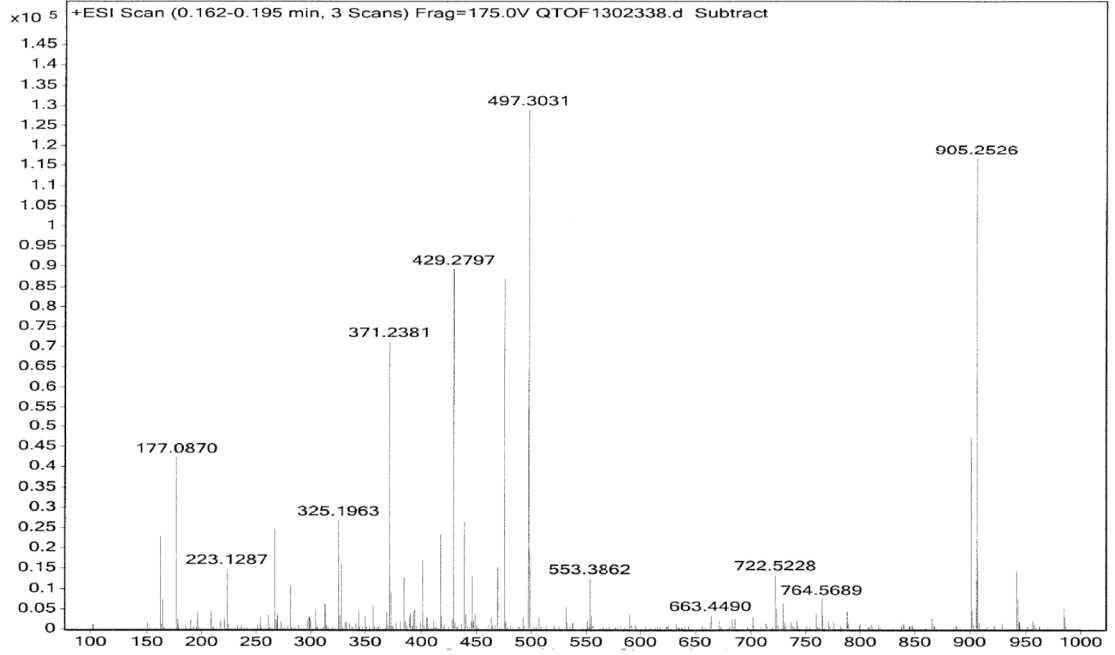


**Mellitic acid (hexa-4-methylphenyl) ester (3)****600 MHz, CDCl<sub>3</sub>**

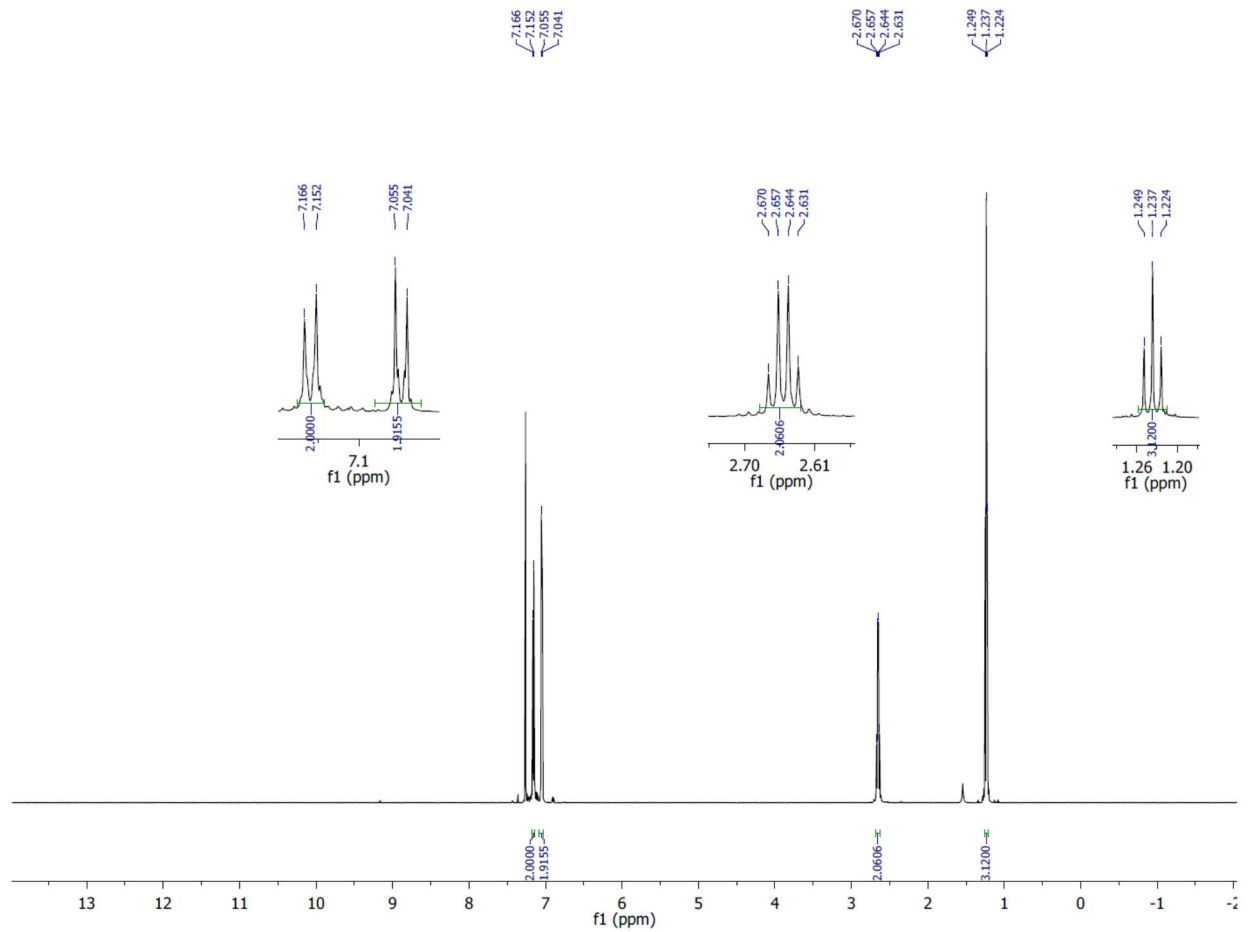
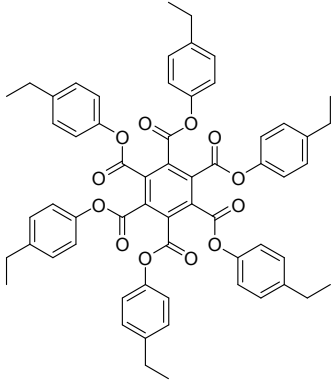


150 MHz, CDCl<sub>3</sub>

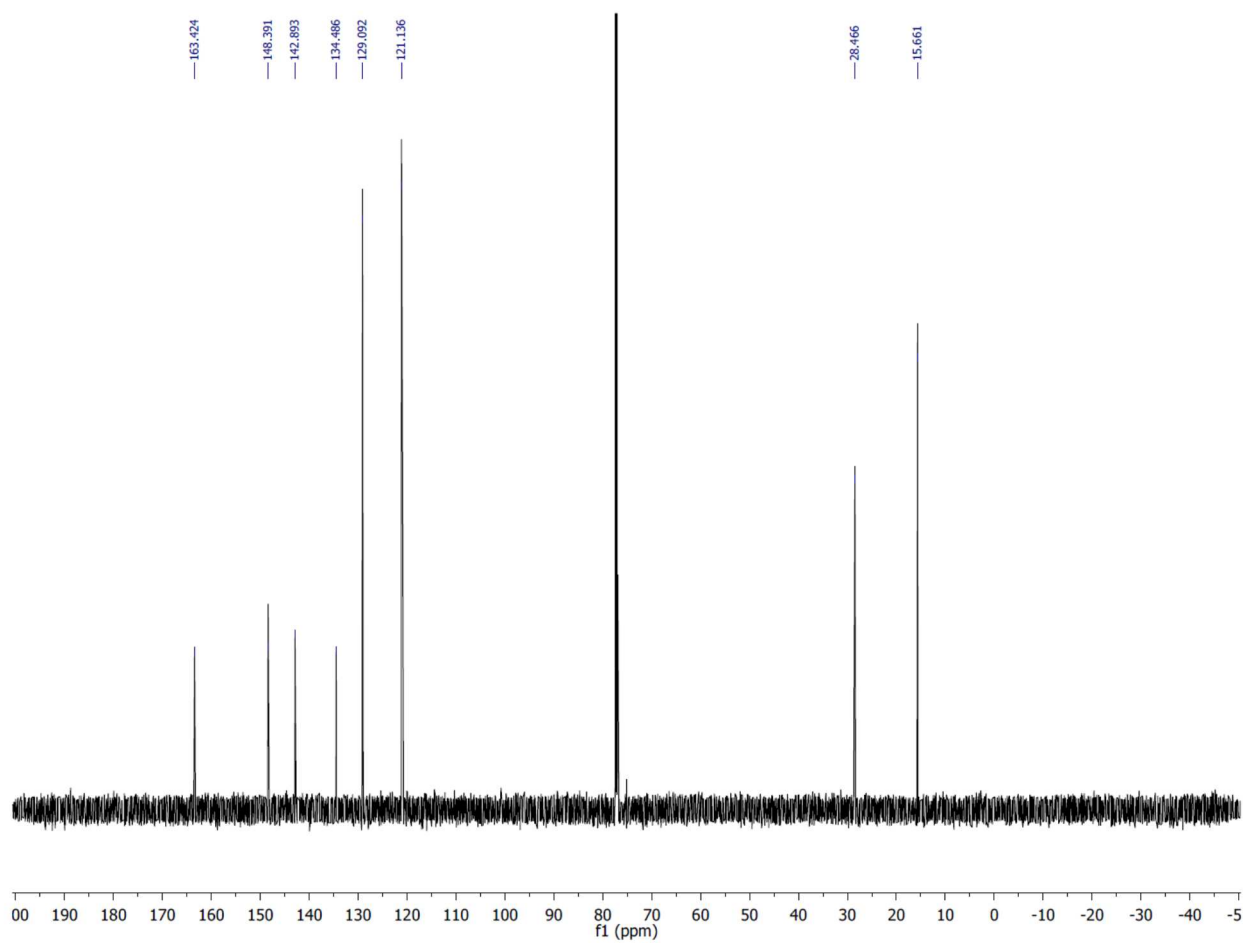
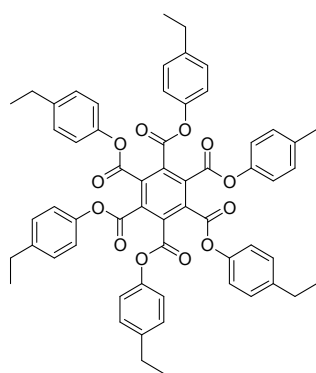
Sample Name	Exp48	Position	vial1	Instrument Name	QTOF	User Name	CIF-PC\admin
Inj Vol	1	InjPosition		SampleType	Sample	IRM Calibration Status	Success
Data Filename	QTOF1302338.d	ACQ Method	ESI2-pos.m	Comment		Acquired Time	8/27/2013 10:22:30



### Mellitic acid (hexa-4-ethylphenyl) ester (4)

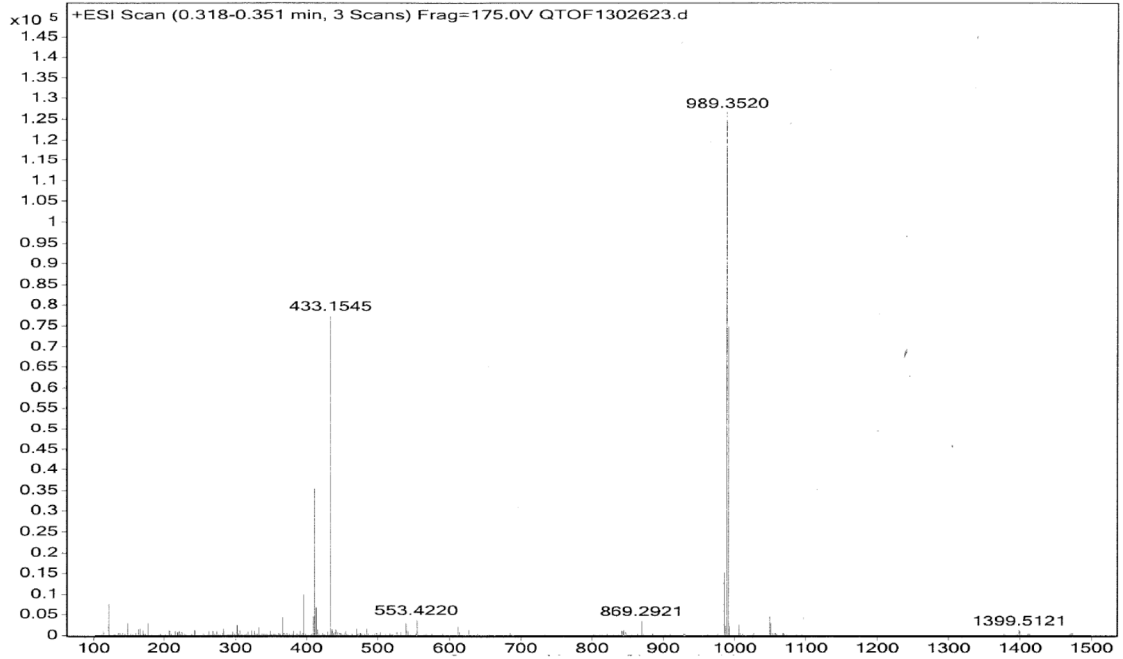


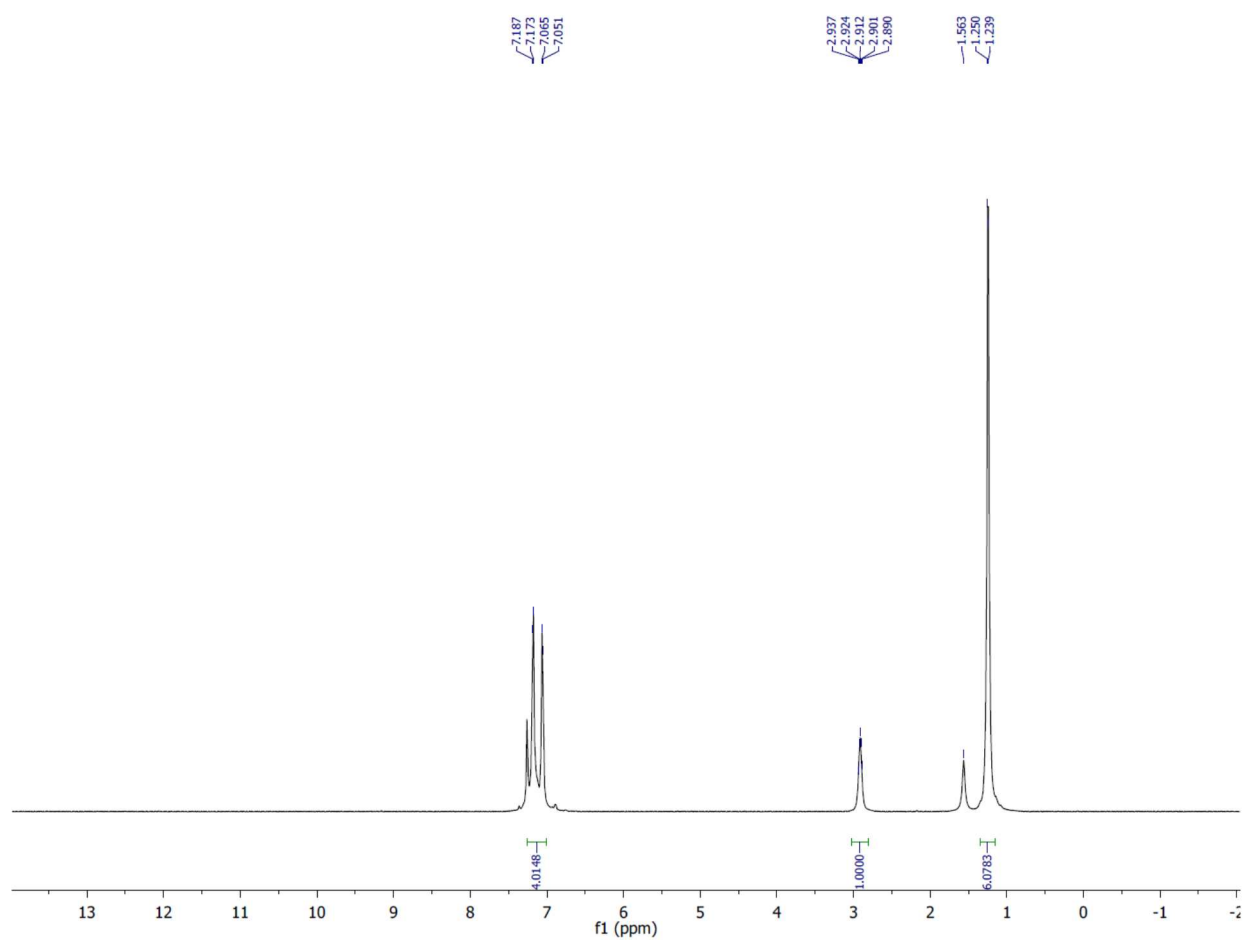
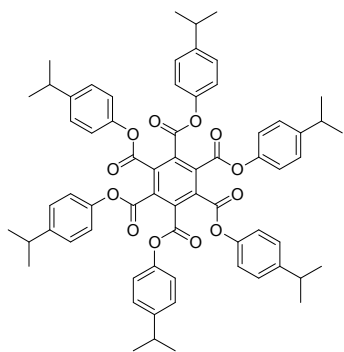
600 MHz,  $\text{CDCl}_3$

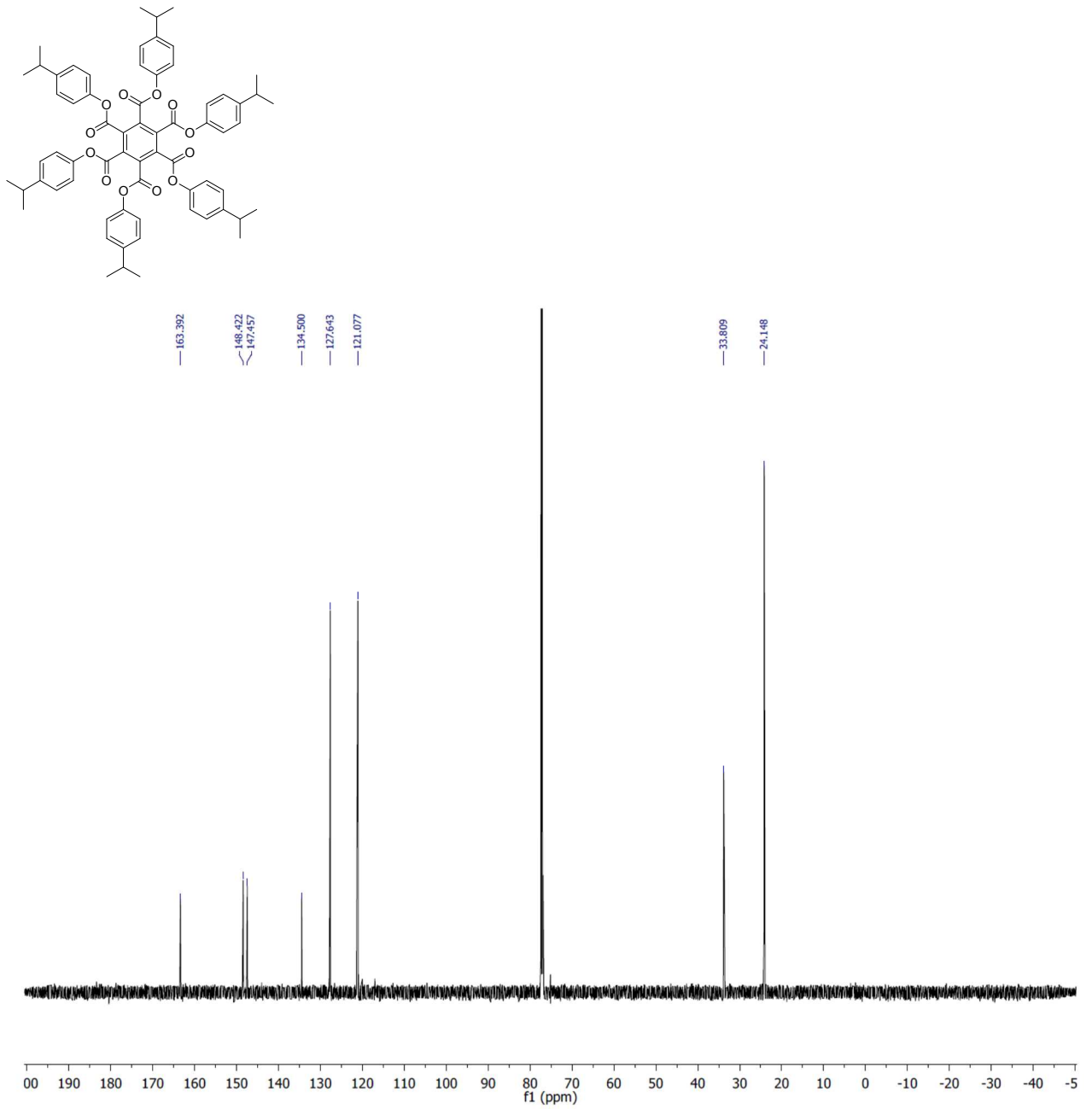


150 MHz, CDCl<sub>3</sub>

Sample Name	Exp55	Position	vial1	Instrument Name	QTOF	User Name	CIF-PC\admin
Inj Vol	0.3	InjPosition		SampleType	Sample	IRM Calibration Status	Success
Data Filename	QTOF1302623.d	ACQ Method	AESI-100-1000-pos.m	Comment		Acquired Time	10/17/2013 10:4



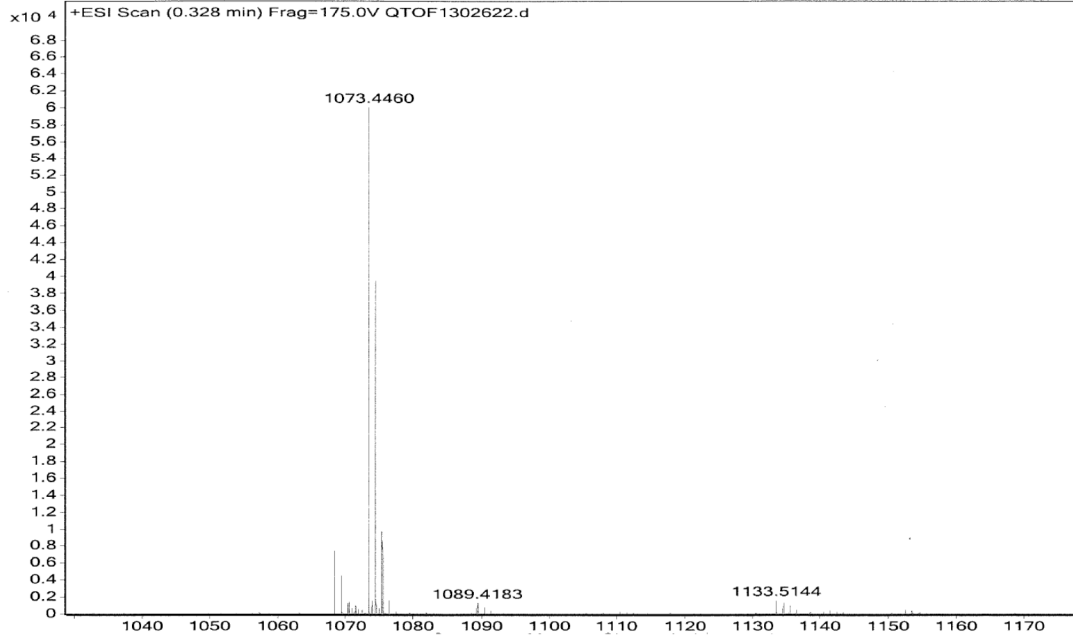
**Mellitic acid (hexa-4-isopropylphenyl) ester (5)****600 MHz, CDCl<sub>3</sub>**



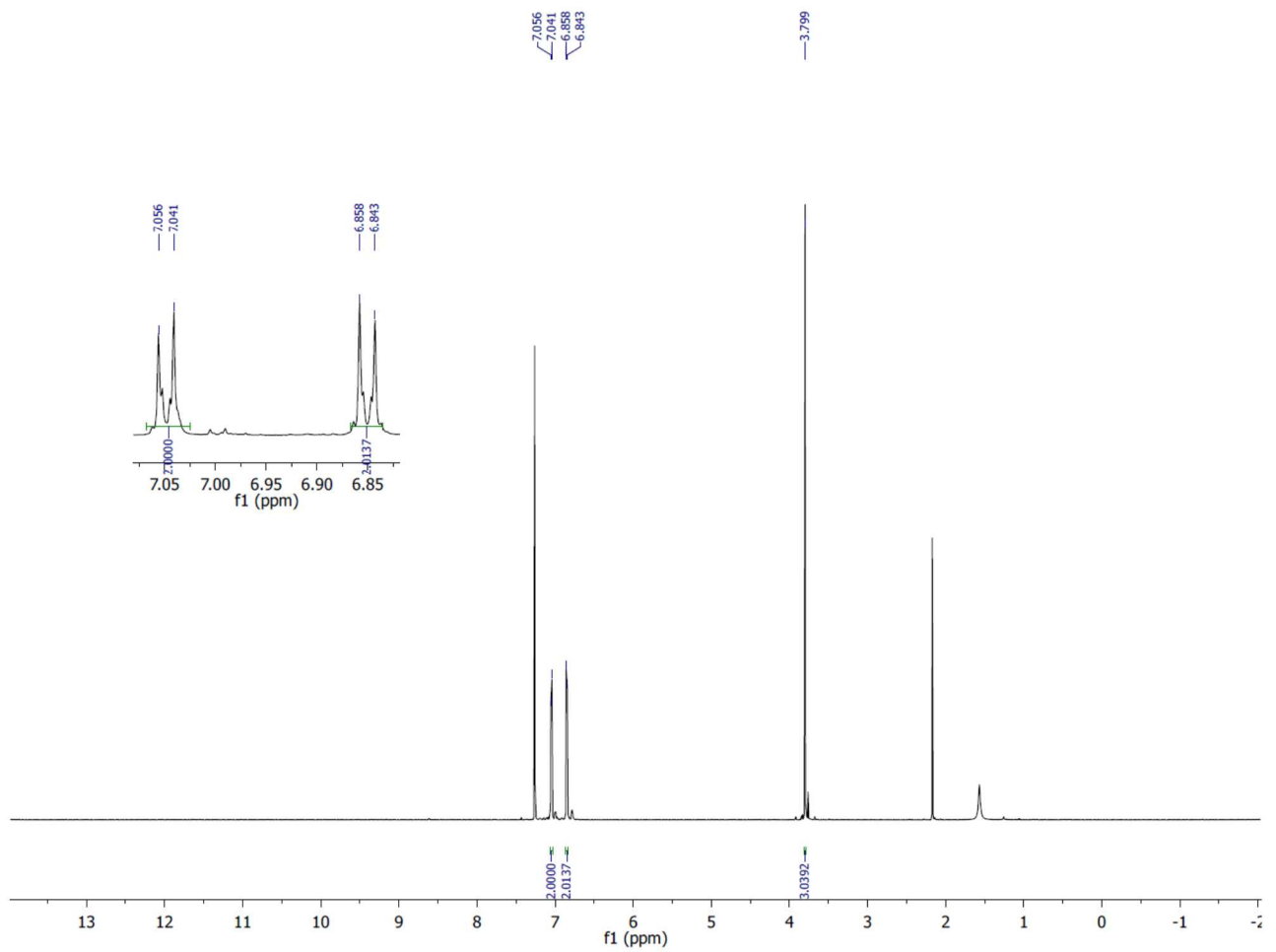
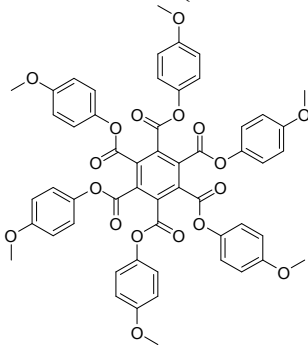
150 MHz, CDCl<sub>3</sub>

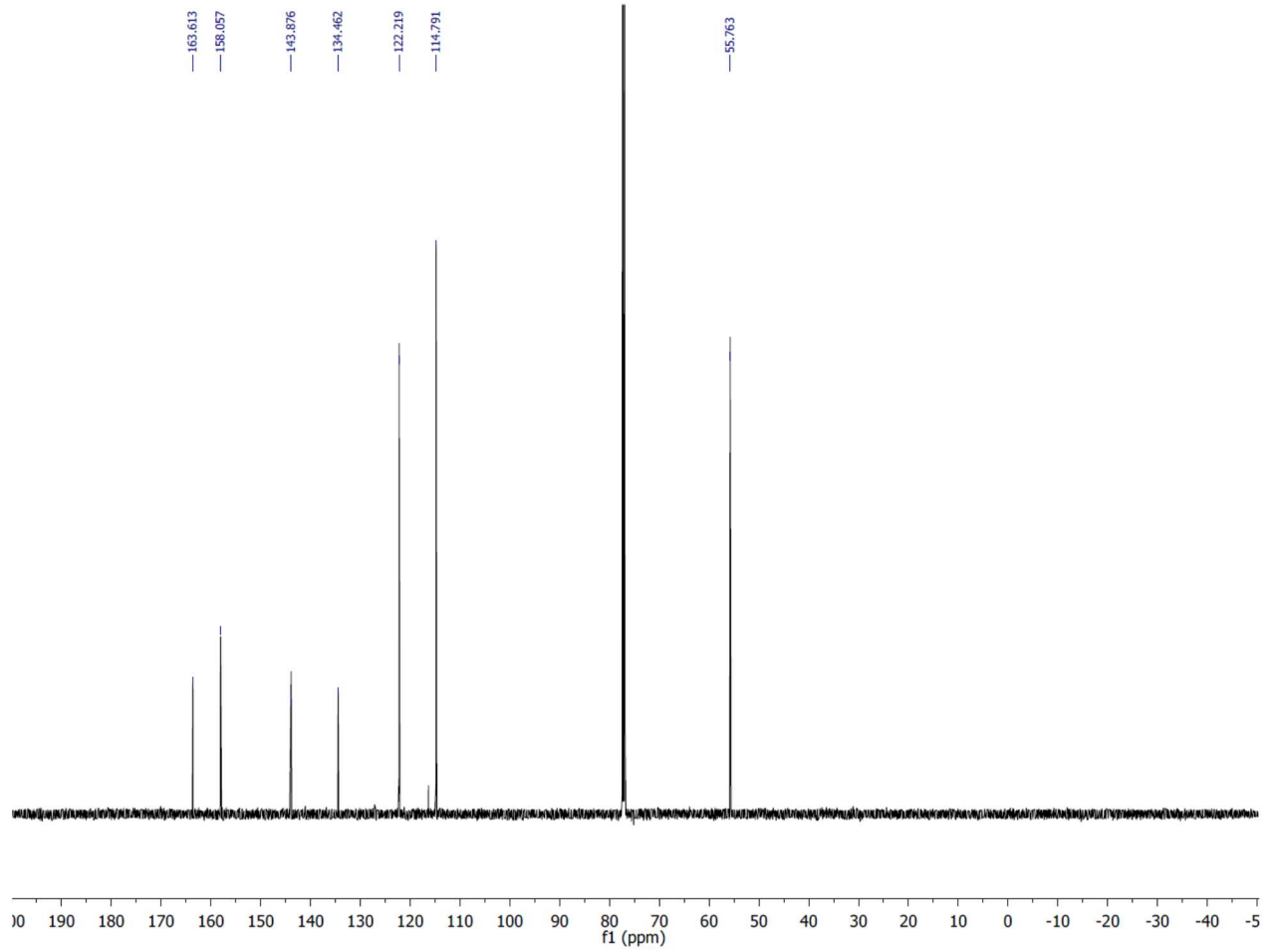
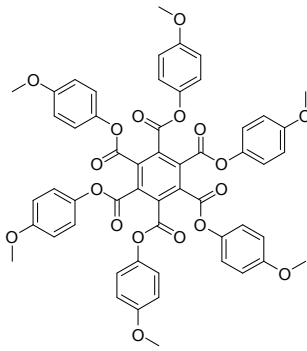


Sample Name	Exp <sup>2</sup>	Position	vial1	Instrument Name	QTOF	User Name	CIF-PC\admin
Inj Vol	0.3	InjPosition		SampleType	Sample	IRM Calibration Status	Success
Data Filename	QTOF1302622.d	ACQ Method	AESI-100-1000-pos.m	Comment		Acquired Time	10/17/2013 10:3



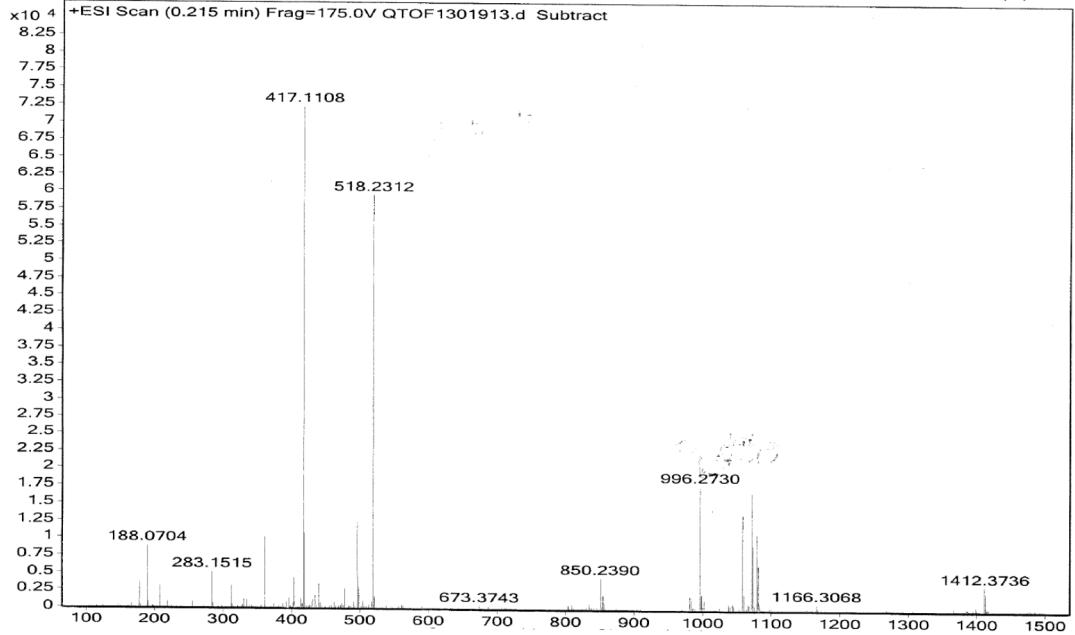
**Mellitic acid (hexa-4-methoxyphenyl) ester (6)**



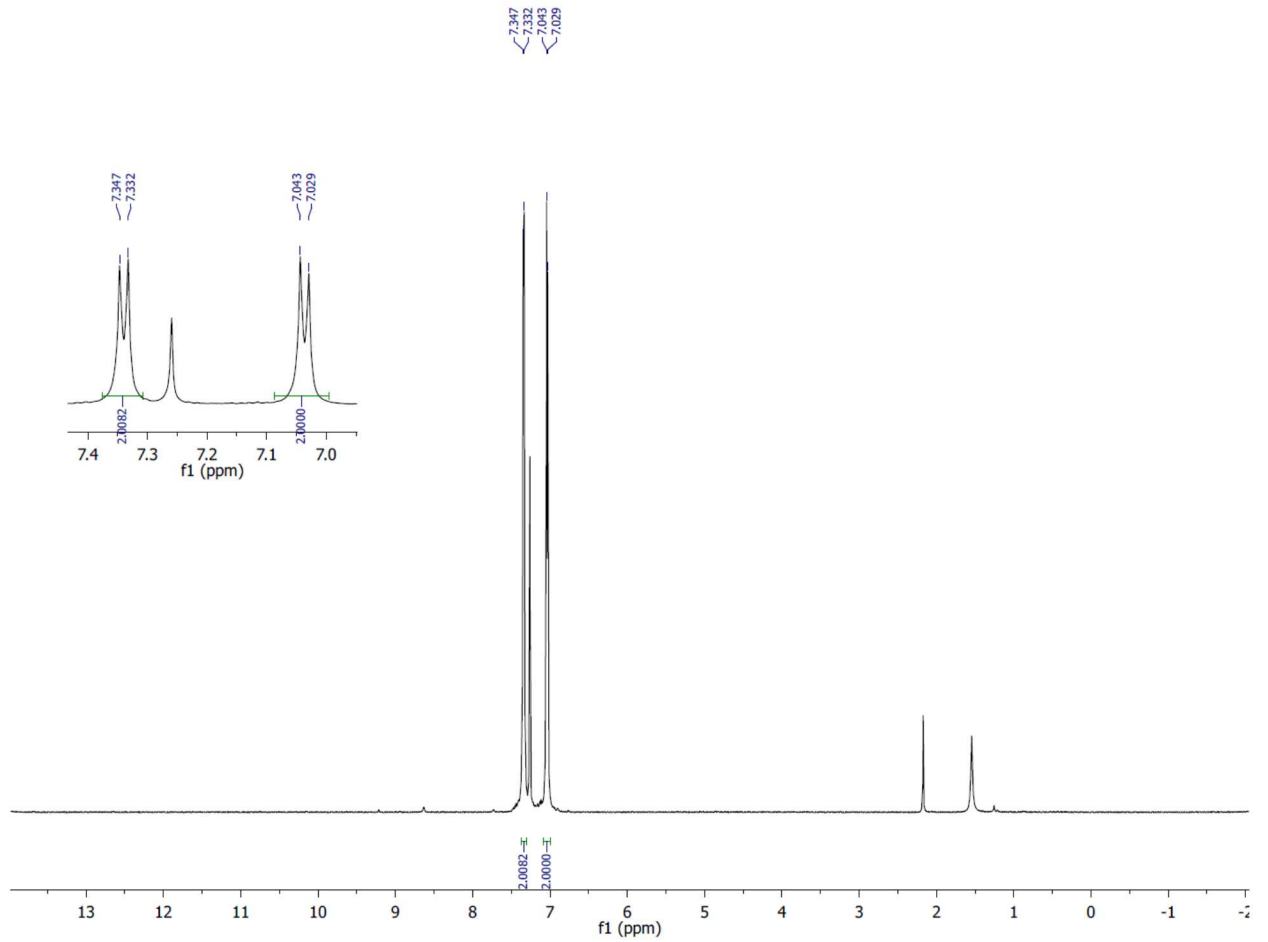
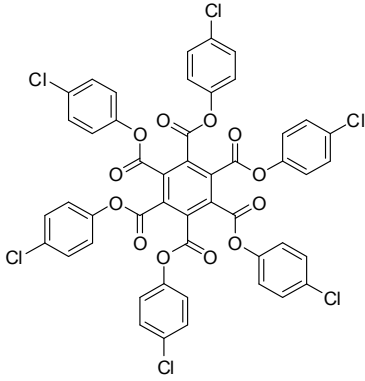


150 MHz, CDCl<sub>3</sub>

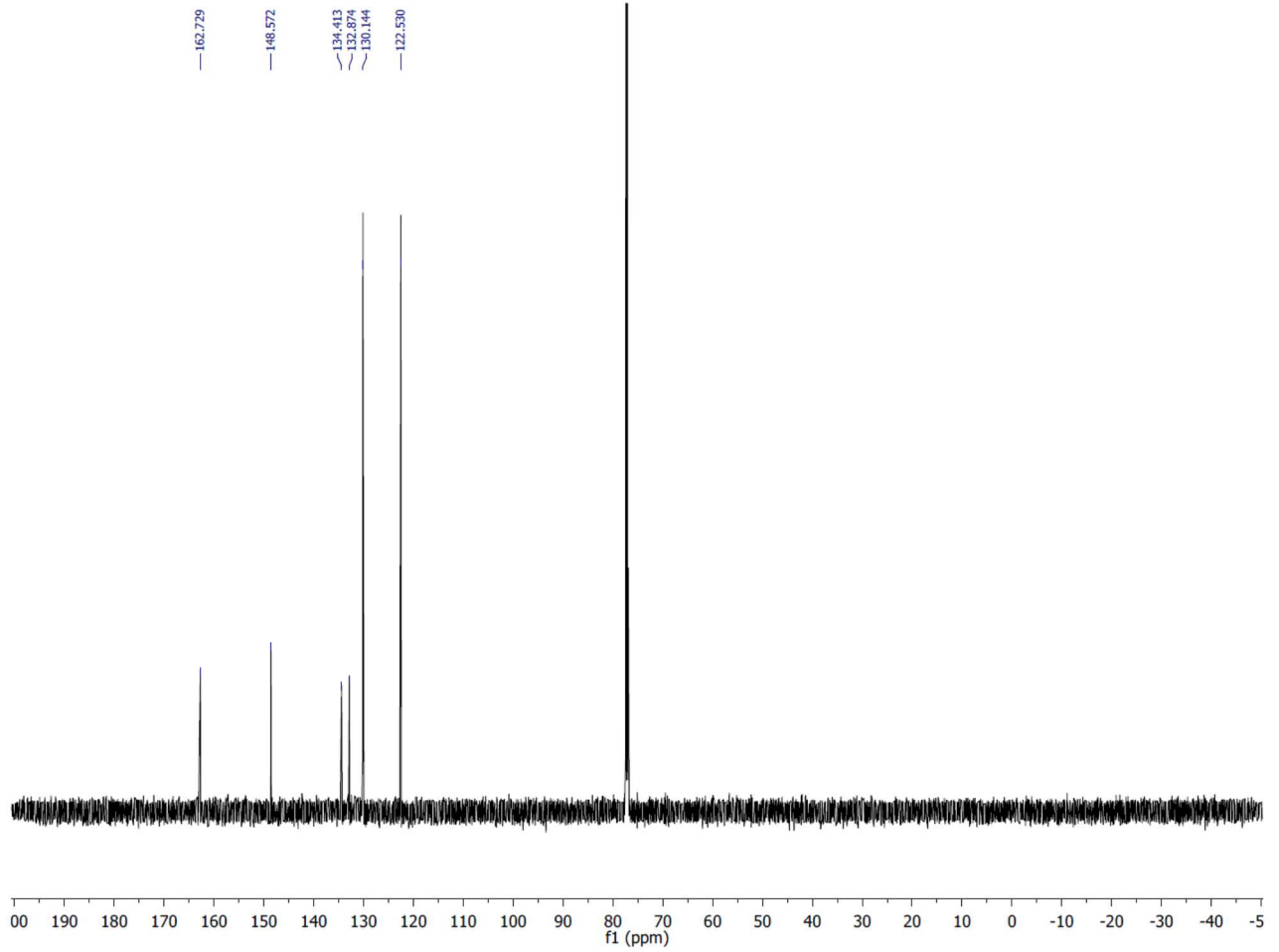
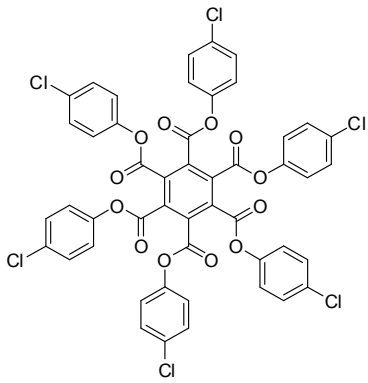
Sample Name	459	Position	vial1	Instrument Name	QTOF	User Name	CIF-PC\admin
Inj Vol	1	InjPosition		SampleType	Sample	IRM Calibration Status	Success
Data Filename	QTOF1301913.d	ACQ Method	ESI-pos.m	Comment		Acquired Time	6/25/2013 4:09:32 PM



### Mellitic acid (hexa-4-chlorophenyl) ester (7)

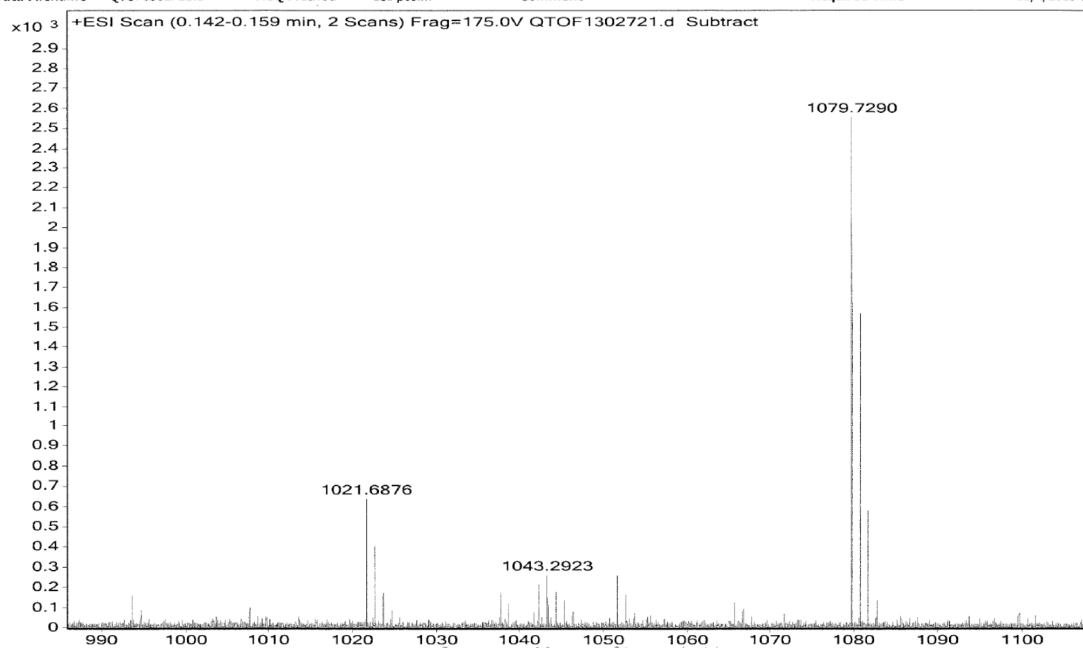


600 MHz, CDCl<sub>3</sub>

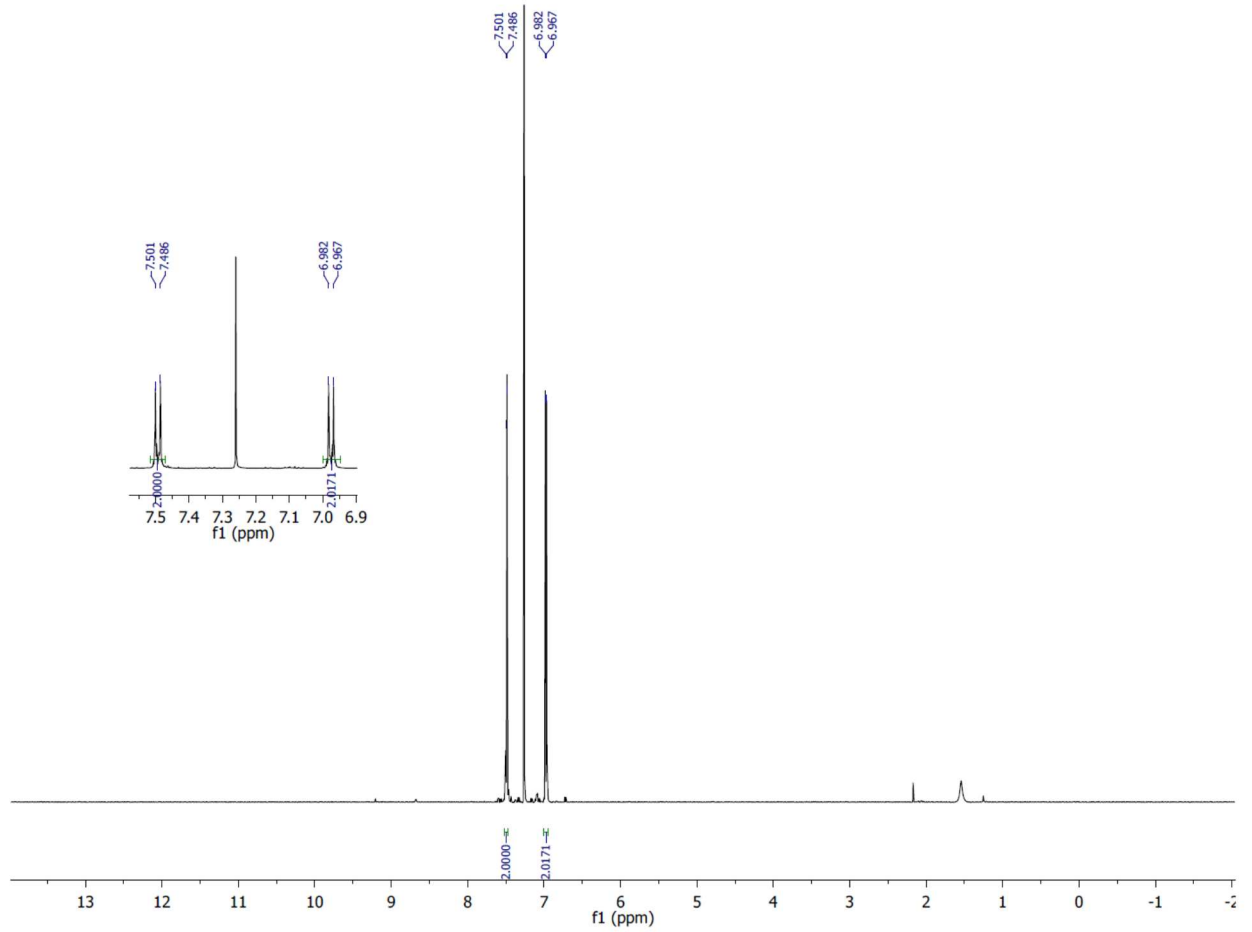
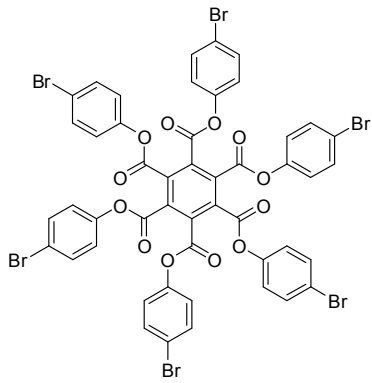


150 MHz, CDCl<sub>3</sub>

Sample Name	Exp47	Position	vial1	Instrument Name	QTOF	User Name	CIF-PC\admin
Inj Vol	2	InjPosition		SampleType	Sample	IRM Calibration Status	Success
Data Filename	QTOF1302721.d	ACQ Method	ESI-pos.m	Comment		Acquired Time	11/4/2013 9:55:32 A

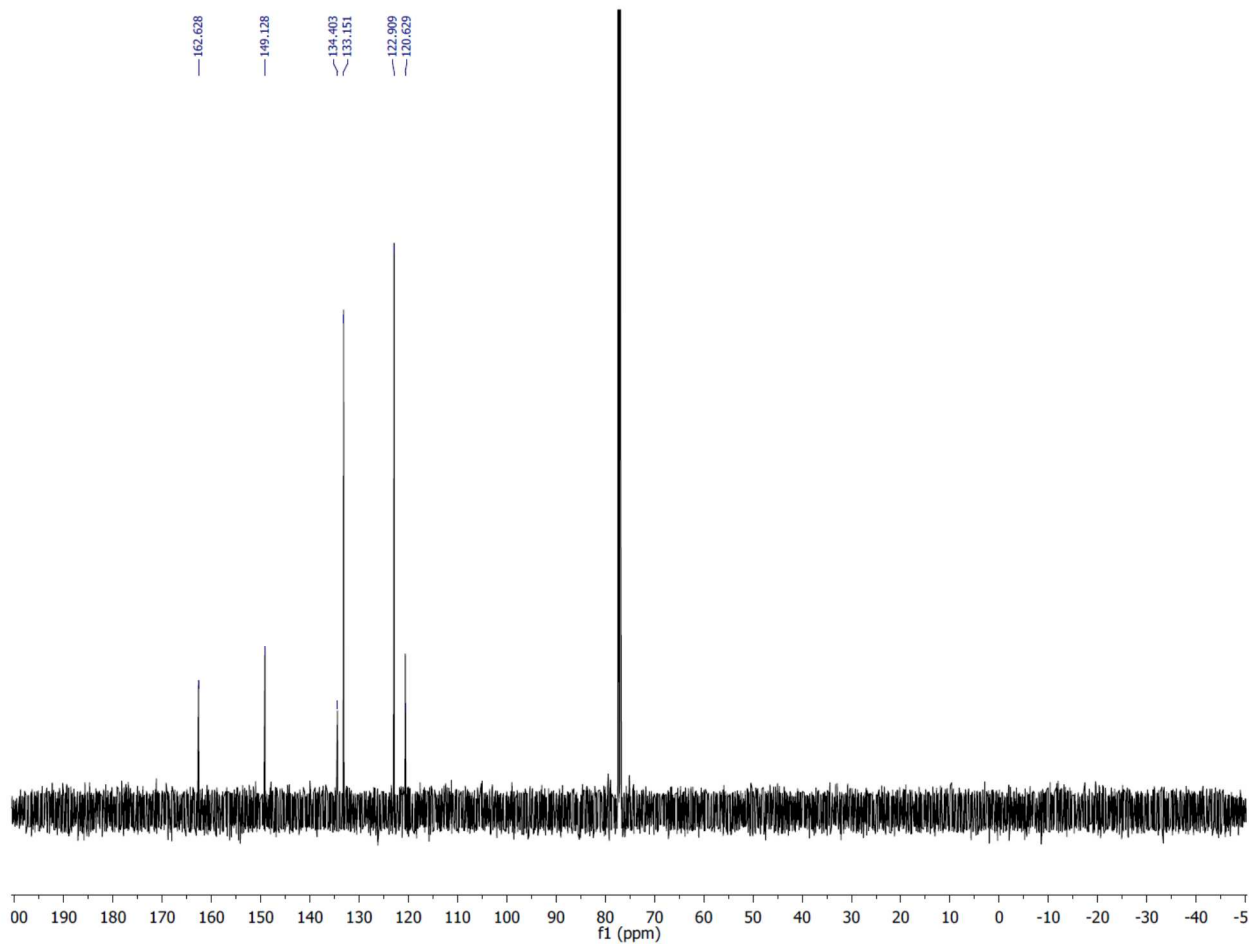
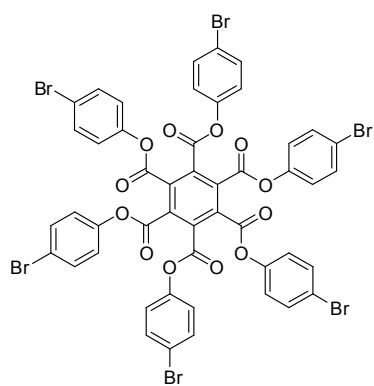


**Mellitic acid (hexa-4-bromophenyl) ester (8)**



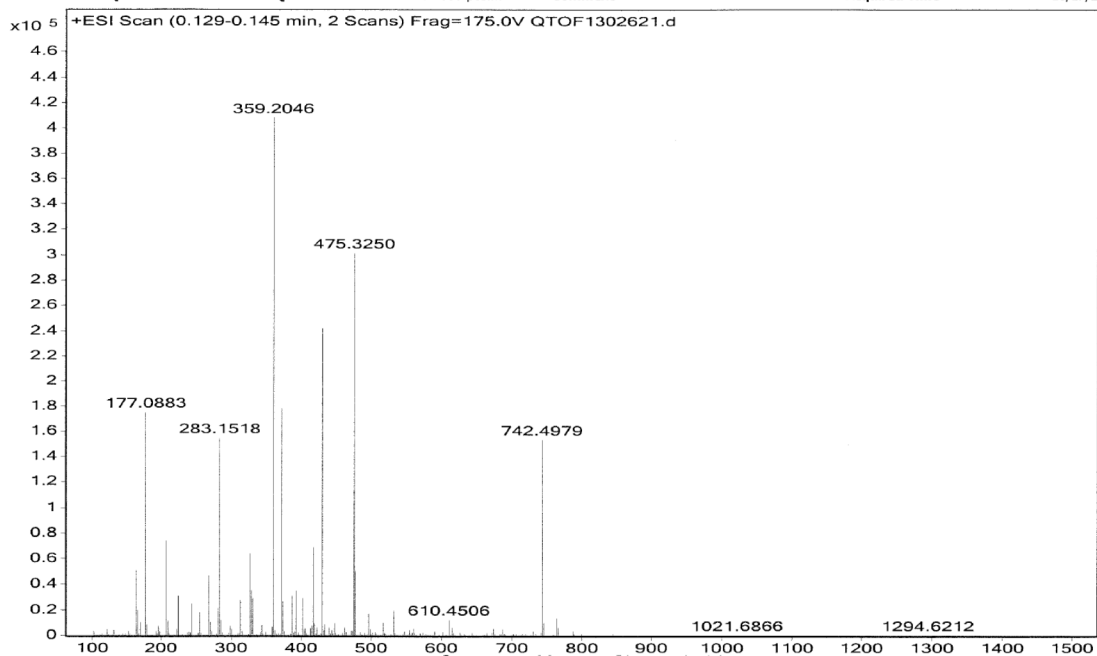
600 MHz, CDCl<sub>3</sub>

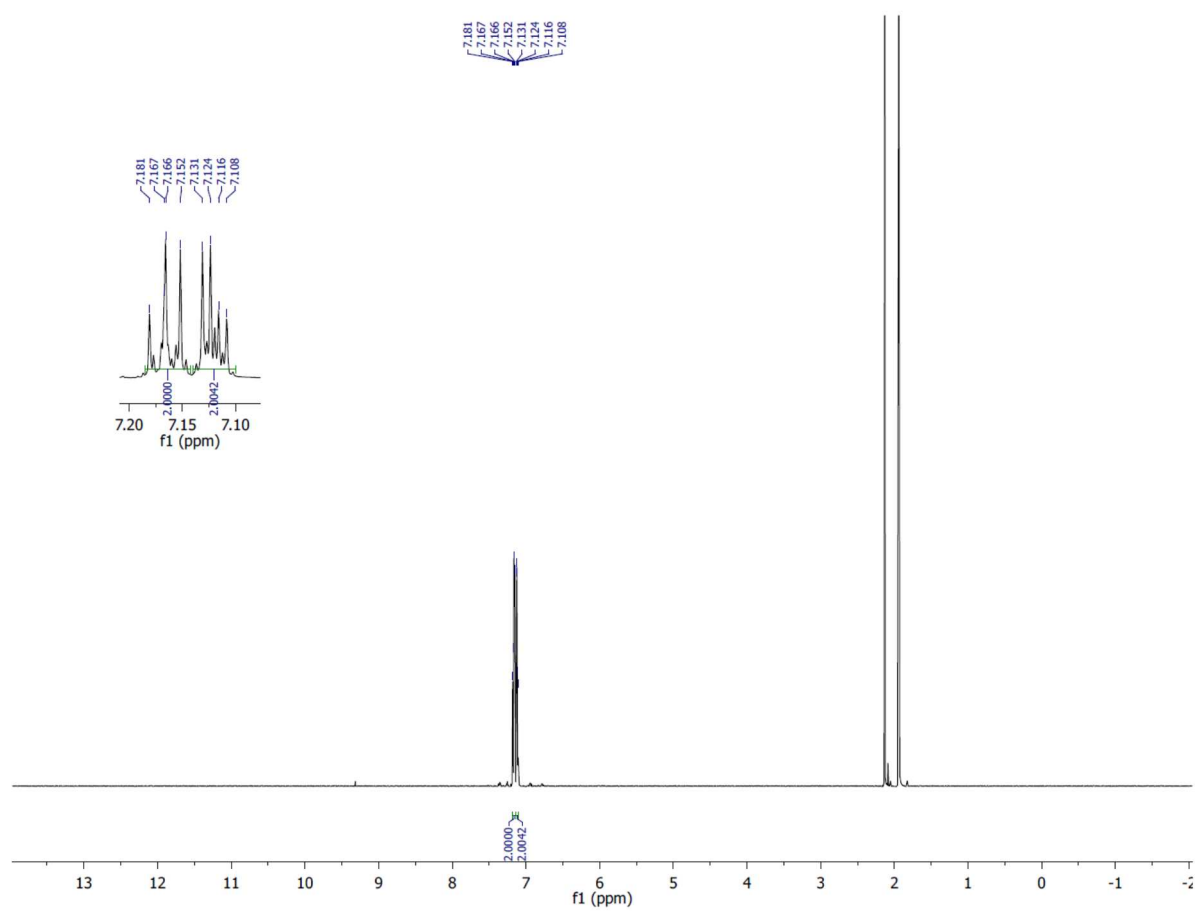
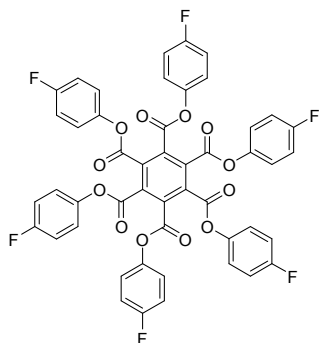


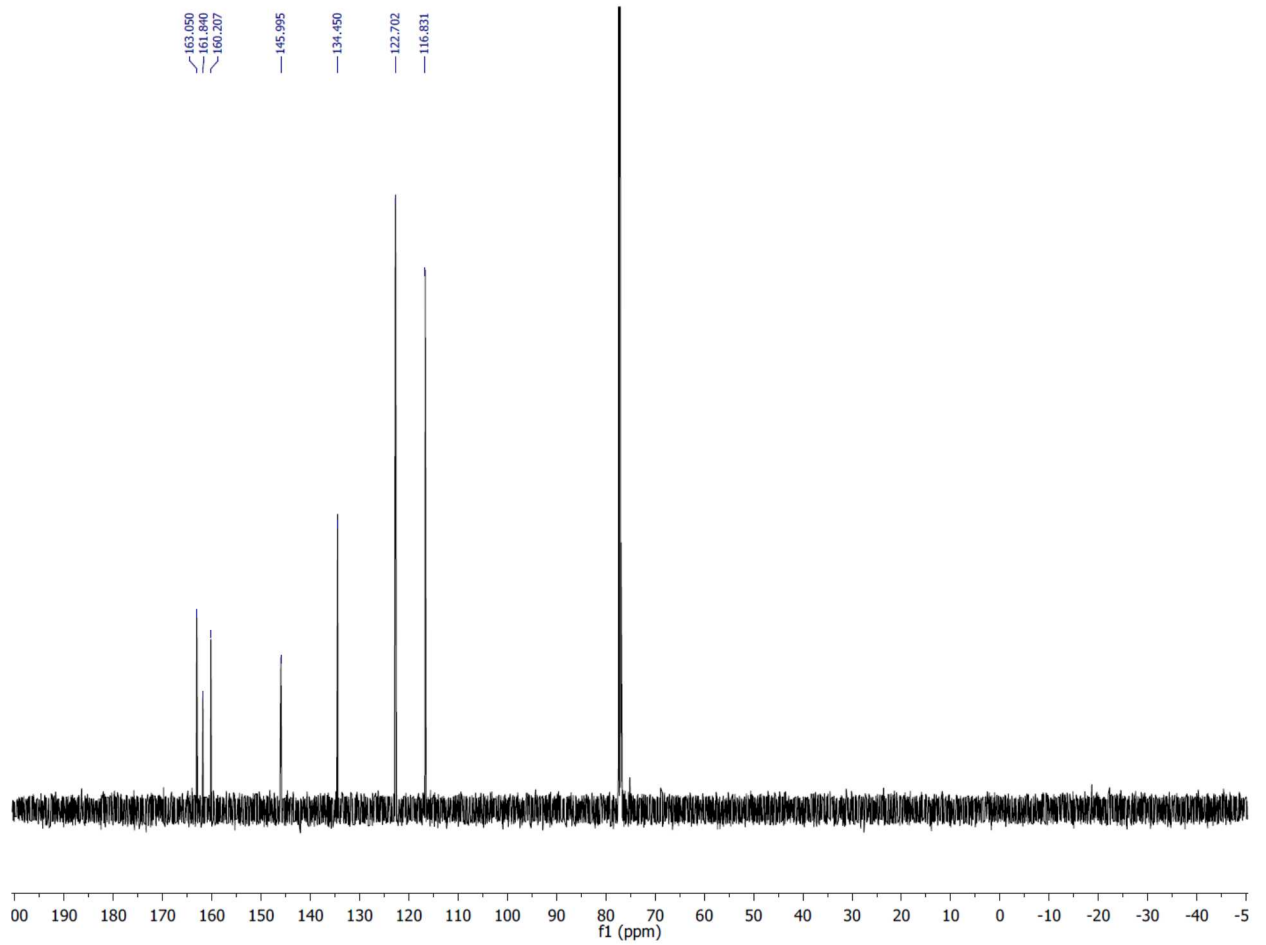
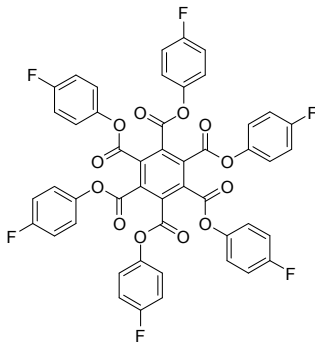


150 MHz, CDCl<sub>3</sub>

Sample Name	Exp62	Position	vial1	Instrument Name	QTOF	User Name	CIF-PC\admin
Inj Vol	1	InjPosition		SampleType	Sample	IRM Calibration Status	Success
Data Filename	QTOF1302621.d	ACQ Method	AESI-100-1000-pos.m	Comment		Acquired Time	10/17/2013 11

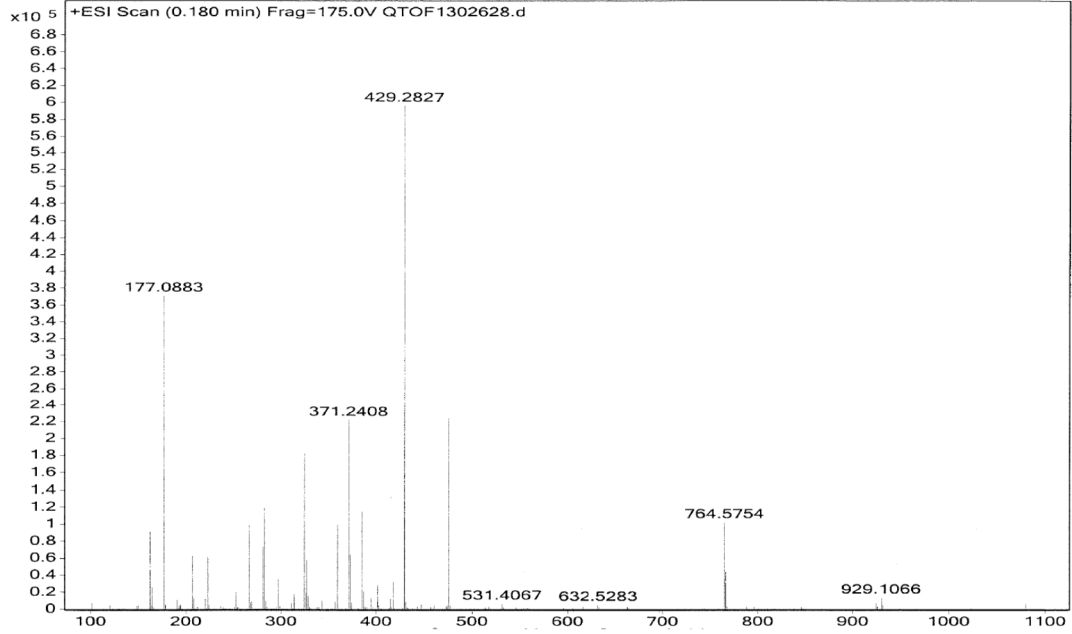


**Mellitic acid (hexa-4-fluorophenyl) ester (9)****600 MHz, CD<sub>3</sub>CN**

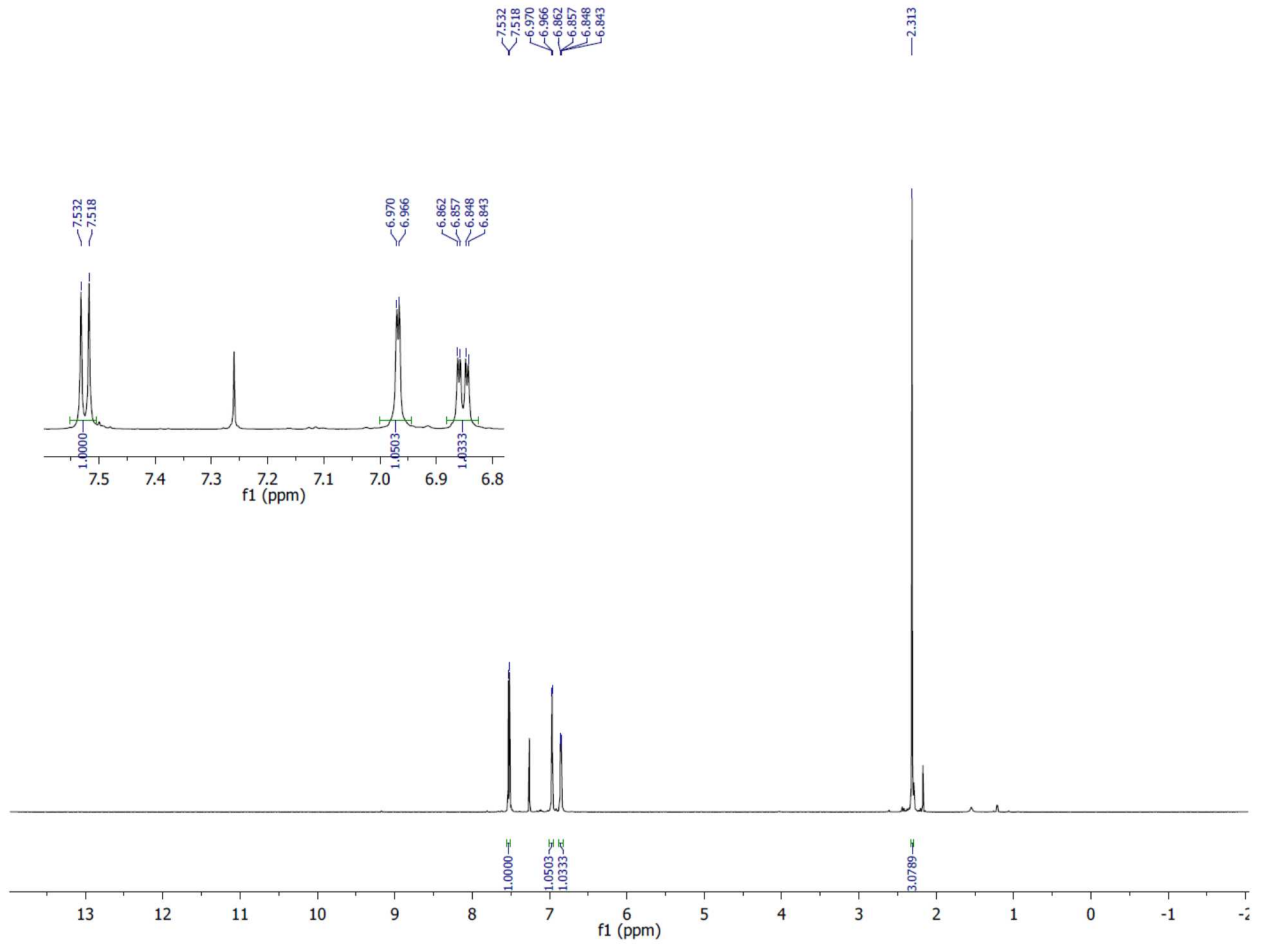
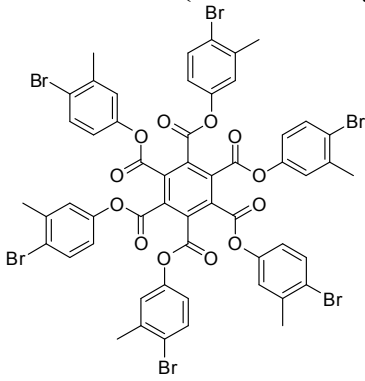


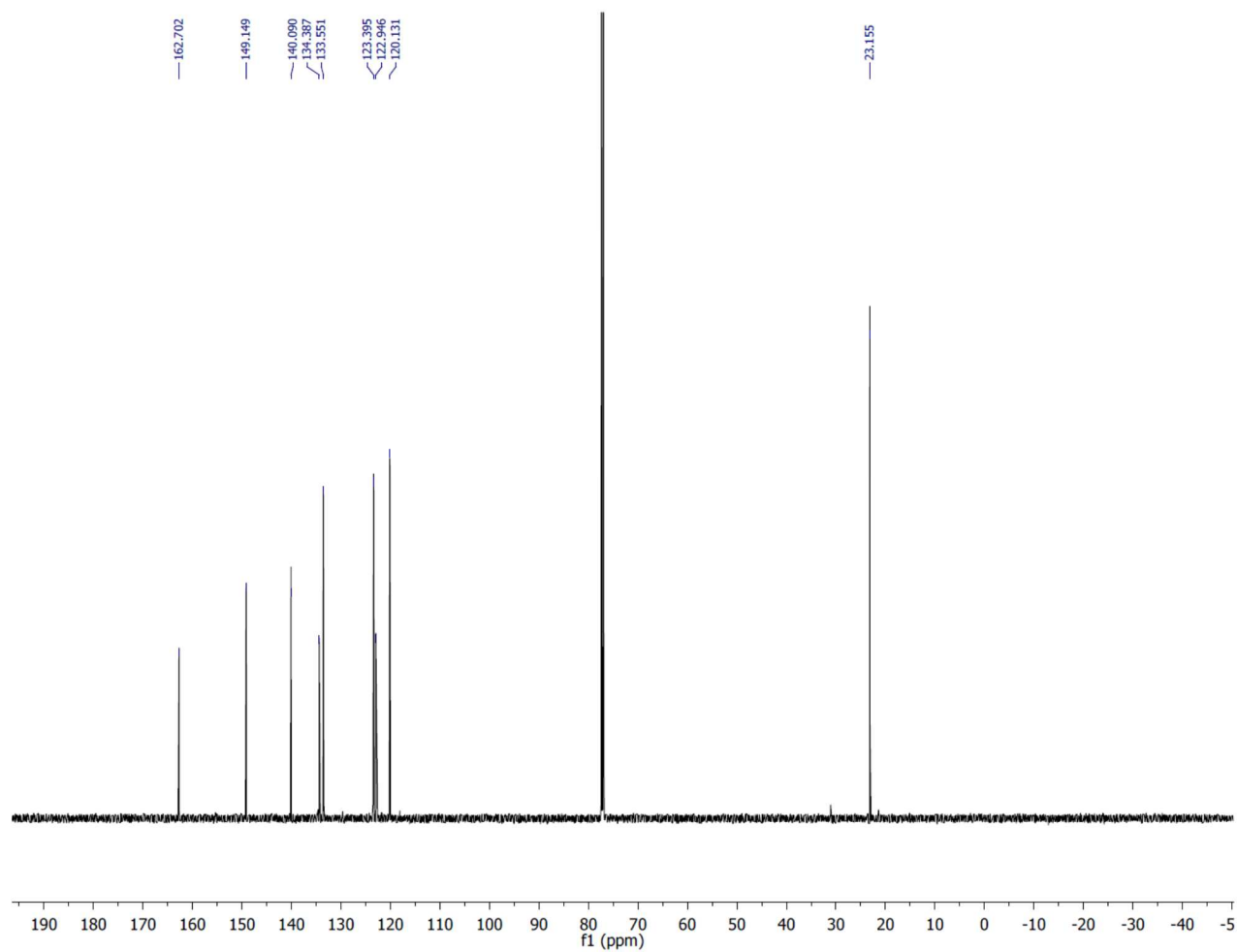
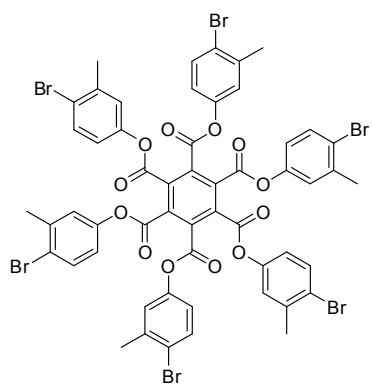
150 MHz, CDCl<sub>3</sub>

Sample Name	Exp54	Position	vial1	Instrument Name	QTOF	User Name	CIF-PC\admin
Inj Vol	4	InjPosition		SampleType	Sample	IRM Calibration Status	Success
Data Filename	QTOF1302628.d	ACQ Method	ESI2-pos.m	Comment		Acquired Time	10/17/2013 1:46:44 P



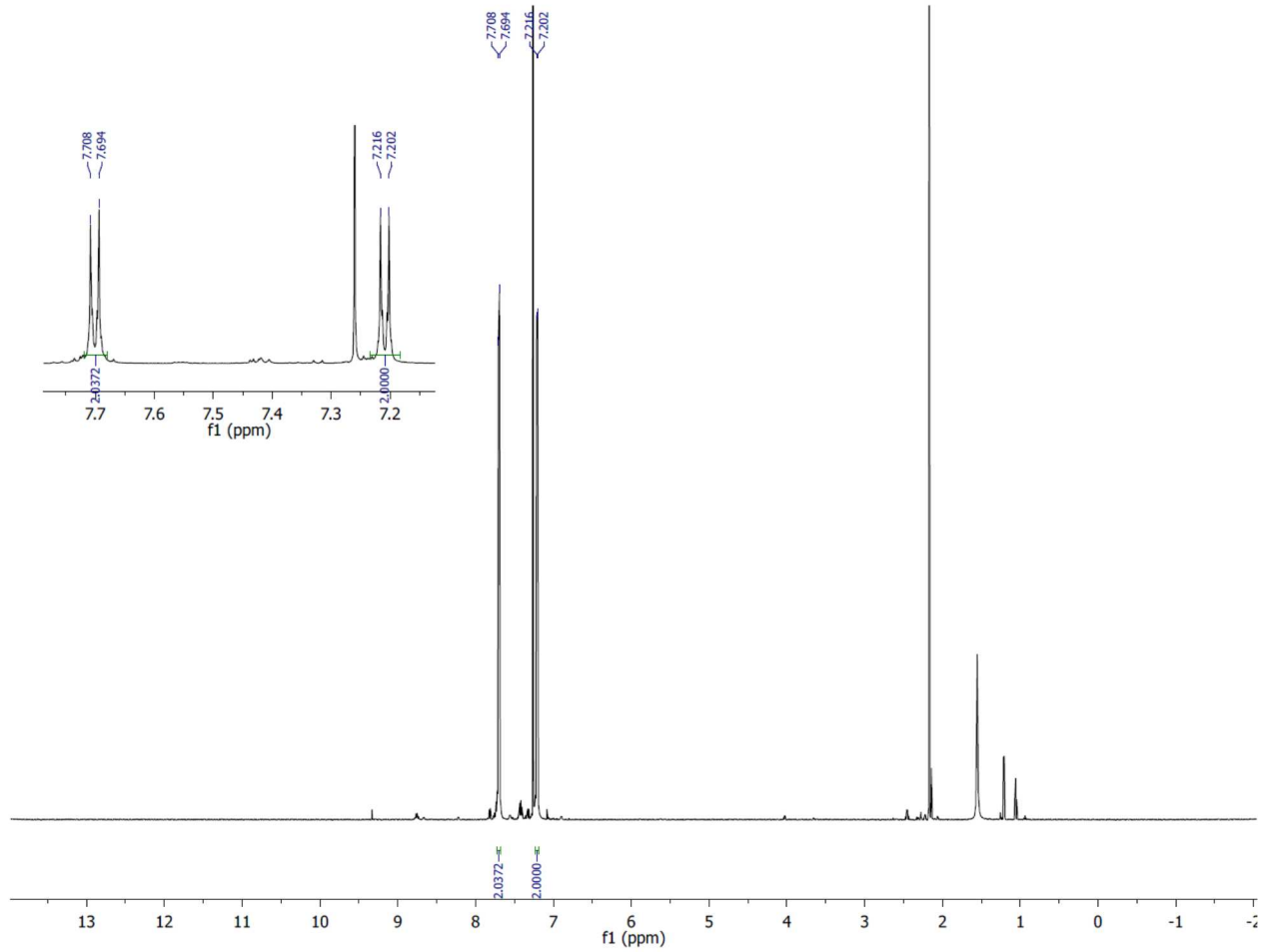
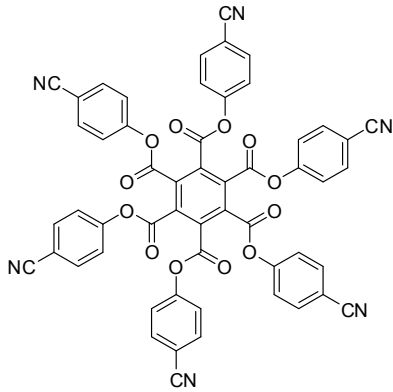
### Mellitic acid (hexa-3-methyl-4-bromophenyl) ester (10)





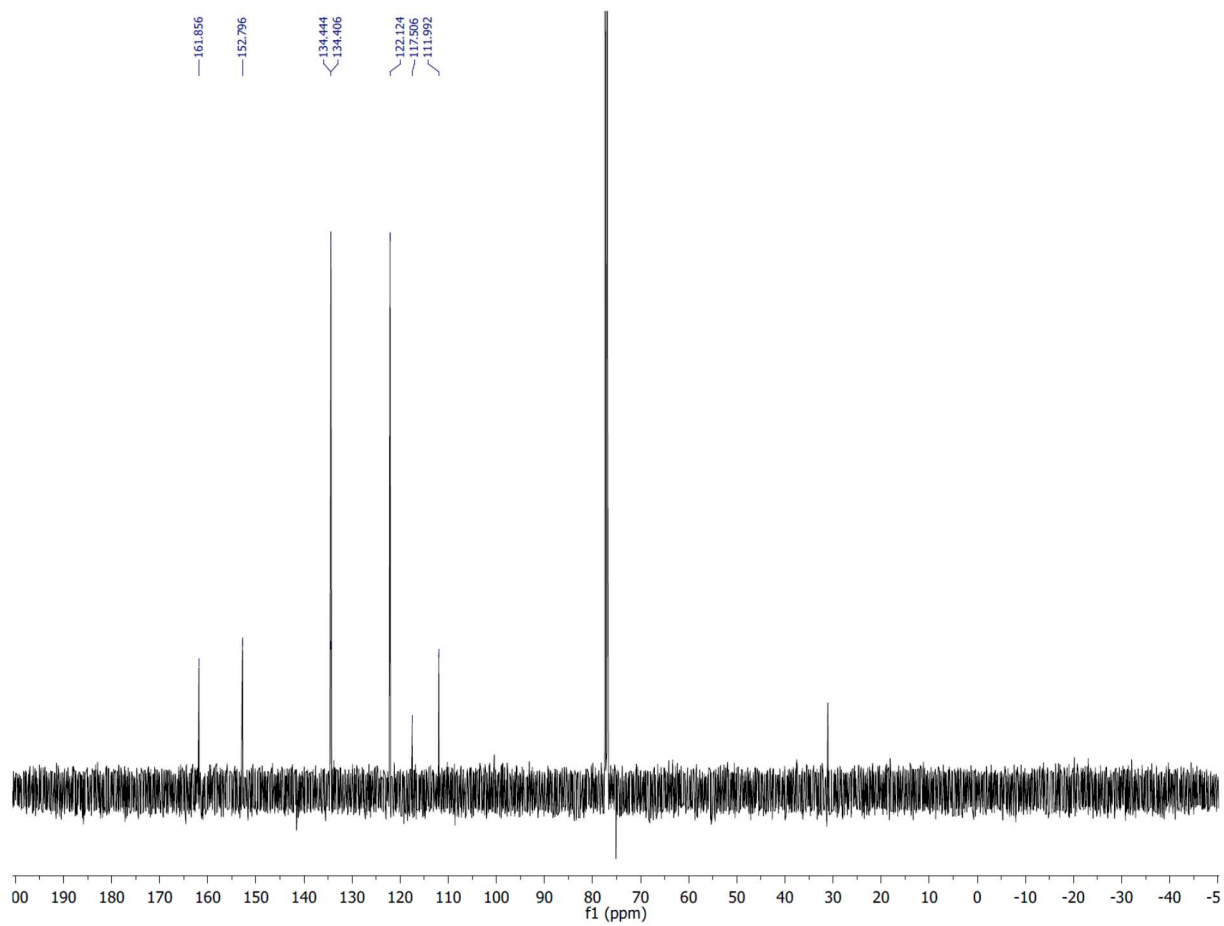
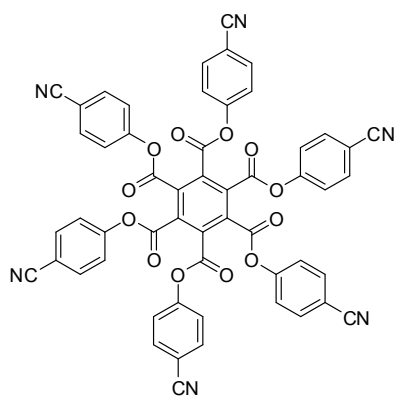
150 MHz, CDCl<sub>3</sub>

### Mellitic acid (hexa-4-cyanophenyl) ester (11)



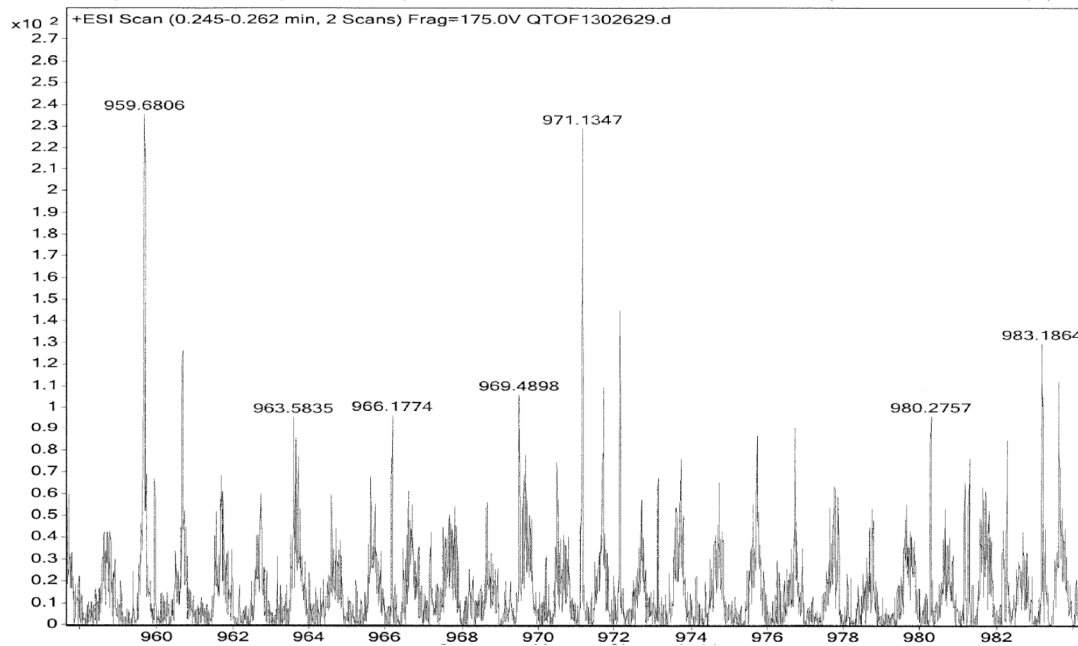
600 MHz, CDCl<sub>3</sub>





150 MHz, CDCl<sub>3</sub>

Sample Name	Exp61	Position	vial1	Instrument Name	QTOF	User Name	CIF-PC\admin
Inj Vol	4	InjPosition		SampleType	Sample	IRM Calibration Status	Success
Data Filename	QTOF1302629.d	ACQ Method	ESI2-pos.m	Comment		Acquired Time	10/17/2013 1:50:33



## APPENDIX B. SUPPORTING INFORMATION FOR CHAPTER 3

### Selection of chemical amplifier

Many properties of pharmacological drugs can be improved with the careful implementation of proper drug delivery systems.<sup>129</sup> One area where improvement could be used is the chemical linker by which the payload is delivered.<sup>130</sup> The ideal chemical linker should have a switch that, when activated, releases a chemical payload or cargo and meet certain criteria for practical use.<sup>131</sup> For our purposes, the linker is subject to the following criteria: kinetics faster than those previously reported ( $\tau < 1$  hour), stable in water for long enough for the payload to be delivered ( $\tau > 1$  day), with benign byproducts, and a synthetic scheme that would allow for placement of drug molecules as a payload. Proper selection of the chemical linker could then be used in more advanced molecules and molecular machines, such as a chemical amplifier.

Self-immolative linkers have become indispensable molecules for connecting a cleavable mask to an output cargo molecule.<sup>132-134</sup> Upon an input reaction that cleaves the mask, self-immolative linkers release their output cargo, and the molecule “self-destructs” into harmless byproducts. Self-immolative linkers have proven to be extremely useful in enzyme-activated prodrugs,<sup>135-140</sup> chemical sensors,<sup>141-143</sup> traceless linkers,<sup>144-147</sup> biological probes,<sup>148-151</sup> and degradable polymers.<sup>152-154</sup> Released chemical cargoes are often biomolecules, drugs, or reporters such as fluorescent dyes. Linker structure can aid prodrugs by improving stability, solubility, biodistribution, pharmacokinetics, bioavailability and activation.

The ideal self-immolative linker is simple, stable, compatible with water, and transforms into a benign byproduct upon releasing the output cargo. Furthermore, such linkers should be easy to synthesis, readily adaptable to a variety of inputs and outputs, and quickly release the output cargo upon the input reaction. In particular, some common self-immolative linkers suffer from slow release of their output cargo. New linkers that incorporate these desirable features would be highly useful.

### **Experimental:**

Phenyl hydrogen phthalate, was synthesized according to a known procedure.<sup>155</sup>

Synthesis of both cis and trans- 2-((p-methoxyphenoxy)carbonyl)cyclohexanecarboxylic acid and p-methoxy phenyl hydrogen phthalate were prepared by adapting the method described in literature.<sup>155</sup> Phenyl hydrogen phthalate and p-methoxy phenyl hydrogen phthalate had <sup>13</sup>C-NMR and <sup>1</sup>H-NMR in good agreement with literature values. The cis and trans cyclohexane 1,2 p-methoxy phenolate carboxylate had <sup>13</sup>C-NMR and <sup>1</sup>H-NMR in good agreement with expected values. For full synthetic procedures, see chapter 7.

### **Kinetics:**

Kinetic experiments were performed using the Agilent 8453 UV-Visible spectrometer and plotted using Kaleida graph version 4.1.1 plots were fitted to find the rate constant (k) or  $1/k = \tau$  Phthalic anhydride was monitored at 300 nm, phenol was monitored at 270 nm and p-methoxy phenol was monitored at 285. All studies were done at 10 mM concentrations in phosphate buffered solutions with ultra pure water.

## Computational methods:

All the molecular geometries of the electronic states of all molecules were optimized and transition states were found under the DFT level of theory using the B3LYP or M06-2X functionals and the 3-21+G\* or 6-311++G\* basis set.<sup>40</sup> The stationary points were found to have zero imaginary frequencies, and all energies contain a correction for the zero-point energy. All the single-reference computations were computed with GAMESS suit.<sup>41</sup> The hybrid B3LYP functional used consists of the Becke 3-parameter exchange<sup>42, 43</sup> functional with the correlation functional of Lee, Yang, and Parr<sup>44</sup>. This and related DFT functionals have been shown to give quite reasonable geometries for ground state molecules.<sup>45-47</sup> The M06-2X is a meta hybrid GGA functional with double exchange energy (54% hartree fock exchange energy) that has been shown to be a very good functional for main group elements and kinetics. Polarizable continuum model (PCM) was used to approximate solvent conditions in water. Further solvent approximations were attempted but were too computationally expensive to be studied to satisfaction.

## Results and Discussion:

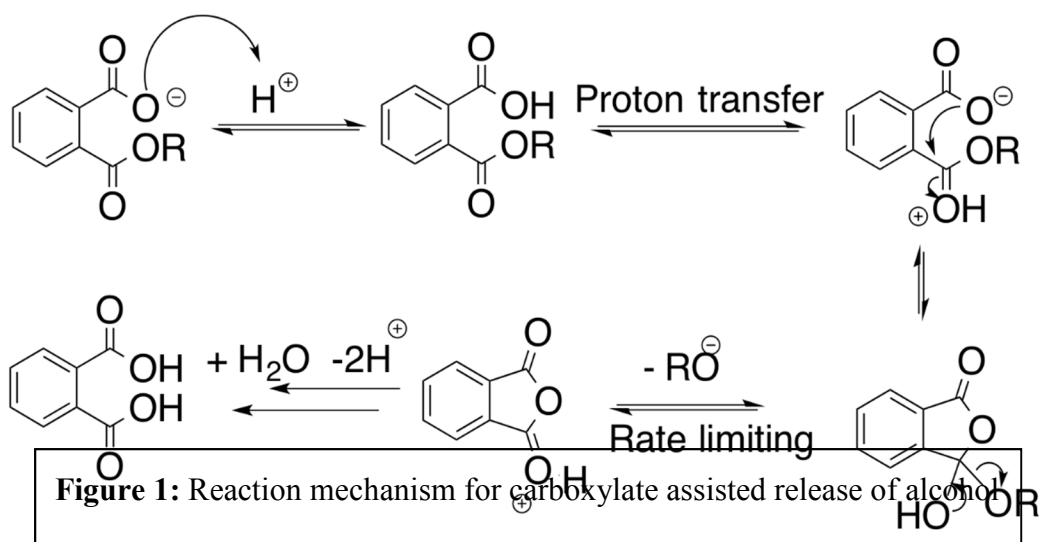


**Figure 1:** Reaction mechanism for carboxylate assisted release of alcohol

There are three parts to the selected linker: the trigger, the base system, and the payload released. The phenyl hydrogen phthalate has been shown to be a good candidate for a system and is the metric to which other linkers are compared. Shown below is the mechanism that was computationally determined for a neutral pH system. Given this mechanism, we would expect, and we observe, a pH dependence on the system.

**Cargo:**

The ultimate payload release should have some sort of functionality or emulate some functionality. However, for our purposes of a proof of concept study, any alcohol that is easily observable and demonstrated appropriate kinetics could be considered. Aliphatic alcohols were for the most part not extensively explored because of the known slow reaction times, even in the hydrogen phthalate case. Molecules useful for chemical sensing, such as coumarin and coumarin derivatives have been shown to be appropriate, particularly in the hydrogen phthalate case<sup>131</sup>, but are not discussed here. In particular, phenol and the phenolic derivative p-methoxy phenol were used. Phenol serves as a good analogue because several drugs contain a phenolic alcohol group that could be used as the esterified alcohol in our linker system. P-methoxy phenol was used to show that even with some electron donating character (which we expect to, and was observed to slow down the reaction), phenolic esters could still be useful.

After synthesis of p-methoxy phenolate hydrogen phthalate and phenyl hydrogen phthalate, the two alcohols could be compared for potential use. In the p-methoxy phenol case, a UV-wavelength of 285 was selected because it is conveniently far from any other species' wavelength, thus the kinetic plots show only growth that corresponds to the alcohol. The anhydride formation was not observed because, unlike the aromatic case,

the aliphatic cyclohexanes do not strongly absorb UV-light. For the phenol case, phenol has a UV-spectrum that overlaps with the phthalic ester, therefore the formation of the anhydride was the species observed, as the anhydride absorbs at a sufficiently different wavelength than any other species. Thus we can see the release of phenol (growth in the plot corresponding to the formation of the anhydride) and the anhydride ring opening to the phthalic acid (decay of the curve).

In both instances it can be shown that the release is pH dependent. For both phenol and p-methoxy phenol, neutral pH (~7, phosphate buffer) showed faster kinetics for release of the payload than lower pH (~5.1 phosphate buffer). This is consistent with the computational data observation that the protonation accompanied with a lower pH raises the barrier of activation. In the case of the phenol, the release of the alcohol was so fast that we were unable to observe the kinetics at neutral pH, only the reopening of the anhydride was observed. Unsurprisingly the p-methoxy phenol was slower than the phenol, as ether groups (the para substituted methoxy) are traditionally electron donating, thus destabilizing the released phenolate.

It should be noted that amide type linkers were investigated. However, amide linkers are slow to release the amine payloads at neutral pH. In very acidic conditions, (such as those that might be found in the stomach), the release kinetics were much faster. For the purposes of our chemical amplifier, the amide was not further considered since we deemed it to be unsuited to our criteria of appropriate kinetics at neutral pH. However, for other applications, amides may be considered, especially in the context of a pH sensitive linker.

**Base system:**

The hydrolysis of hydrogen phthalate is a classic case of neighboring group participation. The phenyl hydrogen phthalate has particularly been extensively investigated because of its fast kinetics of release in water at neutral pH, the mechanism of which has seen previous investigation.<sup>156-159</sup> It is also shown that the mechanism is pH dependant, such that the phenyl hydrogen phthalate is a shelf-stable compound when stored away from moisture, but this compound hydrolyzes rapidly in water at neutral pH. We discuss a more generalized case of the phthalate system with different chemical payloads and bases, as it pertains to potential use in further functionalized systems. It has been determined that the fast ester hydrolysis of this compound is a case of intramolecular catalysis wherein the neighboring carboxylate group displaces the alcohol to generate a water-unstable anhydride that in turn spontaneously hydrolyzes to phthalic acid. These factors make the phthalate system ideal for the fast release of a chemical payload in further functionalized systems.

Although the phthalic acid system is a good candidate because of its kinetics, increasing the number of carboxylate groups on the ring system make the aromatic base system difficult to work with and transform because of the complex electronic and steric environment involved. A number of unpublished experiments were done demonstrating this fact, even with as few as three carboxylate groups. Because of this, cyclohexane-1,2-dicarboxylic acid was investigated for potential use in both the cis and trans forms.

We identify our target kinetics to have tau values of less than 1 hour at room temperature and under neutral conditions in order to be competitive with other published amplifiers. In the case of the trans base, the tau values were so high as to be difficult to obtain accurately in the timeframe we investigated for the p-methoxy phenol. When a



better leaving group of phenol was used, the tau value was still  $15,625 \text{ s}^{-1}$  (see figure 2). Given this, it was determined that the trans-cyclohexanes carboxylic acid would be poor candidates for linkers since these values fell outside of the range of interest. The high tau values are likely a result of the trans-five member ring junction that would be required for the neighboring group participation required to kick off the phenolic alcohol.

The cis cyclohexane dicarboxylic acid was also investigated for potential use as a linker. The all cis-cyclohexane hexacarboxylic acid is commercially available and can be esterified through simple Fischer esterification methods making it a convenient candidate. Additionally, the model studies conducted were promising from a kinetics point of view. The tau value of the phenol was  $127 \text{ s}^{-1}$  and the p-methoxy phenol was  $692 \text{ s}^{-1}$ . Both of these values were within the acceptable range for kinetic, even though they were considerably slower than the hydrogen phthalate case. Of concern is cis-trans epimerization with the cis cyclohexane carboxylic acid and its ester derivatives. At neutral conditions and low heat, epimerization is slow, but at either basic or acidic conditions, epimerization happens more readily to the less sterically strained trans cyclohexanes. This is especially evident as the number of carboxylic acids on the ring increases. For purposes of use as an amplifier, the cis bases system was not investigated for this reason.

However, even though the cis base system may not be an ideal candidate for the use in an amplifier system, it may be useful for other applications. Particularly, if some binding event needs to happen before release, relatively slow hydrolysis-even after activation may be desirable. For drug delivery systems, this may be especially important. Such application is currently being investigated.

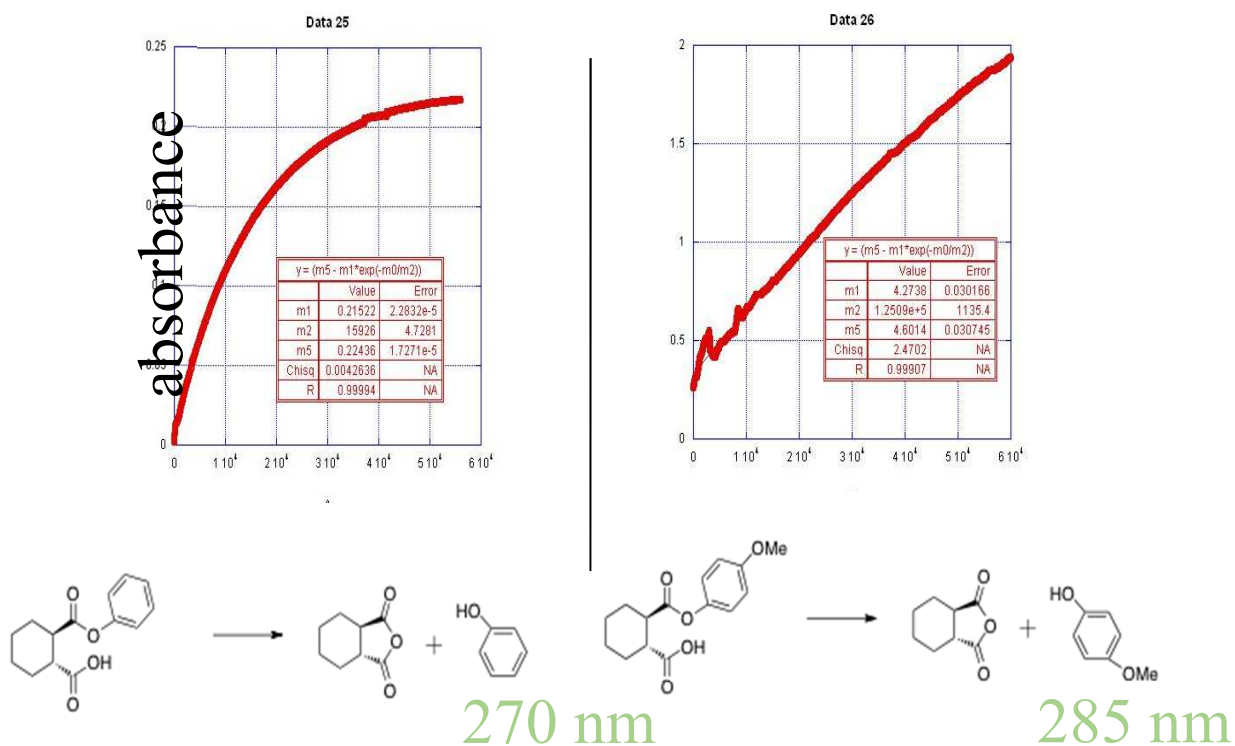


**Figure 2:** UV plots of the trans phenol (left) and trans p-methoxy phenol (right). Both are very slow, indicating that the trans may not be suitable for a base system.

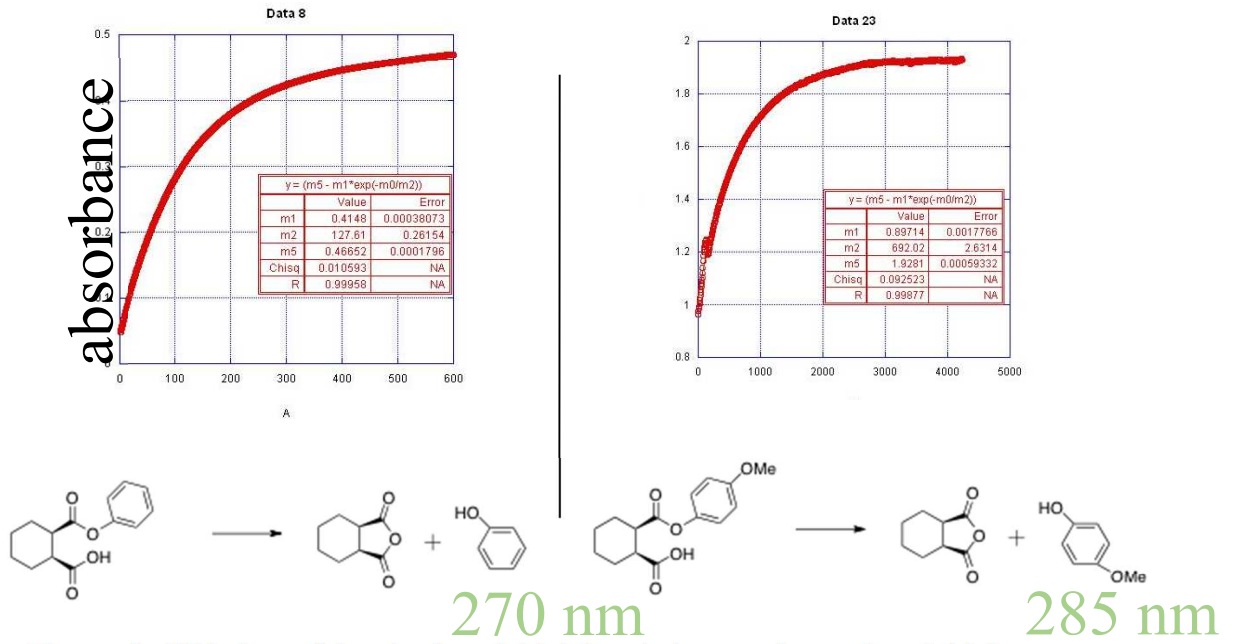


**Figure 3:** UV plots of the cis phenol (right) and cis p-methoxy phenol (right). Both are on a kinetics scale that makes them appropriate for use.

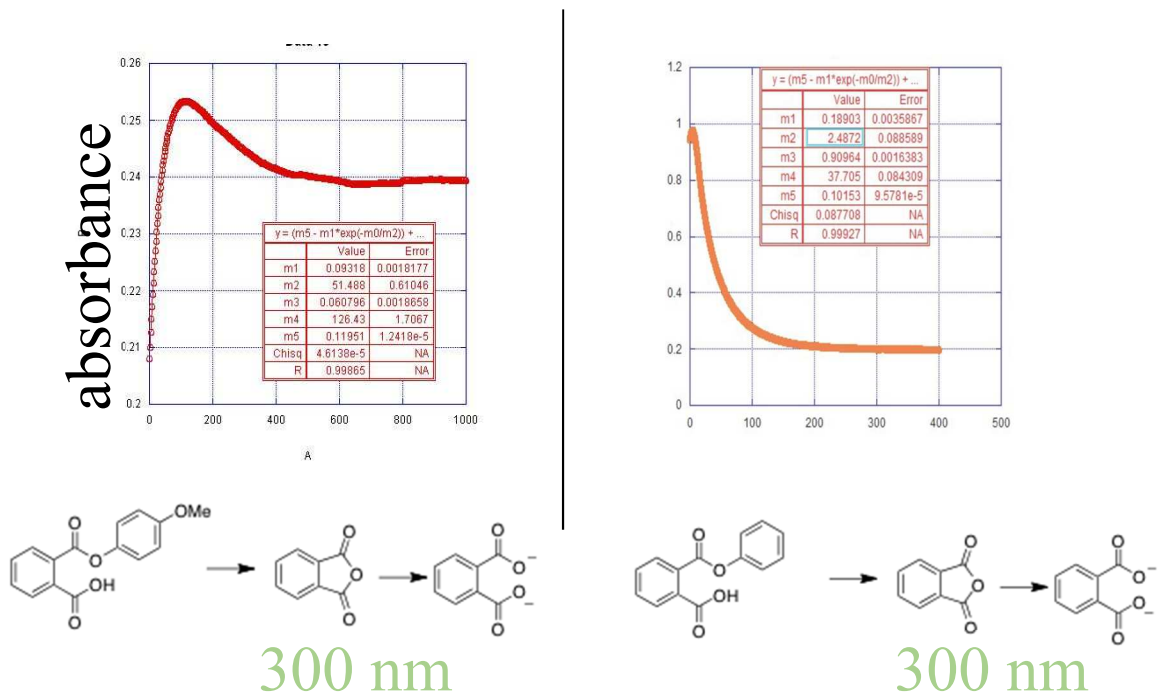


**Figure 4:** UV plots of the phthalate phenol and phthalate p-methoxy phenol (right). Both are quick and very desirable for kinetics purposes.

Tau values (s <sup>-1</sup> )				
	pH7 Phthalic	pH 7 trans	pH 7 cis	pH 4 Pthalic
Phenol	2.4	125000	127	50 (pH 5)
p-methoxy phenol	50.2	16000	692	114
p-nitro aniline	Very high	Not measured	Not measured	347

**Figure 5:** A summary of the tau values of relevant kinetics (as determined by UV) in different pHs. Other, amide linkers were also investigated but were too slow to measure over the indicated pH ranges **The**

**Trigger:**

Two triggers that have been previously investigated have been 2-(trimethylsilyl) ethanol (TMSE) and 2-nitro benzyl alcohol.<sup>131</sup> The TMSE group is sensitive to the fluoride ion and the 2-nitro benzyl alcohol is sensitive to UV-light irradiation. Both triggers have proven to be compatible with the phthalic system and the triggers are not further discussed here. These two triggers serve mostly as a proof of concept.

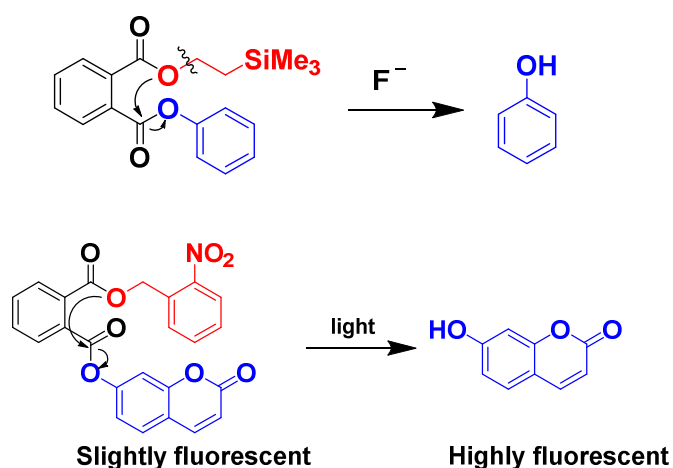


**Figure 6:**

Top: A TMSE trigger, activated by fluorine

Bottom: A 2-nitrobenzyl alcohol trigger, activated by UV-light

**Conclusion:**

Using a fluoride-sensitive 2-(trimethylsilyl)ethyl ether group to mask the catalytic carboxyl group, in combination with phenolic cargos, we find that aryl phthalate esters can indeed be exploited as self-immolative linkers. The saturated analogues of phthalic esters, cis and trans cyclohexane carboxylic acid, were also investigated. Although we did find these to have many of the criteria for a good linker, the kinetics made them less than ideal for investigation for more functionalized chemical machines, particularly chemical amplifiers.

Dendritic systems have been investigated for chemical amplification with some previous success.<sup>160-164</sup> Unlike most dendritic systems that rely solely on the number of functional groups, dendrimers for chemical amplification, also rely heavily on their structural relationship in order to undergo some transformation.<sup>132</sup> This transformation can then be used to do some useful “work”. We can therefore define these dendritic amplifiers as chemical machines capable of performing tasks such as chemical gating, signal amplification (taking one signal and transforming it into another, stronger signal) or drug delivery.<sup>132, 163, 165</sup>

The existing systems studied are limited in scope of what they are able to release, as they require specific molecules to act as triggers and specific linking systems. We propose a proof of concept of an amplification system that can accommodate a variety of prodrugs and have precisely controlled kinetics of release. Based on the discussion in chapter 3, we determined that mellitic acid with aromatic leaving groups as analogues for potential prodrug payloads with a single trigger attached would be the ideal target.

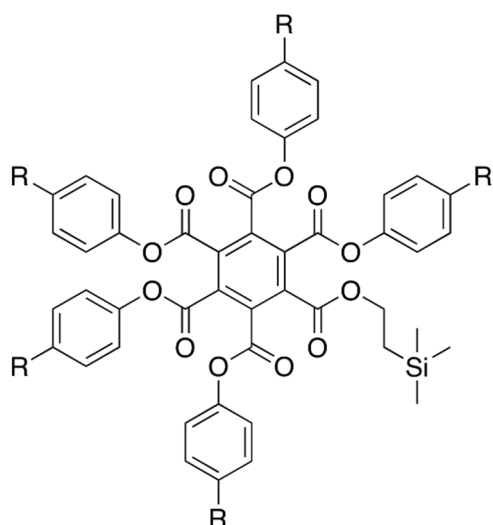


**Figure 1:** Target molecule where R=H, OMe or NO<sub>2</sub>

Mellitic acid provides several challenges as a base system, however, particularly synthetically. Mellitic acid cannot be easily esterified, even with the use of common coupling reagents, because of complex electronics and high steric hindrance.<sup>130</sup> Two techniques that have been shown to be successful in the synthesis of these systems are the cyclotrimerization of diester butynes and the previously discussed oxidative aromatization.<sup>166</sup> Both the cyclotrimerization and oxidative aromatization synthetic methods are discussed below for use as potential amplifier synthesis pathways.

### **Experimental:**

Syntheses of the benzene hexaesters were prepared via the oxidative aromatization as described in chapter 2. Transesterifications were done under high pressure and with increased temperatures to give modest yields. Cyclotrimerization was done catalytically with a bis-allyl ruthenium (IV) precatalyst that showed good tolerance for sterically

hindered butyne diesters.<sup>166</sup> Stoichiometric cyclotrimerizations were done with a zirconacyclopentadiene reagent using a modified literature preparation.<sup>167</sup> For exact synthetic procedures, see chapter 7.

### **Results and discussion:**

We were able to successfully synthesize the hexakis benzyl esters using two different methodologies, each with its own advantages. For the cyclotrimerization synthetic route, a dicarboxylate butyne would give the desired benzylic system. This was successfully done in high yields to give hexakis (4-methoxy phenyl) benzene-1,2,3,4,5,6-hexacarboxylate. Although the catalytic cyclotrimerization give good yields and nearly pure product, (figure 2) they are limited by the fact that only the homosubstituted esters could be created, or at least with no selectivity in the hexaester system. Using this method, it would be difficult to synthetically dictate where a single trigger molecule would be placed on our system without having multiple trigger substituents . We have also shown that with a stoichiometric cyclotransesterification agent, selectable substituted benzenes hexacarboxylates could be synthesized (Figure 3). Unfortunately this synthetic pathway is limited by the dicarboxylate butynes synthesized. So far the only dibutyl carboxylates synthesized are the methyl, ethyl, and p-methoxy derivatives. The synthesis of the dicarboxylate butynes is a several step synthesis, which makes creating a library of suitable compounds more difficult. This reaction path does add possible versatility, however, and is still being investigated with different ester groups.

Also considered was making benzylic ethers and then oxidizing to the appropriate esters. Although the benzylic ether could be fairly simply synthesized by the William

ether synthesis, the oxidation did not readily happen. Again this indicates that the electronics and/or sterics of the hexa-substituted benzyl esters are complicated.

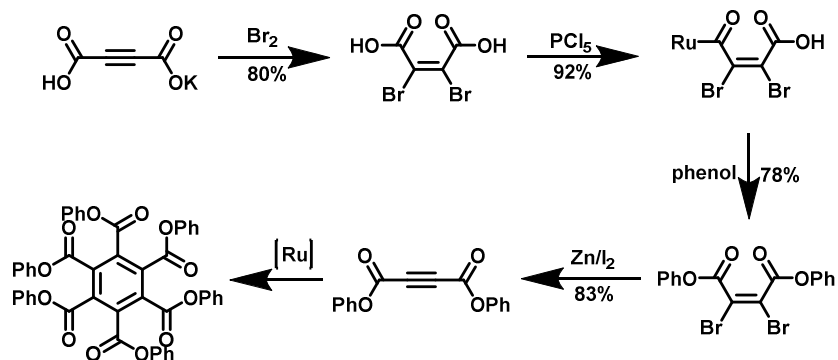


**Figure 2:** Catalytic cyclotrimerization demonstrating the ability of cyclotrimerization to produce sterically hindered hexaesters

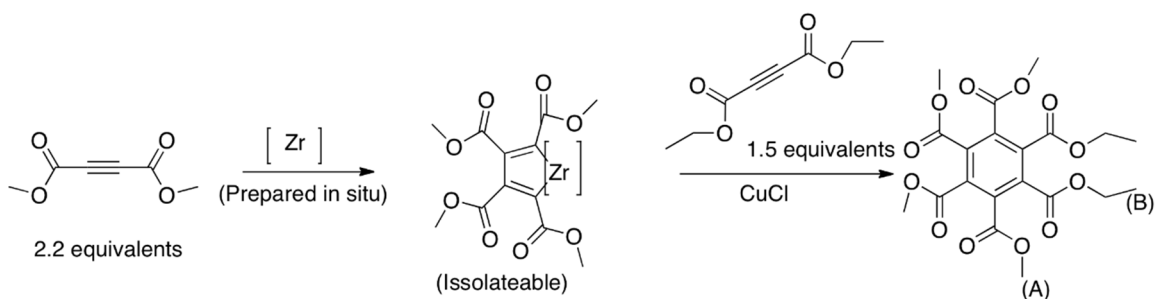


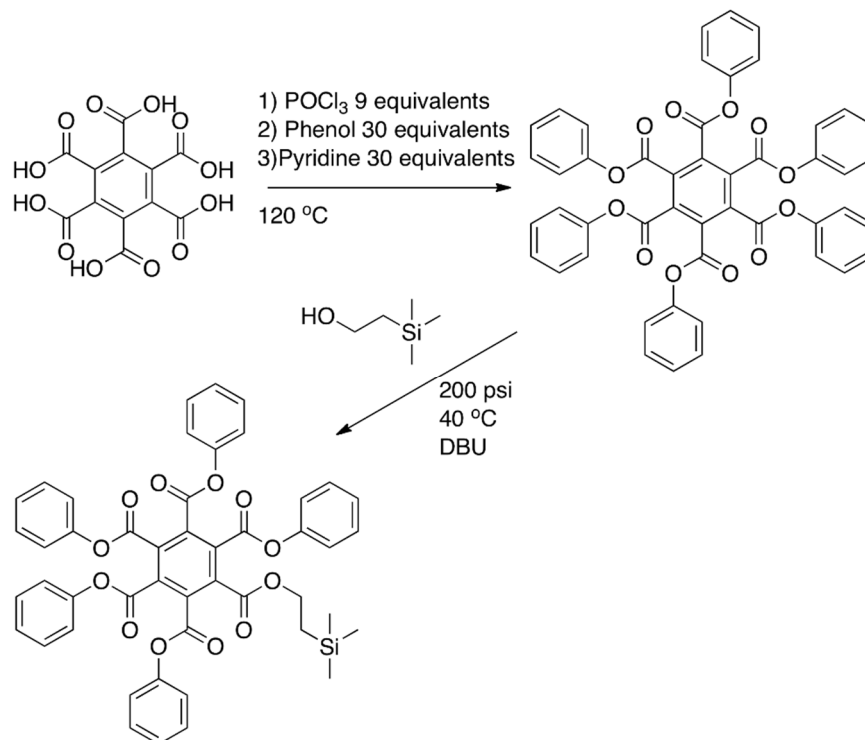
**Figure 3:** Cyclotrimerization using stoichiometric zirconium reagent that gives selective substitution

As discussed in chapter 2, hexester systems could also be prepared by our oxidative aromatization technique. Since this is a one pot synthesis, a wider variety of molecules could be synthesized much quicker than with the cyclotrimerization



techniques. Like the catalytic trimerization, however, selectivity is difficult in this synthetic pathway, without previously functionalizing our system.

The transesterification reactions were non-trivial due to the restrictive steric



system and the complicated electronics that made the direct esterification of the mellitic acid derivatives difficult. However, high-pressure systems have been shown to give moderate yields in sterically hindered transesterifications.<sup>168</sup> Even with the high pressure and increased temperature, a labile leaving group was necessary. The transesterification reaction failed with the hexakis (4-methoxy phenyl) benzene 1,2,3,4,5,6 hexacarboxylate, and provided only modest yields even with the high pressure transesterification of the phenolate derivative. Further transesterification with better leaving groups (such as p-nitrophenol or coumarins) are expected to give even higher yields.

Additionally, the transesterification using the 2-nitro benzyl alcohol photocage as the nucleophile proved unsuccessful. It is conceivable that with a better leaving group, the transesterification may be done with the photocage, however previously reported studies of sterically hindered transesterification showed difficulty with benzyl type alcohols.<sup>168</sup> Otherwise, cyclotrimerization may be a viable alternative for getting different triggers onto the amplifier system.

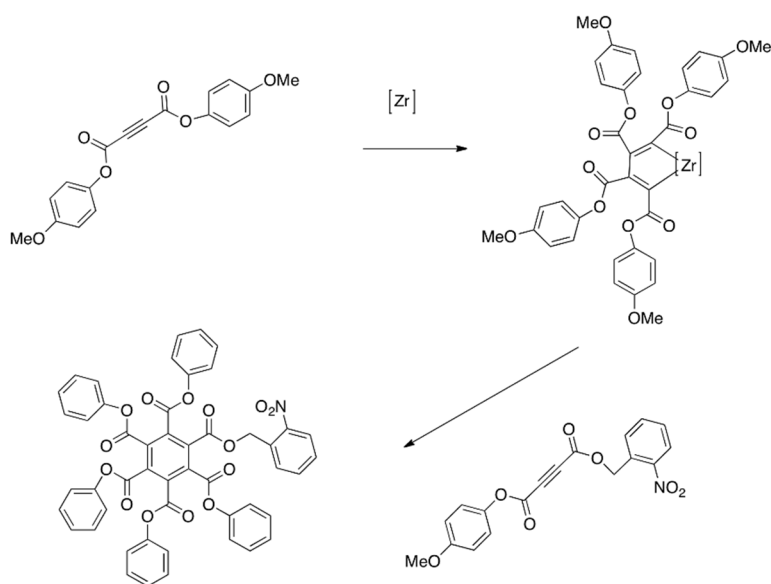


**Figure 6:** Proposed scheme for synthetic route for cyclotrimerization approach to making chemical amplifier

To test the stability to unwanted hydrolysis of the hexaester, 10 mg of the hexakis 4-methoxy phenyl benzene-1,2,3,4,5,6-hexacarboxylate was dissolved in 100  $\mu\text{L}$  of dioxane. 10  $\mu\text{L}$  of this solution was placed into 1 mL of  $\text{D}_2\text{O}$ . The  $\text{D}_2\text{O}$ /dioxane solution

was monitored by  $^1\text{H-NMR}$  for appearance of phenol. The NMR tube, with sample, was kept in a  $37^\circ\text{C}$  water bath between NMR runs. No phenol was observed over the first 24

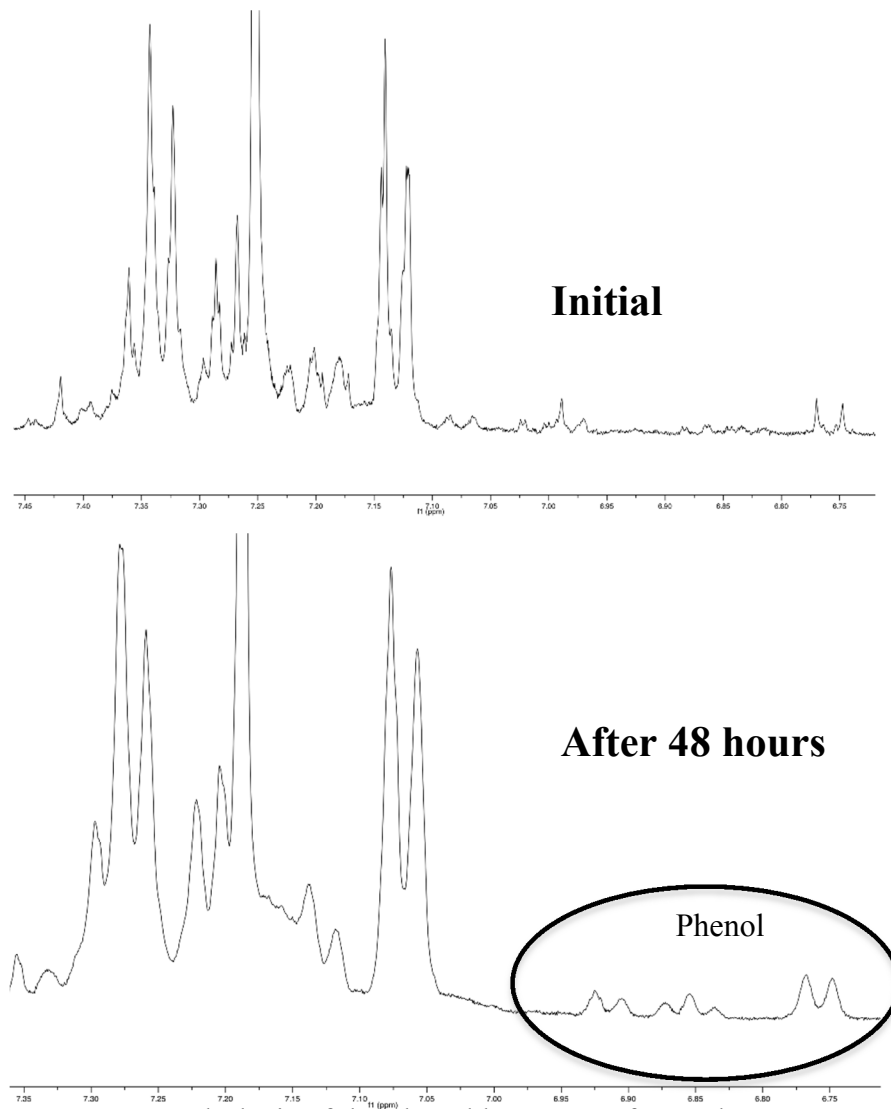


**Figure 7:** Hydrolysis of the phenol hexaester after 48 hours at  $37^\circ\text{C}$  in a dioxane/water solution (some chloroform impurity as well)

hours, demonstrating that the substrate is suitably water stable for our purposes. A small amount of phenol was detected after 48 hours indicating a small, but acceptable amount of hydrolysis. To help with solubility, the synthesis is being repeated with nitro groups added to the alcohol (eg. p-nitro phenol). Adding the nitro groups should also increase

the rate of kinetics. Alternatively, with lower concentrations and purer product, kinetic studies could be done via UV-vis spectroscopy in a water/dioxane mixture.

Studies testing the effect of the amplifier are currently ongoing. However, initially studies seem to be promising. The 1,2,3,4,5-pentaphenyl 6-(2-(trimethylsilyl)ethyl) benzene-1,2,3,4,5,6-hexacarboxylate, synthesized by the transesterification method and with impurities, was dissolved in THF and subjected to tetra-n-butylammonium fluoride in order to activate the trigger. After 1 hour the reaction mixture was placed in pH 7 phosphate buffered water and reaction was monitored by UV. Release of phenol was nearly immediately observed by UV, on addition to the water, indicating that our system retains the quick kinetics of the model linker system.

### **Conclusion:**

Using our newly developed oxidative aromatization technique we were able to quickly synthesize several hexaester benzyl derivatives. Using criteria that we laid out in chapter 3, and with the transesterification goal in mind, hexakis phenyl benzene-1,2,3,4,5,6-hexacarboxylate was synthesized and transesterified with a fluorine sensitive trigger, which has been shown to work well with similar systems.<sup>131</sup> Current work is in purification of the amplifier and studies that prove the amplifier effect. After proving release on activation of a trigger, a variety of other alcohols, such as p-nitro phenol and 7-hydroxy coumarin, could be considered. These have better utility as reporter molecules because of their inherent fluorescence.

## APPENDIX C. SUPPORTING INFORMATION FOR CHAPTER 4

### Synthesis of Polymer:

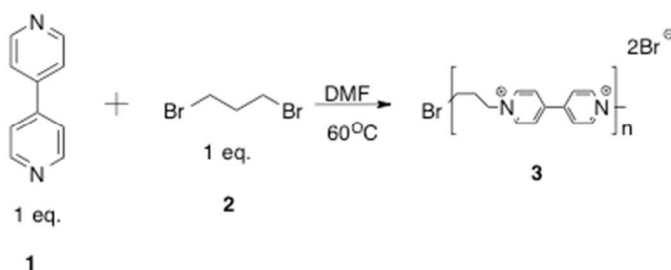


**Figure S1.** Synthesis of ionene polymer

**Synthesis of poly(propyl viologen) (3):** The synthesis was adapted from a known procedure.<sup>90</sup> 0.75 g of 4,4'-bipyridine was added to 20 mL of DMF in a 50 mL rbf. The solution was stirred with a stir bar until the bipyridine completely dissolved. To the bipyridine solution was added 0.653 mL of 1,3-dibromopropane and the entire solution was sealed and stirred at 60°C for 5 days. After 5 days, an additional 0.2514 g of bipyridine was dissolved in 10 mL of DMF and added to the solution. This was allowed to react for an additional day. The solution was then allowed to cool to room temperature where the solid that crashed out could be removed via filtration and washing with ethyl acetate. After washing, the solid was dissolved in minimal amounts of methanol and poured into a beaker filled with ethyl acetate. This new solid was removed via filtration, washed with ethyl acetate, and allowed to dry under vacuum. <sup>1</sup>H-NMR and <sup>13</sup>C-NMR were consistent with reported polymers.<sup>90</sup>

**Determination of molecular weight:** Average molecular weight of the polymer was determined by integration of the  $^1\text{H-NMR}$  due to practical difficulties of MALDI and GPC. The synthesis of (**3**) resulted in polymers that were terminated by bipyridines, as evidenced by the relatively small peaks related to the  $\text{CH}_2\text{Br}$  hydrogens. Degree of polymerization ( $X_n$ ) could therefore be determined by the ratio of the peaks attributed to the H in the chain viologen (the aromatic doublets, for a relative integration value of 4 hydrogens per unit each) over twice the doublet at 7.96, assigned to the end bipyridine, with a relative integration value of 4 when accounting for both ends. Since the chain lengths are sufficiently short, 1 is added to this number to account for the unit on the end. Polymers synthesized using the above procedure have  $X_n$  between 9-20, with the polymers used for all the experiments tested falling around  $X_n = 15$ . Multiplying this number by the monomer molecular weight (358.08) gives an average molecular weight between ( $M_n$ )=3,200 and 7,100 which was near the range previously reported for this polymer.

**UV-Vis studies:** The UV-Vis spectrum were collected with the Agilent 8453 UV-Vis spectrometer and Agilent chemstation software. A constant temperature bath equipped with a water pump was used for temperature control.

**Temperature switching:** A 100  $\mu\text{M}$  solution of the propyl-linked polymer (**3**) dissolved in pH = 9.6 sodium hydroxide/sodium bicarbonate buffer was degassed using sparging. Meanwhile, the sodium dithionite was retrieved from a glove box and sealed in a round-bottomed flask to maintain an inert atmosphere. Once sparging was done, the analyte solution was cannulated into the rbf containing the sodium dithionite. Finally the reduced

analyte solution was cannulated into a septummed 1cm pathlength quartz cuvette. The cuvette was kept under an argon atmosphere for the duration of the experiments. Spectrum were taken every 5°C, allowing 15 minutes for temperature to equilibrate. Decay of signal was monitored at 499nm (figure S4). The new peak growth at 960 required a correction to accommodate the overlapping decay of a broader peak. The correction was made by drawing a straight line from the absorbance at 900nm to the absorbance at 1000 nm and taking the difference in absorbance between the absorbance at 960nm to this new baseline (figure S6).

**Jobs Plot Experiment:** The jobs plot experiment was carried out by titration of 2.5 mL of degassed 100  $\mu$ M solution of the propyl-linked polymer (**3**) reduced by sodium dithionite in pH = 9.6 sodium hydroxide/sodium bicarbonate buffer using 0.01 M CB[7] solution degassed in the same buffer in a 1 cm path length quartz cuvette. The CB[7] was added to form molar ratios ( $\chi$ ) 0.0, 0.1, 0.2, 0.3, 0.4, 0.5, 0.6, 0.7, 0.8, 0.9, and 0.99 through subsequent additions of CB[7] to the same cuvette. This was completed by first scanning **3** then 2.8  $\mu$ L of the CB[7] solution was added and scanned again. Another 3.5  $\mu$ L of CB[7] was added for a total volume of 6.3  $\mu$ L and scanned again. This process was continued with total CB[7] volumes of 10.8, 16.8, 25.1, 37.6, 58.6, 100.6, 220.6, and 660.6  $\mu$ L for molar ratios 0.3, 0.4, 0.5, 0.6, 0.7, 0.8, 0.9, and 0.99, respectively.

### EPR Experiments

**CB[7] Switching:** 3 mL of 10 mM solution of the propyl-linked polymer (**3**) dissolved in pH = 9.6 sodium hydroxide/sodium bicarbonate buffer was degassed using sparging.

Meanwhile, the sodium dithionite was retrieved from a glove box and sealed in a round-

bottomed flask to maintain an inert atmosphere. 0.034 g of CB[7] was also weighed into a third rbf, sealed with a septum, and degassed. Once sparging was done, the analyte solution was cannulated into the rbf containing the sodium dithionite and swirled to stir. The reduced solution was cannulated into the CB[7] and swirled to allow for binding. Finally, the reduced analyte solution was cannulated into a custom made EPR tube, 3mm ID/4mm OD top and ~30mm of 1mm ID/2mm OD bottom, capped by a septum. The solution was then cycled in the EPR using a nitrogen flow to maintain the heat. The spin concentration was calculated via double integration of the signal versus the known standards in the Bruker software for our EPR.

**Temperature Switching:** A 10 mM solution of the propyl-linked polymer (**3**) dissolved in pH = 9.6 sodium hydroxide/sodium bicarbonate buffer was degassed using sparging. Meanwhile, the sodium dithionite was retrieved from a glove box and sealed in a round-bottomed flask to maintain an inert atmosphere. Once sparging was done, the analyte solution was cannulated into the rbf containing the sodium dithionite. Finally the reduced analyte solution was cannulated into a custom made EPR tube, 3mm ID/4mm OD top and ~30mm of 1mm ID/2mm OD bottom, capped by a septum. The solution was then cycled in the EPR using a nitrogen flow to maintain the heat. The spin concentration was calculated via double integration of the signal versus the known standards in the Bruker software for our EPR.

The EPR parameters for all experiments are as follows: Modulation Frequency = 100 kHz, Modulation Amplitude = 1.0 G, Receiver Gain = 50 dB, time constant = .08 ms, conversion time = 20.48 ms, sweep time = 83.89 s, center field = 3335 G, sweep width =



70.0 G, microwave attenuation = 20 dB, microwave power = 1.984 mW, number of points = 4096, and number of averaged scans = 8.

Experiment	Spin Conc. (M)	Percent Radical
25 C with CB[7]	0.002779	27.79
25 C Cycle 1	0.0009395	9.395
90 C Cycle 1	0.001115	11.15
25 C Cycle 2	0.0009394	9.394
90 C Cycle 2	0.001089	10.89
25 C Cycle 3	0.0009317	9.317
90 C Cycle 3	0.00116	11.6
25 C Cycle 4	0.0009263	9.263
90 C Cycle 4	0.00106	10.6

**Figure S2.** EPR experimental results of the temperature and CB[7] switching. Spin concentration calculated from double integration of the EPR signal.

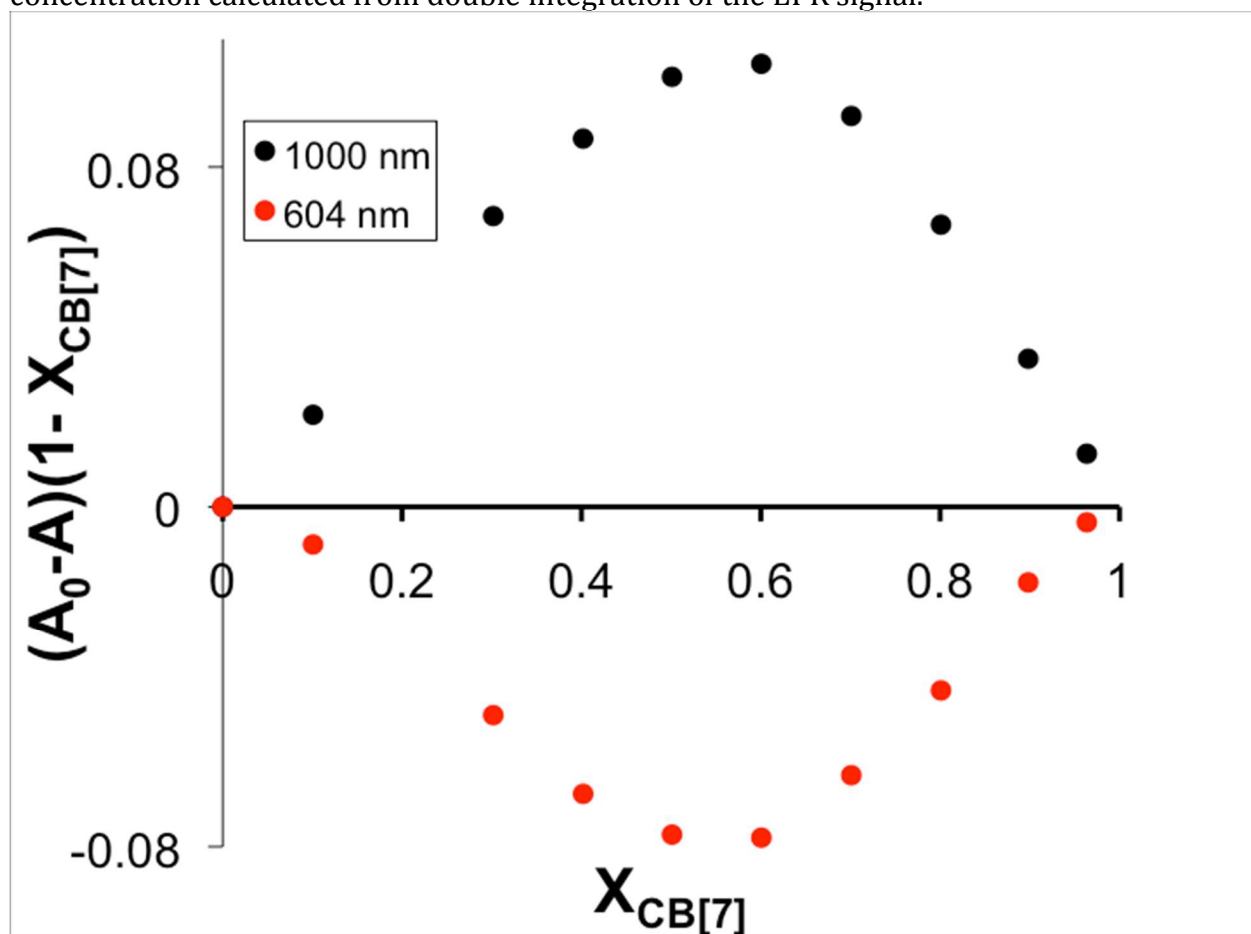


**Figure S3.** Graphical results of the JOBS Plot with increasing mole fraction of CB[7] monitored at 604 nm (red) and 100 nm (black).

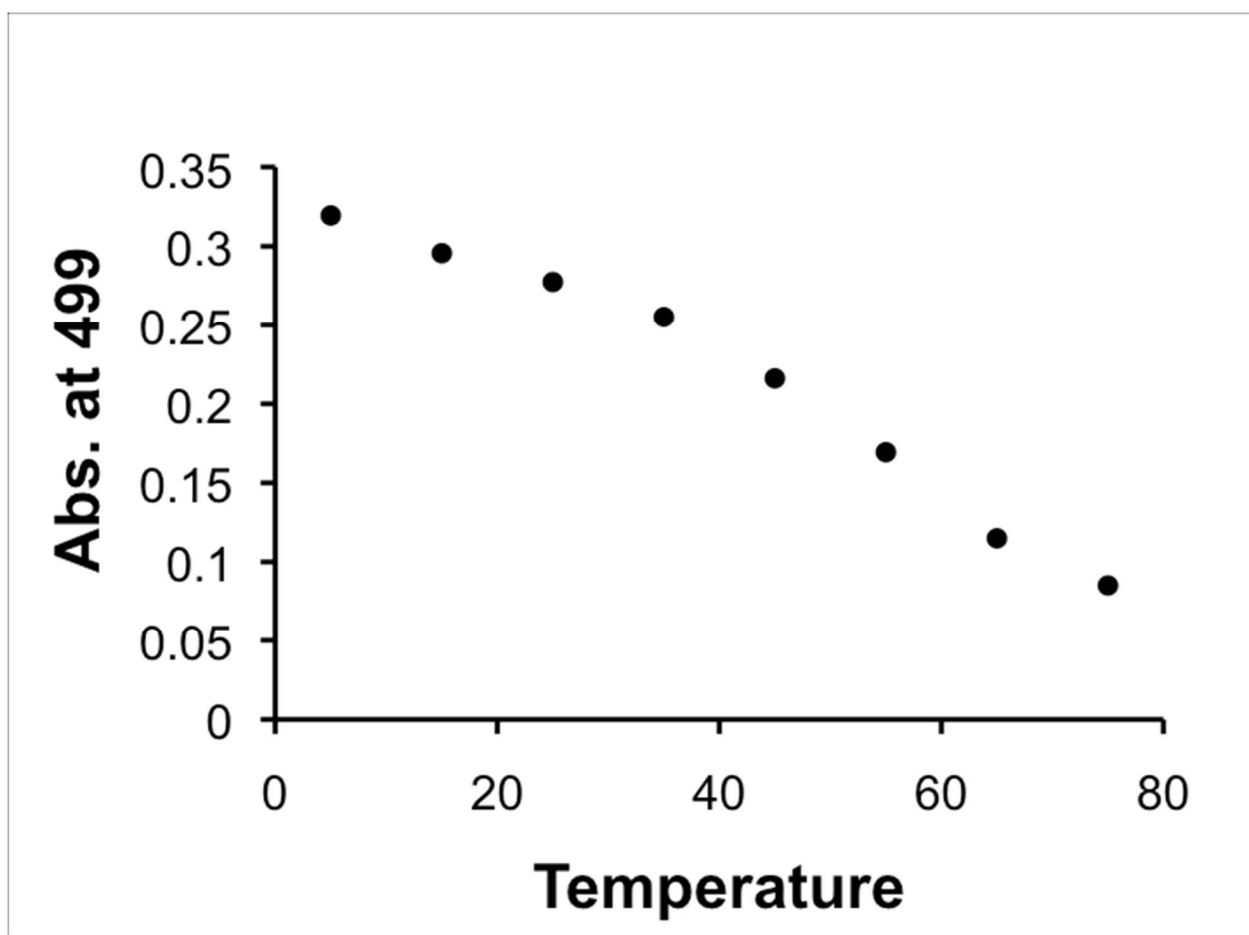


**Figure S4.** Plot of UV-Vis absorbance of the reduced version of **3** at 499 nm with increasing temperature from 5°C-65°C

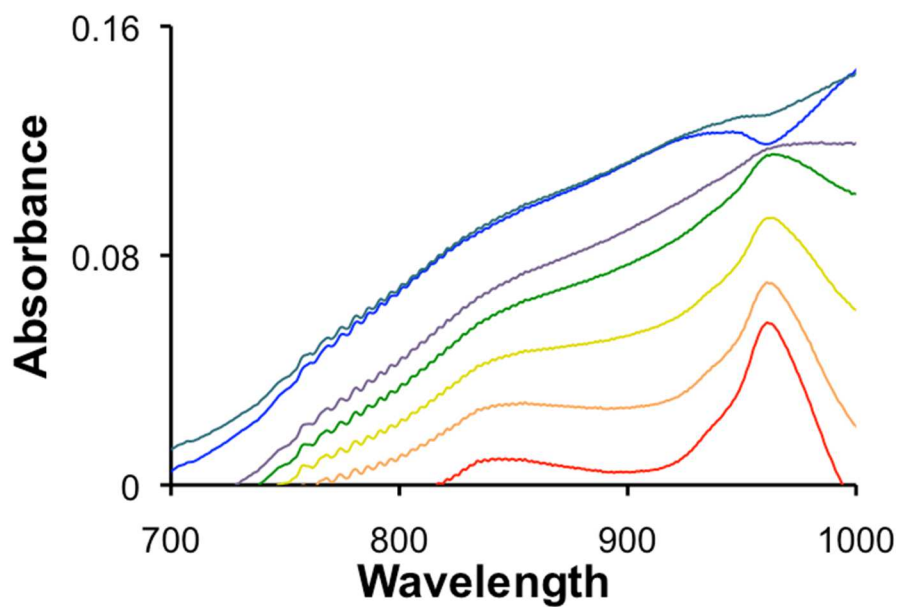


**Figure S5.** UV-vis of the reduced form of **3** in buffered aqueous solution at 100  $\mu\text{M}$ , highlighting the growth of the 960 nm peak (figure 4b).

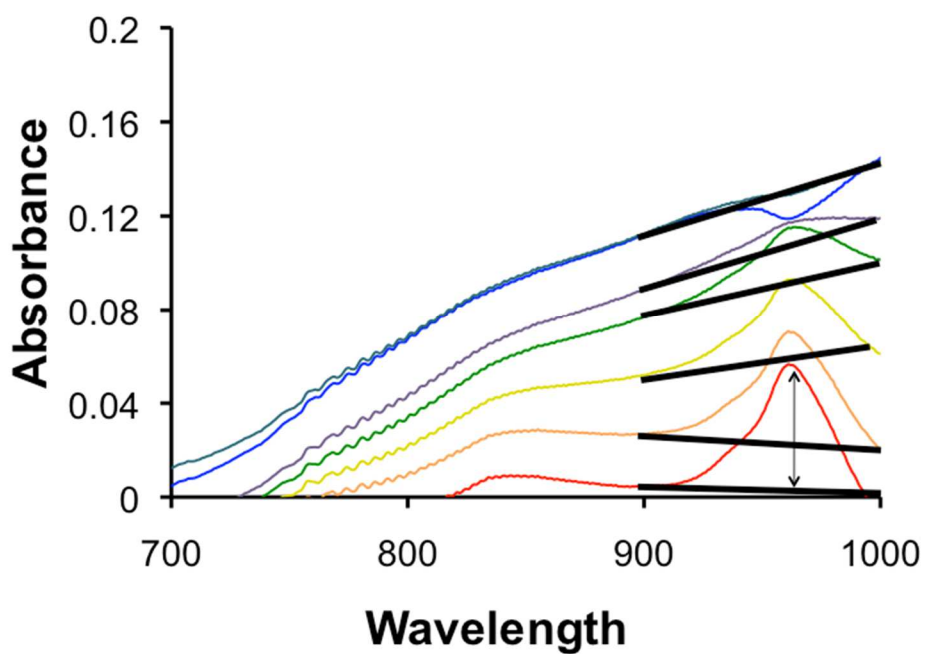


**Figure S6.** UV-vis of figure S5 showing the straight-line correction for the growth of the peak at 960nm.

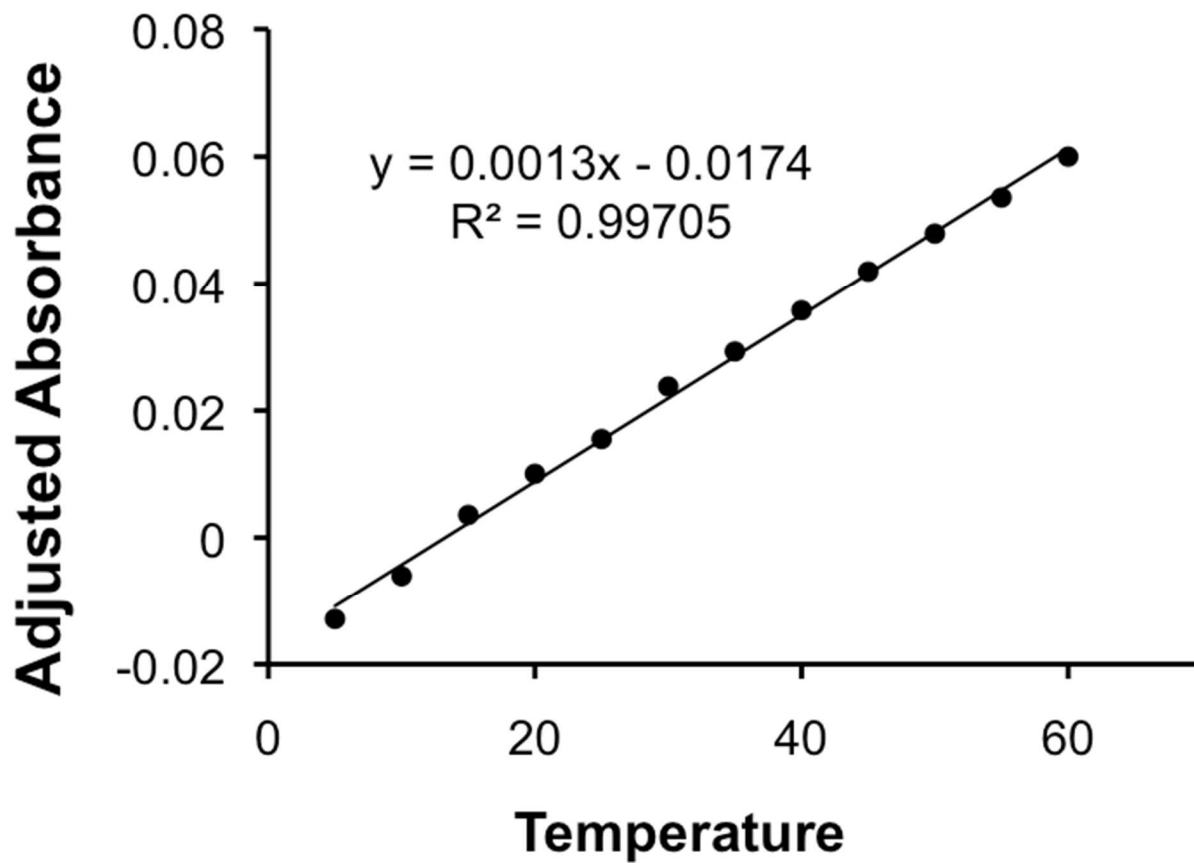


**Figure S7.** Plot of the absorbance (from the baseline linear correction of figure S6 of the reduced form of **3** at increasing temperatures.

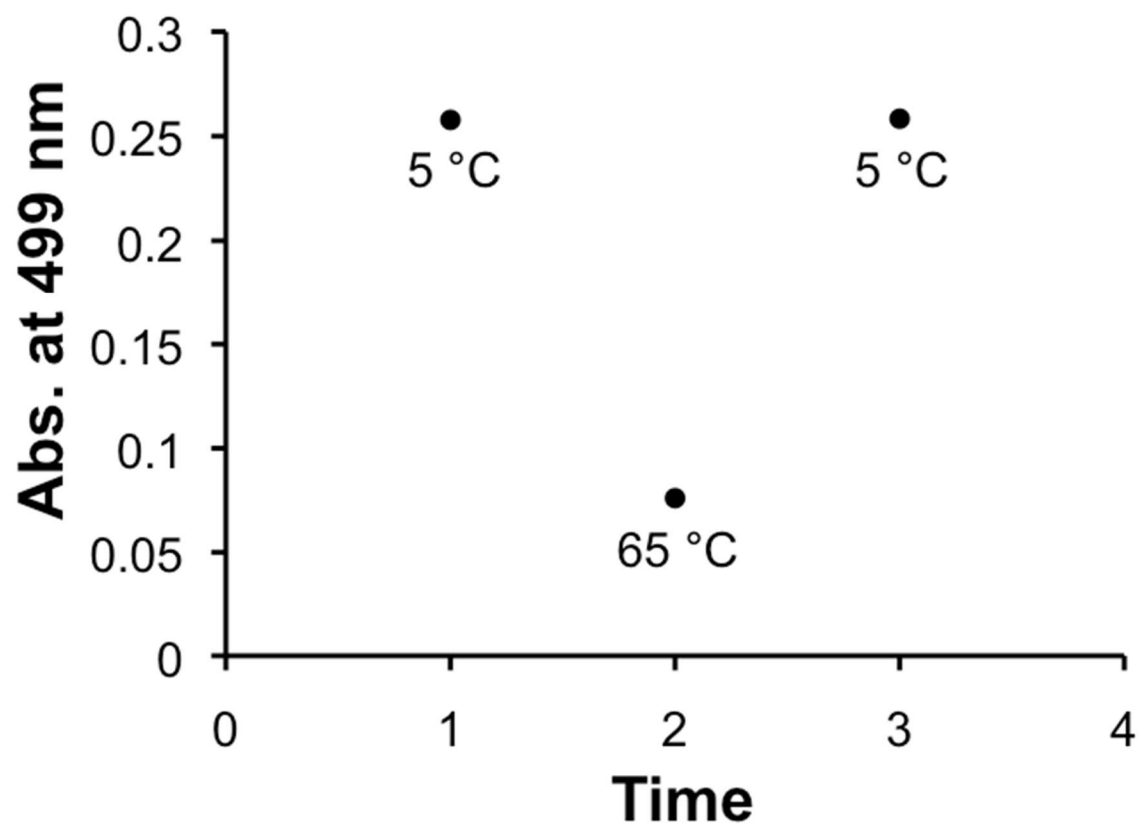


**Figure S8.** Absorbance of the reduced form of **3** at 5 °C to 65 °C back to 5 °C. Amount of time between scans was based on how long it took for absorbance to remain constant, which for heating was approximately 30 minutes, and for cooling was approximately 3 hours.

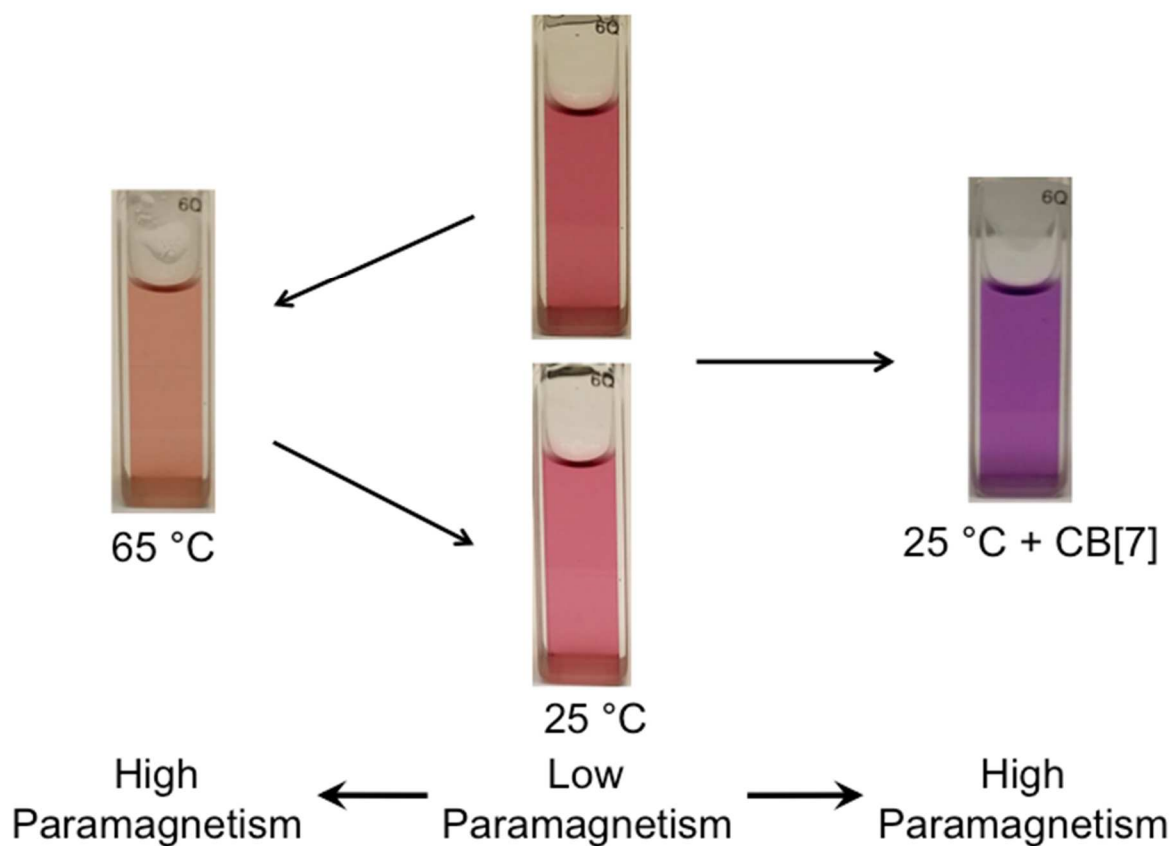


**Figure S9.** Aqueous buffer solution of the reduced **3** at 25°C (top middle) with color change to dark purple by addition of CB[7] (right) or to peach with heating (left). Color returned to the original fushia upon cooling to room temperature (bottom middle). The middle two and the figure on the right are all from the same experiment. The cuvette on the right is a representative color change from a different experiment.

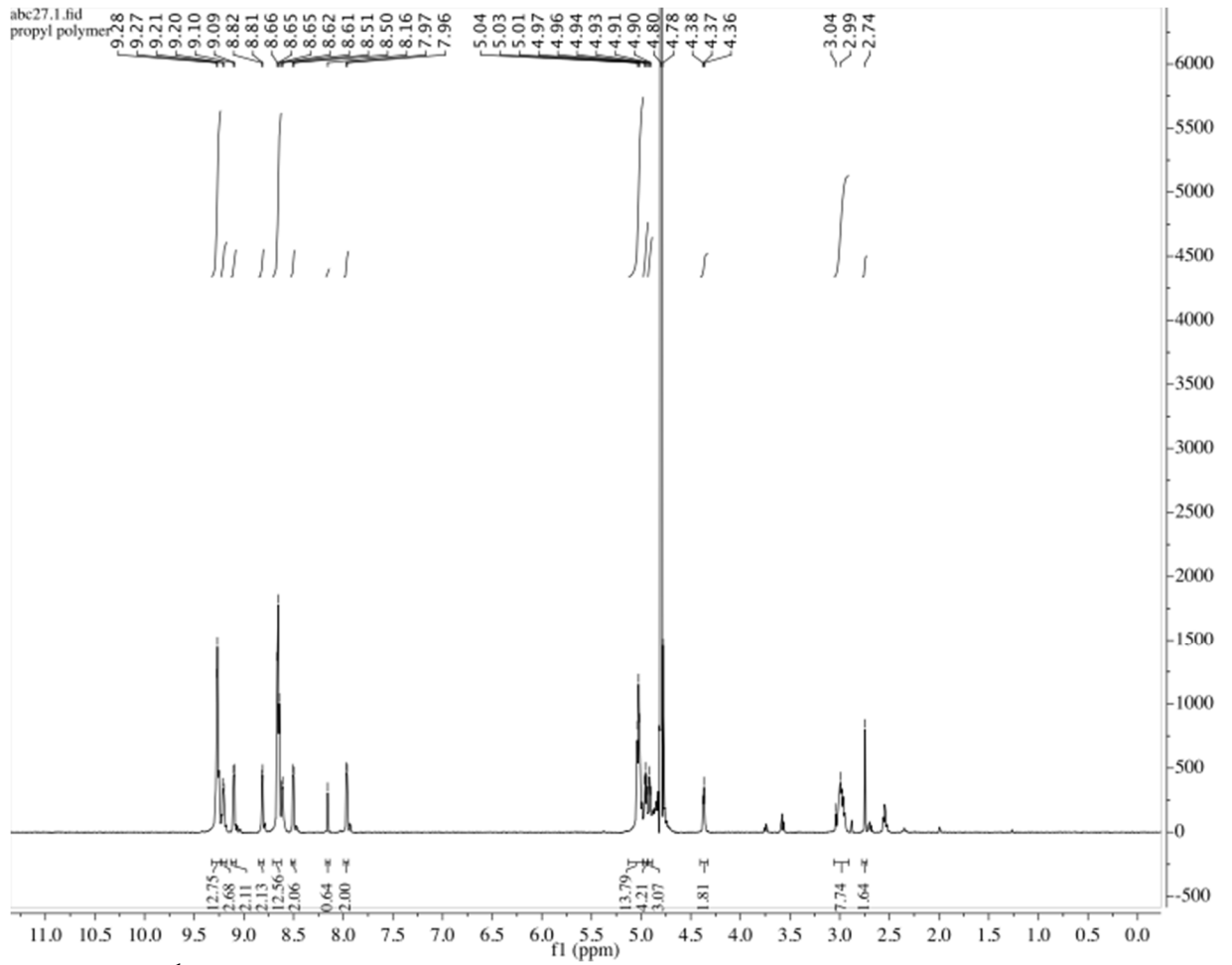
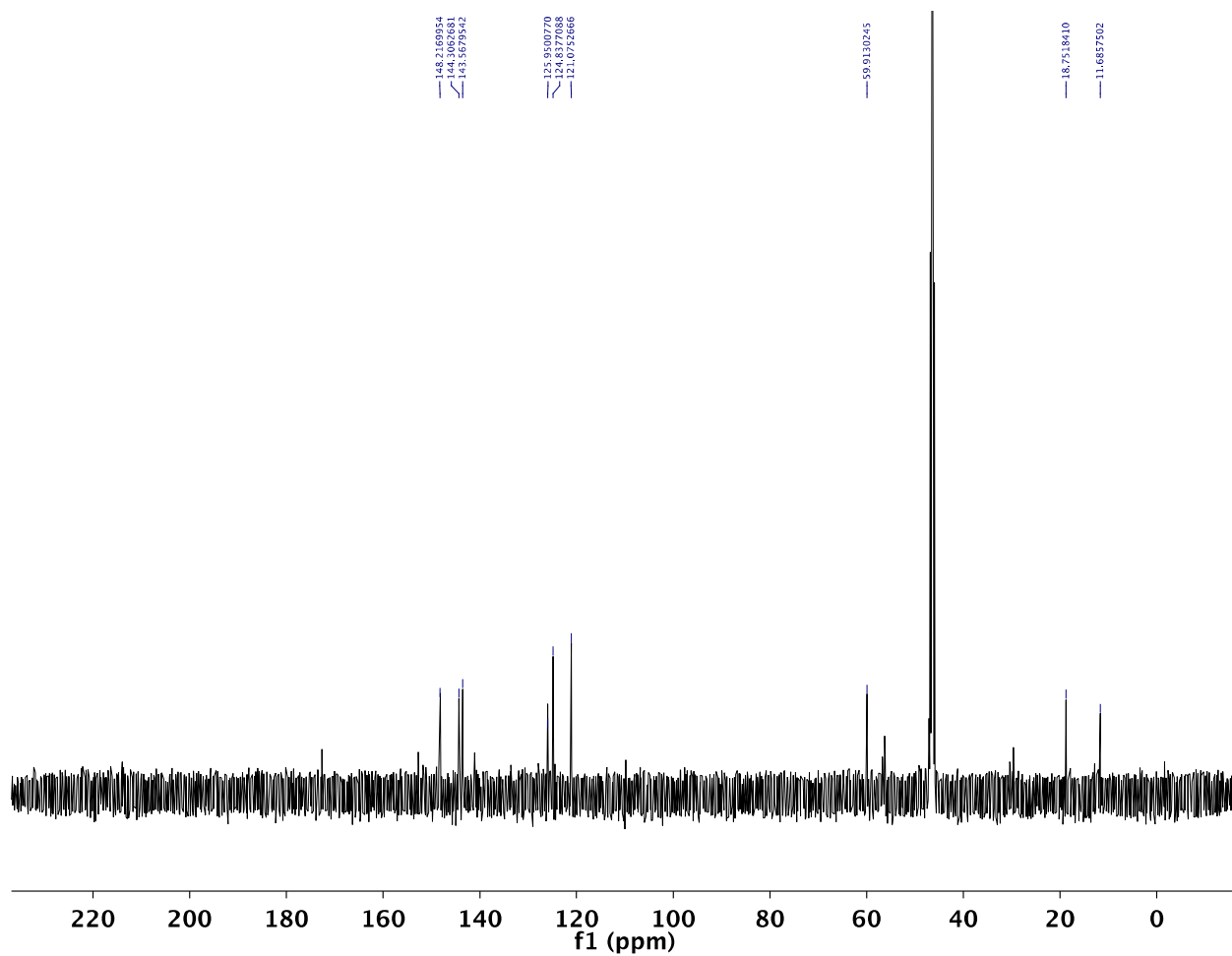


Figure S10.  $^1\text{H-NMR}$  of **3** in  $\text{D}_2\text{O}$





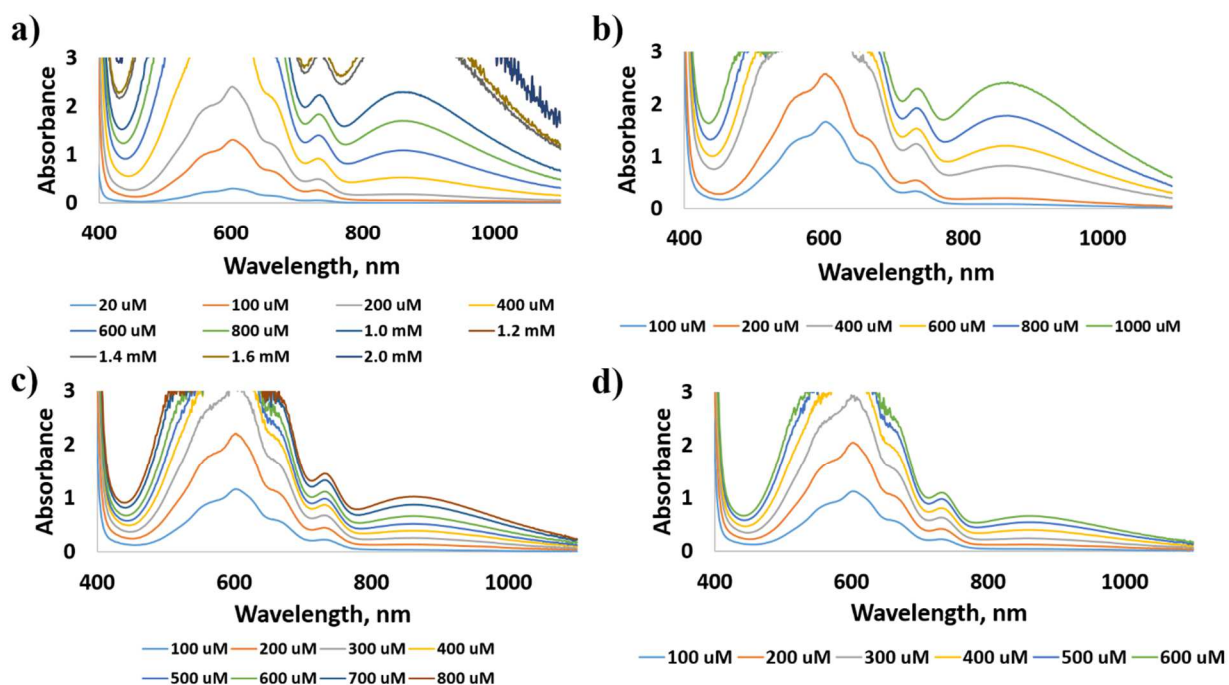
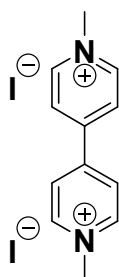
**Figure S11.**  $^{13}\text{C}$ -NMR of **3** in 95% Deuterated methanol 5% water

(1) Shimomura, M.; Utsugi, K.; Horikoshi, J.; Okuyama, K.; Hatozaki, O.; Oyama, N. *Langmuir* **1991**, *7*, 760.

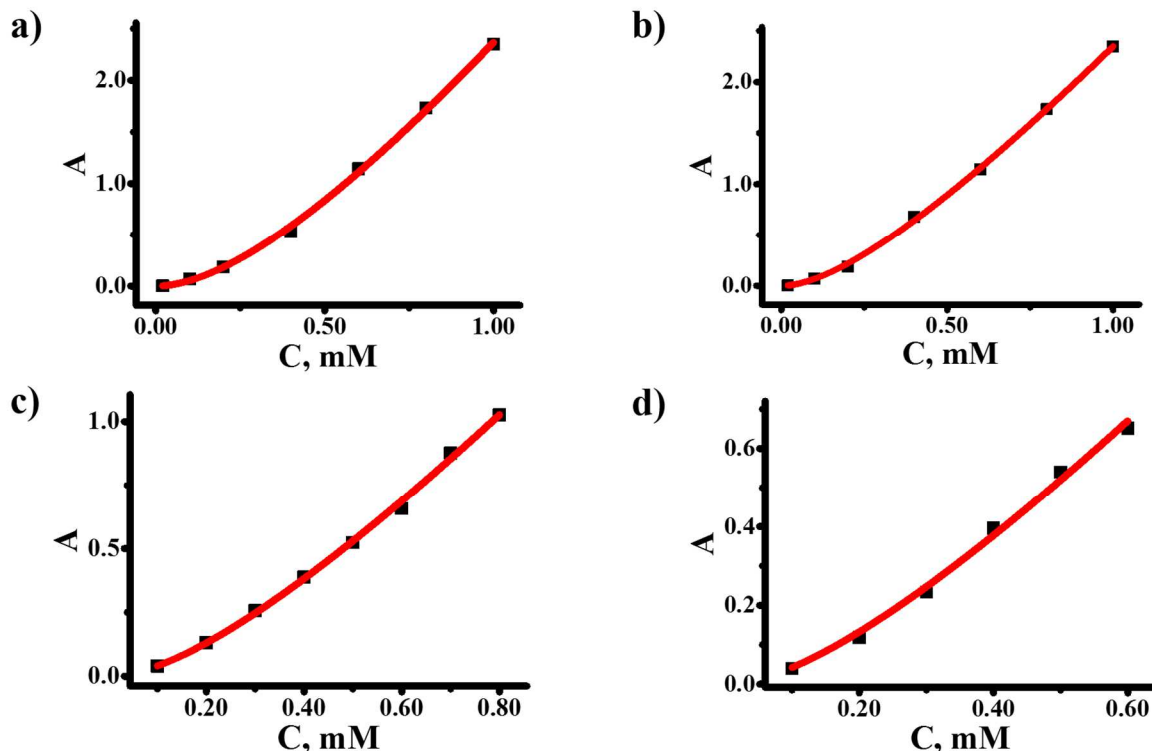
## APPENDIX D: SUPPORTING INFORMATION FOR CHAPTER 5

**General information.** Compounds and solvents were used as received from commercial suppliers without prior purification. NMR spectra were obtained using a spectrometer 600 and 150 MHz for  $^1\text{H}$  and  $^{13}\text{C}$ , respectively. The QTOF mass analyzer was used for the HRMS measurements.

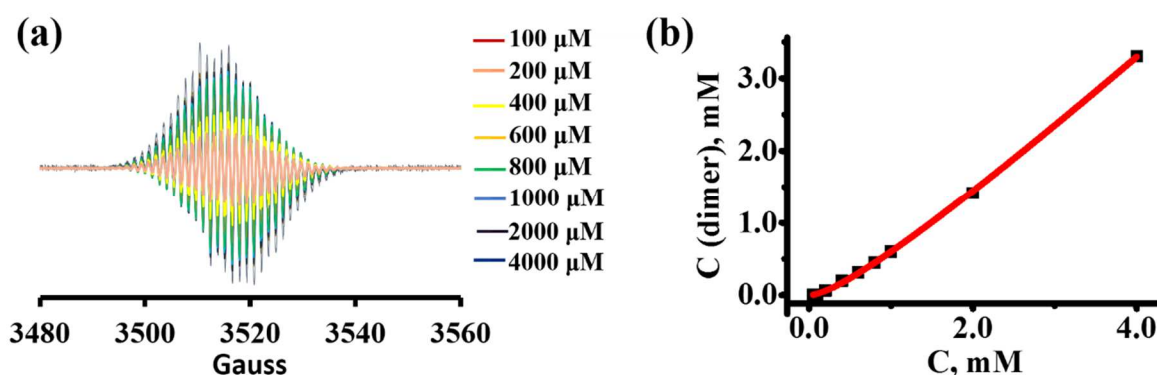
### 1,1'-Dimethyl-4,4'-bipyridinium diiodide (1).



**Supplementary figure S1.** Representative uv-vis spectra of 1,1'-dimethyl-4,4'-bipyridinium diiodide (1) aqueous buffer solutions at: (a) pH 9.6 run 1 (b) pH 9.6 run 2; (c) pH 7 run 1 (d) pH 7 run 2.

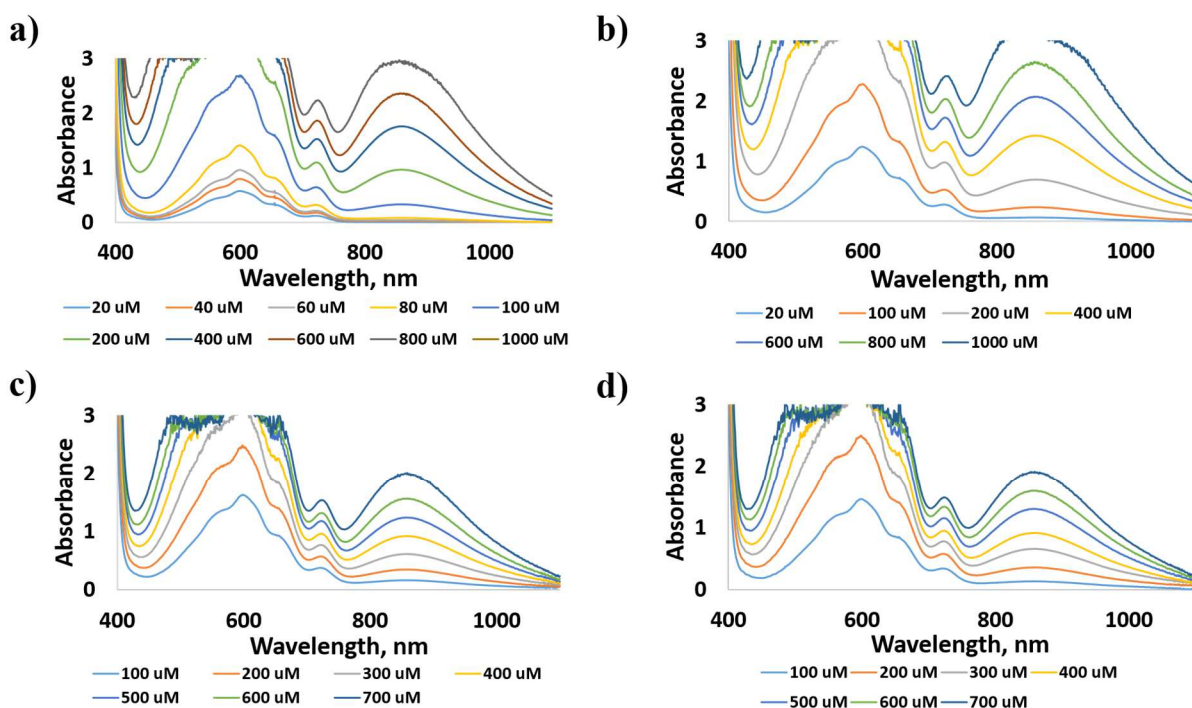
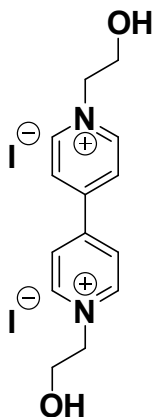


**Supplementary figure S2.** Representative origin fitting plots for uv-vis data of 1,1'-dimethyl-4,4'-bipyridinium diiodide (1) aqueous buffer solutions at: (a) pH 9.6 run 1 (b) pH 9.6 run 2; (c) pH 7 run 1 (d) pH 7 run 2.

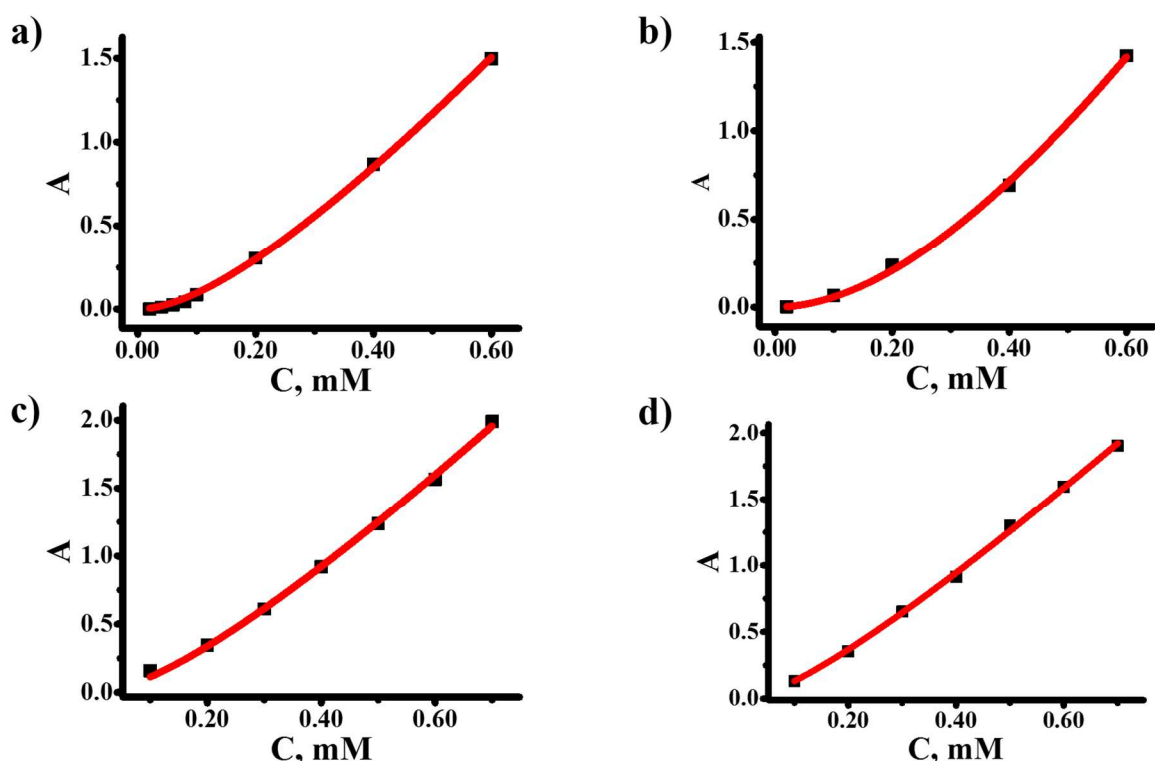


**Supplementary figure S3.** Representative EPR spectrum and origin fitting plot for 1,1'-dimethyl-4,4'-bipyridinium diiodide (1) aqueous buffer solution at pH 7 (a) Isothermal EPR dilution experiment spectrum (b) Nonlinear fitting curve: the dimer concentration vs total concentration of viologen derivative.

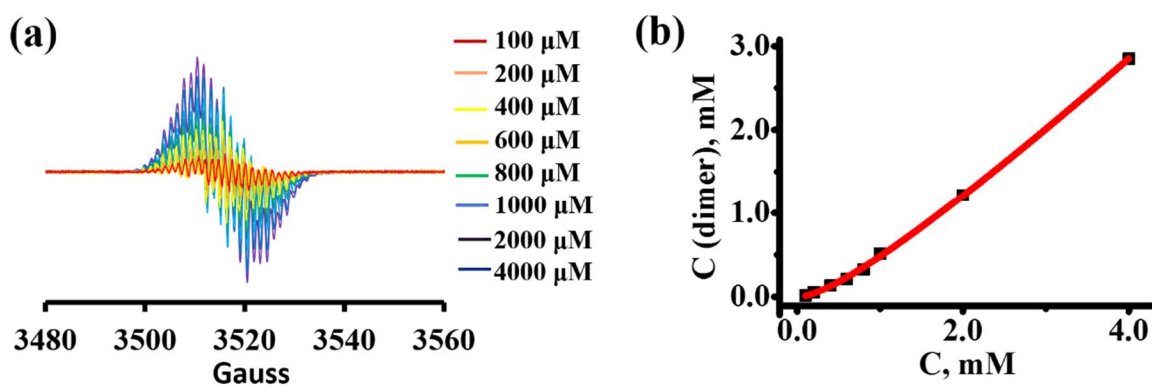
**1,1'-Bis(2-hydroxyethyl)-4,4'-bipyridinium diiodide (2).**



**Supplementary figure S5.** Representative uv-vis spectra of 1,1'-bis(2-hydroxyethyl)-4,4'-bipyridinium diiodide (2) aqueous buffer solutions at: **(a)** pH 9.6 run 1 **(b)** pH 9.6 run 2; **(c)** pH 7 run 1 **(d)** pH 7 run 2.

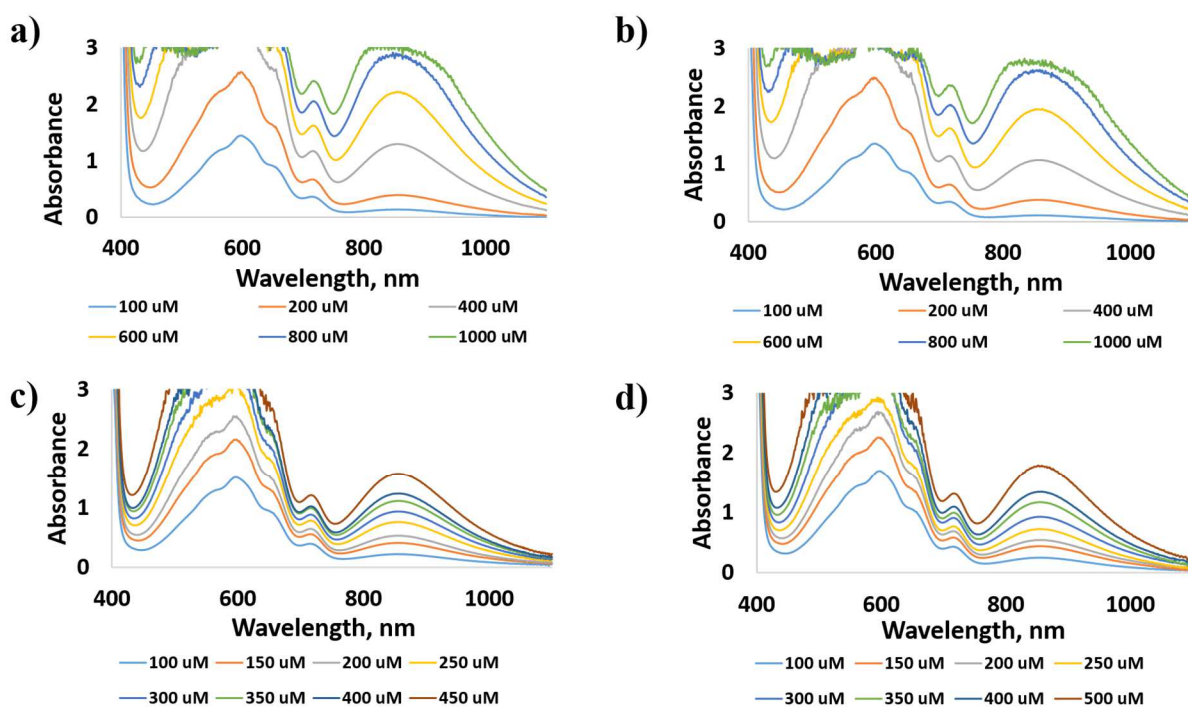
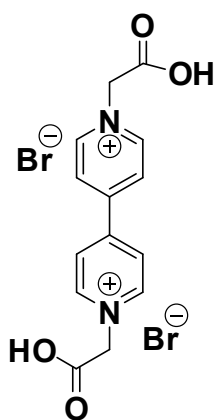


**Supplementary figure S6.** Representative origin fitting plots for uv-vis data of 1,1'-bis(2-hydroxyethyl)-4,4'-bipyridinium diiodide (2) aqueous buffer solutions at: (a) pH 9.6 run 1 (b) pH 9.6 run 2; (c) pH 7 run 1 (d) pH 7 run 2.

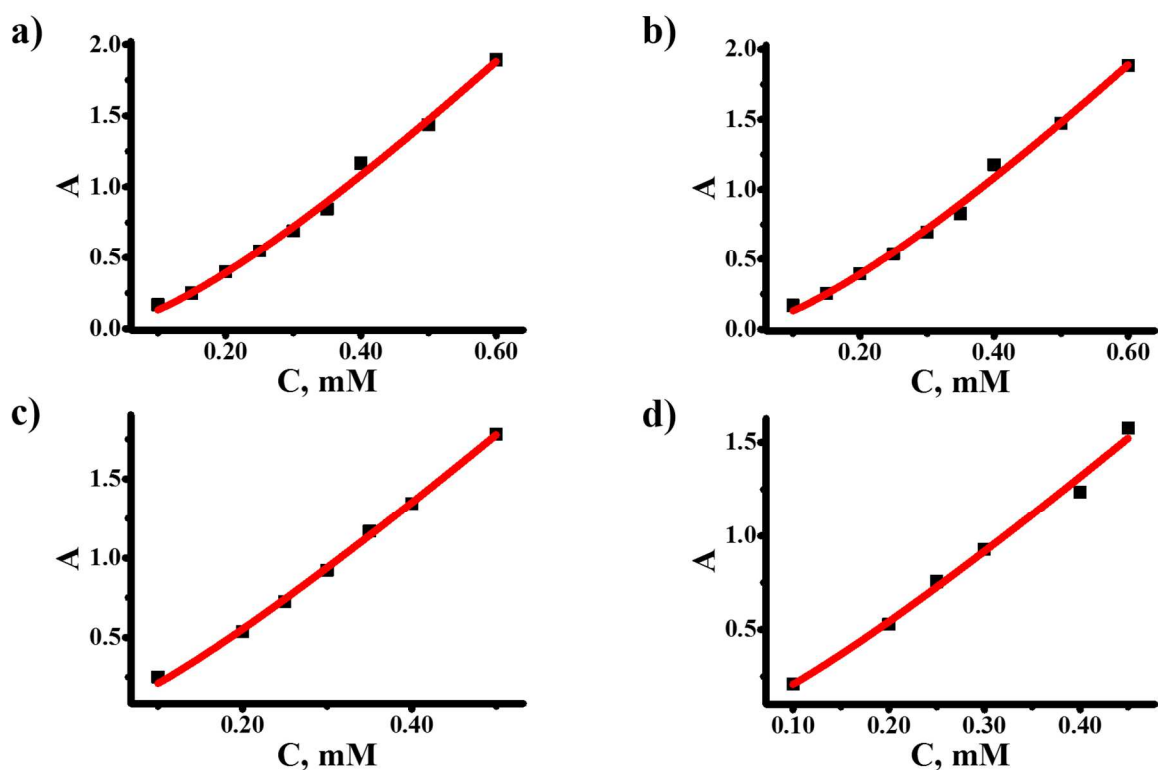


**Supplementary figure S7.** Representative EPR spectrum and origin fitting plot for 1,1'-bis(2-hydroxyethyl)-4,4'-bipyridinium diiodide (2) aqueous buffer solution at pH 7 (a) Isothermal EPR dilution experiment spectrum (b) Nonlinear fitting curve: the dimer concentration vs total concentration of viologen derivative.

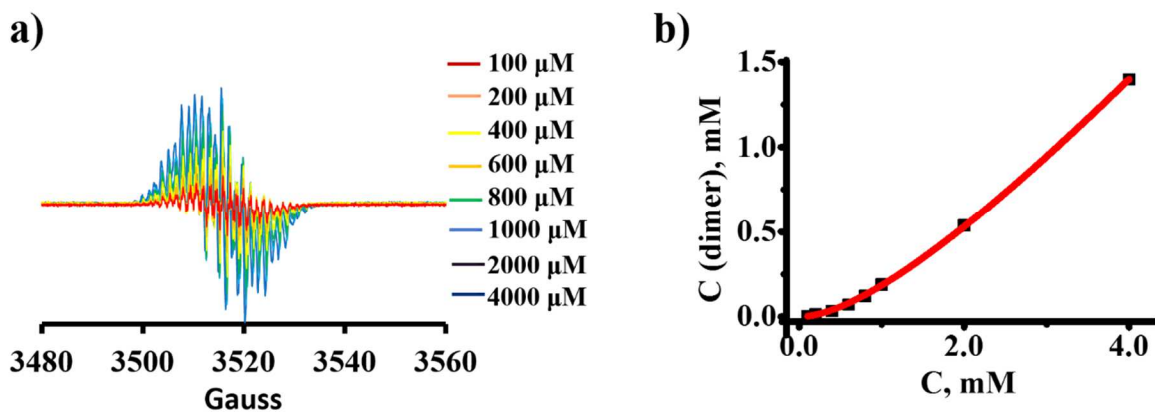
**1,1'-Bis(carboxymethyl)-4,4'-bipyridinium dibromide (3).**



**Supplementary figure S9.** Representative uv-vis spectra of 1,1'-bis(carboxymethyl)-4,4'-bipyridinium dibromide (3) aqueous buffer solutions at: (a) pH 9.6 run 1 (b) pH 9.6 run 2; (c) pH 7 run 1 (d) pH 7 run 2.



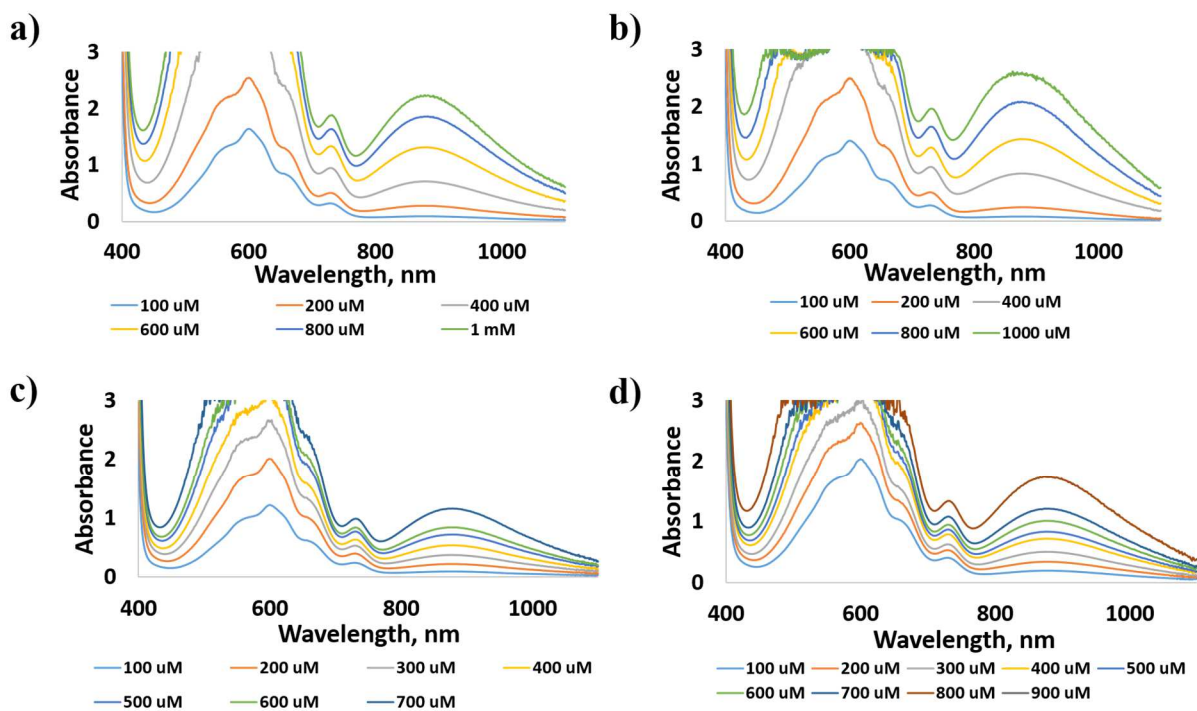
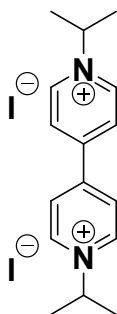
**Supplementary figure S10.** Representative origin fitting plots for uv-vis data of 1,1'-bis(carboxymethyl)-4,4'-bipyridinium dibromide (3) aqueous buffer solutions at: (a) pH 9.6 run 1 (b) pH 9.6 run 2; (c) pH 7 run 1 (d) pH 7 run 2.



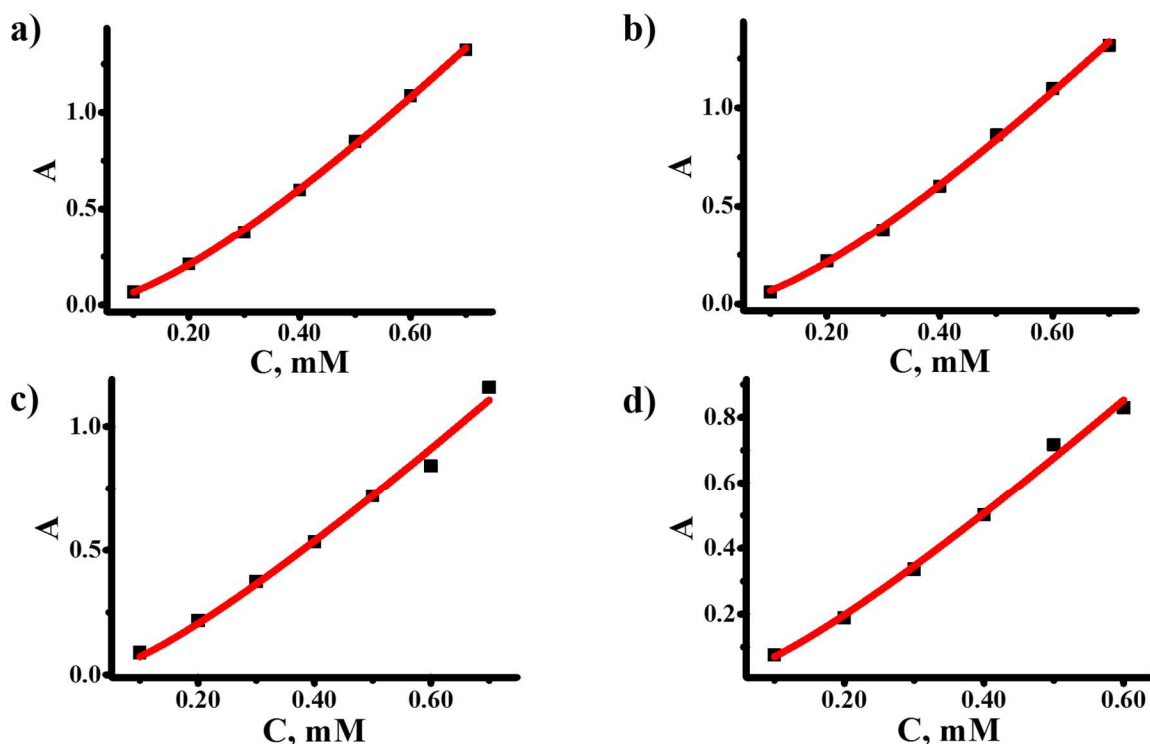
**Supplementary figure S11.** Representative EPR spectrum and origin fitting plot for 1,1'-bis(carboxymethyl)-4,4'-bipyridinium dibromide (3) aqueous buffer solution at pH 7 (a) Isothermal EPR dilution experiment spectrum (b) Nonlinear fitting curve: the dimer concentration vs total concentration of viologen derivative.



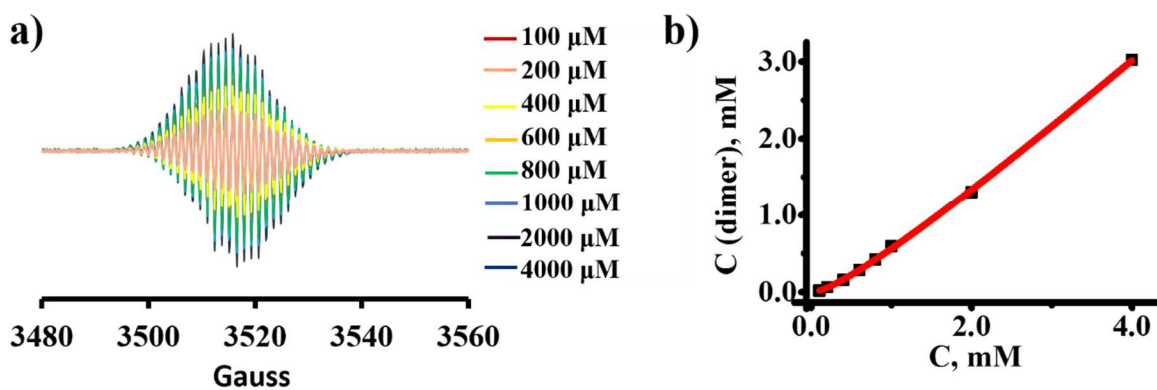
**1,1'-Diisopropyl-4,4'-bipyridinium diiodide (4).**



**Supplementary figure S13.** Representative uv-vis spectra of 1,1'-diisopropyl-4,4'-bipyridinium diiodide (4) aqueous buffer solutions at: **(a)** pH 9.6 run 1 **(b)** pH 9.6 run 2; **(c)** pH 7 run 1 **(d)** pH 7 run 2.

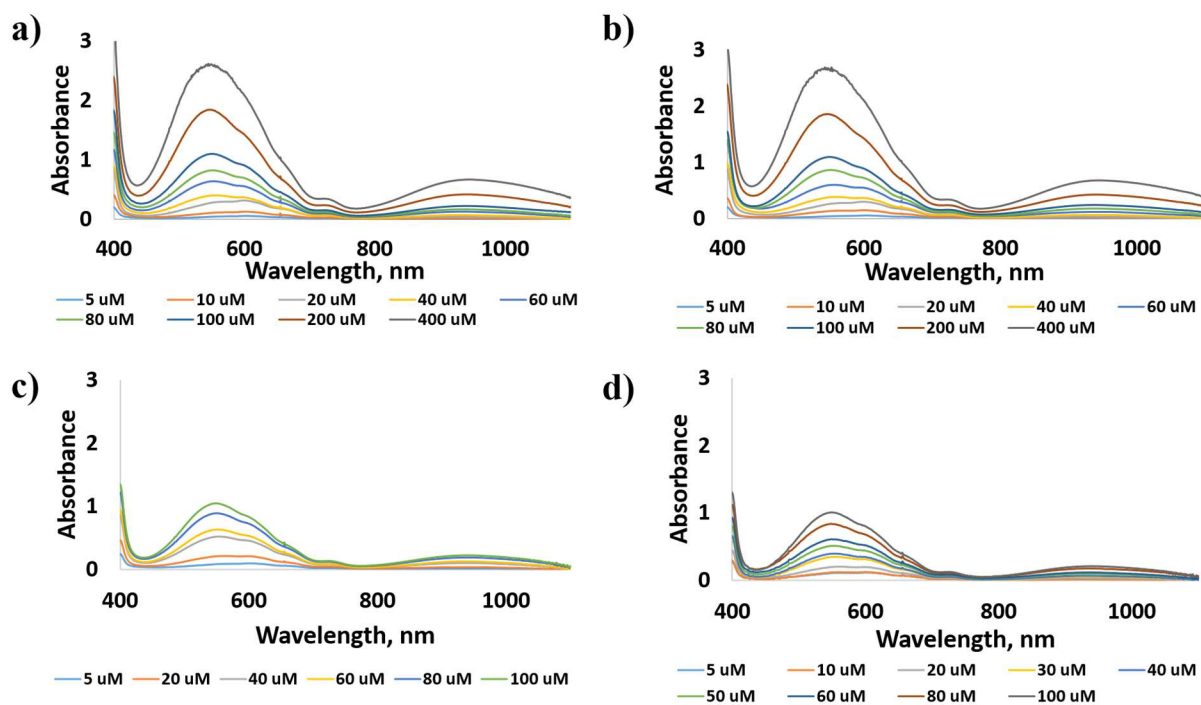
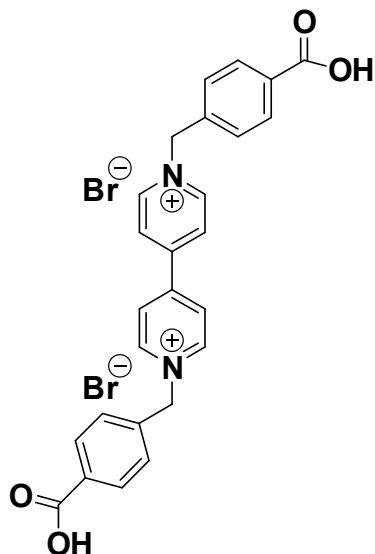


**Supplementary figure S14.** Representative origin fitting plots for uv-vis data of 1,1'-diisopropyl-4,4'-bipyridinium diiodide (4) aqueous buffer solutions at: (a) pH 9.6 run 1 (b) pH 9.6 run 2; (c) pH 7 run 1 (d) pH 7 run 2.

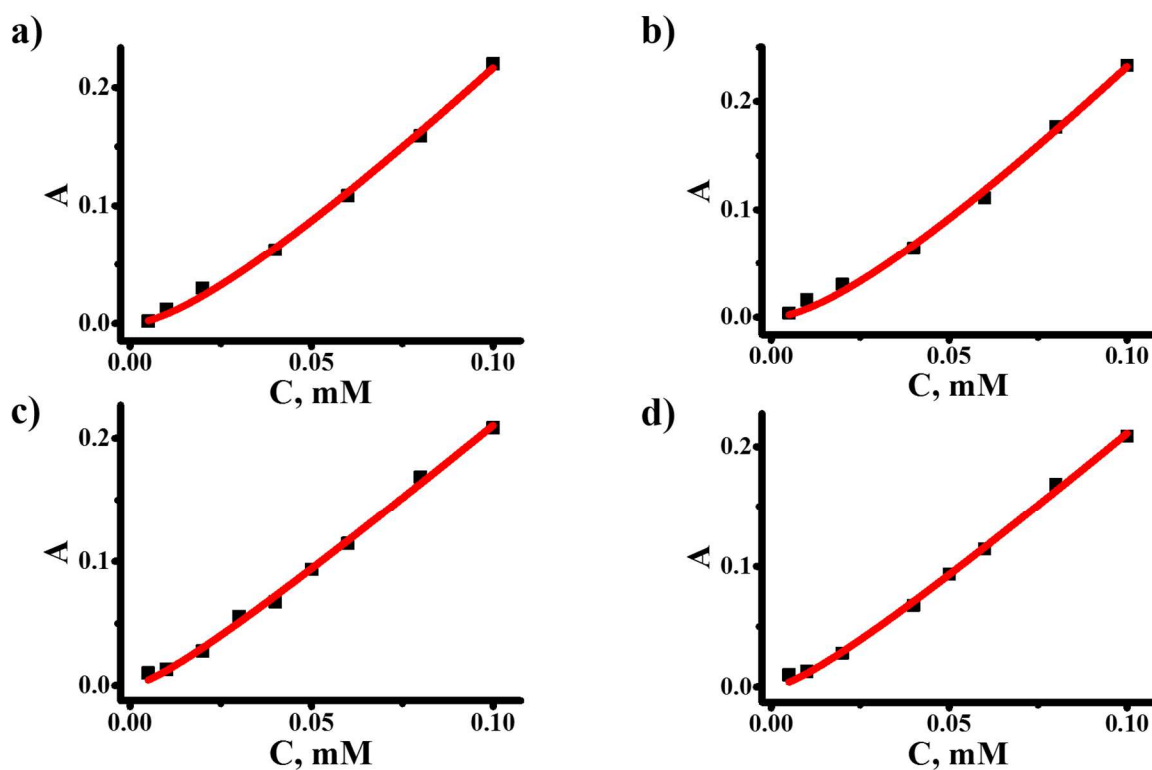


**Supplementary figure S15.** Representative EPR spectrum and origin fitting plot for 1,1'-diisopropyl-4,4'-bipyridinium diiodide (4) aqueous buffer solution at pH 7 (a) Isothermal EPR dilution experiment spectrum (b) Nonlinear fitting curve: the dimer concentration vs total concentration of viologen derivative.

**1,1'-Bis(4-carboxybenzyl)-4,4'-bipyridinium dibromide (5).**

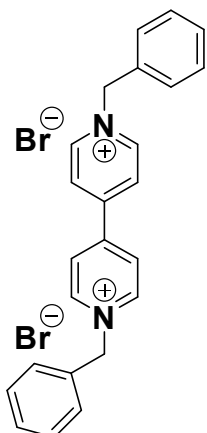


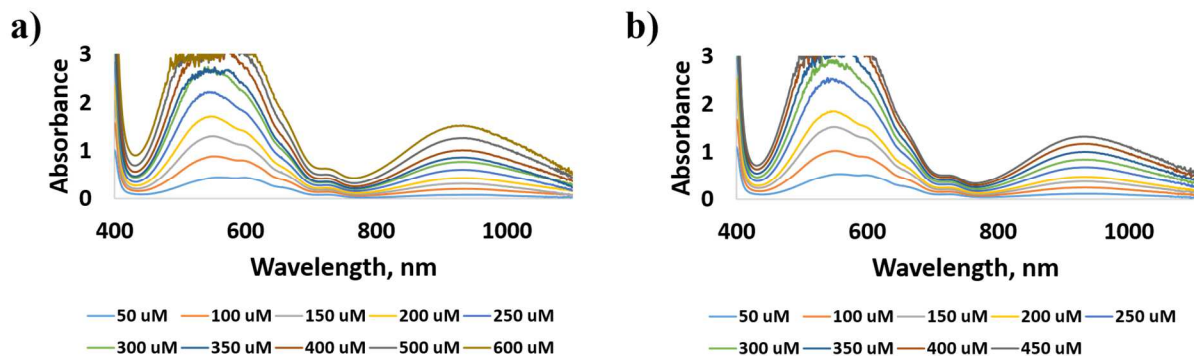
**Supplementary figure S17.** Representative uv-vis spectra of 1,1'-bis(4-carboxybenzyl)-4,4'-bipyridinium dibromide (5) aqueous buffer solutions at: (a) pH 9.6 run 1 (b) pH 9.6 run 2; (c) pH 7 run 1 (d) pH 7 run 2.



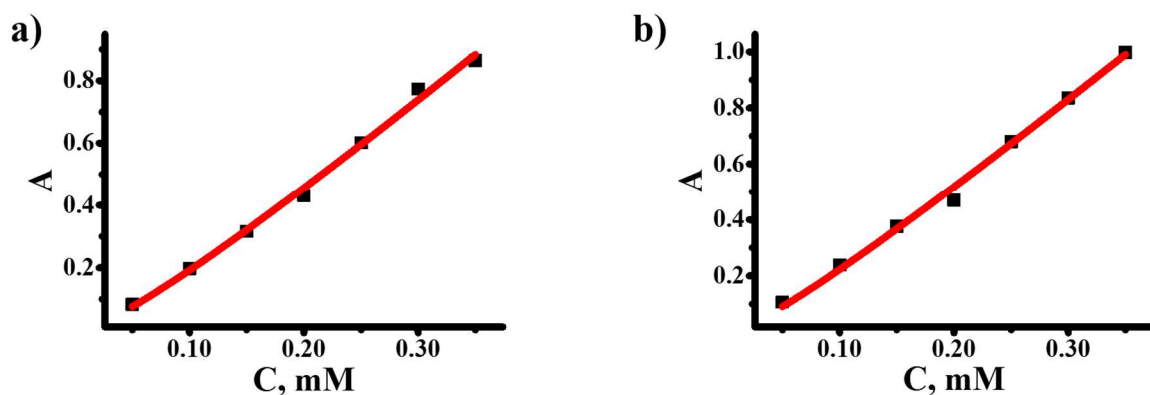
**Supplementary figure S18.** Representative origin fitting plots for uv-vis data of 1,1'-bis(4-carboxybenzyl)-4,4'-bipyridinium dibromide (5) aqueous buffer solutions at: (a) pH 9.6 run 1 (b) pH 9.6 run 2; (c) pH 7 run 1 (d) pH 7 run 2.

### 1,1'-Dibenzyl-4,4'-bipyridinium dibromide (6).





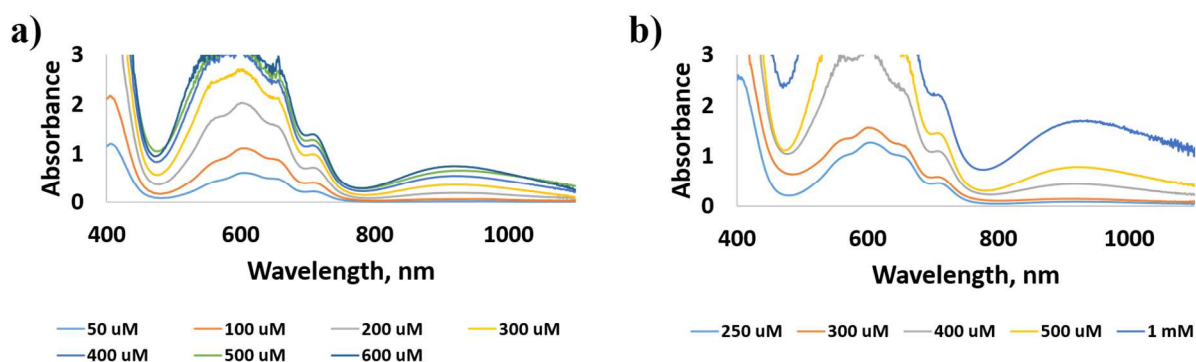
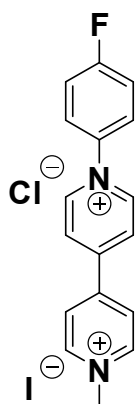
**Supplementary figure S21.** Representative uv-vis spectra of 1,1'-dibenzyl-4,4'-bipyridinium dibromide (6) aqueous buffer solutions at pH 7 (\*at pH 9.6 the compound crashes out the solution upon reduction): (a) run 1 (b) run 2.



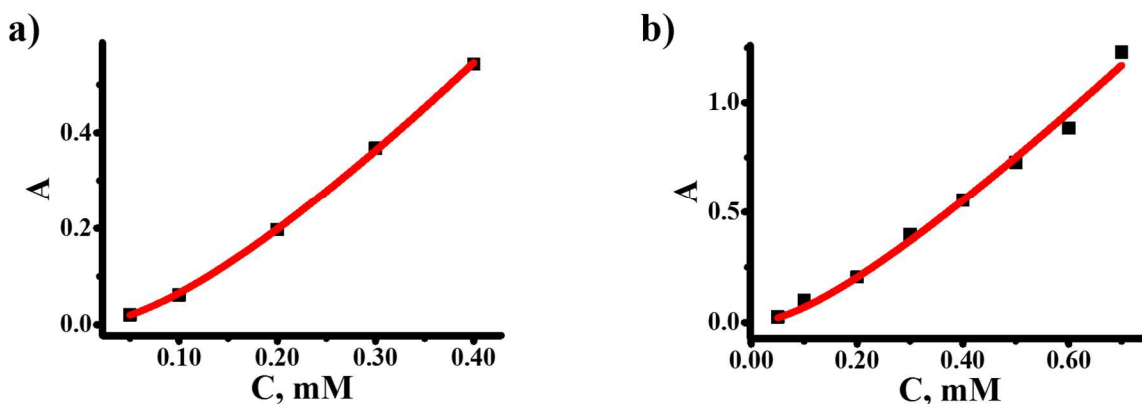
**Supplementary figure S22.** Representative origin fitting plots for uv-vis data of 1,1'-dibenzyl-4,4'-bipyridinium dibromide (6) aqueous buffer solutions at pH 7 (\*at pH 9.6 the compound crashes out the solution upon reduction): (a) run 1 (b) run 2.

\*EPR spectra are not possible to obtain due to the poor stability and/or solubility of the formed radical.

**1-(4-Fluorophenyl)- 1'-methyl -4,4'-bipyridinium iodide/chloride (7).**



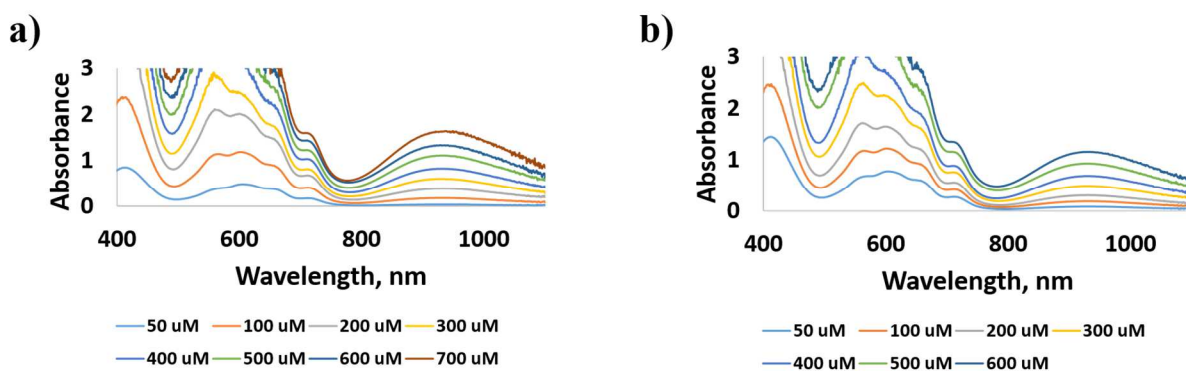
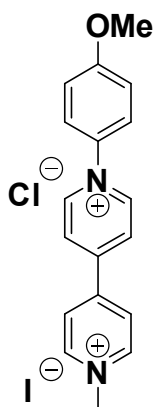
**Supplementary figure S23.** Representative uv-vis spectra of 1-(4-fluorophenyl)-1'-methyl-4,4'-bipyridinium iodide/chloride (7) aqueous buffer solutions at pH 7 (\*at pH 9.6 the radical is unstable to obtain uv-vis spectra): (a) run 1 (b) run 2.



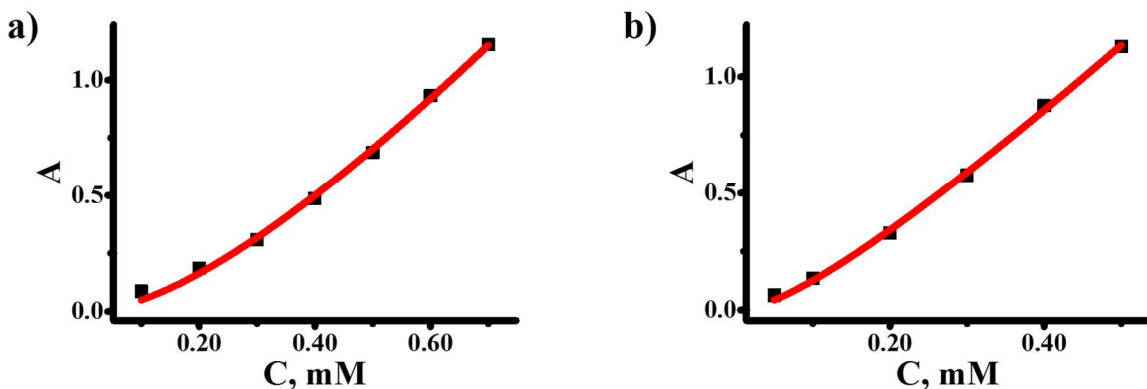
**Supplementary figure S24.** Representative origin fitting plots for uv-vis data of 1-(4-fluorophenyl)-1'-methyl-4,4'-bipyridinium iodide/chloride (7) aqueous buffer solutions at pH 7 (\*at pH 9.6 the radical is unstable to obtain uv-vis spectra): (a) run 1 (b) run 2.

\*EPR spectra are not possible to obtain due to the poor stability and/or solubility of the formed radical.

**1-(4-Methoxyphenyl)- 1'-methyl -4,4'-bipyridinium iodide/chloride (8).**



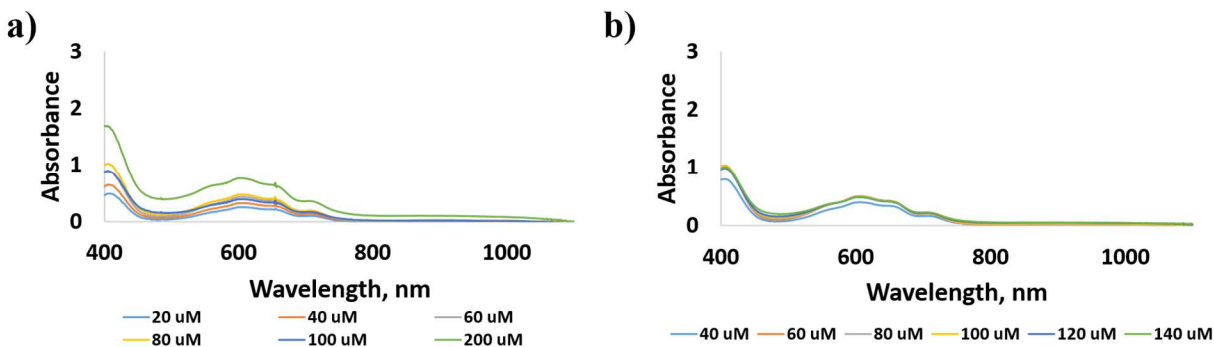
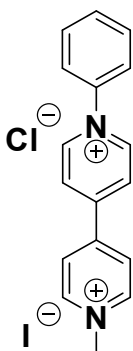
**Supplementary figure S25.** Representative uv-vis spectra of 1-(4-methoxyphenyl)- 1'-methyl -4,4'-bipyridinium iodide/chloride (8) aqueous buffer solutions at pH 7 (\*at pH 9.6 the radical is unstable to obtain uv-vis spectra): **(a)** run 1 **(b)** run 2.



**Supplementary figure S26.** Representative origin fitting plots for uv-vis data of 1-(4-methoxyphenyl)-1'-methyl-4,4'-bipyridinium iodide/chloride (8) aqueous buffer solutions at pH 7 (\*at pH 9.6 the radical is unstable to obtain uv-vis spectra): (a) run 1 (b) run 2.

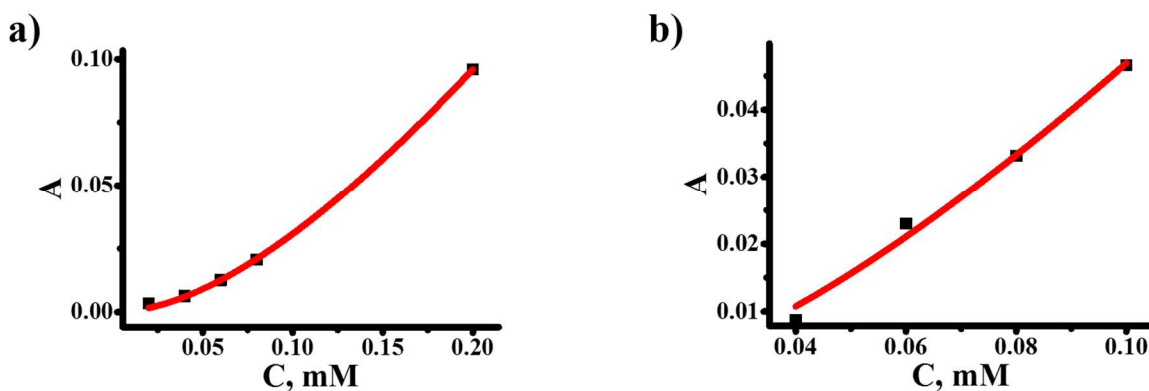
\*EPR spectra are not possible to obtain due to the poor stability and/or solubility of the formed radical.

### 1-Phenyl-1'-methyl-4,4'-bipyridinium iodide/chloride (9).





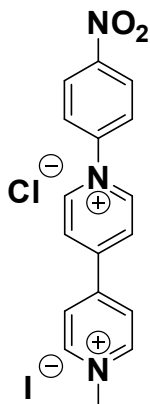
**Supplementary figure S27.** Representative uv-vis spectra of 1-phenyl-1'-methyl-4,4'-bipyridinium iodide/chloride (9) aqueous buffer solutions at pH 7 (\*at pH 7 the radical has poor stability and at pH 9.6 the radical is unstable to obtain uv-vis spectra): (a) run 1 (b) run 2.

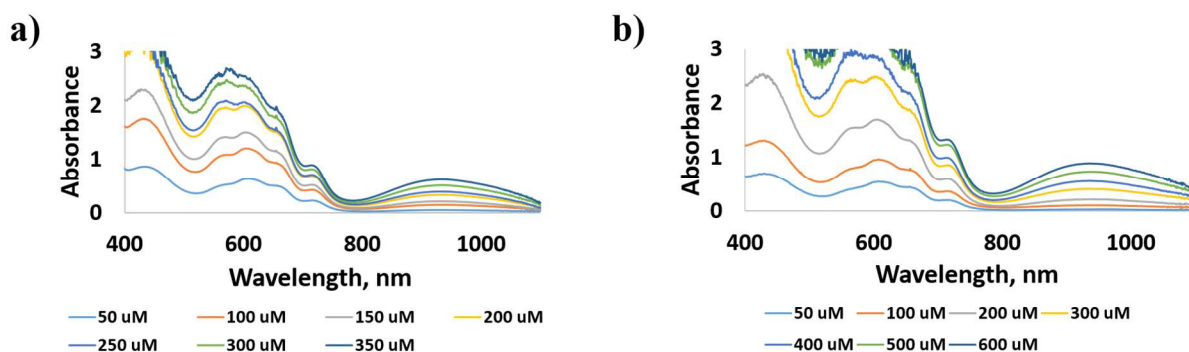


**Supplementary figure S28.** Representative origin fitting plots for uv-vis data of 1-phenyl-1'-methyl-4,4'-bipyridinium iodide/chloride (9) aqueous buffer solutions at pH 7 (\*at pH 7 the radical has poor stability and at pH 9.6 the radical is unstable to obtain uv-vis spectra): (a) run 1 (b) run 2.

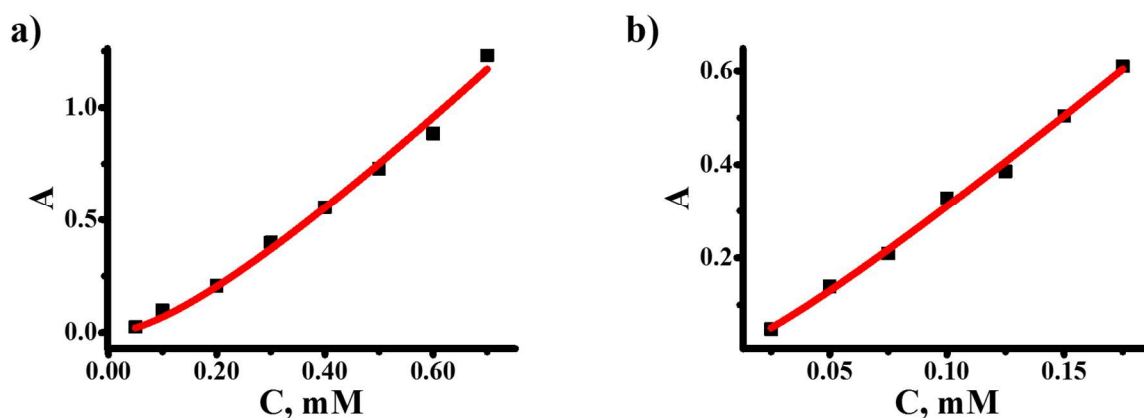
\*EPR spectra are not possible to obtain due to the poor stability and/or solubility of the formed radical.

**1-(4-Nitrophenyl)-1'-methyl-4,4'-bipyridinium iodide/chloride (10).**





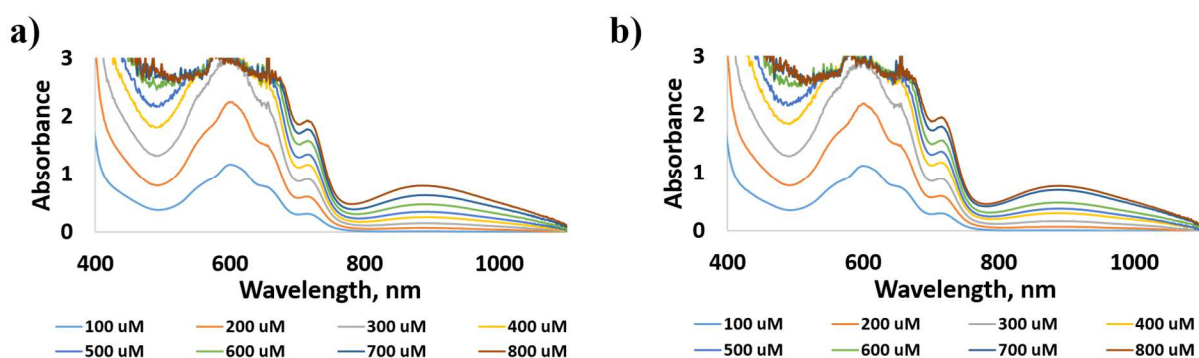
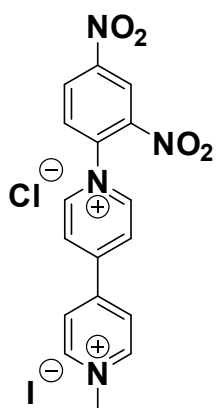
**Supplementary figure S29.** Representative uv-vis spectra of 1-(4-nitrophenyl)- 1'-methyl -4,4'-bipyridinium iodide/chloride (10) aqueous buffer solutions at pH 7 (\*at pH 9.6 the radical is unstable to obtain uv-vis spectra): (a) run 1 (b) run 2.



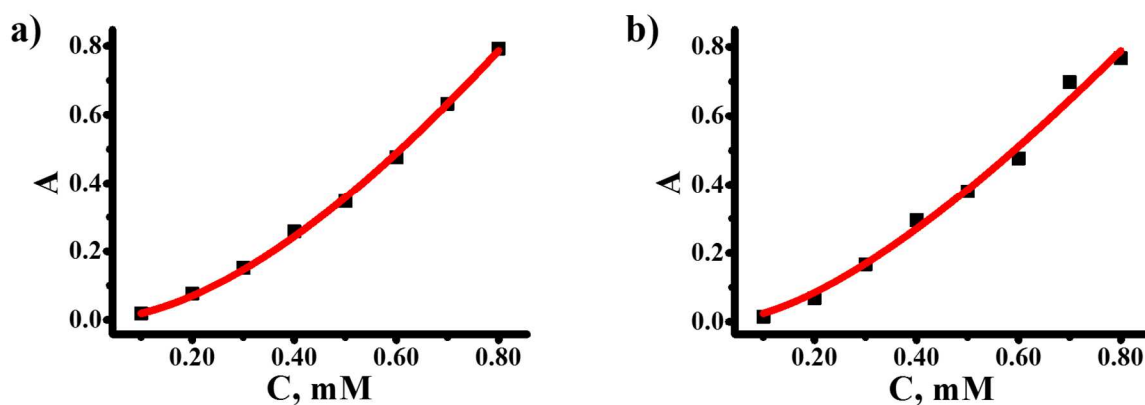
**Supplementary figure S30.** Representative origin fitting plots for uv-vis data of 1-(4-nitrophenyl)- 1'-methyl -4,4'-bipyridinium iodide/chloride (10) aqueous buffer solutions at pH 7 (\*at pH 9.6 the radical is unstable to obtain uv-vis spectra): (a) run 1 (b) run 2.

\*EPR spectra are not possible to obtain due to the poor stability and/or solubility of the formed radical.

**1-(2,4-Dinitrophenyl)-1'-methyl -4,4'-bipyridinium iodide/chloride (11).**



**Supplementary figure S31.** Representative uv-vis spectra of 1-(2,4-dinitrophenyl)-1'-methyl -4,4'-bipyridinium iodide/chloride (11) aqueous buffer solutions at pH 7 (\*at pH 9.6 the radical is unstable to obtain uv-vis spectra): (a) run 1 (b) run 2.

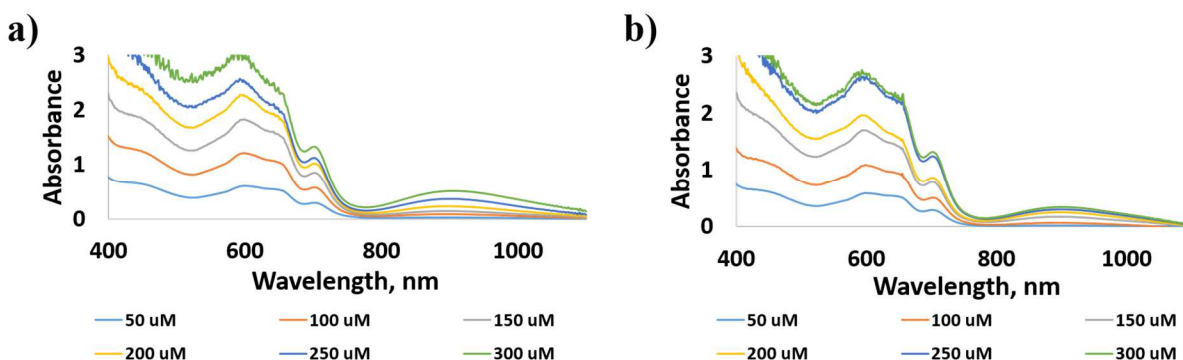
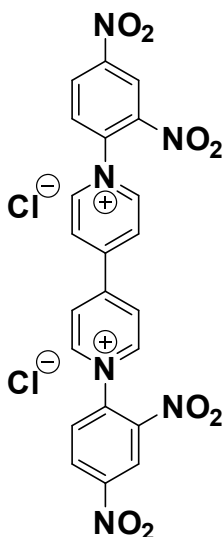


**Supplementary figure S32.** Representative origin fitting plots for uv-vis data of 1-(2,4-dinitrophenyl)-1'-methyl -4,4'-bipyridinium iodide/chloride

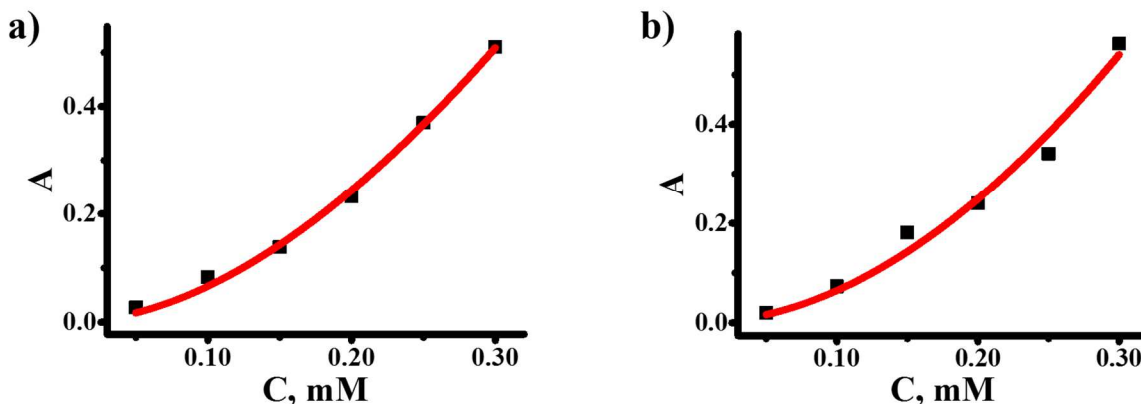
(11) aqueous buffer solutions at pH 7 (\*at pH 9.6 the radical is unstable to obtain uv-vis spectra): **(a)** run 1 **(b)** run 2.

\*EPR spectra are not possible to obtain due to the poor stability and/or solubility of the formed radical.

**1,1'-Di-2,4-dinitrophenyl-4,4'-bipyridinium dichloride (12).**



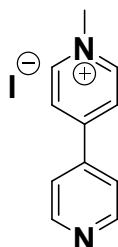
**Supplementary figure S33.** Representative uv-vis spectra of 1,1'-di-2,4-dinitrophenyl-4,4'-bipyridinium dichloride (12) aqueous buffer solutions at pH 7 (\*at pH 9.6 the radical is unstable to obtain uv-vis spectra): **(a)** run 1 **(b)** run 2.

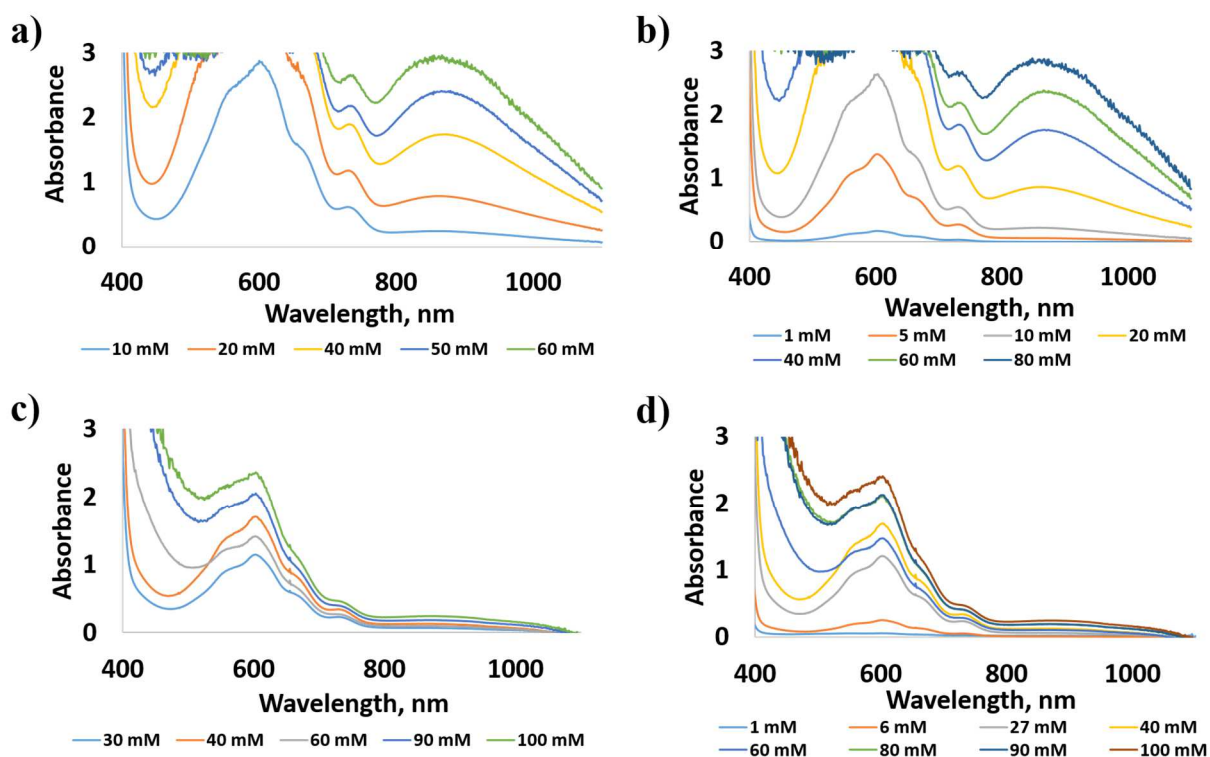


**Supplementary figure S34.** Representative origin fitting plots for uv-vis data of 1,1'-di-2,4-dinitrophenyl-4,4'-bipyridinium dichloride (12) aqueous buffer solutions at pH 7 (\*at pH 9.6 the radical is unstable to obtain uv-vis spectra): **(a)** run 1 **(b)** run 2.

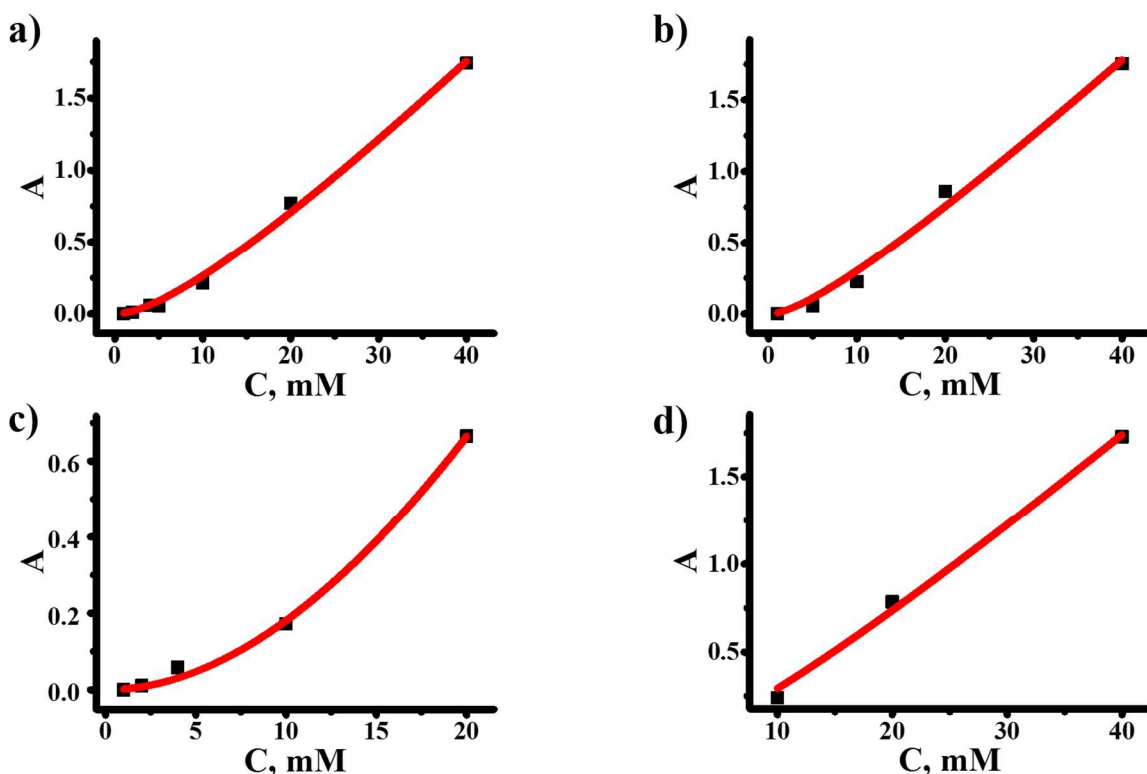
\*EPR spectra are not possible to obtain due to the poor stability and/or solubility of the formed radical.

### 1-Methyl-4,4'-bipyridinium iodide (13).





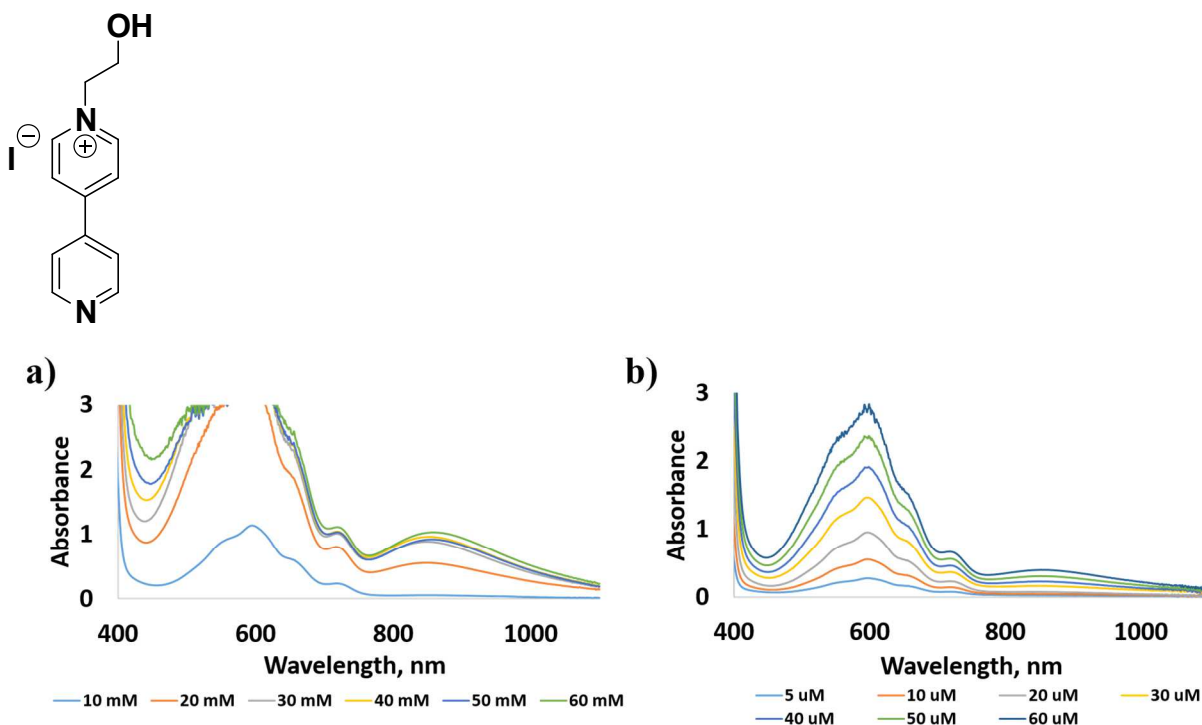
**Supplementary figure S35.** Representative uv-vis spectra of 1-methyl-4,4'-bipyridinium iodide (13) aqueous buffer solutions at: **(a)** pH 9.6 run 1 **(b)** pH 9.6 run 2; **(c)** pH 7 run 1 **(d)** pH 7 run 2; (\* at pH 7 the radical has poor stability): **(a)** run 1 **(b)** run 2.



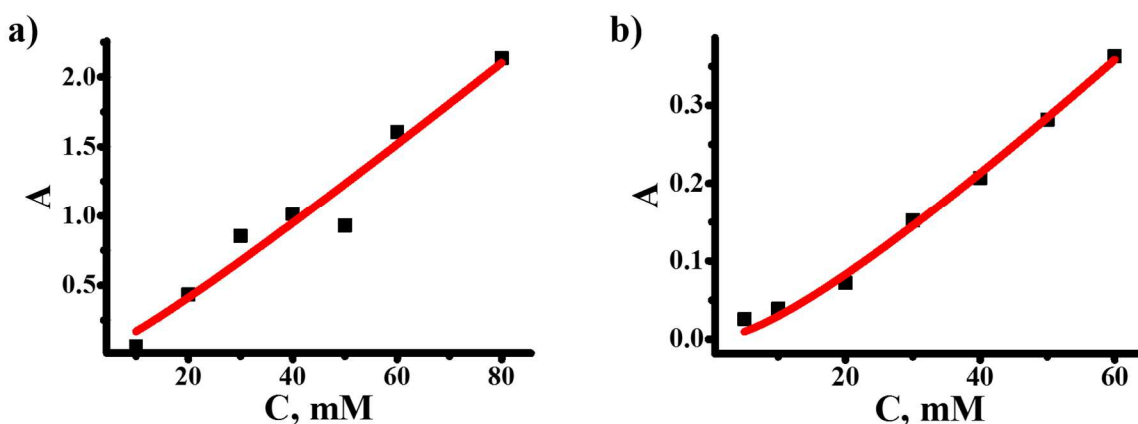
**Supplementary figure S36.** Representative origin fitting plots for uv-vis data of 1-methyl-4,4'-bipyridinium iodide (13) aqueous buffer solutions at: (a) pH 9.6 run 1 (b) pH 9.6 run 2; (c) pH 7 run 1 (d) pH 7 run 2; (\* at pH 7 the radical has poor stability): (a) run 1 (b) run 2.

\*EPR spectra did not show a signal for unpaired electrons at any concentration between 1-100 mM. It is not clear if EPR and uv-vis are monitoring the same process for mono-substituted bipyridinium salts as mono-substituted derivatives exhibit absolutely different behavior for dimerization process and need to be investigated as a separate species from viologen derivatives.

**1-(2-Hydroxyethyl)-4,4'-bipyridinium iodide (14).**



**Supplementary figure S37.** Representative UV-Vis spectra of 1-ethyl alcohol-4,4'-bipyridinium iodide (14) aqueous buffer at (a) pH 9.6 run 1 (b) 9H 7 run 2.



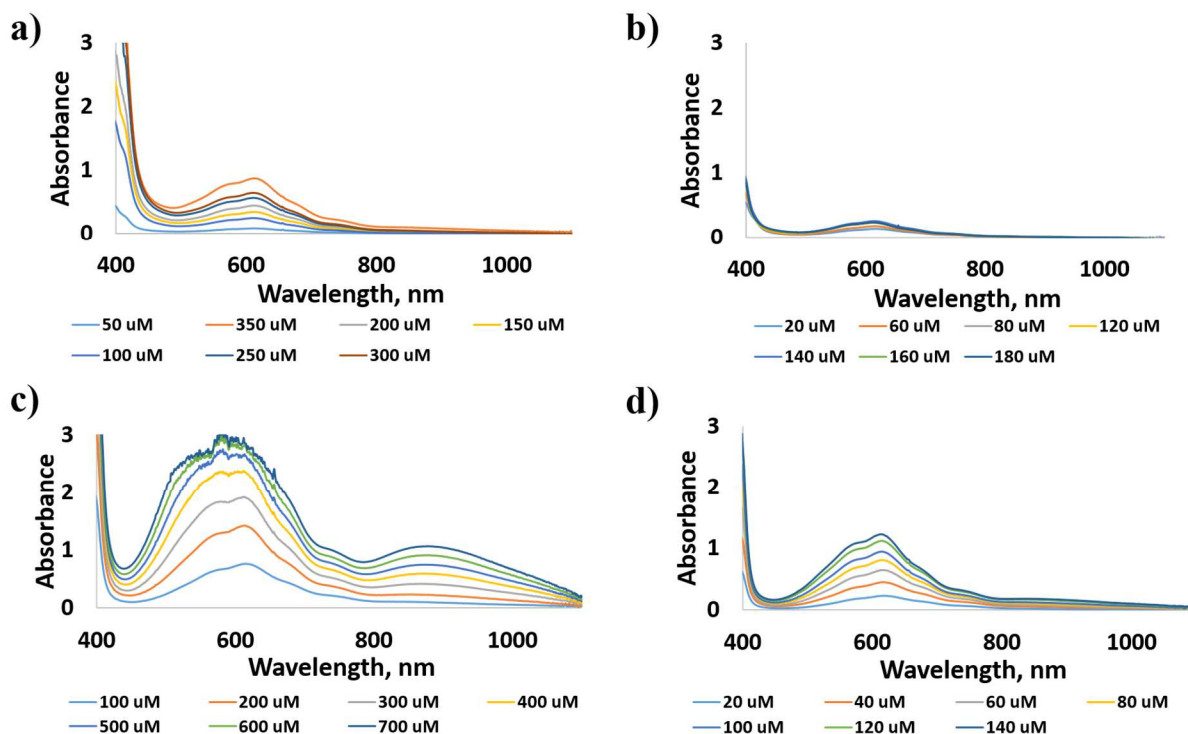
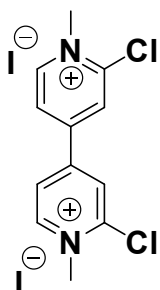
**Supplementary figure S38.** Representative origin fitting plots for UV-Vis data of 1-ethyl alcohol-4,4'-bipyridinium iodide (14) aqueous buffer solutions at pH: (a) pH 9.6 run 1 (b) pH 7 run 2.

\*EPR spectra did not show a signal for unpaired electrons at any concentration between 1-100 mM. It is not clear if EPR and uv-vis are

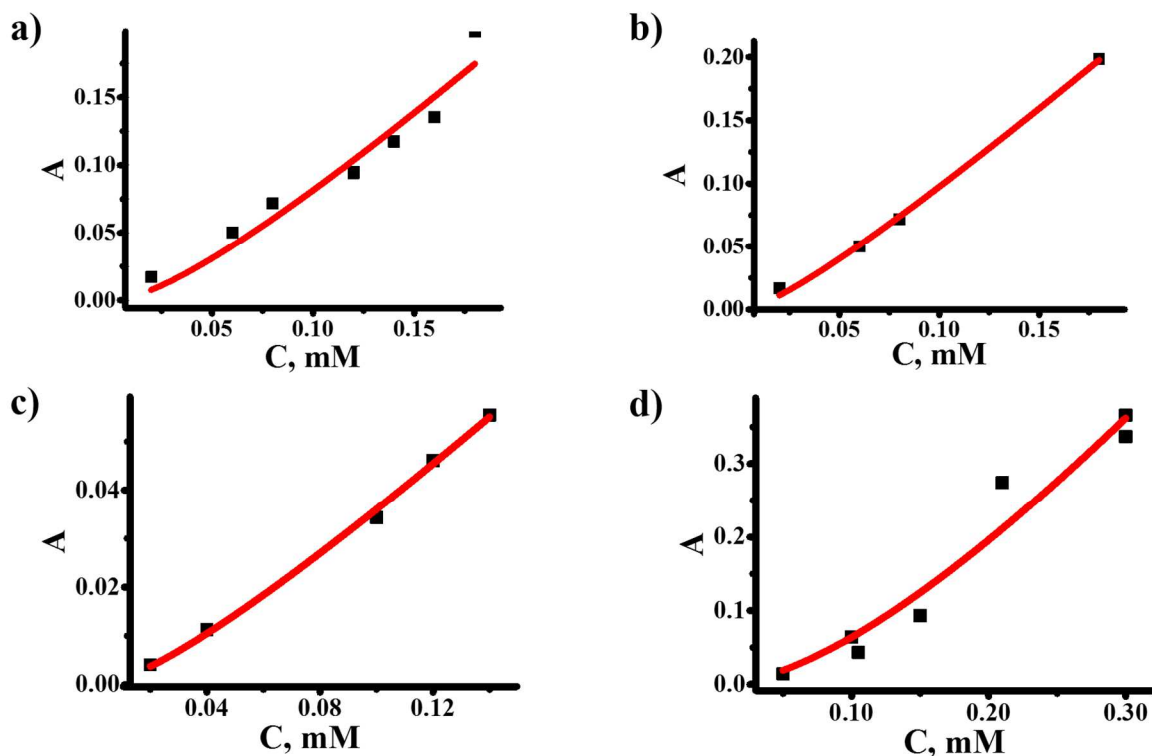


monitoring the same process for mono-substituted bipyridinium salts as mono-substituted derivatives exhibit absolutely different behavior for dimerization process and need to be investigated as a separate species from viologen derivatives.

### 1,1'-Dimethyl-2,2'-dichloro-4,4'-bipyridinium diiodide (15).

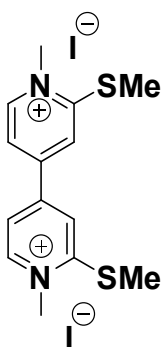


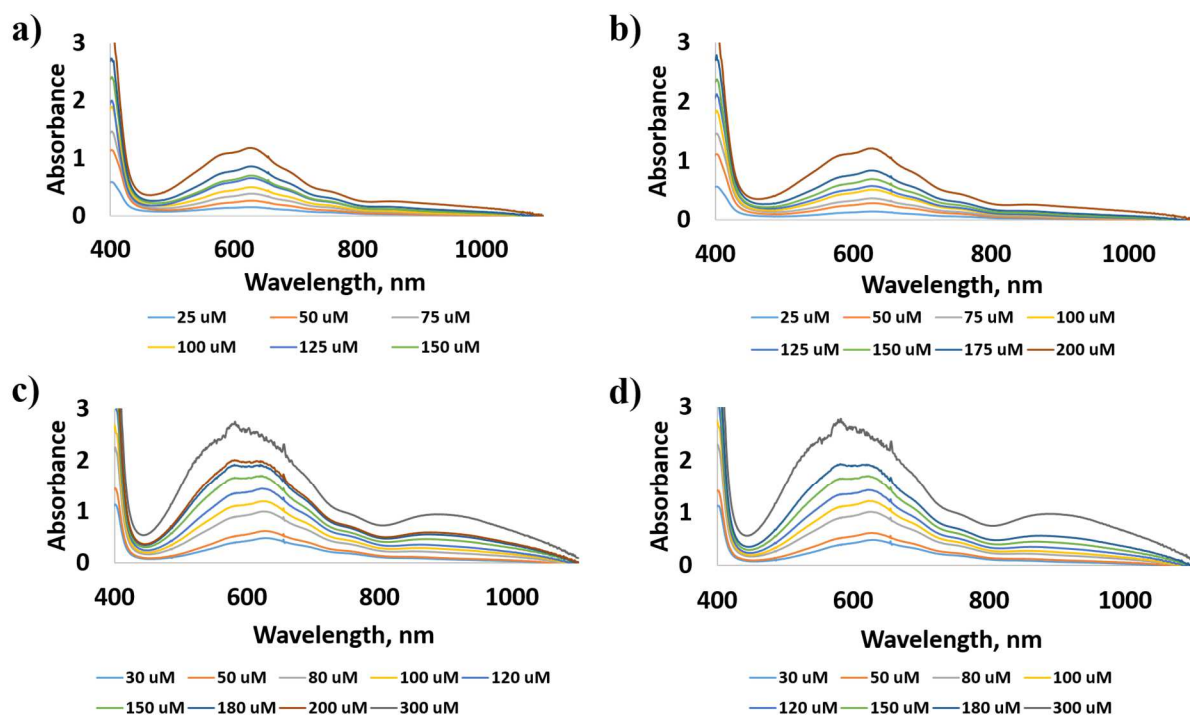
**Supplementary figure S39.** Representative uv-vis spectra of 1,1'-Dimethyl-2,2'-dichloro-4,4'-bipyridinium diiodide (15) aqueous buffer solutions at: (a) pH 9.6 run 1 (b) pH 9.6 run 2; (c) pH 7 run 1 (d) pH 7 run 2; (\* at both pH 9.6 and pH 7 the compound has poor stability).



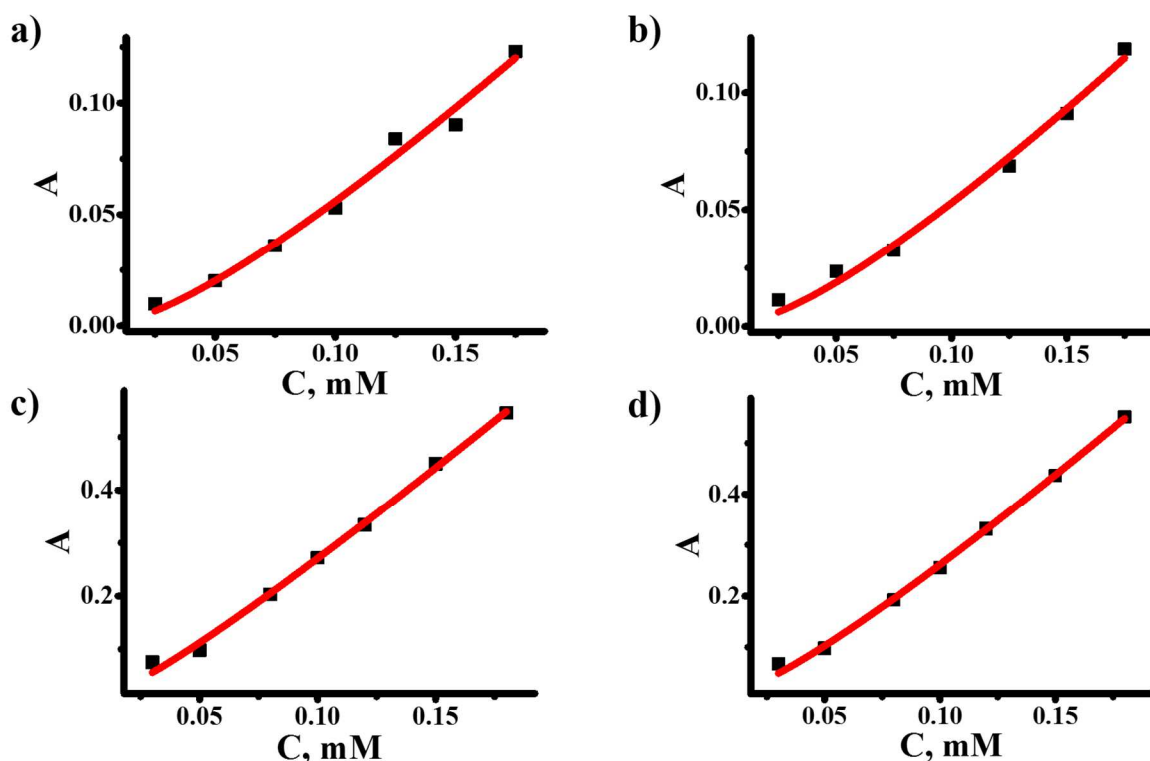
**Supplementary figure S40.** Representative origin fitting plots for uv-vis data of 1,1'-Dimethyl-2,2'-dichloro-4,4'-bipyridinium diiodide (15) aqueous buffer solutions at: (a) pH 9.6 run 1 (b) pH 9.6 run 2; (c) pH 7 run 1 (d) pH 7 run 2; (\*at both pH 9.6 and pH 7 the compound has poor stability).

**1,1'-Dimethyl-2,2'-bis(methylthio)-4,4'-bipyridinium diiodide (16).**

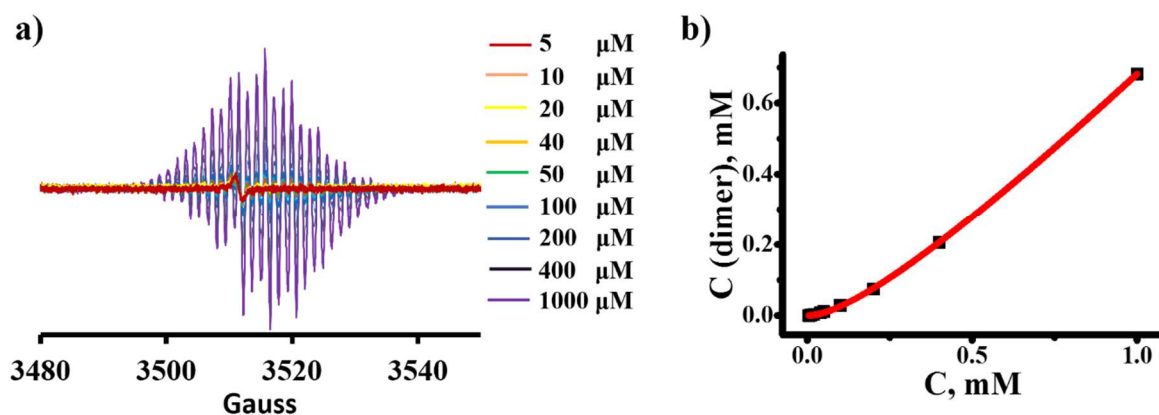




**Supplementary figure S43.** Representative uv-vis spectra of 1,1'-Dimethyl-2,2'-bis(methylthio)-4,4'-bipyridinium diiodide (16) aqueous buffer solutions at: (a) pH 9.6 run 1 (b) pH 9.6 run 2; (c) pH 7 run 1 (d) pH 7 run 2.



**Supplementary figure S44.** Representative origin fitting plots for uv-vis data of 1,1'-Dimethyl-2,2'-bis(methylthio)-4,4'-bipyridinium diiodide (16) aqueous buffer solutions at: (a) pH 9.6 run 1 (b) pH 9.6 run 2; (c) pH 7 run 1 (d) pH 7 run 2.

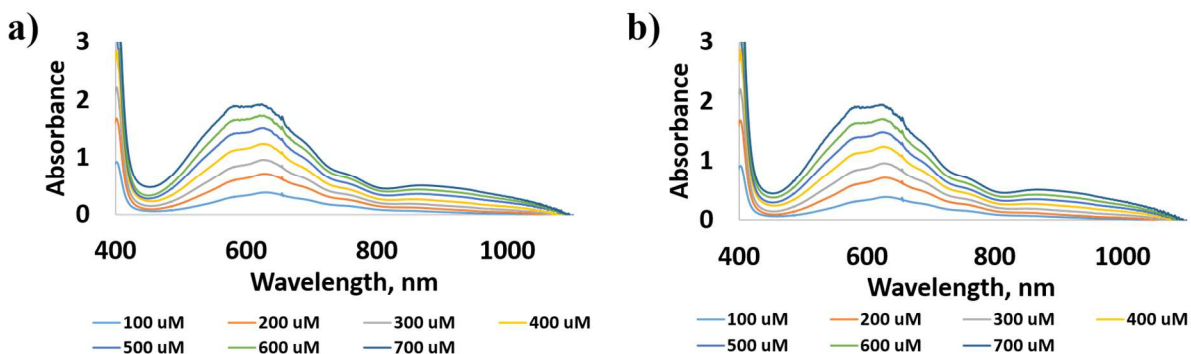
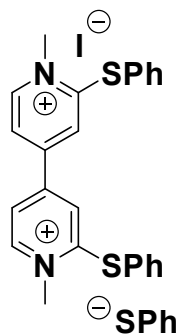


**Supplementary figure S45.** Representative EPR spectrum and origin fitting plot for 1,1'-Dimethyl-2,2'-bis(methylthio)-4,4'-bipyridinium diiodide (16) aqueous buffer solution at pH 7 (a) Isothermal EPR dilution experiment

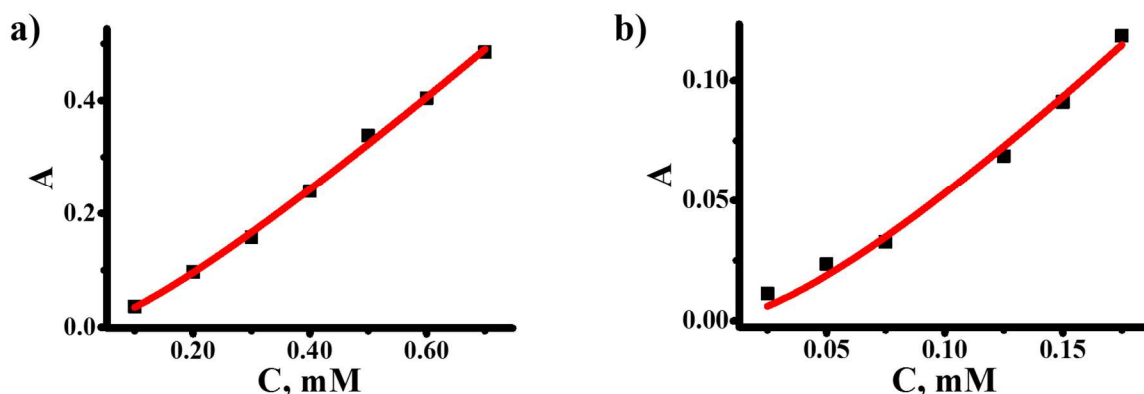
spectrum **(b)** Nonlinear fitting curve the dimer concentration vs total concentration of viologen derivative.

\*EPR spectra at pH 9.6 are not possible to obtain due to the poor stability of the formed radical.

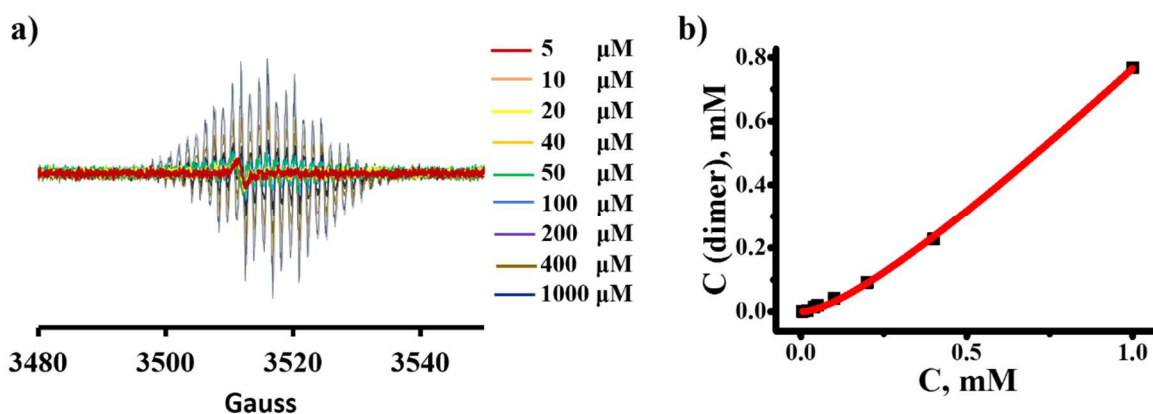
**1,1'-Dimethyl-2,2'-bis(phenylthio)- 4,4'-bipyridinium benzenethiolate iodide (17).**



**Supplementary figure S46.** Representative uv-vis spectra of 1,1'-Dimethyl-2,2'-bis(phenylthio)- 4,4'-bipyridinium benzenethiolate iodide (17) aqueous buffer solutions at pH 7 (\*at pH 9.6 the compound is unstable to obtain uv-vis spectra): **(a)** run 1 **(b)** run 2.



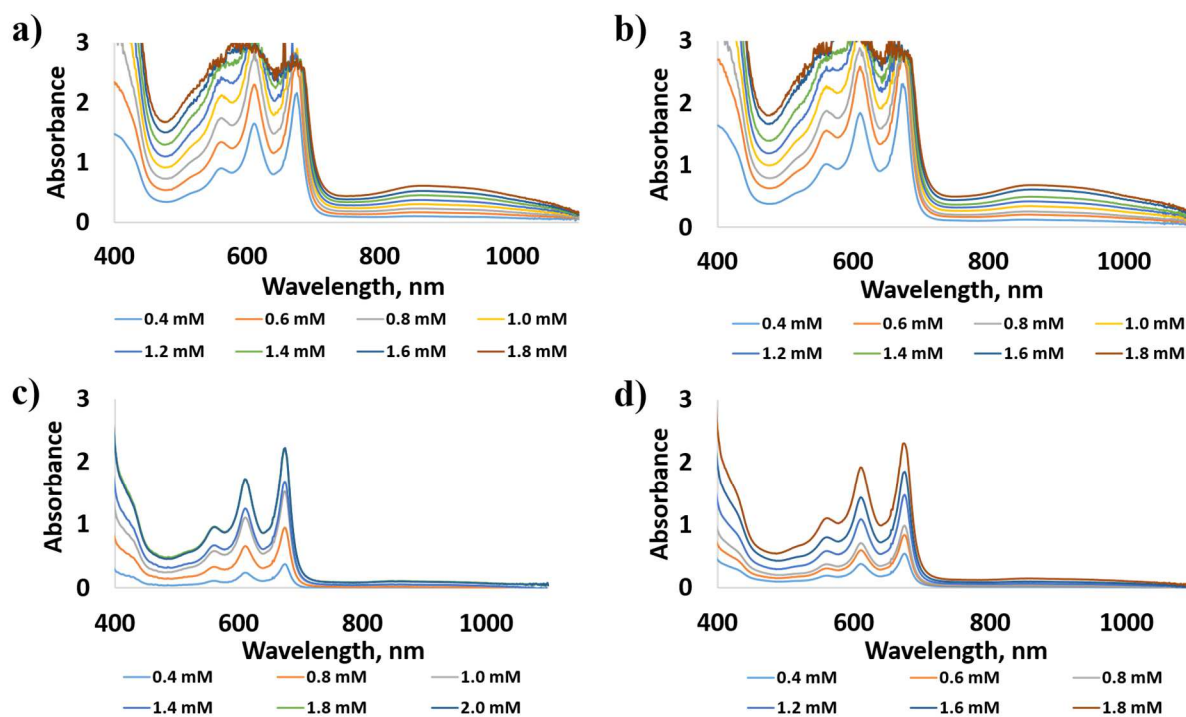
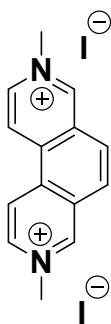
**Supplementary figure S47.** Representative origin fitting plots for uv-vis data of 1,1'-Dimethyl-2,2'-bis(phenylthio)- 4,4'-bipyridinium benzenethiolate iodide (17) aqueous buffer solutions at pH 7 (\*at pH 9.6 the compound is unstable to obtain uv-vis spectra): **(a)** run 1 **(b)** run 2.



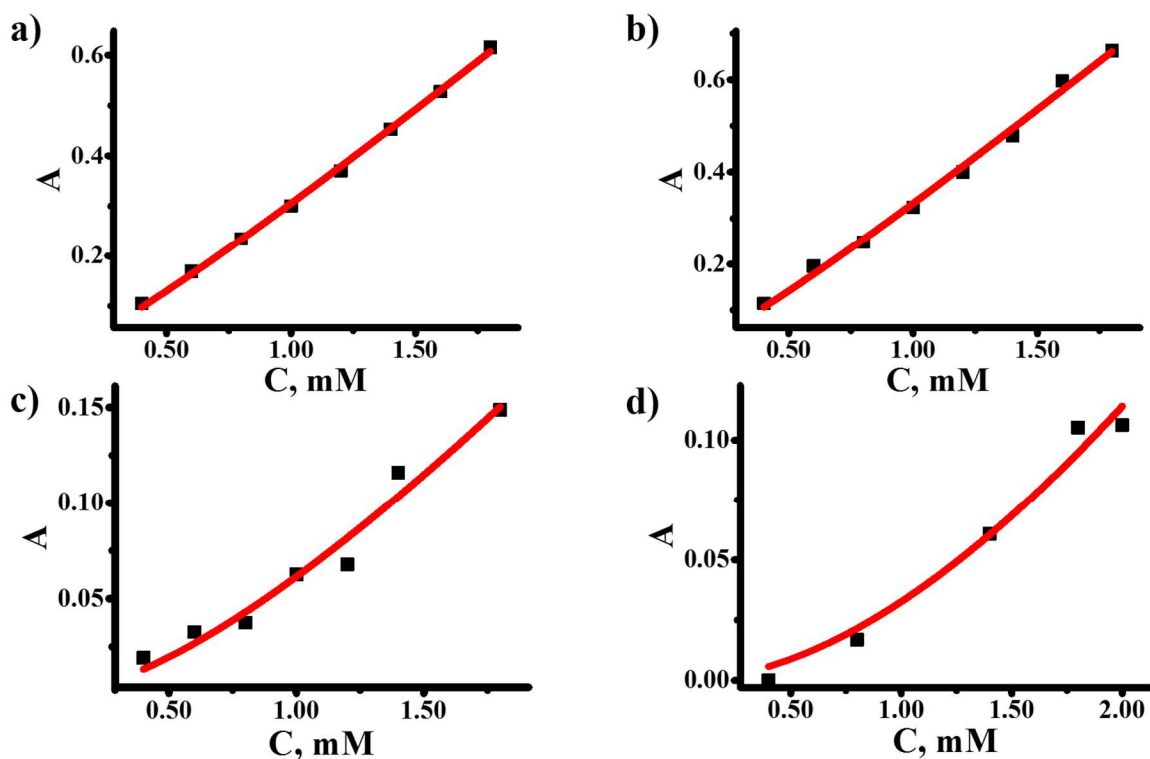
**Supplementary figure S48.** Representative EPR spectrum and origin fitting plot for 1,1'-Dimethyl-2,2'-bis(phenylthio)- 4,4'-bipyridinium benzenethiolate iodide (17) aqueous buffer solution at pH 7 **(a)** Isothermal EPR dilution experiment spectrum **(b)** Nonlinear fitting curve the dimer concentration vs total concentration of viologen derivative.

\*EPR spectra at pH 9.6 are not possible to obtain due to the poor stability of the formed radical.

### 3,8-Dimethyl-3,8-phenanthrolium diiodide (18).



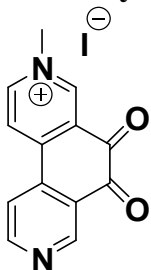
**Supplementary figure S49.** Representative uv-vis spectra of 3,8-dimethyl-3,8-phenanthroline diiodide (18) aqueous buffer solutions at: (a) pH 9.6 run 1 (b) pH 9.6 run 2; (c) pH 7 run 1 (d) pH 7 run 2.



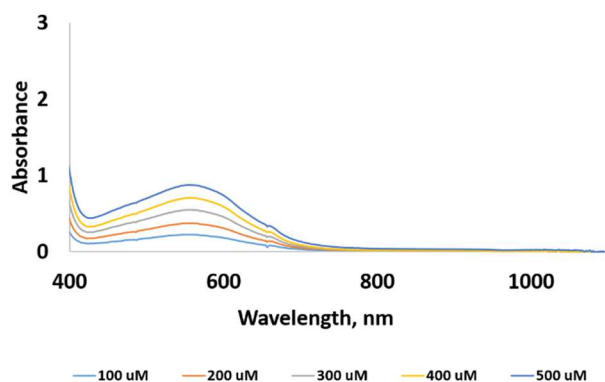
**Supplementary figure S50.** Representative origin fitting plots for uv-vis data of 3,8-dimethyl-3,8-phenanthroline diiodide (18) aqueous buffer solutions at: (a) pH 9.6 run 1 (b) pH 9.6 run 2; (c) pH 7 run 1 (d) pH 7 run 2.

\*EPR spectra are not possible to obtain due to the poor stability and/or solubility of the formed radical.

### 3-Methyl-5,6-dioxo-5,6-dihydro-3,8-phenanthroline iodide (19).







**Supplementary figure S51.** Representative uv-vis spectrum of 3-Methyl-5,6-dioxo-5,6-dihydro-3,8-phenanthroline iodide (19) aqueous buffer solutions at pH 7 (\*at pH 9.6 the compound is unstable to obtain uv-vis spectra).

\*Both, EPR and conclusive uv-vis spectra are not possible to obtain due to the poor stability and/or solubility of the formed radical.

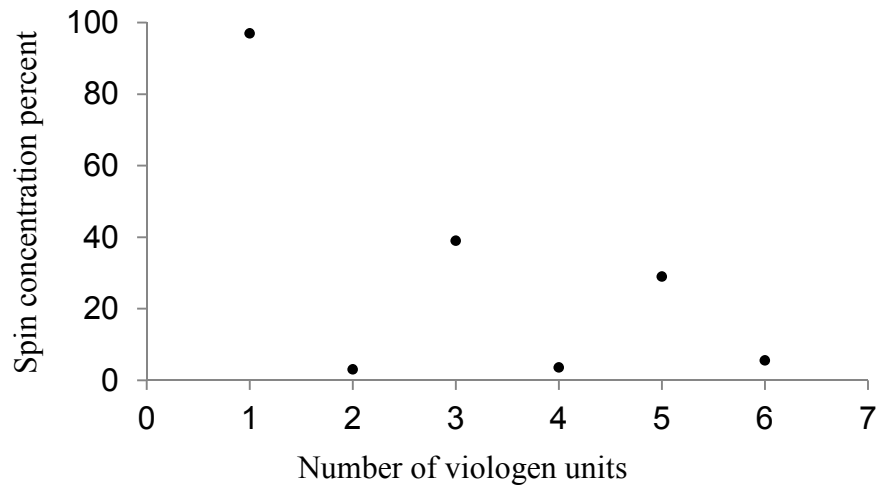


**Figure 5.8** Plot showing how the number of reduced viologen units in a 3 carbon tethered molecule affects total spin concentration

**1,1''-(1,3-Propanediyl)bis-4,4'-bipyridinium dibromide (3, n =3) [1]**

(1 g) was dissolved in dimethylformamide (20 ml) and water (10 ml) and 1,3-dibromopropane (3.9 g) was added. The mixture was heated for six hours at 90° and cooled. On dilution with acetone a yellow precipitate was obtained which was crystallised twice from aqueous ethanol to give the product, mp > 300° (yield 0.6 g). The nmr spectrum (deuterium oxide) consisted of a triplet at 5.238 (2H, central CH<sub>2</sub> protons), a broad quintet at 3.0 (4H, side chain central CH<sub>2</sub> protons), a triplet at 3.7 (4H, CH<sub>2</sub> protons adjacent to hydroxyl groups), a triplet at 4.99 (8H, CH<sub>2</sub> protons adjacent to quaternized nitrogens), a doublet at 8.68 (8H, aromatic protons *meta* to ring nitrogens) and a doublet at 9.30 ppm (8H, aromatic protons *ortho* to ring nitrogens).

**1,1''-(1,4-Butanediyl)bis[r-(4-hydroxybutyl)-4,4'-bipyridinium]-Tetrabromide (4, n = 4).**

1,1''-(1,4-Butanediyl)bis-4,4'-bipyridinium dibromide (3, n = 4) [1] (1 g) was dissolved in dimethylformamide (20 ml) and water (10 ml) and 1,4-dibromobutane (4.1 g) was added. The mixture was heated for six hours at 90° and cooled. On dilution with acetone a yellow precipitate was obtained which was crystallised twice from aqueous ethanol to give the product as the dihydrate mp > 300° (yield 0.8 g). The nmr spectrum (deuterium oxide) consisted of a multiplet at 6 — 1.6-2.4 (12H, four central CH<sub>2</sub> protons and eight side chain central CH<sub>2</sub> protons), a triplet at 3.7 (4H, CH<sub>2</sub> protons adjacent to hydroxyl groups), a multiplet at ~ 4.6-4.9 (8H, CH<sub>2</sub> protons adjacent to quaternized nitrogens), a doublet at 8.55 (8H, aromatic protons *meta* to ring nitrogens) and a doublet at 9.15 ppm (8H, aromatic protons *ortho* to ring nitrogens).

**Octaquaternary Salt 5 (n = 3).**

The tetraquaternary salt 4 (n = 3) (0.4 g) was dissolved in 48% aqueous hydrobromic acid (20 ml) and the solution was refluxed for three hours. After cooling, concentrated aqueous lithium perchlorate was added to precipitate the product as a pale brown powder which was crystallised twice from water, mp > 320° (yield 46%). The nmr spectrum (deuterium oxide) consisted of a multiplet at 5 chain central 2.6CH<sub>2</sub>-3.15 (10H, six central CH<sub>2</sub> protons and four side 2 protons), a triplet at 3.6 (4H, CH<sub>2</sub>Br protons), a multiplet at 4.85-5.10 (16H, CH<sub>2</sub> protons adjacent to quaternized nitrogens), a doublet at 8.60 (16H, aromatic protons *meta* to ring nitrogens) and a doublet at 9.20 ppm (16H, aromatic protons *ortho* to ring nitrogens).

**Octaquaternary Salt 5 (n = 4).**

The tetraquaternary salt 4 (n = 4) (0.4 g) was dissolved in 48% aqueous hydrobromic acid (20 ml) and the solution was refluxed for three hours. After cooling concentrated aqueous lithium perchlorate was added to precipitate the product as a white powder which was crystallised twice from water, mp > 320° (yield 53%). The nmr spectrum (deuterium oxide) consisted of a multiplet at 5 central 1.9-2.4 CH<sub>2</sub> (20 2 protons H, twelve ), a central triplet at CH<sub>2</sub> 3.6 2 protons (4H, CH<sub>2</sub> and 2 Br eight side chain protons), a multiplet at 4.7-4.95 (16H, CH<sub>2</sub> protons adjacent to quaternized nitrogens), a doublet at 8.55 (16H,

aromatic protons *meta* to ring nitrogens) and a doublet at 9.15 ppm (16H, aromatic protons *ortho* to ring nitrogens).

### Decaquaternary Salt 10 (n = 3).

The octaquaternary salt 5 (n = 3) (1 g) and a fourfold excess of 4,4'-bipyridine (0.7 g) were dissolved in dimethyl sulfoxide (15 ml) and the mixture heated at 80° for eight hours. The cooled mixture was diluted with concentrated aqueous lithium perchlorate whereupon a light brown precipitate of the product formed. It was crystallised twice from water as the pentahydrate mp > 300° (yield 61%). The nmr spectrum (deuterium oxide) consisted of a multiplet at 2.8-3.15 (10H, central CH 2 protons), a triplet at 5.0 (20H, CH 2 protons adjacent to quaternized nitrogens) a doublet at 7.9 (4H, aromatic protons *meta* to nitrogen in unquaternized pyridine rings), and a multiplet at 8.45-9.3 ppm (44H, remaining aromatic protons).

### Computational Methods

Computational studies were done using broken-symmetry density functional theory functional (UM06-2X/6-31++G(d,p), guess=read,mix,save)) with SMD water solvation using Gaussian 09.5,6 The monomer and the intermolecular dimer in the doublet and triplet state respectively were first optimized with UM06 6-31++G(d,p). All final geometries showed no imaginary frequencies and  $\langle S \rangle^2$  values of 0.

### Computational Coordinates

#### Viologen radical cation doublet SMD UM06-2X/6-31++G(d,p)

Absolute Energy (a.u., sum of electronic and zero point) = -574.579326 Hartree

Symbol	Coordinates (Angstroms)		
	X	Y	Z
C	0.712887	0.001459	-0.000126
C	1.481291	-1.204448	0.056986
C	2.845654	-1.174847	0.047806
C	2.846721	1.174961	-0.071455
C	1.482079	1.206651	-0.058254

C	-0.712887	0.001458	0.00012
C	-1.48129	-1.20445	-0.056991
C	-2.845653	-1.17485	-0.047806
C	-2.846722	1.174958	0.071454
C	-1.48208	1.206649	0.05825
N	-3.537268	-0.000705	0.028637
N	3.537268	-0.0007	-0.028633
C	-5.000682	-0.002224	-0.024155
H	-5.339791	-0.004284	-1.06266
H	-5.372178	-0.891106	0.485087
H	-5.372364	0.888196	0.48169
C	5.000681	-0.002229	0.024163
H	5.372369	0.888233	-0.481603
H	5.339788	-0.004381	1.062669
H	5.372177	-0.891068	-0.485156
H	-3.44643	-2.075837	-0.095008
H	3.447649	2.075632	-0.120679
H	3.446433	-2.075832	0.095009
H	1.010065	-2.177094	0.120745
H	-1.010064	-2.177096	-0.120754
H	-3.447652	2.075627	0.120681
H	-1.011417	2.180158	0.112312
H	1.011415	2.180159	-0.11232

### Intermolecular Viologen diradical dication singlet SMD UM06-2X/ 6-31++G(d,p)

Absolute Energy (a.u., sum of electronic and zero point) = -1149.179161 Hartree

Symbol	Coordinates (Angstroms)		
	X	Y	Z
C	-0.694969	-1.498412	0.165623
C	-1.720677	-1.560354	-0.831724
C	-3.040374	-1.601333	-0.483526
C	-2.501072	-1.488405	1.798064
C	-1.163458	-1.453483	1.511909
C	0.694878	-1.498465	-0.164787
C	1.163248	-1.454696	-1.51115
C	2.500838	-1.489813	-1.79741

C	3.040351	-1.600643	0.484211
C	1.720686	-1.559428	0.832507
N	3.441021	-1.610679	-0.818658
N	-3.441154	-1.610252	0.819319
C	4.860151	-1.491179	-1.150604
H	5.039708	-1.956642	-2.119602
H	5.143772	-0.434061	-1.193091
H	5.44918	-1.998936	-0.387233
C	-4.860314	-1.490644	1.151104
H	-5.143934	-0.433518	1.193289
H	-5.449277	-1.998629	0.387835
H	-5.039947	-1.95585	2.120214
H	2.876138	-1.443584	-2.813486
H	-2.876506	-1.44122	2.814048
H	-3.832656	-1.653132	-1.223099
H	-1.487141	-1.594945	-1.888166
H	0.481218	-1.371949	-2.349017
H	3.832716	-1.651615	1.223762
H	1.487259	-1.592978	1.889
H	-0.481508	-1.369934	2.349759
C	-0.694845	1.498402	-0.165451
C	-1.163289	1.45359	-1.511801
C	-2.500857	1.488575	-1.798049
C	-3.040339	1.601401	0.483522
C	-1.720691	1.560341	0.831826
C	0.694924	1.49837	0.164934
C	1.72071	1.559373	-0.832444
C	3.040374	1.60067	-0.484267
C	2.501068	1.489645	1.797416
C	1.16347	1.454462	1.511279
N	3.441191	1.610728	0.8186
N	-3.44105	1.610427	-0.819369
C	4.860336	1.491125	1.15038
H	5.14397	0.434002	1.192692
H	5.449312	1.998988	0.387035
H	5.040011	1.956452	2.119424
C	-4.860158	1.490705	-1.151264
H	-5.449239	1.998693	-0.388084
H	-5.039749	1.955859	-2.12041
H	-5.143747	0.433564	-1.193429
H	3.832676	1.651731	-1.223879
H	-3.832679	1.653189	1.223037

H	-2.876213	1.441444	-2.814065
H	-0.481265	1.370073	-2.349602
H	1.487167	1.592889	-1.888919
H	2.876463	1.443327	2.813455
H	0.481534	1.371531	2.349201
H	-1.487251	1.594848	1.888289

### Intermolecular Viologen diradical dication triplet SMD UM06-2X/ 6-31++G(d,p)

Absolute Energy (a.u., sum of electronic and zero point) = -1149.180230 Hartree

Symbol	Coordinates (Angstroms)		
	X	Y	Z
C	-0.689585	-1.666468	0.180946
C	-1.737705	-1.665594	-0.793271
C	-3.049597	-1.622917	-0.422745
C	-2.45893	-1.586185	1.854346
C	-1.130184	-1.63033	1.541524
C	0.689568	-1.666471	-0.180935
C	1.130126	-1.630289	-1.541523
C	2.458862	-1.586125	-1.854382
C	3.0496	-1.622947	0.422688
C	1.737719	-1.665643	0.793252
N	3.424335	-1.596752	-0.891038
N	-3.424371	-1.596782	0.890972
C	4.835317	-1.441397	-1.248715
H	4.999076	-1.872004	-2.236354
H	5.107489	-0.382319	-1.259961
H	5.446669	-1.968466	-0.515873
C	-4.835364	-1.441444	1.248609
H	-5.107549	-0.38237	1.259802
H	-5.446689	-1.968558	0.515776
H	-4.999135	-1.872008	2.236265
H	2.812892	-1.542579	-2.878016
H	-2.812994	-1.542685	2.87797
H	-3.857484	-1.618982	-1.146406
H	-1.52909	-1.690932	-1.855552
H	0.4316	-1.620588	-2.368832

H	3.85751	-1.619027	1.146324
H	1.529144	-1.691024	1.855538
H	-0.43169	-1.62066	2.368859
C	-0.68956	1.666469	-0.180921
C	-1.130142	1.630333	-1.541504
C	-2.458884	1.586197	-1.854343
C	-3.049581	1.622929	0.42274
C	-1.737694	1.665599	0.793283
C	0.689593	1.66647	0.18096
C	1.73773	1.665638	-0.79324
C	3.049616	1.622934	-0.422693
C	2.458909	1.586115	1.854385
C	1.130168	1.630288	1.541543
N	3.424369	1.596734	0.891027
N	-3.424338	1.596799	-0.890983
C	4.835355	1.441365	1.248684
H	5.107518	0.382285	1.25992
H	5.4467	1.968433	0.515836
H	4.999131	1.871965	2.236324
C	-4.835326	1.441474	-1.24864
H	-5.446657	1.968594	-0.515816
H	-4.99908	1.87204	-2.236298
H	-5.10752	0.382402	-1.259836
H	3.857516	1.61901	-1.14634
H	-3.857479	1.618996	1.14639
H	-2.812933	1.542697	-2.877972
H	-0.431635	1.620657	-2.368828
H	1.529139	1.691022	-1.855523
H	2.812953	1.542568	2.878014
H	0.431656	1.620594	2.368864
H	-1.529096	1.690932	1.855567